SYNTHESIS, *IN VITRO* EVALUATION AND STRUCTURE ACTIVITY RELATIONSHIP OF SOME HETEROCYCLIC IMIDAZOAZINE DERIVATIVES

Thesis submitted

by

Richa Goel
(Regn. No.901209002)

In fulfilment of the requirement
for the degree of

Doctor of Philosophy

Under the supervision of

Dr. Kamaldeep Paul
(Associate Professor)

School of Chemistry and Biochemistry
Thapar University
Patiala – 147 004
Punjab, India

May 2016

Certificate

This is to certify that thesis entitled "**Synthesis, *In vitro* evaluation and structure activity relationship of some heterocyclic imidazoazine derivatives**" being submitted by Richa Goel in the fulfilment of the requirement for the award of Degree of Doctor of Philosophy to the School of Chemistry and Biochemistry, Thapar University, Patiala, is a record of candidate's own work carried out by her under my supervision and guidance. The matter presented in the thesis has not been submitted in part or full for the award of any degree in any other University or institute.

(Supervisor)

Dr. Kamaldeep Paul

Associate Professor

School of Chemistry and Biochemistry

Thapar University, Patiala-147004

Punjab (India)

(Professor and Head)

Dr. Bonamali Pal

Professor and Head

School of Chemistry and Biochemistry

Thapar University, Patiala-147004

Punjab (India)

Candidate's Declaration

I, hereby declare that work presented in the thesis entitled" **Synthesis, *In vitro* evaluation and structure activity relationship of some heterocyclic imidazoazine derivatives",** in fulfilment of the requirement for the award of degree of Doctor of Philosophy, School of Chemistry and Biochemistry, Thapar University, Patiala, is an authentic record of my own work under the supervision of Dr. Kamaldeep Paul, Associate Professor, School of Chemistry and Biochemistry, Thapar University, Patiala, India. The matter embodied in this thesis has not been submitted in part or full to any other University or Institute for the award of any degree in India or abroad.

Richa Goel.

Richa Goel

Kamaldeep Paul.

(Supervisor)
Dr. Kamaldeep Paul
Associate Professor
School of Chemistry and Biochemistry
Thapar University, Patiala-147004
Punjab (India)

DEDICATED TO
MY
BELOVED FAMILY

Acknowledgements

Though only my name appears on the cover of this thesis, a great many people have contributed to its production. I owe my gratitude to all those people who have made this dissertation possible and because of whom my graduate experience has been one that I will cherish forever. This thesis is the end of my journey in obtaining my Ph.D. I have not travelled in a vacuum in this journey. This thesis has been kept on track and been seen through to completion with the support and encouragement of numerous people including my well wishers, my friends, colleagues and various institutions.

With humble thanks, I owe it all to Almighty God for granting me the wisdom, health and strength to undertake this research task and who kindly helped me to complete my thesis.

At the outset, I would like to express my appreciation to my supervisor **Dr. Kamaldeep Paul** for his advice during my doctoral research endeavour for the past four years. As my supervisor, he has constantly forced me to remain focused on achieving my goal. His observations and comments helped me to establish the overall direction of the research and to move forward with investigation in depth. I thank him for providing me with the opportunity to work under his guidance and great effort he put into training me in the scientific field. Like a charm!

I am extremely grateful to **Dr. Vijay Luxami** for her support, guidance and contributions towards my research work.

I am profoundly obliged to **Dr. Bonamali Pal**, Professor and Head, School of Chemistry and Biochemistry, Thapar University, Patiala for their good wishes and motivation. I would also like to thank my committee members, **Dr. Manmohan Chhibber**, **Dr. Satyendra Kumar Pandey** and **Dr. Siddharth Sharma** for serving as my committee members even at hardship. Special regards to all faculty members of the School of Chemistry and Biochemistry for providing suggestions and taking interest in the progress of work.

I would like to specially acknowledge staff of School of Chemistry and Biochemistry especially **Mr. Chander Singh Thakur** for always being there to help.

I gratefully acknowledge, **Council of Scientific and Industrial research (CSIR)** for providing the open senior research fellowship **(SRF, Scheme no- 09/677(0020)/2013.EMR-I)** and JRF **(Scheme no- 02(0034)/11/EMR-II)** to complete my research work. Most of the results described in this thesis would not have been possible without the help of laboratories at the institutes like,

SAI labs, Thapar University, Patiala, **SAIF**, Punjab University, Chandigarh, **IISER**, Mohali, **NCI,** USA and **IIRT**, Delhi is gratefully acknowledged for investigating antitumor activities on cancer and normal cell lines respectively.

I am thankful to all my lab mates and colleagues **Dr. Alka Sharma, Dr. Meenakshi Verma, Dr. Prinka Singla, Richa Rani, Akul Sen Gupta, Gulshan Sharma, Ruhi, Richa Bansal and Iqubal Singh** for sharing all bad and good times in this long journey.

A special thanks to my family. Words cannot express how grateful I am to my father **Mr. Kamlesh Goel**, my mother **Mrs. Madhu Goel** and my brother **Deepanshu Goel.** I thank you all for your endless affection and love. Lastly, I thank my beloved husband **Mr. Mohit Mittal** for his continued and unfailing love, support and understanding in completion of my thesis and long journey. Despite all this co-operation rendered generously by one and all, I am solely responsible for any and all the errors and short comings of this dissertation.

Richa Goel

Table of Contents

INTRODUCTION

Cancer is uncontrolled growth of normal cells or division of the abnormal cells. These uncontrolled divisions of cells and its spread, resulted in death. Various factors for induction of cancer are tobacco, unhealthy diet and infectious organisms as well as internal factors like inherited genetic mutations, hormonal changes and immune conditions. Cancer remains a major health issue in developed countries and is the second largest cause of death after heart disease. It is predicted that by 2030, cancer can affect 22 million people.[1] It has been concluded that from estimated 5,89,430 cases of cancer deaths almost 1,71,000 of cancer deaths caused by smoking in 2015.[2] World Cancer Research Fund (WCRF) has estimated that upto 1/3 of the cancer cases occur due to obesity, physical inactivity, and/or poor nutrition in economically developed countries, so could easily be prevented. Infectious agents like human papillomavirus (HPV), hepatitis B virus (HBV), human immunodeficiency virus (HIV) and hepatitis C virus (HCV) can also be the cause of cancer. Treatment of cancer include surgery, use of chemotherapeutic drugs, hormonal therapy, use of radiation and targeted therapy i.e. drugs that interfere with tumor growth.[3] Surgical and radiation therapies for treatment of local cancer is not specific due to tumor position in the body and is not completely successful treatment in removing tumors. Chemotherapy is systemic treatment of cancer involving chemotherapeutic agents that interfere with the growth and normal cell division, inducing apoptosis of tumour cell by signaling pathways that improve and eradicate cancer. Various chemotherapeutic drugs like 5-fluorouracil, methotrexate, doxorubicin, epirubicin etc. are clinically known. Anticancer agents acted through *in vitro* inhibition of various cancer cell lines viz., breast cancer, ovarian cancer, non small cell lung cancer, melanoma, leukemia.

However, because of high mortality rate due to cancer and the development of resistance due to drugs and unwanted side effects, there is need to synthesize novel anticancer agents with reduced unwanted effects.[4-10] Considering cancer cells as highly proliferative tissues, various heterocyclic moieties viz., imidazopyridine,[11-14] quinazoline,[15,16] napthalimides,[17] purines[18] etc have been gaining attention as novel drug candidates for treatment of cancer through inhibition of various cancer cell lines. In addition, DNA is also an important target for development of anticancer agents.[19,20] Therefore, development of DNA targeted compounds becomes one of the most important fields in chemistry, biology and medicine. DNA acted through number of

pathways including DNA alkylating agents, major and minor groove binders and DNA intercalator. DNA intercalaters intercalate into the base pairs due to its planar geometry. Some of the known DNA intercalating molecules are acridine, naphthodiazine and anthraquinone.

Amongst fused heterocyclic moieties, imidazo[1,2-*a*]pyrazine has been gaining significant attention in field of drug discovery, due to its wide array of biological properties like antiinflammatory,[21] antihypertensive,[22] antiulcer,[23] antibronchospastic,[24] antimalarial etc.[25] Imidazo[1,2-*a*]pyrazine derivative **GS-9973** (Figure 1) acted as spleen tyrosine kinase inhibitor and has been selected in clinical trials as lead. Therefore, with a future expectation to grow imidazo[1,2-*a*]pyrazine as anticancer drug, there is a high need to synthesize and modify the imidazo[1,2-*a*]pyrazine core to develop more active pharmacophore with less side effects.

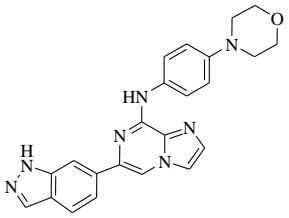

GS-9973

Figure 1

Coumarin is nitrogen based fused heterocyclic moiety that showed versatile biological behaviour. Several studies revealed the use of coumarin pharmacophore viz., 7-hydroxy coumarin, 6-nitro-7-hydroxycoumarin, esculetin (6,7-dihydroxy-2*H*-chromen-2-one) and scopoletin (7-hydroxy-6-methoxy-2*H*-chromen-2-one) for treatment of cancerous cells. It displayed antitumor activities being acted at different stages of tumor such as blocking the cell cycle, and inducing apoptosis etc.[26] Despite the use of coumarins in the cancer treatment, extensive efforts have been put to design and synthesize the novel coumarins with improved anticancer activity. Geiparvarin has been used as an antiproliferative and monoamine oxidase inhibitor. Coumarin and 7-hydroxy coumarin have been used as a potent cytotoxic and cytostatic agents.[27] 6-Nitro-7-hydroxy coumarin acted as anticancer agent that selectively target stress activated protein kinase.[28] Inhibition of leukaemic cells by induction of apoptosis is inhibited by esculetin and scopoletin (Figure 2).[29]

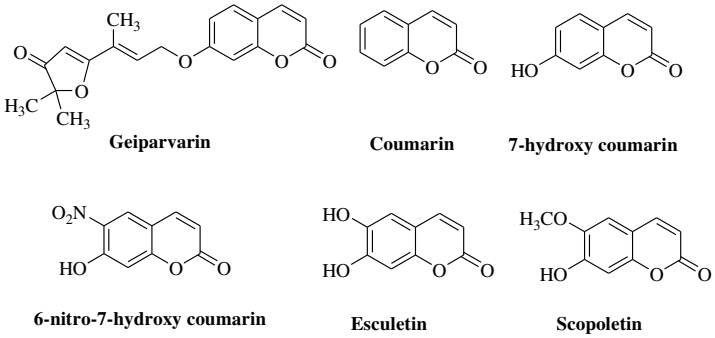

Figure 2

Benzimidazole is a 'Master Key' as it is an important pharmacophore in many compounds acting at different targets to elicit variable pharmacological properties.[30] Derivatives of benzimidazole are found in natural and non-natural products like marine alkaloid kealiiquinone and vitamin B_{12}.[31] Various marketed preparations viz., carbendazim has been used as anti-fungal agent, mebendazole as anti-helmintic agent etc. Benzimidazole derivative, Bendamustine (Figure 3) have been known clinically as potent antitumor agent.

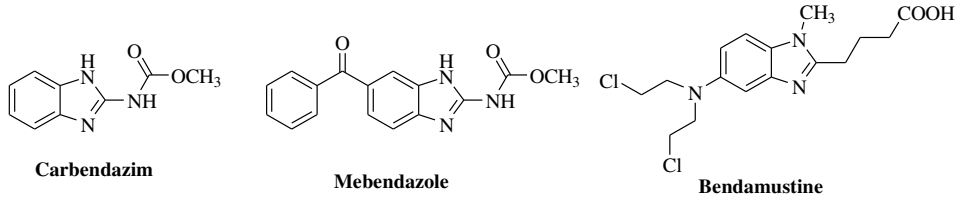

Figure 3

Among the class of DNA intercalators as well as cytotoxic activity, naphthalimide derivatives are one of those members which have gained considerable attention. Naphthalimide based drugs, amonafide and mitonafide are the first drugs to reached the clinical trial stage. But due to unpredictable side effects like central neurotoxicity, amonafide failed to enter clinical phase III.[20] Mitonafide has been studied in phase I and phase II clinical trials where it showed good inhibition against solid tumors despite of the toxic side effects.[32] LU 79553 and DMP 840 belonging to bis-naphthalimide series, have been in the clinical trials (Figure 4).[33-35]

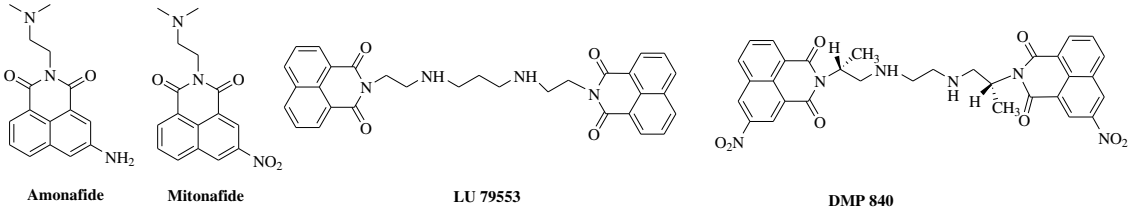

Figure 4

Herein, we have synthesized various imidazo[1,2-*a*]pyrazine derivatives bearing aryl group at different positions (C3, C6 or C8) along with its *in vitro* evaluation against cancer cell lines, synthesis of triazole tethered imidazo[1,2-*a*]pyrazine-coumarin and triazole tethered imidazo[1,2-a]pyrazine-benzimidazole conjugates by applying click chemistry and Suzuki coupling approach and then studied its photophysical properties. Structure activity relationship has also been predicted for the relation of activity with change of substituents.

Present work has been divided into following parts:

Chapter 1: Review of literature

Chapter 2: Arylated Imidazo[1,2-*a*]pyrazine derivatives

Chapter 3: Imidazo[1,2-*a*]pyrazine-coumarin hybrids

Chapter 4: (I) Imidazo[1,2-*a*]pyrazine-triazole-coumarin conjugates

(II) Imidazo[1,2-*a*]pyrazine-triazole-benzimidazole conjugates

Chapter 5: Photophysical and DNA interaction studies of naphthalimide derivatives

References

1. http://www.who.int/mediacentre/factsheets/fs297/en/(accessed on 05.01.16)
2. American Cancer Society. *Cancer Facts & Figures 2015*. Atlanta: American Cancer Society; 2015.
3. http://www.cancer.org/acs/groups/content/@research/documents/webcontent/acspc 041787.pdf (accessed 05.01.16).
4. Y. Li, Y. Xu, X. Qian, B. Qu, *Tetrahedron Lett*., 2004, **45**, 1247.
5. Y. Xu, B. Qu, X. Qian, Y. Li, *Bioorg. Med. Chem. Lett*., 2005, **15**, 1139.
6. F. Liu, X. Qian, J. Cui, Y. Xiao, R. Zhanga, G. Lia, *Bioorg. Med. Chem*., 2006, **14**, 4639.
7. Y. Li, Y. Xu, X. Qian, B. Qu, *Bioorg. Med. Chem. Lett*., 2003, **13**, 3513.
8. H. B. Mereyala, M. Joe, *Curr. Med. Chem. Anti-Cancer Agents*, 2001, **1**, 293.
9. M. F. Bran˜ a, A. Ramos, *Curr. Med. Chem. Anti-Cancer Agents*, 2001, **1**, 237.
10. X. Qian, Y. Li, Y. Xu, B. Qu, *Bioorg. Med. Chem. Lett*., 2004, **14**, 2665.
11. M. A. Vilchis-Reyes, A. Zentella, M. A. Martinez-Urbina, A. Guzman, O. Vargas, M. T. R. Apan, J. L. V. Gallegos, E. Diaz, *Eur. J. Med. Chem.,* 2010, **45,** 379.
12. M. A. Martinez-Urbina, A. Zentella, M. A. Vilchis-Reyes, A. Guzman, O. Vargas, M. T. R. Apan, J. L. V. Gallegos, E. Diaz, *Eur. J. Med. Chem.,* 2010, **45,** 1211.

13. N. Dahan-Farkas, C. Langley, A. L. Rousseau, D. B. Yadav, H. Davids, C. B.de. Koning, *Eur. J. Med. Chem.,* 2011, **46,** 4573.
14. Y.-S. Tung, M. S. Coumar, Y.-S. Wu, H.-Y. Shiao, J.-Y. Chang, J.-P. Liou, P. Shukla, C.-W. Chang, C.-Y. Chang, C.-C. Kuo, T.-K. Yeh, C.-Y. Lin, J.-S. Wu, S.-Y. Wu, C.-C. Liao, H.-P. Hsieh, *J. Med. Chem.,* 2011, **54,** 3076.
15. A. Sharma, V. Luxami, K. Paul, *Bioorg. & Med. Chem. Lett.,* 2013, **23**, 3288.
16. K. Paul, S. Bindal, V. Luxami, *Bioorg. & Med. Chem. Lett.,* 2013, **23**, 3667.
17. M. Verma, V. Luxami, K. Paul, *Eur. J. Med. Chem.*, 2013, **68**, 352.
18. A. Sharma, V. Luxami, K. Paul, *Eur. J. Med. Chem.*, 2015, **93**, 414.
19. X. Li , Q. Wang, Y. Qing, Y. Lin, Y. Zhang, X. Qian, J. Cui, *Bioorg. Med. Chem.*, 2010, **18**, 3279.
20. I. Ott, Y. Xu, J. Liu, M. Kokoschka, M. Harlos, W. S. Sheldrick, X. Qian, *Bioorg. Med. Chem.*, 2008, **16**, 7107.
21. M. G. Rimoli, L. Avallone, P de. Caprariis, E. Luraschi, E. Abignente, W. Filippelli, L. Berrino and F. Rossi, *Eur. J. Med. Chem.*, 1997, **32**, 195.
22. W. C. Lumma, Jr., W. C. Randall, E. L. Cresson, J. R. Huff, R. D. Hartman and T. F. Lyon. *J. Med. Chem.,* 1983, **26**, 357.
23. (*a*) J. J. Kaminski, D. G. Perkins, J. D. Frantz, D. M. Solomon, A. J. Elliott, P. J. S. Chiu and J. F. Long, *J. Med. Chem.,* 1987, **30**, 2047; (*b*) J. J. Kaminski, J. M. Hilbert, B. N. Pramanik, D. M. Solomon, D. J. Conn, R. K. Rizvi, A. J. Elliott, H. Guzik, R. G. Lovey, M. S. Domalski, S.-C. Wong, C. Puchalski, E. H. Gold, J. F. Long, P. J. S. Chiu and A. T. McPhail, *J. Med. Chem.,* 1987, **30**, 2031.
24. P. A. Bonnet, A. Michel, F. Laurent, C. Sablayrolles, E. Rechencq, J. C. Mani, M. Boucard and J. P. Chapat, *J. Med. Chem.,* 1992*,* **35***,* 3353.
25. C. W. McNamara, M. C. S. Lee, C. S. Lim, S. H. Lim, J. Roland, A. Nagle, O. Simon, B. K. S. Yeung, A. K. Chatterjee, S. L. McCormack, M. J. Manary, A.-M. Zeeman, K. J. Dechering, T. R. SanthaKumar, P. P. Henrich, K. Gagaring, M. Ibanez, N. Kato, K. L. Kuhen, C. Fischli, M. Rottmann, D. M. Plouffe, B. Bursulaya, S. Meister, L. Rameh, J. Trappe, D. Haasen, M. Timmerman, R. W. Sauerwein, R. Suwanarusk, B. Russell, L. Renia, F. Nosten, D. C. Tully, C. H. M. Kocken, R. J. Glynne, C. Bodenreider, D. A. Fidock, T. T. Diagana and E. A. Winzeler, *Nature*, 2013, **504**, 248.

26. S. Emami and S. Dadashpour, *Eur. J. Med. Chem*., 2015, **102**, 611.
27. (a) D. Conley and E. M. Marshall, *Proc. Am. Assoc. Cancer Res*., 1987, **28**, 63; (b) M. E. Marshall, J. L. Mohler, K. Edmonds, B. Williams, K. Butler, M. Ryles, L. Weiss, D. Urban, A. Beuschen, M. Markiewicz, *J. Cancer Res. Clin. Oncol*., 1994, **120**, 39; (c) L. D. Raev, E. Voinova, I. C. Ivanov and D. Popov, *Pharmazie,* 1990, **45**, 696.
28. G. Finn, B. Creaven and D. Egan, *Eur. J. Pharmacol*., 2003, **481,** 159.
29. (a) E. K. Kim, K. B. Kwon, B. C. Shin, E. A. Seo, Y. R. Lee, J. S. Kim, J. W. Park, B. H. Park and D. G. Ryu, *Life Sci*. 2005, **77**, 824; (b) C. Y. Chu, Y. Y. Tsai, C. J. Wang, W. L. Lin and T. H. Tseng, *Eur. J. Pharmacol*., 2001**, 416**, 25.
30. (a) G. Singh, M. Kaur and C. Mohan, *Int. J. Pharm*., 2013, **4**, 82; (b) Y. Bansal and O. Silakari, *Bioorg. Med. Chem*., 2012, **20**, 6208.
31. S. Nakamura, N. Tsuno, M. Yamashita, I. Kawasaki, S. Ohta and Y. Ohishi, *J. Chem. Soc. Perkin Trans*., 2001, **1**, 429.
32. M. Llombart, A. Poveda, E. Forner, C. F. Martos, C. Gaspar, M. Munoz, T. Olmos, A. Ruiz, V. Soriano, A. Benavides, M. Martin, E. Schlick, V. Guillem, *Invest. New Drugs*, 1992, **10**, 177.
33. P. LoRusso, L. Demchik, M. Dan, L. Polin, J. L. Gross, T. H. Corbett, *Invest. New Drugs*, 1995, **13**, 195.
34. C. P. Robinson, K. A. Robinson, J. Castaner, *Drugs Future*, 1996, **21**, 239.
35. M. F. Brana, J. M. Castellano, M. Moran, M. J. Perez de Vega, D. Perron, D. Conlon, P. Bousquet, C. A. Romerdahl, S. P. Robinson, *Anti-Cancer Drug Des*., 1996, **11**, 297.

CHAPTER 1

REVIEW OF LITERATURE

Heterocyclic moieties play important roles in synthetic organic chemistry due to its wide variety of applications in medicinal chemistry and pharmaceuticals. Being the structural analogue of purine, it is gaining attention due to its diverse pharmacological properties such as bronchodilatory, cyclic nucleotide phosphodiesterase inhibition, antiinflammatory, inotropic agent, hypoglycaemic, cardiac stimulating, uterine relaxant, antiulcer and antibronchospastic.

1.1. Imidazo[1,2-*a*]pyrazine

Demirayak *et. al.* reported the anticancer activities of compounds **1a-e** having excellent % inhibition against MCF-7, NCI-H460 and SF-268 cancer cell lines. Compound **1c** possessed excellent inhibition with MG-MID $\log_{10}GI_{50}$ value of -6.29 and was even found to be active than standard drug melphalan against leukemia with MG-MID $\log_{10}GI_{50}$ value of -5.09. Structure activity relationship around the synthesized compounds **1b-e** revealed that presence of 8-(4-chlorophenyl) ring was found to be responsible for anticancer effects.[1]

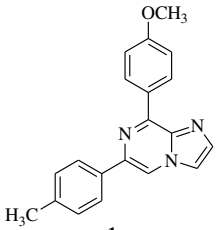

1a

$\log_{10}GI_{50}$ = -5.25

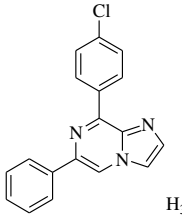

1b

$\log_{10}GI_{50}$ = -5.10

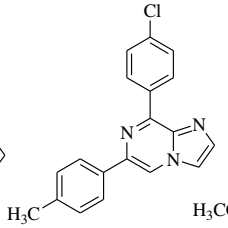

1c

$\log_{10}GI_{50}$ = -6.29

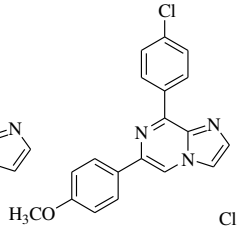

1d

$\log_{10}GI_{50}$ = -5.07

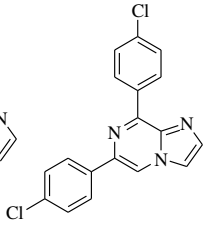

1e

$\log_{10}GI_{50}$ = -4.88

Later on Demirayak *et. al* synthesized 2,3,6,8-tetraarylimidazo[1,2-*a*]pyrazines that displayed potent anticancer activities against various cancer cell lines. Highest activity was found to be for compound **2b** against Central nervous system cancer (-4.62) and Breast cancer (-4.52). Mean

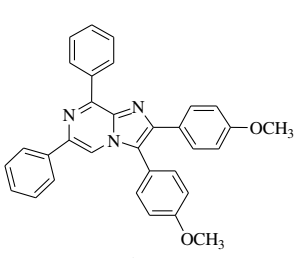

2a

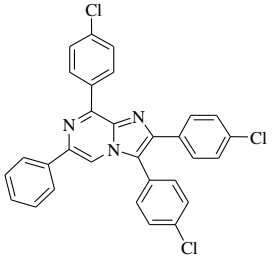

2b

graph midpoint (MG-MID) values of **2a** and **2b** were -4.08 and -4.42 respectively in comparison to standard drugs melphalan (-5.09) and cisplatin (-6.20).[2]

Bavetsias *et. al.* reported selective Aurora kinase A inhibitory activity of 3,6,8-trisubstituted imidazo[1,2-*a*]pyrazines. Unsubstituted C3 position **3d** (IC_{50} = 2.12 $\pm$ 0.63 μM) showed less activity than presence of methyl group **3e** (IC_{50} = 0.208 $\pm$ 0.052 μM) or halogen groups such as C3-Cl in **3a** (IC_{50} = 0.190 $\pm$ 0.138 μM) and C3-Br in **3b** (IC_{50} = 0.152 $\pm$ 0.090 μM). But, the presence of bis 3-pyridyl at C3 and C6 positions **3c** reduced the Aurora A inhibitory activity with IC_{50} value of 4.20 μM.[3]

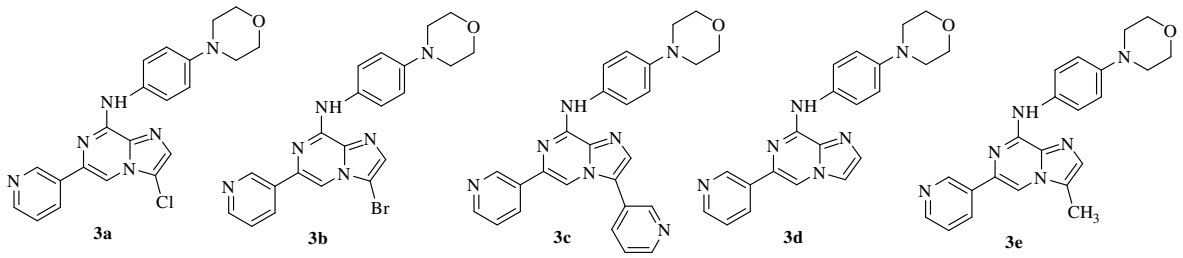

Belanger *et. al.* has reported the presence of CH_3 group at C6 position, 4-pyrazolyl at C3 position and isothiazole ring at C8 position as potent Aurora kinase inhibitors. Presence of polar groups on isothiazolyl ring at C8 position did not affect the cell potency but improved their aqueous solubility. So, this has led to the development of the amino-alcohol **4** (SCH 1473759) as a novel, picomolar inhibitor of Aurora kinases A (IC_{50} = 4 nM) and B (IC_{50} = 13 nM) with high intrinsic aqueous solubility (11 mM).[4]

Later Belanger and co-workers explored the substitution on the pyrazole nitrogen at C3 position of imidazo[1,2-*a*]pyrazine. Primary amide substitution at pyrazole nitrogen **5a** displayed 50 fold selectivity to Aurora kinase B inhibition (IC_{50} = 28 nM) over Aurora A. However, secondary amide substitutions **5b** and **5c** displayed 20 fold inhibitions to Aurora B with IC_{50}

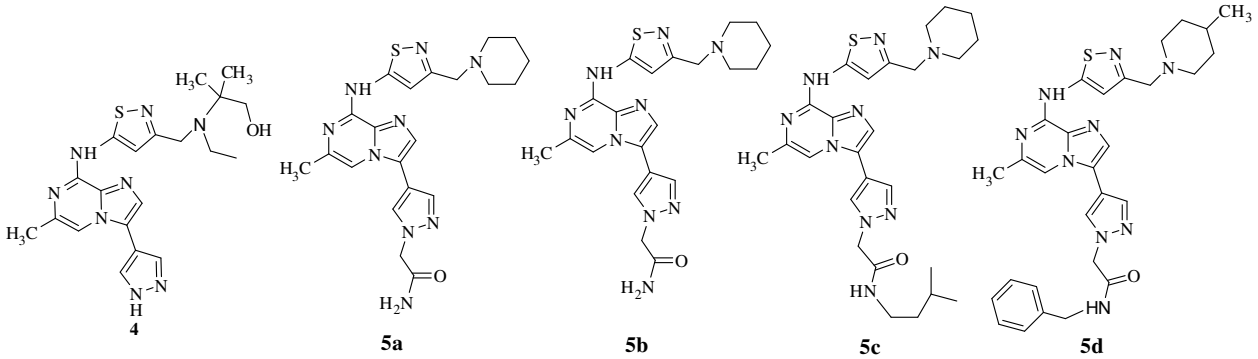

values of 193 nM and 44 nM respectively. However, benzyl amide analogue **5d** resulted in excellent Aurora kinase A (IC_{50} = 21 nM) and B (IC_{50} = 13 nM) inhibition with significant cell activity (EC_{50} = 129 nM).[5]

Incorporation of fluorine affects metabolism and physicochemical properties thereby impacting cell activity, oral absorption and exposure. Difluoroethyl **6** and trifluoroethyl **7** analogues had potent biochemical activity for both Aurora A (IC_{50} = 4 nM) and Aurora B (IC_{50} = 13 nM). Loss in cellular potency (**6**, phos HH3 = 306 nM, Rat PK = 0.28; **7**, phos HH3 = 198 nM, Rat PK = 0.86) is due to addition of fluorine atom that reduces the amine basicity but improved the oral PK (pharmacokinetics). Incorporation of deuterium **8** enabled 3 fold improvements in oral exposure in monkey (phos HH3 = 63 nM, Rat PK = 4.73).[6]

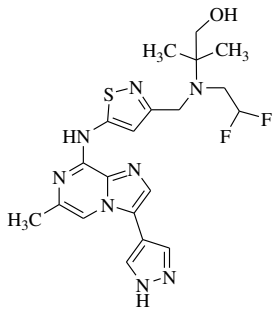

6

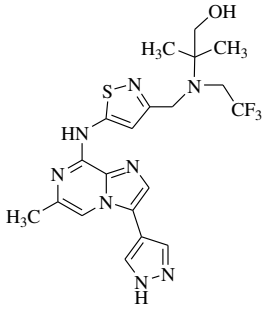

7

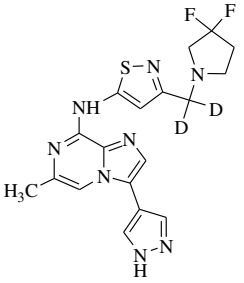

8

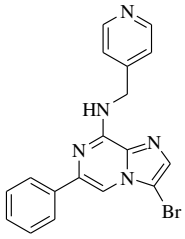

9

3,6,8-Trisubstituted imidazo[1,2-*a*]pyrazine **9** proved as a versatile template for ATP competitive kinase inhibitor as cyclin dependent kinase (CDK) inhibitor. Presence of Br at C3 position was necessary for activity as this analogue inhibited CDK with IC_{50} value of 0.44 μM. Compound **9** was also evaluated *in vitro* for the ability to alter uptake and incorporation of radioactive labelled thymine by living cells with IC_{50} value of 2 μM.[7,8]

Gonzalez *et. al.* reported the trisubstituted imidazo[1,2-*a*]pyrazines as phosphatidyl inositol 3 kinase (PI3K) inhibitor. Presence of methyl group **10a** at 2-position possessed significant inhibition against PI3K (IC_{50} = 0.096 μM). Incorporation of cyclopropyl group **10b** (IC_{50} = 0.340 μM), trifluoromethyl group **10c** (IC_{50} = 0.108 μM) and *N*-mesylpiperazine group **10d** (IC_{50} = 0.037 μM) at C2 position of imidazo[1,2-*a*]pyrazine paved a way for development of lead analogues with excellent inhibition activity. Presence of 3-hydroxy phenyl group is responsible for *in vitro* activity but has limited use for *in vivo* activity due to metabolic instability of this group. In order to overcome this problem, 3-hydroxy phenyl ring was isosterically replaced with

indazole **11** (IC_{50} = 0.095 μM) at C6 position of imidazo[1,2-*a*]pyrazine that gave an important advancement in discovery of imidazo[1,2-*a*]pyrazines as PI3K inhibitors.[9]

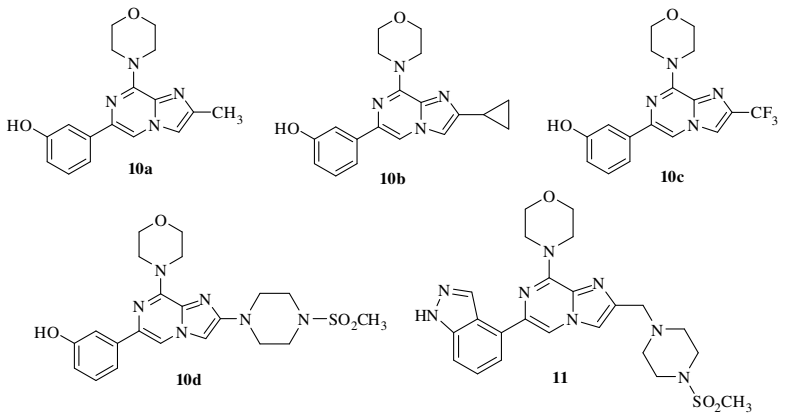

Imidazo[1,2-*a*]pyrazinamines acted as breast tumour kinase (Brk)/protein tyrosine kinase inhibitors which are important enzymes in signal transduction pathway in cancer. Substitution at C2 position **12** (IC_{50} = 1524 nM) and **13-15** (IC_{50} > 10,000 nM) resulted in substantial loss of inhibitory activity of Brk.[10]

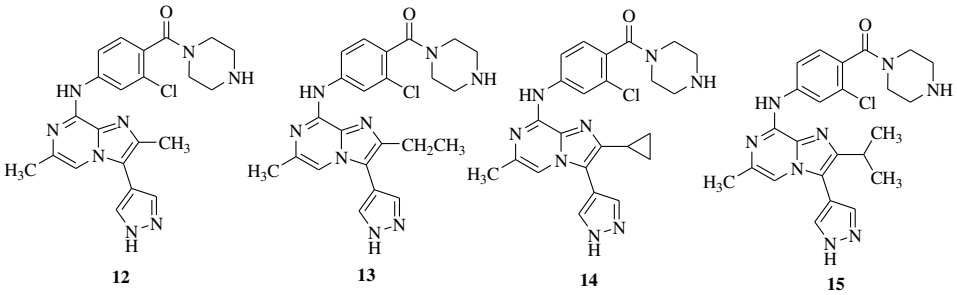

Kettle *et. al.* reported disubstituted imidazo[1,2-*a*]pyrazines based inhibitor of AKT kinase with improved potency and physiochemical properties. These compounds behaved as downstream biomarkers in *in vivo* and inhibited the tumor growth in breast cancer xenograft model. Compound **16** showed significant reduction of log D (1.3) value representing high solubility (2500 μM) and free level of drugs (37.1%). It also inhibited the phosphorylation of Thr308 on AKT in BT474 cells (IC_{50} = 0.386 μM) and Ser473 on AKT in MDMBA468 cells (IC_{50} = 0.365 μM).[11] 6,8-Disubstituted imidazo[1,2-*a*]pyrazines possessed potent activity against EphB4, responsible for inhibiting the formation of new blood vessels. Substitutions with 4-pyridyl at C8 position **17a** proved to be most potent with IC_{50} value of 0.062 μM in comparison to 3-pyridyl **17b** with IC_{50} value of 7.8 μM. It indicated the role of appropriate positioning of the pyridyl nitrogen atom for significant binding interaction with the protein.[12]

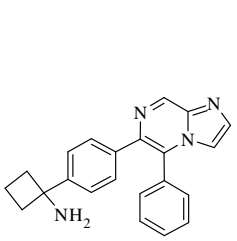

16

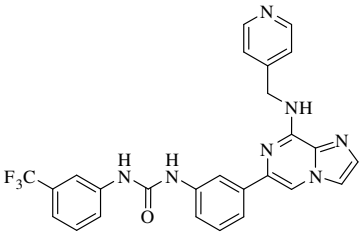

17a

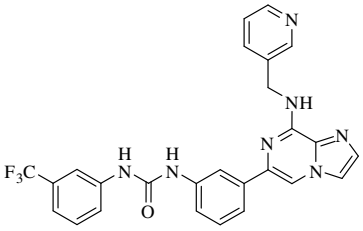

17b

Imidazo[1,2-*a*]pyrazines **18-20** with different substitutions at C2 and C3 positions, inhibited the human topoisomerase-II in DNA catenation, relaxation and intercalation. Clonogenic and MTT cell survival assay of kidney cancer cell (HEK-293) revealed that these compounds not only showed potent anticancer activity in comparison to standard drugs etoposide and 5-fluorouracil but also having low toxicity to normal cells.[13]

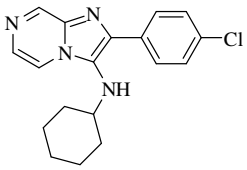

18

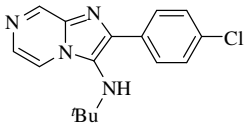

19

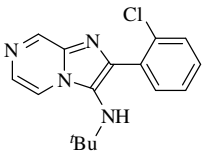

20

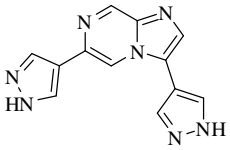

21a

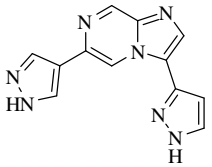

21b

3,6-Diheteroaryl imidazo[1,2-*a*]pyrazines **21a-b** have been evaluated as ATP competitive inhibitors of CHK1. SAR around diheteroaryl imidazo[1,2-*a*]pyrazine showed that bis-pyrazolyl analogues **21a** and **21b** inhibited the CHK1 potency in micromolar range (IC_{50} = 5.0 and 1.5 µM). These compounds also showed wide variety of activities against several other tyrosine kinases viz., ABL, FYN, LYN, LCK and SRC with > 94 % inhibition at 10 µM concentration.[14]

1.2. Coumarins

Coumarin is a fused heterocyclic moiety made of benzene and 2-pyrone ring. Coumarins being a member of flavonoid group of plant secondary metabolite, exhibited different biological activities which prompted the researchers to explore the pathways to target cancer *viz.,* kinase inhibition, cell cycle arrest, angiogenesis inhibition etc.

Reddy *et. al.* discovered amide functionality at C3 position as potent anticancer agents. Compound **22** acted as a potent inhibitor of cancer against breast cancer cell lines SkBr3 and BT474 (IC_{50} = 16.3-94 µM) and normal cells (Human lung fibroblasts).[15] Wells *et. al.* reported coumarin-pyrrolobenzodiazepines conjugate **23** having propylene linker that showed anticancer activity with IC_{50} value of 3.20 µM.[16]

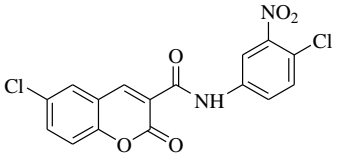

22

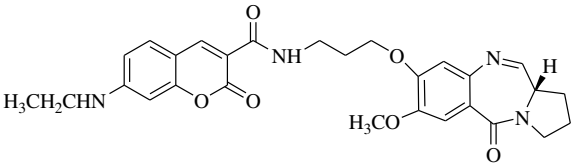

23

Mohareb and co-workers reported the evaluation of hydrazide-hydrazone derivatives of coumarin for anticancer activities against various cancer cell lines such as CNS cancer (SF268) and breast cancer (MCF7). The maximum inhibitory effect of compound **24** was exerted against non small cell lung cancer (NCIH460) with IC_{50} value of 10 μM.[17] Coumarins possessing 3-aryl moiety exhibited promising anticancer effects against KV, MCF7/ADR and nasopharyngeal (KB) cancer cell lines. Compound **25** bearing 7,8-diacetoxy substitutent showed excellent activity against KB cell line (IC_{50} = 5.18 μM) which revealed that presence of substituents at 7- and 8-positions with aryl moiety at C3 position was responsible for cytotoxic effects.[18]

Liu *et. al*. reported coumarin-pyrazoline derivative having thioacetyl moiety. This derivative showed potent antiproliferative activity in comparison to 5-fluorouracil against Bcap37, SGC7901, MGC803 and HepG2 cell lines. TRAP assay proved compound **26** having *n*-butylthio group as the potent inhibitor of telomerase with IC_{50} value of 0.92 $\pm$ 0.09 μM. Cellular proliferation was efficiently suppressed through cell cycle arrest in G_0/G_1 phase.[19]

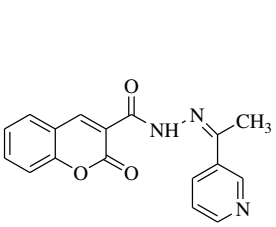

24

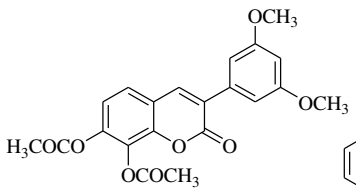

25

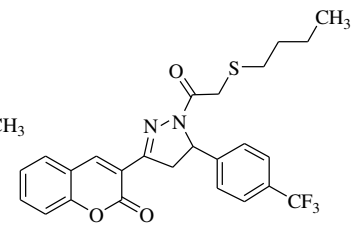

26

Dysregulation of various signal transduction pathways such as RAS/RAF/MEK pathways, resulted in cancer.[20] Various inhibitors blocking Raf pathway for cancer treatment have been tested in the clinical trials.[21] 3-Benzyl coumarin derivative **27** showed modest *in vitro* and *in vivo* potency as a selective RAF/Mek inhibitor. Presence of aniline moiety in **27** have disadvantages of metabolic instability and lower bioavailability. So replacement of aniline derivative with pyridinyl moiety bearing sulphonamide group **28** (RO5126766) gave a clinical candidate.[22-24] However, 6-fluoro coumarin derivative **29** proved to be a potent RAF/Mek inhibitor, having weak CYP inhibitory activity and excellent pharmacokinetic profile. It also showed good *in vitro*

and *in vivo* profile against HCT-116 cells with IC_{50} value of 8 nM and HCT-116 xenografts with ED_{50} value of 4.8 mg/kg respectively.[25]

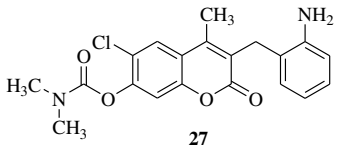

27

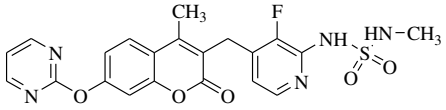

28 (RO5126766)

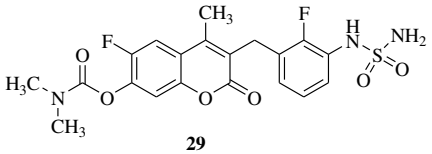

29

Basanagouda and co-workers reported 4-substituted coumarins as novel anticancer agents. Presence of 6-Cl or 7-Cl substituents on 4-iodophenoxy methyl coumarin **30** possessed excellent cytotoxic activity against MDA-MB human breast cancer cell line and human lung carcinoma cells (A549). SAR studies revealed that phenoxy moiety containing iodo group at 4-position was responsible for cytotoxic activity.[26,27] Previously, vitamin K and quinonoid derivatives were found to affect the cdc25 activity and cellular proliferation.[28] All three isoforms of cdc25 was inhibited by coumarin-quinone **31** (IC_{50} < 9 µM). *In vitro* cell viability assay showed potent antiproliferative activity against breast cancer cell lines viz., MDA-MB-231 and MCF-7 cells with IC_{50} value of < 11 µM vs. hTERT-HME1 with IC_{50} value of < 18 µM.[29] Puttaraju and co-workers synthesized dihydrobenzo[4,5]imidazo[1,2-*a*]pyrimidine-4-one-coumarin conjugate **32** as a cytotoxic agent against DAL cell line at 100 µg/ml concentration using trypan blue dye exclusion method.[30]

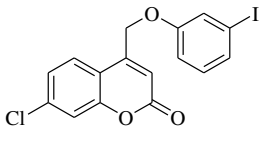

30

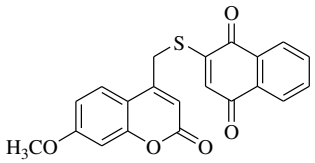

31

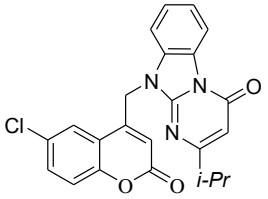

32

Various targets to control cancer cell progression include monocarboxylate transporter that act as lactate carrier. Literature study revealed that presence of monocarboxylate group was found to be responsible for lactate transport inhibition.[31] α-Cyano-4-hydroxy cinnamate **33** as a parent compound was first MCT inhibitor.[32] Substitution of *N*-methyl benzyl moiety at 7-position of coumarin **34** was found to be more potent inhibitor of MCT than the parent compound **33**.[33]

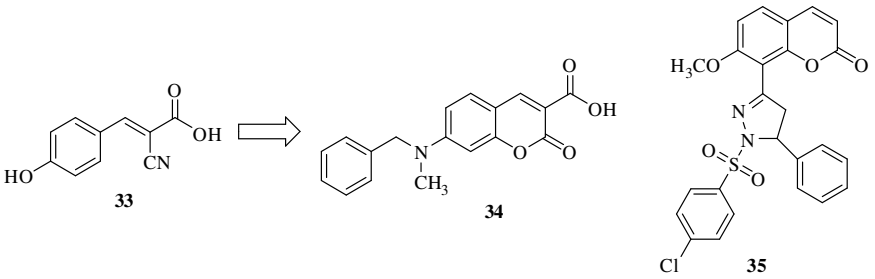

33 34 35

N-(4-Chlorophenylsulphonyl)pyrazoline derivative of coumarin **35** showed potent cytotoxic activity against HCT-116 cell line having IC_{50} value of 0.01 µM in comparison to standard drug doxorubicin with IC_{50} value of 0.63 µM. Presence of 4-Cl on phenylsulphonyl moiety at 8-position of coumarin was responsible of antitumor activity.[34] Chen *et. al.* reported the triphenylethylene-coumarin hybrids possessing aminoethoxy side chains that were evaluated for its anticancer activity against various cancer cell lines. Introduction of two aminoalkyl chains at 4- and 7-positions of coumarin **36a-c** showed promising anticancer activity against cancer cell lines with IC_{50} value of < 12.35 µM.[35] Literature reports revealed that 3,4-diphenyl coumarin moiety possessing appropriate aminoalkyl chains was responsible for cytotoxic activity. Later on, triphenylethylene-coumarin hybrids **37-38** possessing aminoethoxy side chains were synthesized that showed pronounced anticancer activities.[36]

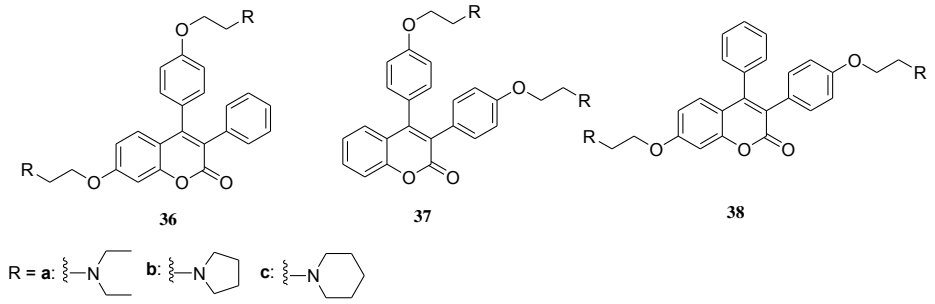

36 37 38

R = **a**: **b**: **c**:

Pingaew *et. al.* reported chalcone-coumarin hybrids **39** and **40** with 1,2,3-triazole linker being assessed for the anticancer activity against cancer cell lines viz., HepG2, A549, HuCCA1 and MOLT3. Reference drug etoposide showed lower activity in comparison to compounds against HepG2 cells. Good anticancer activity was observed with compound **40** against A549, HepG2 and huCCA1 cells with IC_{50} value of 4.81-8.18 µM. No toxicity was observed with normal vero cells.[37]

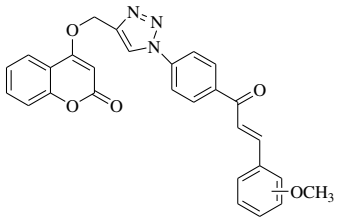

39

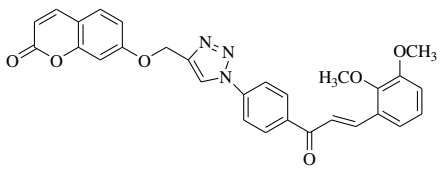

40

Coumarin-chalconoids hybrids **41** and **42** were reported to be Histone deacetylase (HDAC) inhibitor which is an important target for anticancer therapy.[38] Presence of 4-methoxy phenyl and 3,4-dimethoxy phenyl groups on coumarin moiety showed 20-50% inhibition of HDAC activity at 100 μM concentration.[39] Saidu and co-workers have synthesized biscoumarins having polysulfide linkage. Compound **43** was evaluated for antiproliferative activity against HCT-116 colorectal cells that induced cell cycle arrest in G2/M phase.[40]

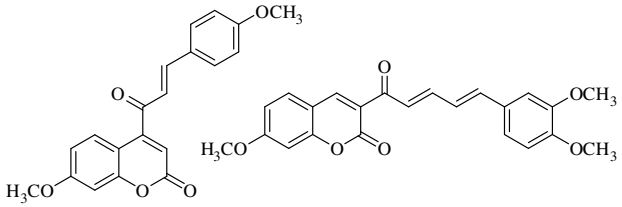

41

42

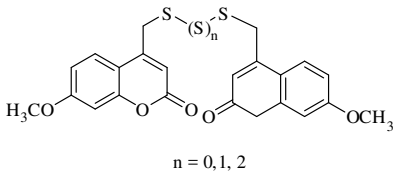

n = 0,1, 2

43

1.3. Benzimidazole

Benzimidazole is an important aromatic heterocyclic compound and acts as a pharmacophore in medicinal chemistry. Mebendazole was the first benzimidazole carbamate followed by flubendazole in humans. Benzimidazole is a key structure found in number of bioactive heterocyclic moieties. It has been formed from the fusion of benzimidazole and imidazole nucleus bearing different functional substituents. Various benzimidazoles and its derivatives exhibited remarkable anticancer/antiproliferative activity.[41,42]

Xiang and co-workers reported benzimidazole derivative **44** as potent antitumor agent through cytosolic vacuolization. Anticancer effect on various cancer cell lines HepG2 and HCT-116 cells was found to be moderate with IC_{50} values of 14.6 μM and 3.9 μM, respectively.[43] Gowda *et. al.* synthesized benzimidazole carboxylic acid derivative **45** as antileukaemic agent. It induced cell death of leukaemic cells with IC_{50} value of 3 μM. Presence of nitro and fluoride respective at 3- and 4- positions exhibited potent growth inhibition against cancer cells.[44] Omar and co-workers synthesized benzimidazoles **46** and **47** with respective acetate and allyl groups that exhibited

more anticancer activity than the standard drug. Presence of quinixalino benzodiazepine moiety at 2-position of benzimidazole resulted in potent anticancer activity. Introduction of allyl group showed significant increase in anticancer activity than presence of acetate group.[45]

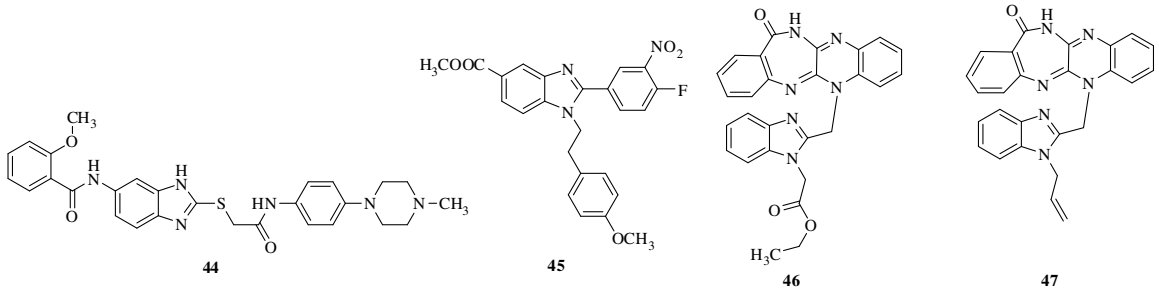

44 **45** **46** **47**

Liu and co-workers discovered that presence of hydrazone moiety in benzimidazole derivative displayed excellent inhibition against cancer cell lines in comparison to standard drugs 5-fluorouracil and SU11248. Introduction of various electron withdrawing groups like hydroxy at 2- and 4-positions of phenyl ring of hydrazone gave the potent derivatives **48** and **49** that displayed highest antitumor activities towards various cell lines like A549 (IC_{50} = 12.36 µM, 10.75 µM), HCT116 (IC_{50} = 4.86 µM, 8.33 µM), PC-9 (IC_{50} = 14.63 µM, 12.2 µM) and A375 (IC_{50} = 5.75 µM, 4.09 µM).[46] Karthikeyan *et. al.* reported benzimidazole carboxylic acid **50** with 3,4-dihydroxy substitutent at phenyl ring as anti-breast cancer agent. However, the substitution of acid group with methyl ester **51** having 2-hydroxy and 5-fluoro substituents showed superior anticancer activity towards breast cancer cell lines; MDA-MB-231 (IC_{50} = 6.23 µM for compound **51** vs 12.85 µM for compound **50**), MDA-MB-468 (IC_{50} = 4.09 µM for compound **51** vs 11.85 µM for compound **50**) and MCF-7 (IC_{50} = 0.18 µM for compound **51** vs 9.23 µM for compound **50**). Less potency of acid derivative is due to the ionization of free acid moiety to carboxylate ion in aqueous medium, thereby interfering with cellular permeability of compounds.[47]

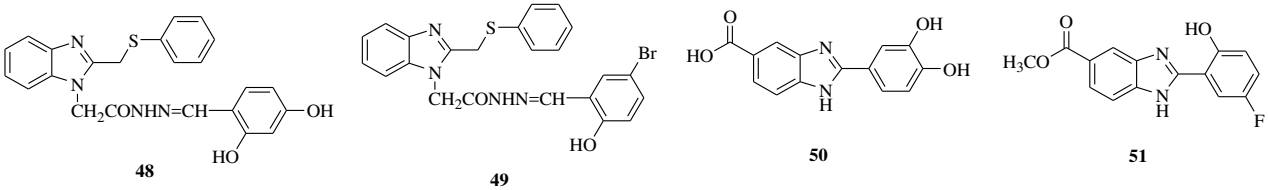

48 **49** **50** **51**

Yoon *et. al.* reported the synthesis of benzimidazole derivative **52** as antitumor agent through inhibition of sirtuin; SIRT1 and SIRT2 with IC_{50} values of 58.43 µM and 45.12 µM respectively. It also exhibited potent inhibitory activity against breast cancer cell lines. SAR studies revealed

that presence of electron donating dimethylamino group on phenyl ring at 2-position of benzimidazole gave potent sirtuin inhibition.[48] 1,2,3,4-Tetrahydro[1,2,4]triazino[4,5-*a*]benzimidazole **53** bearing aryl and heteroaryl substituents at 1-position enhanced the inhibition against MCF-7 with IC_{50} value of 0.039 µM. Presence of electron withdrawing chloro group at *o*-position of the phenyl ring enhanced *in vitro* activity against the cancer cells. In contrast, substitution with *meta* directing groups resulted in decrease in potency.[49]

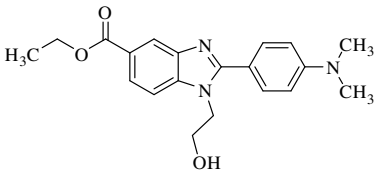

52

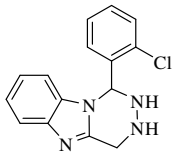

53

Tandon and co-workers reported bis-benzimidazoles as novel topoisomerse-I inhibitors. All derivatives **54a-d** displayed potent inhibitory effect on cancer cell lines. Compounds **54a-b** bearing dihalogenated groups on phenyl ring was found to be the more effective inhibitor (IC_{50} = 5.5 µM and 1.3 µM for MCF-7) than compounds **54c-d** respectively (IC_{50} = 5.3 µM and 16.8 µM for MCF-7) bearing dimethoxyphenyl and trimethoxy phenyl rings.[50]

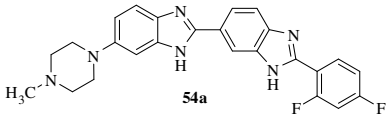

54a

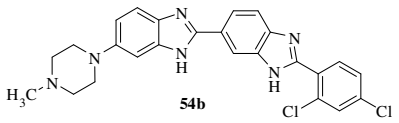

54b

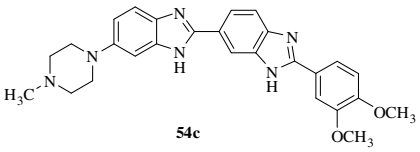

54c

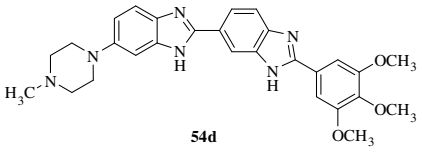

54d

Benzimidazole-1,3-diaminopropane complex with copper **55** intercalate with the base pairs of double helix DNA.[51] Complexes of benzimidazole with platinum **56**-**57** showed potent antiproliferative activity[52] against breast cancer cell line MCF-7 and Hela cervix cancer cell line.[53-57] Silver metal complex with 2-methyl benzimidazole carboxylic acid hydrazide **58** displayed potent cytotoxic activity against cancer cell lines with IC_{50} value of 2 µM.[58] 2-Pyridinyl benzimidazole-5-carboxylic acid complex with copper **59** exerted topoisomerase II inhibitory activity.[59]

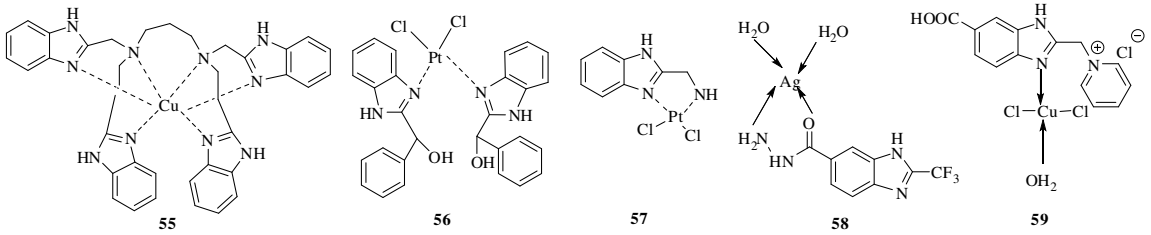

55 56 57 58 59

2-Methyl-5-nitrobenzimidazole containing thiadiazole ring **60** linked with methylene linker at 1-position was responsible for antitumor activity. Presence of nitro at 5-position of benzimidazole is critical for activity.[60] Ng *et. al.* reported 2,5,6-trihalogenated benzimidazole **61** as androgen receptor antagonists for treatment of prostate cancer. SAR revealed that presence of bromobenzyl ring at 1-position of benzimidazole is essential for activity.[61] Benzimidazole quinoline derivative **62** being planar in nature get inserted into space between DNA base pairs resulting in cleavage of DNA. It also exerted potent anticancer activity against cancer cell lines with IC_{50} value of 0.8-30 μM.[62]

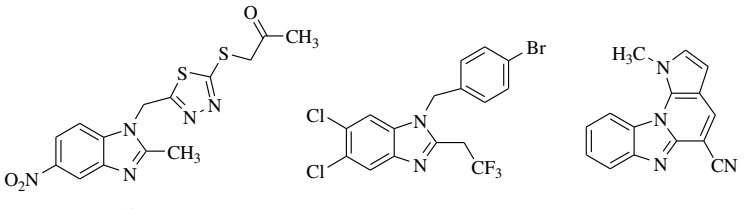

60 61 62

1.4. Naphthalimides

In general, naphthalimides are synthesized by the reaction of naphthalic anhydride with amine. Amongst them, 1,8-naphthalic anhydride exhibited potent anticancer activity against human and murine cells.[63] Presence of amino and nitro groups at 3- and 4-positions of naphthalic anhydride gave highly potent and active compounds, amonafide and mitonafide, respectively. 1,8-Naphthalimides has been used as dye and therapeutic agent. It has also been used for sensing of biologically relevant cations,[64-66] fluorescent bioprobes,[67] chemical probes [68] and laser dyes.[69] Naphthalimides has been used as probe to target the biomolecules and nucleic acids, thereby forming the intermolecular complex with mononucleotide. Due to the planar structure of the aromatic ring, naphthalimide has ability to act as a DNA intercalator which get intercalated itself between the base pairs of DNA. Molecules can bind to DNA through number of ways (i) minor groove binding, (ii) external binding (in case of stacking). UV-visible and fluorescence spectroscopic methods are generally used to observe binding behaviour of molecules with nucleic acids.

Amonafide and mitonafide are the two members belonging to naphthalimide class that have entered into the phase II clinical trials. Excellent antitumor activity was observed against Hela cancer cell line with IC_{50} values of 0.47 μM and 8.80 μM for amonafide and mitonafide respectively.[70] The dihydrochloride salt of Amonafide (Quinamd) manufactured by Chem Genex has been used for treatment of prostate cancer and has entered into phase II clinical trials. Heat denaturation study showed that it stabilized the double stranded DNA.[71] Protein-DNA crosslinking in cultured cells and DNA strand breaks were induced.[72] Unwinding of closed circular DNA by mitonafide resulted in increase in viscosity of sonicated DNA.[73] Both amonafide and mitonafide act through DNA intercalation. Nafidime, another derivative of naphthalimide has been used to inhibit proliferation in animal tumors *in vitro* and *in vivo*.[70] Agarose gel electrophoresis revealed its binding to DNA via intercalation. It also act as a topoisomerase II inhibitor.[72a]

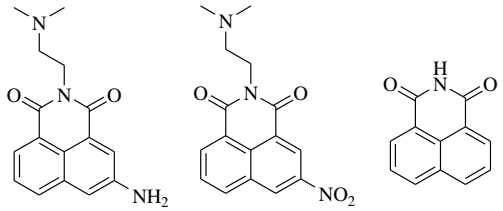

Amonafide **Mitonafide** **Nafidimide**

Bisnaphthalimide **63** in which two naphthalimide moieties are joined by polyamine spacer to increase DNA binding and anticancer activity. It is known to be a bisintercalator due to its ability to unwind the DNA resulting in alteration of closed circular plasmid DNA viscosity and thereby binding to major groove of DNA.[74] Gallego and co-workers using molecular dynamics and NMR spectroscopic techniques that revealed compound **63** bisintercalate itself at TpG and CpA steps in hexameric $d(ATGCAT)_2$ sequence.[75] NMR spectroscopy showed that **63** bind with DNA through two step interaction having dissociation rates of 10^{-2} s^{-1} and 1-4 s^{-1}.[76]

Chen *et. al.* reported bisnaphthalimide **64** as potent antitumor agent against leukaemia and solid tumours *in vivo*.[77a] DNA and RNA biosynthesis was effectively inhibited by **64**, by interfering with incorporation of uridine and thymidine, thereby inducing the single stranded DNA breaks.[77b] Moreover, it also acts as eukaryotic topoisomerase II poison, thereby stabilizing the cleavage complex of topo-II with DNA, causing cell death.[77c]

Compound **65** bearing naphthalimide and phenanthrene moieties was evaluated *in vitro* DNA binding studies using ethidium bromide displacement assay which revealed it to be a effective

DNA binder. Introduction of any electron donating and withdrawing substituents at 6-position of phenanthrene ring did not show any effect in DNA binding. In addition, it also exhibited excellent inhibition against L1210 cancer cell line with IC_{50} value of 0.035 μM.[78]

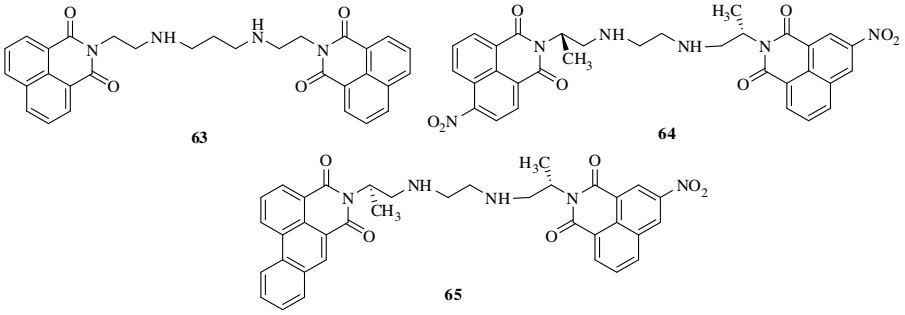

63 **64** **65**

Gunnlaugsson and co-workers reported bisnaphthalimides for DNA targeting linked through Troger moiety.[79] Compounds **66**-**67** bearing terminal nitrogen at the side chain were protonated at physiological pH which resulted in increased water solubility and also favouring the electrostatic interactions with negatively charged phosphate backbone of DNA. These compounds bind to ct-DNA with high affinity (~ 10^6 M^{-1}). Thermal denaturation studies also stabilize the ct-DNA (Δ T_m > 15 ^oC).[80] Naphthalimidobenzamido derivatives **68a-b** were analyzed for interactions with DNA sequences using ethidium bromide displacement assay.[81]

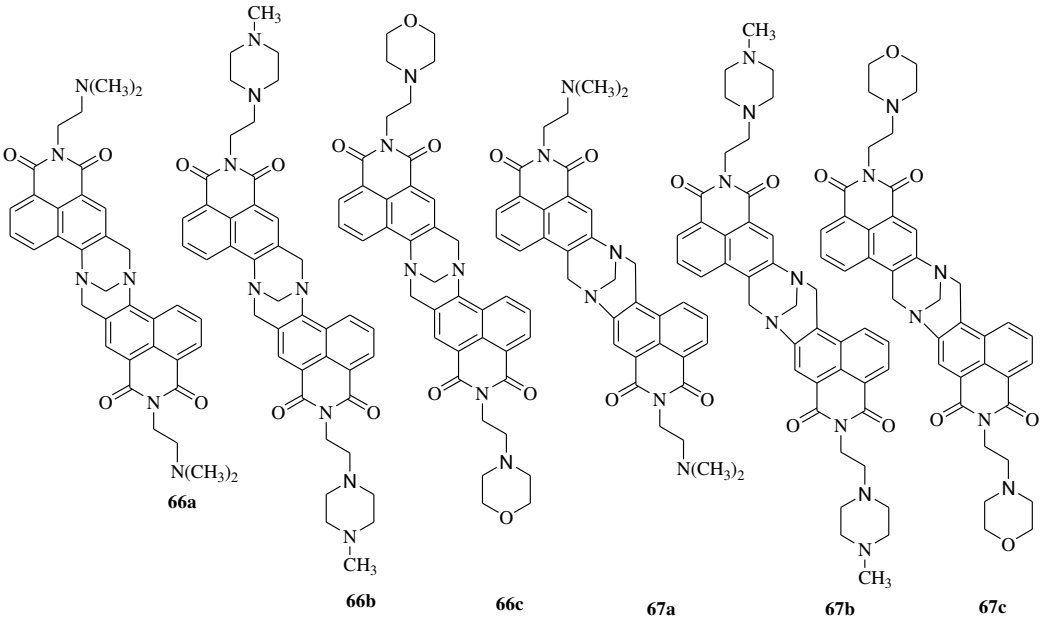

66a **66b** **66c** **67a** **67b** **67c**

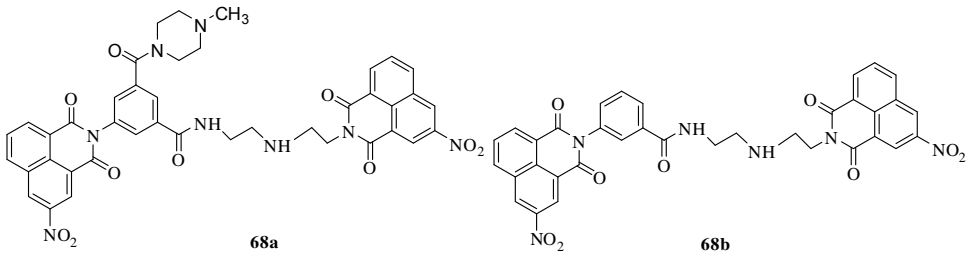

68a **68b**

Keeping in mind for undesirable toxicity of naphthalimide derivatives and to improve the therapeutic index, naphthalimide based pro drugs **69**-**72** bearing *N*-oxide moiety at the terminal side chain have been synthesized.[82] All compounds showed lower affinity towards double stranded DNA as compared to amine due to absence of protonated side chain in the ligand, thereby favouring electrostatic binding with DNA. Li *et. al.* synthesized 1,8-naphthalimide analogues **73**,**74** bearing 2-aminothiazole moiety,[83] being extensively used in parkinsonism while moderate affinity towards ct-DNA was observed (10^4 M^{-1}). Compound **74** with linear heterocyclic fused chromophore was found to be good intercalator than compound **73** with angular chromophore.

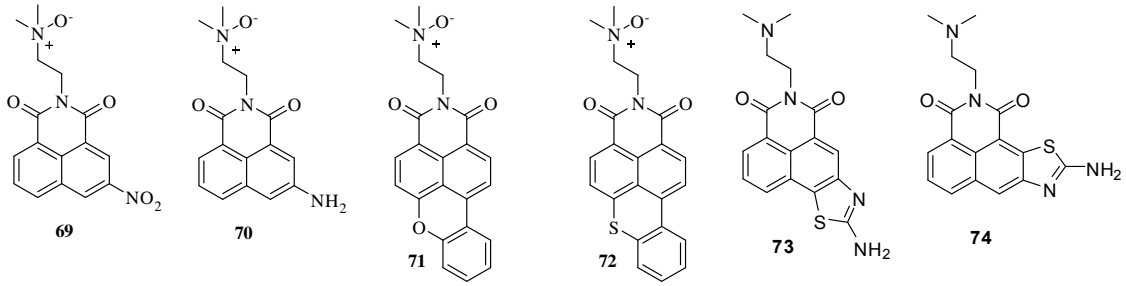

69 **70** **71** **72** **73** **74**

Qian *et. al.* reported naphthalimide based derivatives **75**,**76** linked to amino acid leucine to overcome the poor solubility and to enhance the cellular uptake.[84] These compounds bind to DNA via intercalation, determined by increase in viscosity. Binding of these analogues to DNA was moderate (10^4 M^{-1}). Additionally, these have been found to be cytotoxic to tumor cells and showed strong interaction with bovine serum albumin.

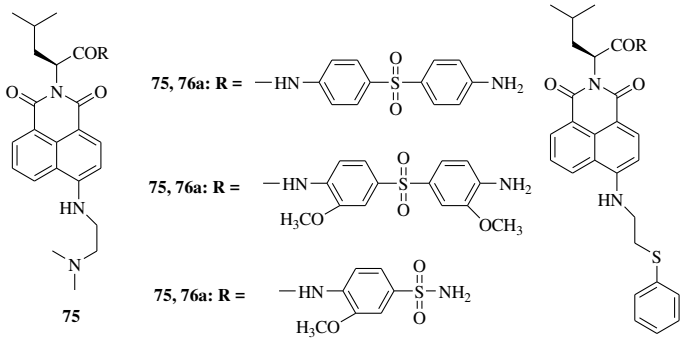

75 **75, 76a: R =** **75, 76a: R =** **75, 76a: R =**

CHAPTER 2

ARYLATED IMIDAZO[1,2-*a*]PYRAZINE DERIVATIVES

2.1. INTRODUCTION

Fused heterocyclic molecular frameworks are found in a large number of biologically active natural and synthetic components.[85] Halogenated heteroaromatic ring systems are valuable monomers because of their ability to participate in cross-couplings including the Heck, Stille and Suzuki reactions.[86] Several procedures for transition-metal-catalyzed by direct C-C functionalization of imidazoazines have been developed, notably in the imidazo[1,2-*a*]pyridine[87] and imidazo[1,2-*a*]pyrimidine[88] series. Imidazo[1,2-*a*]pyrazine, a bicyclic *N*-fused imidazole and pyrazine ring, is a privileged structural motif present in several natural products and pharmacological relevant structures with wide ranges of activities such as Aurora kinase inhibitors,[89] hypoglycaemic,[90] cyclic nucleotide phosphodiesterase inhibition,[91] antiulcer,[92] anticancer[93] and controlling allergic reactions.[94]

A variety of classical methods has been developed for the functionalizations of imidazo[1,2-*a*]pyrazine *viz.,* arylation of 8-methoxy or 8-methylthio-6-bromo-imidazo[1,2-*a*]pyrazines,[95] 3-aryl/alkylamino and 2-aryl/alkyl substituted imidazo[1,2-*a*]pyrazines,[96] through palladium catalyzed cross-coupling reactions (Figure 1). But, imidazo[1,2-*a*]pyrazine series remains almost unexplored for palladium catalyzed direct C-C monoarylation at C8 and diarylation at C6 and C8 positions.

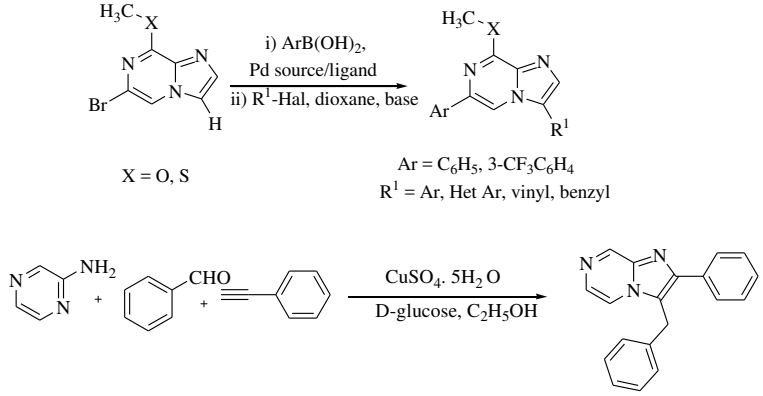

Figure 1 Synthesis of 2,3-diarylated imidazo[1,2-*a*]pyrazine

2.2. OBJECTIVE

Herein, we reported monoarylation at C8 position and symmetrical/unsymmetrical diarylation at C6 and C8 positions of imidazo[1,2-*a*]pyrazine, catalyzed by palladium with and without ligands. The synthesized compounds were then evaluated for 60 human cancer cell lines for their anticancer activities. Structure activity relationship (SAR) as anticancer agents in order to determine the activity profile of the synthesized derivatives has also been discussed.

2.3. CHEMISTRY

To obtain intermediate 6,8-dibromo-imidazo[1,2-*a*]pyrazine, we have used readily available starting material 2-aminopyrazine **1**. Bromination of **1** with *N*-bromosuccinamide (NBS) in DMSO and water at room temperature for 6 h gave 2-amino-3,5-dibromopyrazine **2**[97] in 90% yield followed by cyclization with 50% aqueous solution of chloroacetaldehyde to obtain 6,8-dibromo-imidazo[1,2-*a*]pyrazine **3** in 80% yield (Scheme 1).

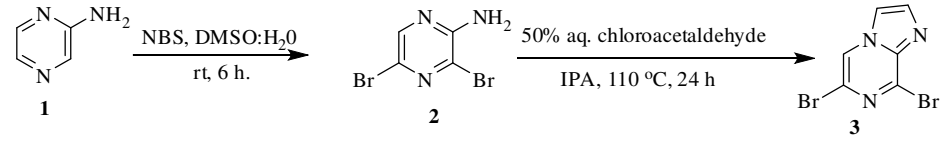

Scheme 1: Synthesis of 6,8-dibromo-imidazo[1,2-*a*]pyrazine.

Palladium catalyzed Suzuki-Miyaura coupling of 6,8-dibromo-imidazo[1,2-*a*]pyrazine **3** with different aryl boronic acids afforded substituted monoarylated and symmetrical diarylated products. Thiophen-2-boronic acid served as a model reactant for optimization of the reaction conditions as thiophene moiety is considered a structural alert in drug design and discovery. Thiophene and thienyl core have attracted the attention of the scientific community due to their therapeutic uses as anti HIV,[98] antitubercular,[99] antimicrobial,[100] tyrosine kinase inhibitor[101] and anticancer agents.[102]

Suzuki-Miyaura coupling reaction between 6,8-dibromo-imidazo[1,2-*a*]pyrazine **3** and thiophen-2-boronic acid with different palladium catalysts like $Pd(PPh_3)_4$, $Pd(PPh_3)_2Cl_2$ and $Pd_2(dba)_3$ has been performed. $Pd(PPh_3)_4$ proved as an effective catalyst for monoarylated and diarylated products, giving 70% and 10% yields, respectively (Table 1, entries 1-3). A survey of different bases (Cs_2CO_3, Na_2CO_3, K_2CO_3 and DIPEA) revealed that Cs_2CO_3 was found to be the

best choice (Table-1, entries 3-6). Recent developments have been carried out in Suzuki–Miyaura coupling by employing ligandless palladium catalysts and employing phase-transfer

Table 1 Optimization of palladium catalyzed Suzuki-Miyaura coupling

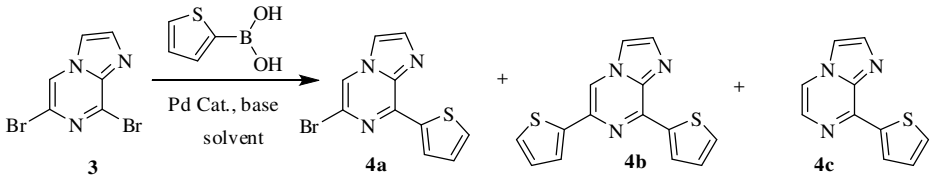

Entry	Time (h)	Catalyst /Ligand	Base	Solvent	Yield (%)[a] 4a/4b/4c
1	12	$Pd(PPh_3)_2Cl_2$	Cs_2CO_3	MeCN:H_2O	30/10/0
2	12	$Pd_2(dba)_3$	Cs_2CO_3	MeCN:H_2O	43/7/0
3	**8**	**$Pd(PPh_3)_4$**	**Cs_2CO_3**	**MeCN:H_2O**	**70/10/0**
4	10	$Pd(PPh_3)_4$	Na_2CO_3	MeCN:H_2O	62/11/0
5	12	$Pd(PPh_3)_4$	K_2CO_3	MeCN:H_2O	60/15/0
6	12	$Pd(PPh_3)_4$	DIPEA	MeCN:H_2O	54/10/0
7	18	$Pd(PPh_3)_4$	Na_2CO_3	Toluene:H_2O	45/5/0
8	19	$Pd(PPh_3)_4$	K_2CO_3	Toluene:H_2O	36/13/0
9	18	$Pd(PPh_3)_4$	DIPEA	Toluene:H_2O	15/0/0
10	12	$Pd(PPh_3)_4$	Cs_2CO_3	Toluene:H_2O	20/10/0
11	19	$Pd(PPh_3)_4$	Cs_2CO_3	THF:H_2O	55/0/0
12	10	$Pd(PPh_3)_4$	K_2CO_3	Acetone	52/15/0
13	10	$Pd(PPh_3)_4$	Cs_2CO_3	DMF	52/0/0
14	15	$Pd(PPh_3)_4$	Cs_2CO_3	1,4-dioxane	44/0/0
15	14	$Pd(PPh_3)_2Cl_2$	Na_2CO_3	MeCN:H_2O	52/7/0
16	14	$Pd(PPh_3)_2Cl_2$	K_2CO_3	MeCN:H_2O	50/5/0
17	15	$Pd(PPh_3)_2Cl_2$	DIPEA	MeCN:H_2O	38/10/0
18	12	$Pd_2(dba)_3$	Na_2CO_3	MeCN:H_2O	43/0/0
19	12	$Pd_2(dba)_3$	K_2CO_3	MeCN:H_2O	65/0/0
20	12	$Pd_2(dba)_3$	DIPEA	MeCN:H_2O	45/0/0
21	20	$Pd(PPh_3)_4$	Cs_2CO_3	MeCN	30/15/0
22	12	$Pd(PPh_3)_4$	Na_2CO_3	IPA	0/0/45
23	8	$Pd(PPh_3)_4$	K_2CO_3	IPA	0/0/55
24	12	$Pd(PPh_3)_4$	Cs_2CO_3	IPA	30/0/60
25	11	$Pd(PPh_3)_4$ + XantPhos	K_2CO_3	MeCN:H_2O	62/10/0
26	10	$Pd(PPh_3)_4$ + JohnPhos	K_2CO_3	MeCN:H_2O	65/0/0
27	10	$Pd(PPh_3)_4$ + Cyclohexyl John Phos	K_2CO_3	MeCN:H_2O	61/5/0
28	9	$Pd(PPh_3)_4$ + BINAP	K_2CO_3	MeCN:H_2O	59/0/0
29	12	$Pd(PPh_3)_4$ + PPh_3	K_2CO_3	MeCN:H_2O	53/0/0

Reaction conditions: 1.0 eq. thiophen-2-boronic acid, 5 mol% catalyst, 5 mol% ligand, 1.0 eq. base, solvent:cosolvent (9:1), reflux, 8-20 h; [a]isolated yields

catalysis or mixture of organic solvents along with water as cosolvent.[103] Use of water is suitable in this coupling reactions as boronic acids are stable in aqueous conditions. Its ability to dissolve

various bases helps in activating boronic acids and enhancing the rate of reaction.[104] The effect of different solvents were also studied and observed that the reaction proceed in both protic and aprotic solvents although significant variations in yields were noticed. The nonpolar aprotic solvents such as MeCN:H_2O (Table 1, entries 1-6 and 15-20), THF:H_2O (Table 1, entry 11) and acetone (Table 1, entry 12) were found to be the most effective solvents and gave excellent results. On the other hand, lower yield was also obtained in the absence of water (Table 1, entry 21). Polar protic solvents like isopropyl alcohol (IPA) with Cs_2CO_3 gave very interesting results as there was formation of 8-thiophen-2-yl-imidazo[1,2-*a*]pyrazine **4c** in 60% yield along with 6-bromo-8-thiophen-2-yl-imidazo[1,2-*a*]pyrazine **4a** in 30% yield due to dehalogenation and C-C coupling, respectively but with K_2CO_3 in IPA gave only 8-thiophen-2-yl-imidazo[1,2-a]pyrazine **4c** in 55% yield (Table 1, entries 22-24). Mixture of acetonitrile and water (9:1) proved to be the best solvent for this transformation. Reaction conditions were also optimized by using Pd catalyst in the presence of different ligands. Use of ligands XantPhos, JohnPhos, Cyclohexyl John Phos, BINAP and PPh_3 (Table 1, entries 25-29), neither improved the yields of diarylated product nor monoarylated product.

Further, by using 1.5 equivalents of thiophen-2-boronic acid in the same ratio of Cs_2CO_3, there was not much variation in monosubstituted and disubstituted products. But by using 2.0 eq. of boronic acid, monosubstituted and disubstituted products were formed in 28% and 54% yields respectively. When 3.0 eq. of boronic acid was used, predominantly disubstituted product was formed with monosubstituted product only in traces (Table 2).

Table 2 Reactions of 6,8-dibromo-imidazo[1,2-*a*]pyrazine with equivalences of boronic acid.

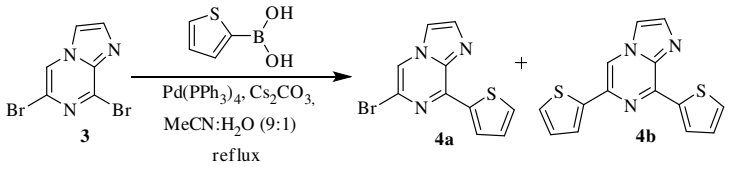

Entry	Thiophen-2-boronic acid (eq.)	Cs_2CO_3	Yield (%)	
			4a	**4b**
1	1.0	1.0	70	10
2	1.5	1.5	65	20
3	2.0	2.0	28	54
4	2.5	2.5	20	60
5	3.0	3.0	traces	90

Table 3 Reactions of 6,8-dibromo-imidazo[1,2-*a*]pyrazine with different boronic acids.

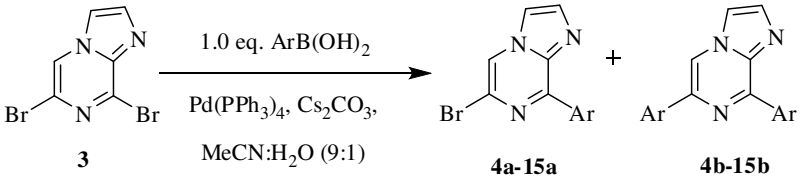

3 **4a-15a** **4b-15b**

Entry	Time (h)	Ar	Products (%)[a]		Yields (%)	
					a	**b**
1	8	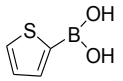	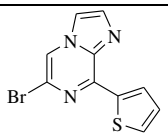	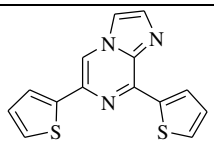	**4a** (70)	**4b** (10)
2	12	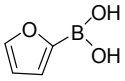	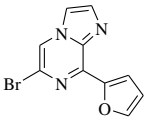	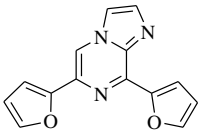	**5a** (56)	**5b** (12)
3	10	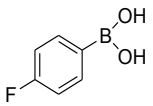	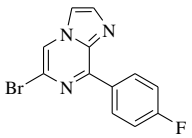	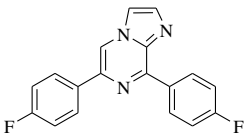	**6a** (52)	**6b** (25)
4	8	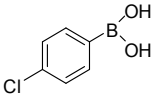	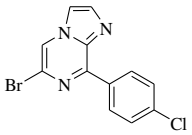	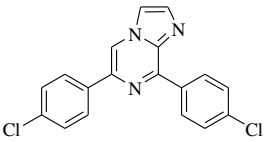	**7a** (70)	**7b** (16)
5	8	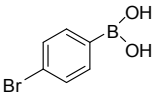	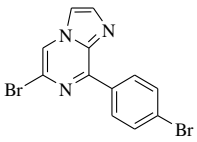	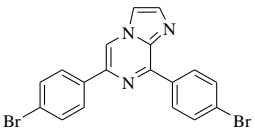	**8a** (68)	**8b** (20)
6	8	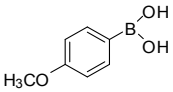	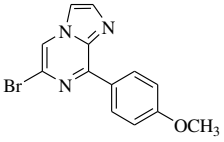	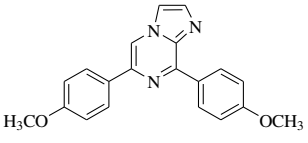	**9a** (69)	**9b** (14)
7	7	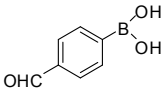	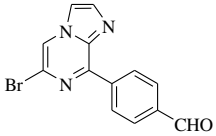	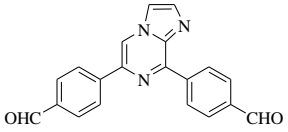	**10a** (70)	**10b** (15)
8	8	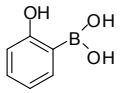	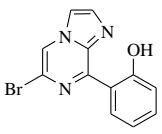	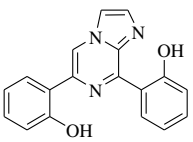	**11a** (57)	**11b** (30)

9	10	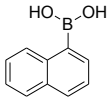	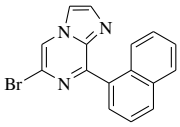	---	**12a** (64)	--
10	10	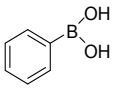	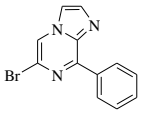	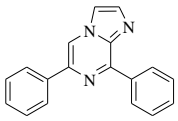	**13a** (50)[b]	**13b** (20)[b]
11	10	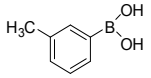	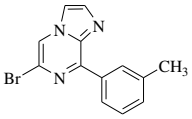	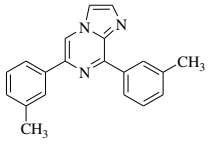	**14a** (53)[b]	**14b** (10)[b]
12	11	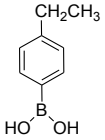	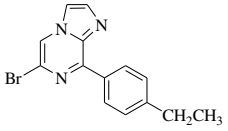	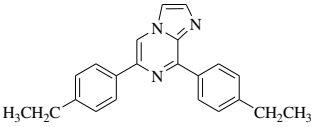	**15a** (65)[b]	**15b** (13)[b]

[a] isolated yields, [b] GC-MS yields.

With the optimized reaction conditions in hand, we have used 1.0 equivalent of thiophen-2-boronic acid, 5 mol% of $Pd(PPh_3)_4$, Cs_2CO_3 (1 eq.) in MeCN:H_2O (9:1) and evaluated the scope of arylation with variety of aryl boronic acids providing a library of monosubstituted **4a-15a** and disubstituted **4b-15b** imidazo[1,2-*a*]pyrazines (Table 3). Electron withdrawing as well as electron donating substituents on aryl boronic acids was well tolerated. The reaction worked well with thiophen-2-boronic acid, furan-2-boronic acid, 4-fluoro, 4-chloro, 4-bromo, 4-methoxy, 4-formyl and 2-hydroxyphenyl boronic acids and good yields of monoarylated and diarylated products were obtained (Table 3, entries 1-8). Among halides, 4-chloro and 4-bromo gave higher yields of monoarylated products as compared to 4-fluoro analogue. Structures of all novel compounds were confirmed by NMR as well as mass spectrometry techniques. Structure of compound **9b** was also confirmed by X-ray crystallography (Figure 2).[105]

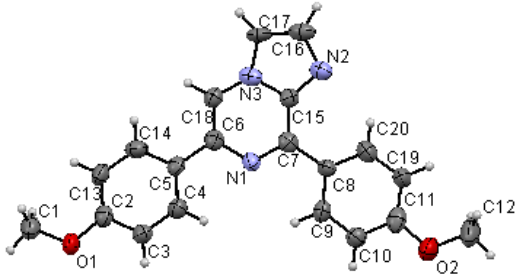

Figure 2 X-ray structure of **9b** (CCDC No. 960038).

In case of napthalen-1-boronic acids, only monoarylated product at C8 position was formed in 64% yield and arylation at C6 position was not obtained (Table 3, entry 9). This is due to the steric hinderance of bulky naphthyl ring at C8 position of imidazo[1,2-*a*]pyrazine. In case of phenyl boronic acid, 3-methylphenyl boronic acid and 4-ethylphenyl boronic acid, monoaryl and diaryl substituted imidazo[1,2-*a*]pyrazine could not be isolated in pure form, but were confirmed by NMR and GCMS (Table 3, entries 10-12).

We took advantage of the monoarylated products to implement an additional cross-coupling reaction which aimed at providing straightforward access to unsymmetrical imidazo[1,2-*a*]pyrazine. Thus, reactions of C8 monosubstituted imidazo[1,2-*a*]pyrazines were carried out with 1.0 equivalent of boronic acids in the presence of $Pd(PPh_3)_4$, Cs_2CO_3 in MeCN:H_2O, gave unsymmetrical diarylated imidazo[1,2-*a*]pyrazines. Monoarylation at C8 position were confirmed by considering 2D NOE difference experiments (Figure 3) that showed negative NOE signal of singlet of C5H proton of imidazo[1,2-*a*]pyrazine and doublet of C2'H of 4-formylphenyl **(10a)**. In unsymmetrical diarylation, substitution of 4-formylphenyl at C8 and 2-thiophene at C6 positions **(25)** were also confirmed by 2D NOE experiment (positive NOE's signal of singlet of C5H proton of imidazo[1,2-*a*]pyrazine with doublet of thiophene and negative NOEs signals of singlet of C5H proton of imidazo[1,2-*a*]pyrazine and doublet of C2'H of 4-formylphenyl. 4-Fluoro, 4-chloro, 4-methoxy and 4-formylphenyl imidazo[1,2-*a*]pyrazine derivatives were employed with thiophen-2-boronic acid, furan-2-boronic acid, 4-methoxy, 2-hydroxy, 4-formyl, 4-chloro and 4-fluorophenyl boronic acids to form the corresponding unsymmetrical imidazo[1,2-*a*]pyrazines (**16-30**) in 50-85% yields (Table 4). The reaction of monosubstituted 4-methoxyphenyl derivative was slow and only traces of desired product was observed when naphthalen-1-boronic acid was reacted under same reaction conditions. Structure of compound **20** was also confirmed by measuring X-ray crystallography (Figure 4).[105]

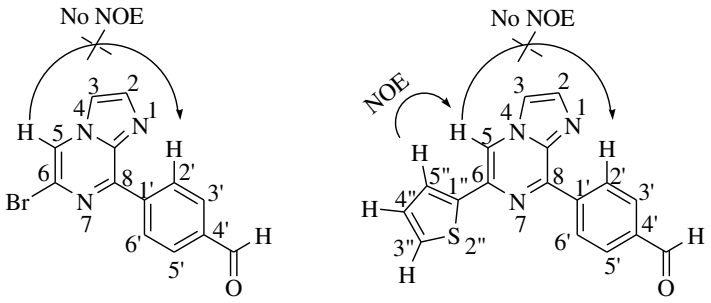

Figure 3 2D NOEs ^1H, ^1H correlations used for structural assignment of compounds **10a** and **25.**

Table 4 Reactions of 8-aryl-6-bromo-imidazo[1,2-*a*]pyrazines with aryl boronic acids

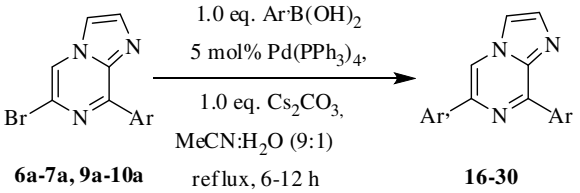

6a-7a, 9a-10a **16-30**

Entry	Time (h)	Monoarylated Imidazopyrazine	Ar'B(OH)$_2$	Product	Yield (%)	mp (^{0}C)
1	6	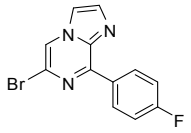	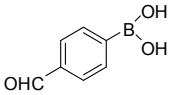	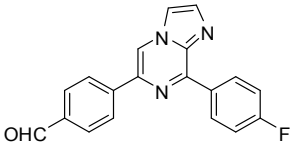	(**16**) 82	208-210
2	7	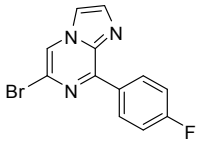	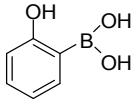	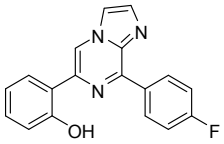	(**17**) 80	158-160
3	6	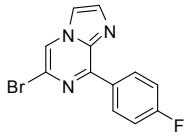	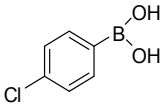	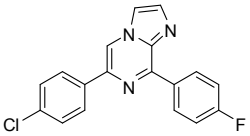	(**18**) 62	136-138
4	9	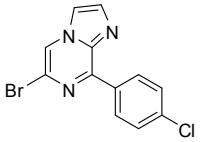	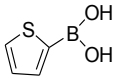	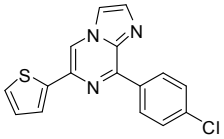	(**19**) 70	135-137
5	8	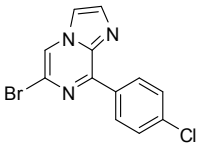	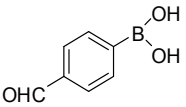	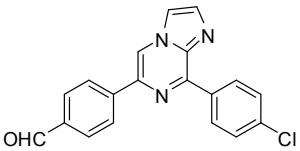	(**20**) 65	204-207
6	8	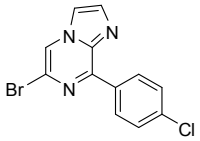	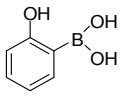	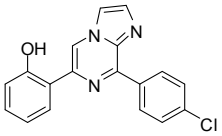	(**21**) 68	172-174
7	10	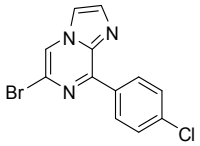	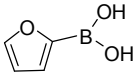	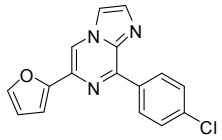	(**22**) 72	159-161

8	7	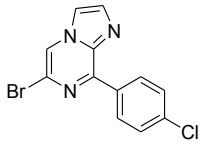	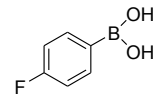	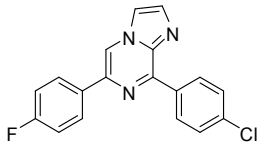	(**23**) 70	134-135
9	7	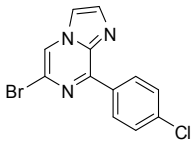	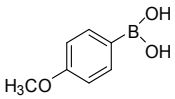	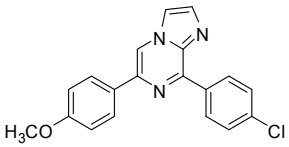	(**24**) 74	115-117
10	9	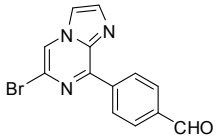	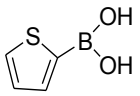	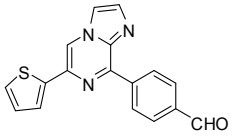	(**25**) 52	165-167
11	7	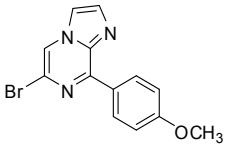	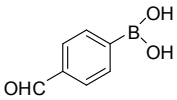	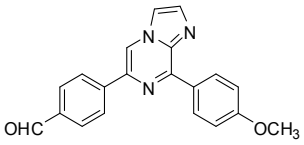	(**26**) 85	190-192
12	7	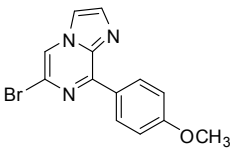	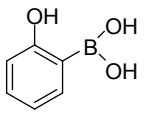	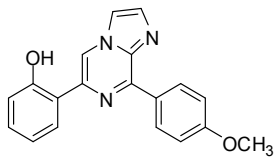	(**27**) 75	125-127
13	10	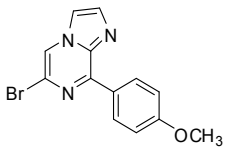	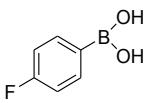	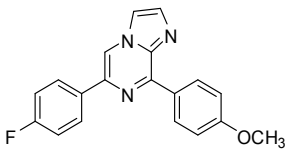	(**28**) 68	108-110
14	10	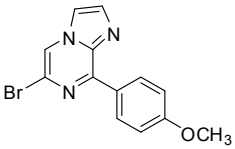	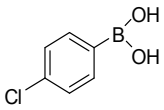	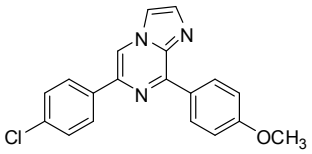	(**29**) 76	119-121
15	12	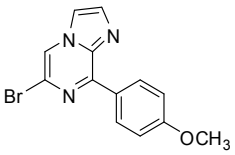	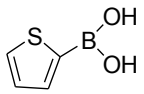	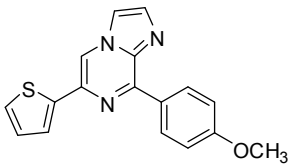	(**30**) 70	120-122

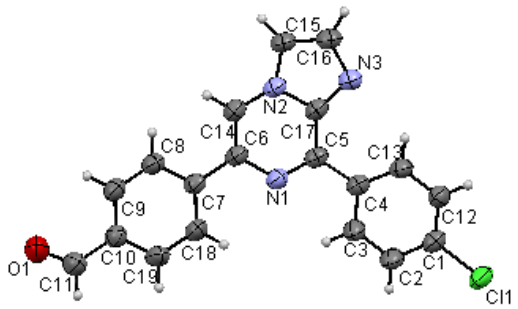

Figure 4 X-ray structure of **20** (CCDC No. 960039)

2.4. *IN VITRO* ANTICANCER SCREENING

Preliminary anticancer activity revealed that monoarylated, symmetrical diarylated compounds **(4a-b, 5a-b, 7a, 8a-b, 9a-b, 11a-b** and **13b)** and unsymmetrical diarylated compounds **(18-19, 21-23, 27-28** and **30)** were selected by National Cancer Institute, Bethesda, Maryland, USA on the basis of structure variation for evaluation of anticancer activity. The selected compounds were subjected to *in vitro* anticancer assay against tumor cells in a full panel of 60-cell lines at single dose concentration of 10 μM, and the percentages of growth inhibition over sixty tested cancer cell lines were determined[106-108] (Table 5, 6). Monosubstituted compounds **(4a-5a, 7a-9a** and **11a)** displayed modest potency against the tested tumor cell lines and considered to be least effective member. Disubstituted compounds (**4b, 5b, 9b** and **13b**) showed lower activity for cancer cell lines but active than monosubstituted compounds (Figure 5). Diarylated compounds (**8b** and **11b**) with respective 4-bromophenyl and 2-hydroxyphenyl imidazo[1,2-*a*]pyrazine showed broad spectrum of anticancer activity as compared to corresponding monoarylated products (**8a** and **11a**), indicating that arylation at both C6 and C8 positions are essential for activity. Disubstituted compound **4b** showed selective potency towards breast cancer cell lines MCF7, T-47D and MDA-MB-468 with GI values of 75.44%, 78.80% and 88.28%, respectively while compound **5b** showed selectivity towards breast cancer cell line MCF7 with GI value of 75.20%. Compound **8b** also showed excellent inhibition against leukaemia cancer cell lines K-562 (83.21%), SR (86.61%), non small cell lung cancer cell line NCI-H460 (83.24%), colon cancer cell lines COLO205 (92.17%), HCT-15 (78.38%), HT29 (90.12%) and SW-620 (74.59%), melanoma cancer cell line MDA-MB-435 (96.92%), ovarian cancer cell line NCI/ADR-RES (80.29%) and breast cancer cell lines BT-549 (82.44%), MCF7 (77.96%), and is

lethal to non small lung cancer cell line NCI-H522 (Figure 6). Compound **11b** also showed selectivity towards colon cancer cell line HCT-15, renal cancer cell line A-498, breast cancer cell lines MCF7 and MDA-MB-231/ATCC with GI values of 59.04%, 68.01%, 59.64% and 69.32% respectively (Table 5).

Table-5 Percentage (%) growth inhibition (GI) of compounds **4a-b**, **5a-b**, **7a, 8a-b**, **9a-b**, **11a-b** and **13b** over the full panel of 60 tumor cell lines at concentration of 10 µM.

Cell line type	Cell line name	4a	4b	5a	5b	7a	8a	8b	9a	9b	11a	11b	13b
Leukemia	CCRF-CEM	-	-	-	-	-	-	55.21	-	-	-	45.26	-
	HL-60(TB)	NT	NT	-	-	NT	-	69.76	NT	NT	NT	NT	NT
	K-562	-	-	-	-	-	-	**83.21**	-	-	-	42.90	-
	MOLT-4	-	NT	-	-	21.13	-	69.64	-	-	29.90	36.39	NT
	RPMI-8226	-	-	-	-	-	-	41.74	-	-	-	45.84	-
	SR	-	-	-	-	-	-	**86.61**	-	-	-	46.69	-
Non-Small Cell Lung Cancer	A549/ATCC	-	-	-	-	-	-	68.14	-	-	-	29.47	-
	HOP-62	-	-	-	-	-	32.79	66.79	-	-	-	-	-
	HOP-92	-	-	-	-	46.37	33.11	44.22	29.33	48.62	-	44.57	-
	NCI-H226	-	-	-	-	25.39	21.94	29.38	-	20.68	-	26.51	-
	NCI-H23	-	-	-	-	-	27.75	40.18	-	-	-	-	-
	NCI-H322M	-	-	-	-	-	-	-	-	-	-	-	-
	NCI-H460	-	-	-	-	-	-	**83.24**	-	-	-	35.82	-
	NCI-H522	-	-	-	-	-	-	**L**	-	-	-	49.20	-
Colon Cancer	COLO 205	-	-	-	-	-	-	**92.17**	-	-	-	-	-
	HCC-2998	-	-	-	-	-	-	39.76	-	-	-	25.73	-
	HCT-116	-	-	-	-	22.16	-	69.96	-	-	-	32.49	-
	HCT-15	-	45.55	-	-	-	-	**78.38**	-	-	-	59.04	-
	HT29	-	-	-	-	-	-	**90.12**	-	-	-	-	-
	KM12	-	25.06	-	-	-	-	65.37	-	-	-	58.16	-
	SW-620	-	-	-	-	-	-	**74.59**	-	-	-	-	-
CNS Cancer	SF-268	-	-	-	-	-	-	43.09	-	-	-	40.05	-
	SF-295	-	-	-	-	-	-	69.38	-	-	-	-	-
	SF-539	-	-	-	-	-	21.39	47.52	-	-	-	33.12	-
	SNB-19	-	-	-	-	-	-	24.23	-	-	-	26.43	-
	SNB-75	-	-	-	-	-	37.71	64.36	21.70	-	-	44.13	29.36
	U251	-	-	-	-	21.82	-	60.82	-	-	-	36.88	-
Melanoma	LOX IMVI	-	-	-	-	22.16	-	56.82	-	-	-	36.88	-
	MALME-3M	-	-	-	-	-	-	60.53	-	-	-	-	-
	M14	-	-	-	-	-	-	47.52	-	-	-	35.81	-
	MDA-MB-435	-	-	-	-	-	-	**96.92**	-	-	-	29.94	-
	SK-MEL-2	NT	NT	-	-	NT	-	69.23	NT	NT	NT	NT	NT
	SK-MEL-28	-	-	-	-	-	-	37.85	-	25.31	-	46.19	-

	SK-MEL-5	-	31.97	-	-	-	-	53.74	-	-	-	-	-
	UACC-257	-	-	-	-	-	-	32.55	-	-	-	-	-
	UACC-62	-	-	-	-	22.63	-	56.36	-	-	-	29.21	-
Ovarian Cancer	IGROV1	-	-	-	-	25.74	23.89	44.23	-	-	-	25.30	-
	OVCAR-3	-	-	-	-	-	-	68.10	-	-	-	39.82	-
	OVCAR-4	-	47.97	-	-	-	-	37.80	-	-	-	29.44	-
	OVCAR-5	-	-	-	-	-	-	-	-	-	-	-	-
	OVCAR-8	-	-	-	-	-	-	48.40	-	-	-	23.89	-
	NCI/ADR-RES	NT	NT	-	-	NT	-	**80.29**	NT	NT	NT	NT	NT
	SK-OV-3	-	-	-	-	-	25.17	44.78	-	-	-	27.05	-
Renal Cancer	786-0	-	-	-	-	-	-	42.16	-	-	-	-	-
	A498	-	-	-	-	23.41	-	64.07	-	29.32	-	68.01	22.64
	ACHN	-	-	-	-	-	22.54	45.39	-	-	-	27.88	-
	CAKI-1	-	-	-	45.67	27.04	28.35	60.43	-	-	-	48.21	-
	RXF 393	-	-	-	-	-	-	53.04	-	-	-	50.82	-
	SN12C	-	-	-	-	-	20.44	46.25	-	-	-	39.90	-
	TK-10	-	-	-	-	-	-	-	-	-	-	30.23	-
	UO-31	-	-	-	-	59.68	49.62	58.36	23.14	27.69	-	53.71	23.29
Prostate Cancer	PC-3	-	-	-	-	-	21.59	33.77	-	-	-	29.85	-
	DU-145	-	-	-	-	-	-	27.33	-	-	-	-	-
Breast Cancer	MCF7	36.45	**75.44**	38.14	**75.20**	35.87	29.97	**77.96**	33.19	-	32.29	59.64	42.69
	MDA-MB-231/ATCC	-	**-**	-	-	30.38	28.08	53.45	-	-	-	69.32	-
	HS 578T	-	**-**	-	-	-	-	38.90	-	20.77	-	37.38	-
	BT-549	-	**-**	38.09	-	-	33.42	**82.44**	-	-	-	37.67	-
	T-47D	-	**78.80**	-	49.11	45.59	47.04	62.84	22.95	-	32.42	47.07	42.48
	MDA-MB-468	-	**88.28**	-	64.74	21.12	-	66.82`	-	-	-	48.29	30.62

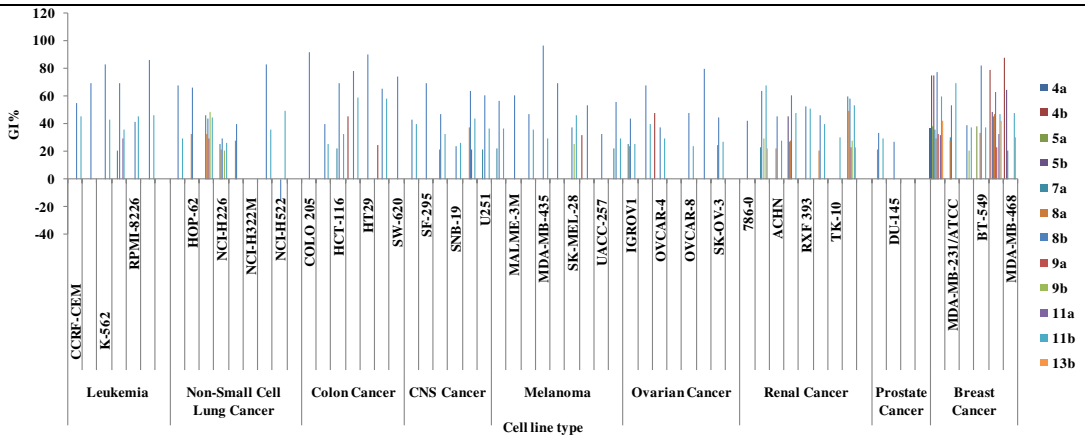

Figure 5 The percentages of growth inhibition of compounds **4a, 4b, 5a, 5b, 7a, 8a, 8b, 9a, 9b, 11a, 11b** and **13b** over the full panel of tumor cell lines.

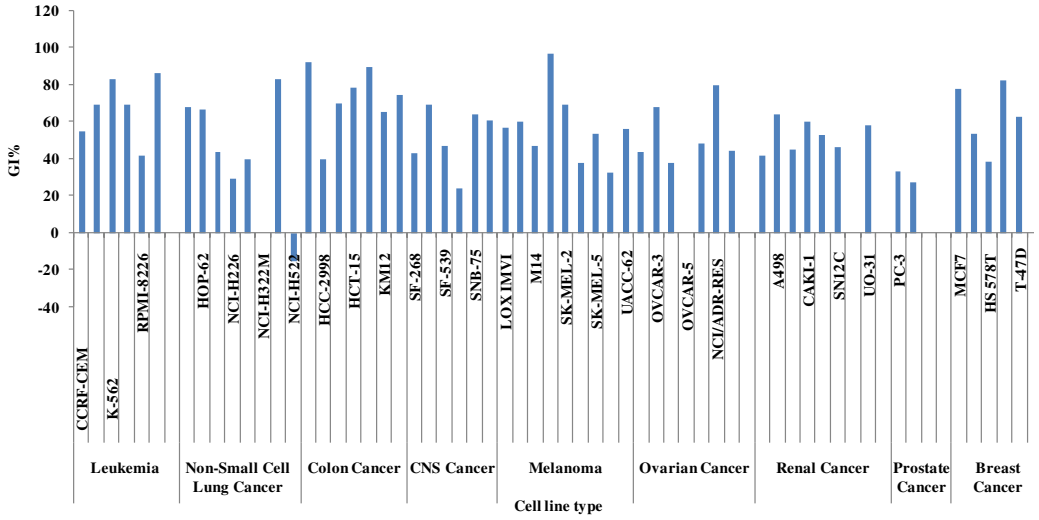

Figure 6 Percentages of growth inhibition of compound **8b** over full panel of tumor cell lines.

Compounds **18**, **27** and **28** are least effective in unsymmetrical disubstituted imidazo[1,2-*a*]pyrazine series indicating that 4-chloro, 2-hydroxy and 4-fluorophenyl at C6 position to the corresponding 4-fluoro and 4-methoxyphenyl at C8 positions of imidazo[1,2-*a*]pyrazine is not essential for activity. Compounds **23** and **30** having 4-fluorophenyl and 2-thiophene moieties at C8 position with respective 4-chlorophenyl and 4-methoxyphenyl at C6 position of imidazo[1,2-*a*]pyrazine showed moderate antitumor activity while compounds **21** and **22** with 2-hydroxyphenyl and 2-furan at C6 position with 4-chlorophenyl at C8 position showed broad spectrum of antitumor activity. Leukaemia cancer cell line K-562 proved to be sensitive towards compounds **19**, **21** and **23** with GI values of 73.90%, 78.51% and 70.71%, respectively. Non small lung cancer cell lines NCI-H322M and NCI-H460 showed sensitivity towards compound **22** with GI values of 88.56% and 85.47%, respectively while NCI-H522 showed sensitivity towards compound **21** with GI value of 82.59%. Compound **19** showed selectivity towards melanoma cancer cell line MDA-MB-435, breast cancer cell lines MCF7 and T-47D with GI values of 76.92%, 80.94% and 83.67%, respectively. Compound **22** showed selectivity towards CNS cancer cell line SF-295 with GI value of 84.86% and renal cancer cell line ACHN, TK-10 and UO-31 with GI values of 91.41%, 88.07% and 92.94%, respectively. These results revealed that unsymmetrical diarylated compounds have been found to be most effective for anticancer activity than monoarylated or symmetrical diarylated compounds (Table 6, Figure 7).

Table-6 Percentages (%) growth inhibition (GI) of compounds **18**-**19**, **21**- **23**, **27**- **28** and **30** over the full panel of 60 tumor cell lines at concentration of 10 µM.

Cell line type	Cell line name	18	19	21	22	23	27	28	30
Leukemia	CCRF-CEM	-	34.75	25.29	21.65	33.43	-	-	22.66
	HL-60(TB)	-	-	-	-	-	-	-	-
	K-562	-	**73.90**	**78.51**	31.05	**70.71**	-	-	37.83
	MOLT-4	23.61	37.56	53.12	20.05	28.64	-	20.53	24.60
	RPMI-8226	-	35.34	-	47.08	-	30.11	-	28.61
	SR	20.98	40.51	58.89	36.61	41.09	30.77	-	29.92
Non-Small Cell Lung Cancer	A549/ATCC	25.93	42.59	48.62	**L**	32.55	-	22.65	-
	HOP-62	22.21	42.27	49.45	68.64	41.11	21.79	30.09	38.49
	HOP-92	30.33	-	28.35	65.30	30.62	-	22.34	32.10
	NCI-H226	22.22	28.04	21.60	53.72	30.49	21.69	-	30.91
	NCI-H23	-	28.90	27.89	38.99	-	-	-	-
	NCI-H322M	-	-	-	**88.56**	-	-	-	-
	NCI-H460	-	-	22.26	**85.47**	-	-	-	-
	NCI-H522	24.24	72.01	**82.59**	38.45	47.09	27.13	-	50.23
Colon Cancer	COLO 205	-	28.91	-	24.95	26.84	-	-	-
	HCC-2998	-	52.20	23.30	41.81	-	-	-	28.38
	HCT-116	20.00	31.98	48.02	49.85	37.95	-	-	21.97
	HCT-15	21.20	68.84	60.41	NT	63.12	35.05	-	51.50
	HT29	-	58.37	41.70	59.69	43.15	-	-	20.93
	KM12	-	49.45	38.53	51.30	39.34	-	-	32.70
	SW-620	-	42.67	56.77	27.26	44.25	-	-	-
CNS Cancer	SF-268	-	-	24.20	35.73	-	-	-	-
	SF-295	-	-	22.27	**84.86**	27.87	-	-	26.78
	SF-539	-	23.30	29.70	37.84	-	-	-	26.14
	SNB-19	-	-	21.09	69.43	20	-	-	-
	SNB-75	26.73	31.87	32.81	67.97	52.25	36.35	33.53	39.07
	U251	-	-	31.37	**L**	23.29	-	-	24.92
Melanoma	LOX IMVI	-	38.60	46.47	44.76	29.61	25.46	-	31.06
	MALME-3M	-	-	22.40	22.96	-	-	-	-
	M14	-	38.48	46.18	-	46.88	25.49	-	41.72
	MDA-MB-435	-	**76.92**	**81.62**	21.44	-	23.60	-	51.97
	SK-MEL-2	-	29.41	34.10	-	-	-	-	32.65
	SK-MEL-28	-	-	-	-	-	-	-	-
	SK-MEL-5	-	46.78	27.13	42.03	27.87	26.32	-	43.51
	UACC-257	-	29.76	23.60	24.77	-	-	-	-
	UACC-62	-	39.83	43.90	-	38.69	-	-	28.30
Ovarian Cancer	IGROV1	20.33	39.06	42.46	59.29	33.81	-	-	-
	OVCAR-3	-	27.40	24.26	49.26	-	-	-	21.05
	OVCAR-4	-	35.44	-	58.70	21.48	-	-	25.52
	OVCAR-5	-	-	-	-	-	-	-	-
	OVCAR-8	-	-	25.34	50.21	-	-	-	-

	NCI/ADR-RES	-	44.46	54.11	29.85	34.08	31.88	-	34.70
	SK-OV-3	22.64	49.84	43.58	**L**	35.01	-	27.57	41.97
Renal Cancer	786-0	-	-	-	**L**	-	-	-	-
	A498	21.83	-	26.82	63.21	23.22	-	-	-
	ACHN	-	-	-	**91.41**	-	-	-	-
	CAKI-1	30.38	41.01	34.72	49.82	43.45	31.71	25.42	36.11
	RXF 393	-	-	20.90	58.40	38.85	-	-	33.85
	SN12C	-	-	20.55	34.30	22.85	-	-	-
	TK-10	-	39.27	-	**88.07**	-	-	-	-
	UO-31	40.53	54.06	51.83	**92.94**	52.29	46.56	40.95	45.06
Prostate Cancer	PC-3	22.49	37.62	27.31	39.85	27.36	21.00	20.87	21.61
	DU-145	-	-	-	32.73	-	-	-	-
Breast Cancer	MCF7	39.00	**80.94**	56.98	**72.83**	57.41	25.48	24.89	42.68
	MDA-MB-231/ATCC	23.35	33.47	47.39	26.00	37.60	36.97	21.64	39.19
	HS 578T	-	-	23.39	-	20.47	20.07	-	22.18
	BT-549	-	NT	NT	NT	NT	39.50	NT	33.41
	T-47D	36.98	**83.67**	29.74	59.78	35.2	36.65	40.92	**76.26**
	MDA-MB-468	-	**L**	-	**L**	23.47	-	-	69.70

NT-not tested, L- lethal

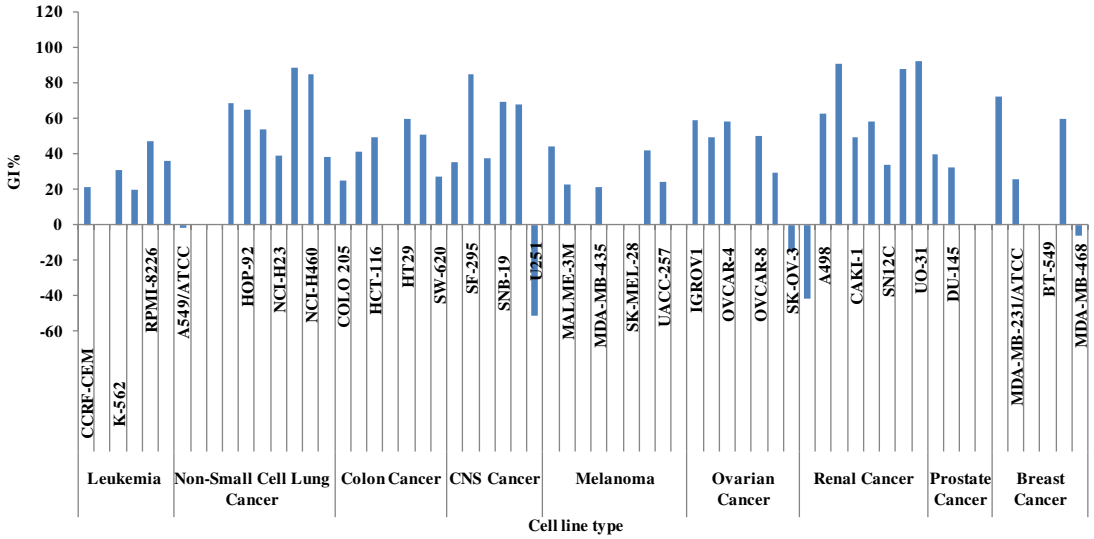

Figure 7 Percentages of growth inhibition of compound **22** over full panel of tumor cell lines.

2.5. STRUCTURE ACTIVITY RELATIONSHIP (SAR) STUDIES

The structure-activity relationship (SAR) studies showed that monoaryl and diaryl imidazo[1,2-*a*]pyrazines were well tolerated for *in vitro* anticancer activities. (i) The monosubstituted and disubstituted imidazo[1,2-*a*]pyrazines with variations of different functional groups on aryl moiety play a key role in varying the efficiency of antitumor activities. (ii) The diaryl imidazo[1,2-*a*]pyrazines positively influence the antitumor effectiveness, inducing good activity

than mono aryl imidazo[1-2-*a*]pyrazines against most of the cancer cell lines. (iii) Unsymmetrical diaryl imidazo[1,2-*a*]pyrazine showed broad spectrum antitumor activity than symmetrical diaryl analogue. (iv) Introduction of 2-hydroxy phenyl (**21**), 2-furanyl (**22**) and 4-fluorophenyl (**23**) at C6 position with 4-chlorophenyl at C8 position of imidazo[1,2-*a*]pyrazine led to broad spectrum antitumor activity. Thus 4-chloro phenyl at C8 position of imidazo[1,2-*a*]pyrazine plays an important role for the activity. (v) Presence of 4-chlorophenyl (**19**) and 4-methoxyphenyl (**30**) at C8 position and 2-thiophene at C6 position of imidazo[1,2-*a*]pyrazine has slightly improved the activity. (vi) Amongst symmetrical diaryl analogues, 4-bromophenyl at C6 and C8 positions of imidazo[1,2-*a*]pyrazine (**8b**) has improved the antitumor activity.

2.6. CONCLUSION

In summary, palladium catalyzed direct C-C coupling has been developed from the easily accessible 6,8-dibromo-imidazo[1,2-*a*]pyrazines, allowing the straightforward functionalization at both C6 and C8 positions to a series of monoarylation and symmetrical diarylation products. In addition, facile access to 8-functionalized imidazo[1,2-*a*]pyrazines were also demonstrated by implementing unsymmetrical diarylation in moderate to high yields. Preliminary analysis of the anticancer activities revealed that unsymmetrical diarylated imidazo[1,2-*a*]pyrazines showed more selectivity than monoarylated and symmetrical diarylated analogues. Compounds **21** and **22** showed broad spectrum antitumour activities in most of the cancer cell lines amongst these series. Overall, we believed that the developed reaction method and novel series of arylated imidazo[1,2-*a*]pyrazine should be considered as important advancement in the medicinal and pharmaceutical chemistry.

2.7. EXPERIMENTAL SECTION

2.7.1. Instrumentations and chemicals:

All commercially available compounds (Spectrochem, Aldrich, Merck etc.) were used without purification. All reactions were run under argon or nitrogen atmosphere. All solvents used in the reactions were purified before use. The reactions were carried out in an oil bath using Microwave Vials (10-15 ml). Melting points were determined in open capillaries and were uncorrected. ^{1}H and ^{13}C NMR spectra were performed on Jeol 400 NMR spectrometer, which was operated at 400 MHz for ^{1}H nuclei and 100 MHz for ^{13}C nuclei, using $CDCl_3$ as solvent. Chemical shifts are

reported in parts per million (ppm) with TMS as internal reference and *J* values are given in hertz. Mass Spectra of the synthesized compounds were recorded at Water Micromass-Q-T of Micro in SAIF, Punjab University. GCMS analyses were carried out on an Agilent Technologies with Scion Mass spectrometer. The Bruker AXS KAPPA APEX II system is used for single crystal X-ray diffraction. Reactions were monitored by thin layer chromatography (TLC) with silica plate coated with silica gel HF-254 and column chromatography was performed with silica gel 60-120/100-200 mesh. Hexane/ethylacetate and chloroform/methanol were adopted solvent systems.

2.7.2. Synthesis of 2-amino-3,5-dibromopyrazine (2)

N-Bromosuccinamide (14.95 g, 83.99 mmol) was added over 50 min to a mixture of 2-aminopyrazine (3.80 g, 40 mmol) in 80 ml DMSO and 2 ml H_2O below 15 ^oC. Mixture was then stirred for 6 h at room temperature. After completion of reaction, mixture was then extracted with water and ethyl acetate. Ethyl acetate layer was dried over sodium sulphate and concentrated in vacuum. Crude product was purified by column chromatography using hexane: ethyl acetate (9:1) as eluents.

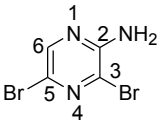

Spectral data 2-amino-3,5-dibromopyrazine (2): White solid; Yield: 90%; mp 115-116 ^oC (lit. M.p. 117-118 ^oC) [1]; ^1H NMR ($CDCl_3$, 400 MHz): δ 5.12 (bs, 1H, NH_2), 8.04 (s, 1H, C_6H); ^{13}C NMR ($CDCl_3$, 100 MHz): δ 123.57, 123.90, 143.09, 151.84; MS (EI): m/z 254 (M^++1).

2.7.3. Synthesis of 6,8-dibromoimidazo[1,2-*a*]pyrazine (3):To 2-amino-3,5-dibromopyrazine (5.0 g, 19.8 mmol) in 100 ml of isopropyl alcohol (IPA), 50% aqueous solution of chloroacetaldehyde (99 mmol) was added dropwise. The reaction mixture was refluxed at 110 ^oC for 24 h. After the completion of the reaction, cooled to room temperature and then extracted with water and chloroform. Chloroform layer was dried over sodium sulphate and concentrated in vacuum to get the crude product. The product was purified by column chromatography using hexane:ethyl acetate (6:4) as eluent.

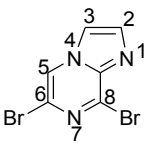

Spectral data 6,8-dibromoimidazo[1,2-*a*]pyrazine (3): White solid; Yield: 80%; mp 163-165 ^oC (lit. M.p. 165-166 ^oC)[2]; ^1H NMR ($CDCl_3$, 400 MHz): δ 7.80 (d, *J* = 0.92 Hz, 1H, C_2H), 7.86 (d, *J* = 1.36 Hz, 1H, C_3H), 8.29 (s, 1H, C_5H); ^{13}C

NMR ($CDCl_3$, 100 MHz): δ 115.92, 119.32, 119.97, 137.03, 137.39, 142.54; MS (EI): m/z 278 (M^++1).

2.7.4. General procedure for synthesis of compounds 4-15: A vial equipped with stirring bar was charged with 6,8-dibromo-imidazo[1,2-*a*]pyrazine (0.5 g, 1.8 mmol), Cs_2CO_3 (0.6 g, 1.8 mmol) and boronic acid (1.8 mmol), dissolved in MeCN:H_2O (9:1) at 100 ^oC under inert atmosphere. Then, 5 mol% of $Pd(PPh_3)_4$ was added and vial was capped. The reaction mixture was refluxed for 7-12 h. After the completion of the reaction (monitored by TLC), cooled the reaction mixture, and then extract with water and chloroform. Organic layer was dried over sodium sulphate, filtered and concentrated under *vacuo* to get crude product. The residue was purified by silica gel (60-120 mesh) column chromatography using hexane: ethyl acetate as eluents to give pure solid.

Spectral data 6-bromo-8-(thiophen-2'-yl)imidazo[1,2-*a*]pyrazine (4a) : Green solid;

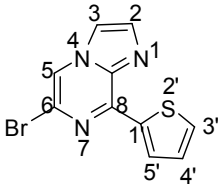

Yield:70%; mp 149-151 ^oC; ^1H NMR ($CDCl_3$, 400 MHz): δ 7.23 (t, *J* = 4.12 Hz, 1H, $C_{4'}H$), 7.62 (d, *J* = 5.04 Hz, 1H, $C_{5'}H$), 7.67 (s, 1H, C_2H), 7.83 (s, 1H, C_3H), 8.14 (s, 1H, C_5H), 8.77 (d, *J* = 3.68 Hz, 1H, $C_{3'}H$); ^{13}C NMR ($CDCl_3$, 100 MHz): δ 114.19, 117.25, 122.37, 128.57, 131.67, 132.99, 135.97, 137.10, 138.96, 144.62 (ArC); GC-MS: m/z 279 (M^+).

Spectral data 6,8-di(thiophen-2'-yl)imidazo[1,2-*a*]pyrazine (4b): Green solid; Yield: 10%;

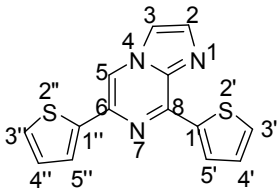

mp 140-142 ^oC; ^1H NMR ($CDCl_3$, 400 MHz): δ 7.12 (t, *J* = 4.36 Hz, 1H, $C_{4''}H$), 7.24 (t, *J* = 4.36 Hz, 1H, $C_{4'}H$), 7.38 (d, *J* = 5.04 Hz, 1H, $C_{5''}H$), 7.56 (d, *J* = 3.68 Hz, 1H, $C_{3''}H$), 7.59 (d, *J* = 5.04 Hz, 1H, $C_{5'}H$), 7.69 (d, *J* = 0.92 Hz, 1H, C_2H), 7.81 (d, *J* = 0.92 Hz, 1H, C_3H), 8.29 (s, 1H, C_5H), 8.79 (d, *J* = 3.64 Hz, 1H, $C_{3'}H$); ^{13}C NMR ($CDCl_3$, 100 MHz): δ 111.52, 114.52, 123.53, 126.67, 128.11, 128.46, 130.74, 132.19, 134.90, 135.33, 137.22, 140.34, 141.38, 144.29 (ArC); GC-MS: m/z 283 (M^+).

Spectral data 8-(thiophen-2'-yl)imidazo[1,2-*a*]pyrazine (4c): Light green solid; Yield: 60%;

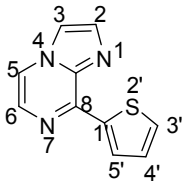

mp 135-137 ^oC; ^1H NMR ($CDCl_3$, 400 MHz): δ 7.26-7.23 (m, 1H, $C_{4'}H$), 7.58 - 7.57 (dd, ^2J = 5.04 Hz, ^3J = 0.92 Hz, 1H, $C_{5'}H$), 7.77 (d, *J* = 0.92 Hz, 1H, C_2H), 7.85 (d, *J* = 0.95 Hz, 1H, C_3H), 7.87 (d, *J* = 4.56 Hz, 1H, C_5H), 7.99 (d, *J* = 4.56 Hz, 1H, C_6H), 8.82-8.80 (dd, ^2J = 4.16 Hz, ^3J = 1.1 Hz, 1H, $C_{3'}H$); ^{13}C NMR ($CDCl_3$, 100 MHz): δ 114.06, 117.33, 128.58, 129.05, 130.23, 132.12, 134.93 (ArC); MS (EI):

m/z 202 (M^++1).

Spectral data 6-bromo-8-(furan-2'-yl)imidazo[1,2-*a*]pyrazine (5a): Light brown solid;

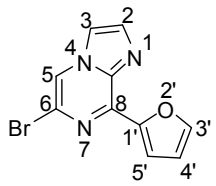

Yield: 56%; mp 124-126 ^oC; ^1H NMR ($CDCl_3$, 400 MHz): δ 6.68-6.67 (dd, ^2J = 3.20 Hz, ^3J = 1.60 Hz, 1H, $C_{5'}H$), 7.69 (d, J = 0.92 Hz, 1H, C_2H), 7.77 (t, J = 0.92 Hz, 1H, $C_{4'}H$), 7.83 (d, J = 0.92 Hz, 1H, C_3H), 8.10 (d, J = 3.2 Hz, 1H, $C_{3'}H$), 8.17 (s, 1H, C_5H); ^{13}C NMR ($CDCl_3$, 100 MHz): δ 112.82, 114.30, 117.42, 118.88, 122.57, 136.05, 136.46, 140.30, 146.42, 148.30 (ArC); GC-MS: m/z 263 (M^+).

Spectral data 6,8-di(furan-2'-yl)imidazo[1,2-*a*]pyrazine (5b): Light brown solid; Yield:

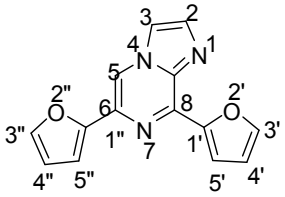

12%; mp 140-142 ^oC; ^1H NMR ($CDCl_3$, 400 MHz): δ 6.56-6.55 (dd, ^2J = 3.20 Hz, ^3J = 1.82 Hz, 1H, $C_{4''}H$), 6.68-6.67 (dd, ^2J = 3.64 Hz, ^3J = 1.62 Hz, 1H, $C_{4'}H$), 7.13 (d, J = 2.76 Hz, 1H, $C_{5''}H$), 7.50 (d, J = 1.8 Hz, 1H, $C_{5'}H$), 7.73 (d, J = 1.4 Hz, 1H, C_2H), 7.77 (d, J = 1.36 Hz, 1H, $C_{3''}H$), 7.81 (d, J = 1.36 Hz, 1H, C_3H), 8.07 (d, J = 4.12 Hz, 1H, $C_{3'}H$), 8.36 (s, 1H, C_5H); ^{13}C NMR ($CDCl_3$, 100 MHz): δ 108.66, 111.79, 111.98, 112.37, 114.69, 117.44, 132.01, 135.18, 136.50, 140.62, 142.61, 145.58, 149.18, 151.16 (ArC); GC-MS: m/z 251 (M^+).

Spectral data 6-bromo-8-(4'-fluorophenyl)imidazo[1,2-*a*]pyrazine (6a): Light yellow solid;

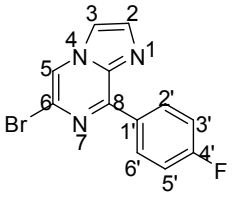

Yield: 52%; mp 157-159 ^oC; ^1H NMR ($CDCl_3$, 400 MHz): 7.23-7.18 (m, 2H, $C_{2'}H$ and $C_{6'}H$), 7.70 (s, 1H, C_2H), 7.84 (s, 1H, C_3H), 8.21 (s, 1H, C_5H), 8.81-8.79 (dd, ^2J = 8.68 Hz, ^3J = 5.48 Hz, 2H, $C_{3'}H$ and $C_{5'}H$); ^{13}C NMR ($CDCl_3$, 100 MHz): δ 114.12, 115.49, 115.71, 118.08, 122.62, 130.99 132.19, 132.28, 136.17, 138.45, 148.10 (ArC); GC-MS: m/z 291(M^+).

Spectral data 6,8-bis(4'-fluorophenyl)imidazo[1,2-*a*]pyrazine (6b): Light yellow solid; Yield:

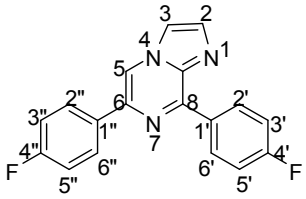

25%; mp 162-164 ^oC; ^1H NMR ($CDCl_3$, 400 MHz): δ 7.27-7.17 (m, 4H, $C_{2'}H$, $C_{6'}H$, $C_{2''}H$ and $C_{6''}H$), 7.78 (d, J = 1.36 Hz, 1H, C_2H), 7.86 (d, J = 1.36 Hz, 1H, C_3H), 8.04-8.00 (m, 2H, $C_{3''}H$ and $C_{5''}H$), 8.40 (s, 1H, C_5H), 8.89 - 8.92 (m, 2H, $C_{3'}H$ and $C_{5'}H$); ^{13}C NMR ($CDCl_3$, 100 MHz): δ 113.65, 114.48, 115.38, 115.59, 115.87, 116.09, 128.04, 128.12, 131.91, 131.99, 132.21, 132.78, 135.46, 138.07, 138.61, 147.72, 162.10, 163.21, 164.57, 165.71 (ArC); GC-MS: m/z 307 (M^+).

Spectral data 6-bromo-8-(4'-chlorophenyl)imidazo[1,2-*a*]pyrazine (7a): White solid; Yield:

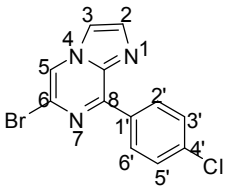

70%; mp 157-159 ^{o}C; ^{1}H NMR ($CDCl_3$, 400 MHz): δ 7.50 (d, *J* = 8.72 Hz, 2H, $C_{2'}H$ and $C_{6'}H$), 7.72 (d, *J* = 0.88 Hz, 1H, C_2H), 7.86 (d, *J* = 0.92 Hz, 1H, C_3H), 8.24 (s, 1H, C_5H), 8.74 (d, *J* = 8.72 Hz, 2H, $C_{3'}H$ and $C_{5'}H$); ^{13}C NMR ($CDCl_3$, 100 MHz): δ 114.14, 118.35, 122.63, 128.78, 131.31, 133.22, 136.25, 137.44, 138.49, 148.02 (ArC); GC-MS: m/z 309 (M^+).

Spectral data 6,8-bis(4'-chlorophenyl)imidazo[1,2-*a*]pyrazine (7b): Off white solid; Yield:

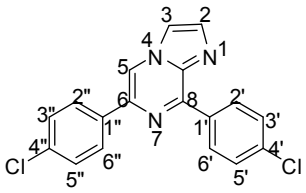

16%; mp 139-141 ^{o}C; ^{1}H NMR ($CDCl_3$, 400 MHz): δ 7.47 (d, *J* = 8.72 Hz, 2H, $C_{2''}H$ and $C_{6''}H$), 7.53 (d, *J* = 8.72 Hz, 2H, $C_{2'}H$ and $C_{6'}H$), 7.78 (s, 1H, C_2H), 7.86 (s, 1H, C_3H), 7.98 (d, *J* = 8.72 Hz, 2H, $C_{3''}H$ and $C_{5''}H$), 8.43 (s, 1H, C_5H), 8.84 (d, *J* = 8.72 Hz, 2H, $C_{3'}H$ and $C_{5'}H$); ^{13}C NMR ($CDCl_3$, 100 MHz): δ 114.13, 114.58, 127.52, 128.71, 129.20, 131.12, 134.41, 134.87, 135.01, 135.57, 136.86, 137.80, 138.63, 147.60 (ArC); GC-MS: m/z 340 (M^+).

Spectral data 6-bromo-8-(4'-bromophenyl)imidazo[1,2-*a*]pyrazine (8a): White solid; Yield:

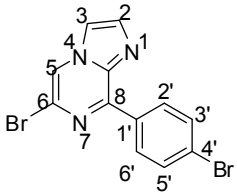

68%; mp 138-140 ^{o}C; ^{1}H NMR ($CDCl_3$, 400 MHz): δ 7.65 (d, *J* = 8.72 Hz, 2H, $C_{2'}H$ and $C_{6'}H$), 7.71 (d, *J* = 0.92 Hz, 1H, C_2H), 7.85 (d, *J* = 0.92 Hz, 1H, C_3H), 8.24 (s, 1H, C_5H), 8.66 (d, *J* = 8.72 Hz, 2H, $C_{3'}H$ and $C_{5'}H$); ^{13}C NMR ($CDCl_3$, 100 MHz): δ 114.13, 118.38, 122.63, 126.08, 131.50, 131.73, 133.65, 136.26, 138.45, 148.05 (ArC); Mass (EI): m/z 351 (M^++1).

Spectral data 6,8-bis(4'-bromophenyl)imidazo[1,2-*a*]pyrazine (8b): White solid; Yield:

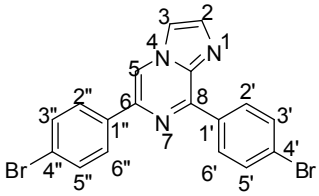

20%; mp 145-147 ^{o}C; ^{1}H NMR ($CDCl_3$, 400 MHz): δ 7.63 (d, *J* = 8.72 Hz, 2H, $C_{2''}H$ and $C_{6''}H$), 7.69 (d, *J* = 8.24 Hz, 2H, $C_{2'}H$ and $C_{6'}H$), 7.79 (s, 1H, C_2H), 7.87 (d, *J* = 0.80 Hz, 1H, C_3H), 7.92 (d, *J* = 8.68 Hz, 2H, $C_{3''}H$ and $C_{5''}H$), 8.45 (s, 1H, C_5H), 8.76 (d, *J* = 8.72 Hz, 2H, $C_{3'}H$ and $C_{5'}H$); ^{13}C NMR ($CDCl_3$, 100 MHz): δ 114.17, 114.59, 123.15, 125.47, 127.82, 131.14, 131.68, 132.16, 134.85, 135.47, 135.60, 137.88, 138.62, 147.73 (ArC); Mass (EI): m/z 428 (M^++1).

Spectral data 6-bromo-8-(4'-methoxyphenyl)imidazo[1,2-*a*]pyrazine (9a): White solid;

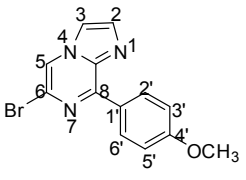

Yield: 69%; mp 138-140 ^{o}C; ^{1}H NMR ($CDCl_3$, 400 MHz): δ 3.89 (s, 3H, OCH_3), 7.05 (d, *J* = 9.16 Hz, 2H, $C_{2'}H$ and $C_{6'}H$), 7.67 (d, *J* = 1.36 Hz, 1H, C_2H), 7.83 (d, *J* = 0.92 Hz, 1H, C_3H), 8.16 (s, 1H, C_5H), 8.77 (d, *J* = 9.16 Hz, 2H, $C_{3'}H$ and $C_{5'}H$); ^{13}C NMR ($CDCl_3$, 100 MHz): δ 55.53 (OCH_3),

113.93, 117.28, 122.37, 122.80, 127.48, 131.76, 135.83, 138.52, 148.95, 162.10 (ArC); GC-MS: m/z 303 (M^+).

Spectral data 6,8-bis(4'-methoxyphenyl)imidazo[1,2-*a*]pyrazine (9b): White solid; Yield:

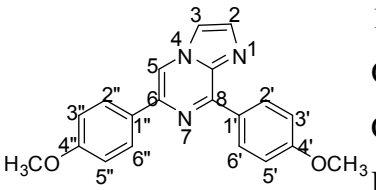

14%; mp 162-164 ^oC; ^1H NMR ($CDCl_3$, 400 MHz): δ 3.86 (s, 3H, OCH_3), 3.90 (s, 3H, OCH_3), 7.01 (d, *J* = 9.16 Hz, 2H, $C_{2''}H$ and $C_{6''}H$), 7.07 (d, *J* = 9.16 Hz, 2H, $C_{2'}H$ and $C_{6'}H$), 7.67 (d, *J* = 1.36 Hz, 1H, C_2H), 7.80 (d, *J* = 0.92 Hz, 1H, C_3H), 7.97 (d, *J* = 9.16 Hz, 2H, $C_{3''}H$ and $C_{5''}H$), 8.27 (s, 1H, C_5H), 8.87 (d, *J* = 8.72 Hz, 2H, $C_{3'}H$ and $C_{5'}H$); ^{13}C NMR ($CDCl_3$, 100 MHz): δ 55.49 (2×OCH_3), 112.38, 113.79, 114.15, 114.28, 127.52, 129.03, 129.44, 131.40, 134.90, 138.61, 148.17, 160.13, 161.52, 161.91 (ArC); GC-MS: m/z 331 (M^+).

Spectral data 4'-(6-bromoimidazo[1,2-*a*]pyrazin-8-yl)benzaldehyde (10a): Yellow solid;

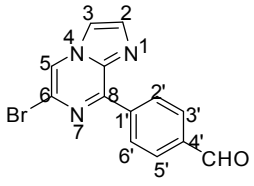

Yield: 70%; mp 176-178 ^oC; ^1H NMR ($CDCl_3$, 400 MHz): δ 7.76 (d, *J* = 1.36 Hz, 1H, C_2H), 7.90 (d, *J* = 0.88 Hz, 1H, C_3H), 8.03 (d, *J* = 8.68 Hz, 2H, $C_{2'}H$ and $C_{6'}H$), 8.30 (s, 1H, C_5H), 8.93 (d, *J* = 8.24 Hz, 2H, $C_{3'}H$ and $C_{5'}H$), 10.11 (s, 1H, CHO); ^{13}C NMR ($CDCl_3$, 100 MHz): δ 111.42, 119.04, 122.69 129.70, 130.57, 136.66, 137.59, 138.71, 140.16, 147.76 (ArC), 192.20 (CHO); GC-MS: m/z 301 (M^+).

Spectral data 4',4"-imidazo[1,2-*a*]pyrazine-6,8-diyl)dibenzaldehyde (10b): Light yellow

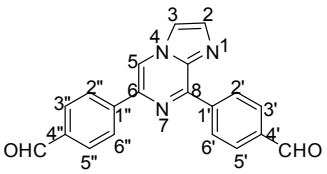

solid; Yield: 15%; mp 229-231 ^oC; ^1H NMR ($CDCl_3$, 400 MHz): δ 7.86 (s, 1H, C_2H), 7.93 (d, *J* = 0.92 Hz, 1H, C_3H), 8.03 (d, *J* = 8.24 Hz, 2H, $C_{2''}H$ and $C_{6''}H$), 8.08 (d, *J* = 8.24 Hz, 2H, $C_{2'}H$ and $C_{6'}H$), 8.25 (d, *J* = 8.28 Hz, 2H, $C_{3''}H$ and $C_{5''}H$), 8.63 (s, 1H, C_5H), 9.06 (d, *J* = 8.28 Hz, 2H, $C_{3'}H$ and $C_{5'}H$), 10.09 (s, 1H, CHO), 10.14 (s, 1H, CHO); ^{13}C NMR ($CDCl_3$, 100 MHz): δ 114.93, 115.97, 126.76, 129.73, 130.43, 130.49, 136.19, 136.44, 137.44, 137.61, 138.92, 141.29, 142.07, 147.67 (ArC), 191.83, 192.25 (CHO); GC-MS: m/z 327 (M^+).

Spectral data 2'-(6-bromoimidazo[1,2-*a*]pyrazin-8-yl) phenol (11a): Yellow solid; Yield:

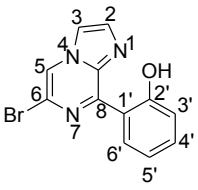

57%; mp 190-192 ^oC; ^1H NMR ($CDCl_3$, 400 MHz): 7.32-7.26 (m, 2H, $C_{5'}H$ and $C_{6'}H$), 7.45-7.40 (m, 2H, $C_{3'}H$ and $C_{4'}H$), 7.65 (d, *J* = 0.88 Hz, 1H, C_2H), 7.75 (d, *J* = 0.92 Hz, 1H, C_3H), 7.97 (s, 1H, C_5H); ^{13}C NMR ($CDCl_3$, 100 MHz): δ 115.34, 115.51, 119.30, 121.76, 125.89, 129.58, 132.63, 135.24, 152.11, 152.16 (ArC); Mass (EI): m/z 290 (M^++1).

Spectral data 2',2"-(imidazo[1,2-*a*]pyrazin-6,8-diyl)diphenol (11b): Yellow solid; Yield:

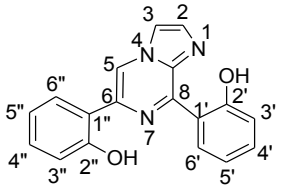

30%; mp 228-230 ^{o}C; ^{1}H NMR ($CDCl_3$, 400 MHz): δ 6.97–6.92 (m, 1H, $C_{5"}H$), 7.03 (d, J = 8.24 Hz, 1H, $C_{6"}H$), 7.11-7.07 (m, 1H, $C_{5'}H$), 7.15-7.13 (dd, ^{2}J = 8.28 Hz, ^{3}J = 1.38 Hz, 1H, $C_{6'}H$), 7.33-7.29 (m, 1H, $C_{4"}H$), 7.49-7.45 (m, 1H, $C_{4'}H$), 7.63-7.60 (dd, ^{2}J = 7.76 Hz, ^{3}J = 1.38 Hz, 1H, $C_{3"}H$), 7.84 (d, J = 1.40 Hz, 1H, C_2H), 7.85 (d, J = 0.92 Hz, 1H, C_3H), 8.29-8.26 (dd, ^{2}J = 8.28Hz, ^{3}J = 1.82 Hz 1H, $C_{3'}H$), 8.55 (s, 1H, C_5H); ^{13}C NMR ($CDCl_3$, 100 MHz): δ 113.28, 115.25, 117.78, 118.59, 119.92, 120.73, 121.38, 125.67, 130.87, 131.23, 133.56, 133.70, 137.60, 139.84, 147.88, 157.56, 158.02 (ArC); Mass (EI): m/z 303 (M^{+}+1).

Spectral data 6-bromo-8-(napthalen-1'-yl)imidazo[1,2-*a*]pyrazine (12a): White solid; Yield:

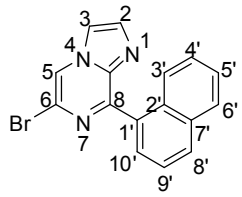

64%; mp 192-194 ^{o}C; ^{1}H NMR ($CDCl_3$, 400 MHz): δ 7.53-7.46 (m, 2H, $C_{8'}H$ and $C_{10'}H$), 7.62 (t, J = 7.79 Hz, 1H, $C_{9'}H$), 7.78 (d, J = 0.92 Hz, 1H, C_2H), 7.83 (d, J = 0.92 Hz, 1H, C_3H), 7.91 - 7.93 (m, 1H, $C_{6'}H$), 8.08-8.00 (m, 3H, $C_{3'}H$, $C_{4'}H$ and $C_{5'}H$), 8.36 (s, 1H, C_5H); ^{13}C NMR ($CDCl_3$, 100 MHz): δ 114.28, 118.50, 122.53, 125.02, 125.29, 126.22, 126.94, 128.61, 129.27, 130.94, 131.26, 131.86, 134.12, 136.85, 139.93, 152.17 (ArC); GC-MS: m/z 323 (M^{+}).

2.7.5. General procedure for synthesis of compounds 16-30: A vial equipped with stirring bar was charged with 6-bromo-8-substituted-imidazo[1,2-*a*]pyrazine (0.1 g, 0.323 mmol), Cs_2CO_3 (0.105 g, 0.323 mmol) and boronic acid (0.323 mmol), dissolved in MeCN:H_2O (9:1) at 100 ^{o}C under inert atmosphere. Then, 5 mol% of $Pd(PPh_3)_4$ was added, vial was capped and refluxed for 6-12 h. After the completion of the reaction (monitored by TLC), cooled the reaction mixture, and then extracted the reaction mixture with water and chloroform. Organic layer was dried over sodium sulphate, filtered and concentrated under *vacuo* to get crude product. The residue was purified by silica gel (100-200 mesh) column chromatography using hexane:ethyl acetate as eluent to give pure solid.

Spectral data 4"-(8-(4'-fluorophenyl)imidazo[1,2-*a*]pyrazin-6-yl)benzaldehyde (16): Off

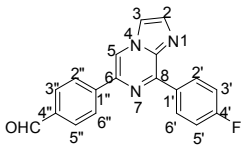

white solid; Yield: 82%; mp 208-210 ^{o}C; ^{1}H NMR ($CDCl_3$, 400 MHz): δ 7.29-7.25 (m, 2H, $C_{2'}H$ and $C_{6'}H$), 7.83 (d, J = 0.92 Hz, 1H, C_2H), 7.90 (d, J = 1.36 Hz, 1H, C_3H), 8.03 (d, J = 8.68 Hz, 2H, $C_{2"}H$ and $C_{6"}H$), 8.26 (d, J = 8.72 Hz, 2H, $C_{3"}H$ and $C_{5"}H$), 8.58 (s, 1H, C_5H), 8.95-8.92 (dd, ^{2}J = 9.16 Hz, ^{3}J = 5.70 Hz, 2H, $C_{3'}H$ and $C_{5'}H$), 10.10 (s, 1H, CHO); ^{13}C NMR ($CDCl_3$, 100 MHz): δ 114.71,

115.11, 115.37, 115.58, 126.61, 130.34, 131.88, 131.97, 135.68, 136.19, 137.27, 138.64, 142.27, 147.95, 163.22, 165.73 (ArC), 191.83 (CHO); Mass (EI): m/z 318 (M^++1).

Spectral data 2”-(8-(4’-fluorophenyl)imidazo[1,2-*a*]pyrazin-6-yl)phenol (17): Yellow solid;

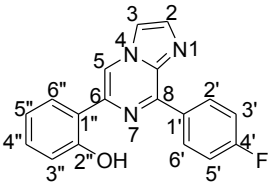

Yield: 80%; mp 158-160 ^oC; ^1H NMR ($CDCl_3$, 400 MHz): δ 6.96 (t, *J* = 7.56 Hz, 1H, $C_{5”}H$), 7.06 (d, *J* = 8.24 Hz, 1H, $C_{6”}H$), 7.35 -7.26 (m, $C_{2’}H$, 3H, $C_{6’}H$ and $C_{4”}H$), 7.65-7.63 (dd, ^2J = 8.24 Hz, ^3J = 1.40 Hz, 1H, $C_{3”}H$), 7.87 (s, 1H, C_2H), 7.95 (s, 1H, C_3H), 8.58 (s, 1H, C_5H), 8.69-8.66 (dd, ^2J = 8.68 Hz, ^3J = 5.50 Hz, 2H, $C_{3’}H$ and $C_{5’}H$); ^{13}C NMR ($CDCl_3$, 100 MHz): δ 113.41, 115.00, 115.79, 116.00, 117.32, 118.59, 119.55, 124.88, 130.73, 130.76, 130.95, 131.69, 131.77, 136.50, 137.61, 139.06, 146.35, 157.97, 163.32, 165.83 (ArC); Mass (EI): m/z 306 (M^++1).

Spectral data 6-(4”-chlorophenyl)-8-(4’-fluorophenyl)imidazo[1,2-*a*]pyrazine (18): Light

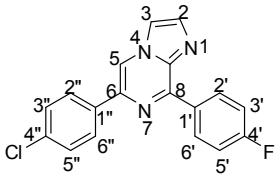

green solid; Yield: 62%; mp 136-138 ^oC; ^1H NMR ($CDCl_3$, 400 MHz): δ 7.27-7.23 (m, 2H, $C_{2’}H$ and $C_{6’}H$), 7.47 (d, *J* = 8.72 Hz, 2H, $C_{2”}H$ and $C_{6”}H$), 7.78 (d, *J* = 1.40 Hz, 1H, C_2H), 7.86 (d, *J* = 0.92 Hz, 1H, C_3H), 7.98 (d, *J* = 8.72 Hz, 2H, $C_{3”}H$ and $C_{5”}H$), 8.42 (s, 1H, C_5H), 8.92-8.88 (dd, ^2J = 9.16 Hz, ^3J = 5.74 Hz, 2H, $C_{3’}H$ and $C_{5’}H$); ^{13}C NMR ($CDCl_3$, 100 MHz): δ 113.73, 114.40, 115.20, 115.42, 127.29, 128.98, 131.75, 131.83, 131.98, 132.01, 134.63, 134.88, 135.32, 137.49, 138.44, 147.46, 163.06, 165.56 (ArC); Mass (EI): m/z 324 (M^++1).

Spectral data 8-(4’-chlorophenyl)-6-(thiophen-2”-yl)imidazo[1,2-*a*]pyrazine (19): Green

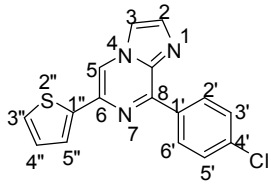

solid; Yield: 70%; mp 135-137 ^oC; ^1H NMR ($CDCl_3$, 400 MHz): δ 7.14 (t, *J* = 4.36 Hz, 1H, $C_{4”}H$), 7.40 (d, *J* = 5.04 Hz, 1H, $C_{5”}H$), 7.51 (d, *J* = 8.72 Hz, 2H, $C_{2’}H$ and $C_{6’}H$), 7.56 (d, *J* = 3.20 Hz, 1H, $C_{3”}H$), 7.74 (s, 1H, C_2H), 7.84 (s, 1H, C_3H), 8.39 (s, 1H, C_5H), 8.85 (d, *J* = 9.16 Hz, 2H, $C_{3’}H$ and $C_{5’}H$); ^{13}C NMR ($CDCl_3$, 100 MHz): δ 112.31, 114.44, 123.31, 126.76, 128.17, 128.66, 131.16, 134.16, 134.87, 135.46, 136.86, 138.52, 141.57, 147.37 (ArC); Mass (EI): m/z 312 (M^++1).

Spectral data 4”-(8-(4’-chlorophenyl)imidazo[1,2-*a*]pyrazin-6-yl)benzaldehyde (20):

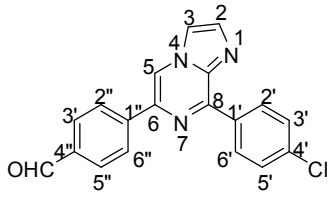

Light yellow solid; Yield: 65%; mp 204-207 ^oC; ^1H NMR ($CDCl_3$, 400 MHz): δ 7.56 (d, *J* = 8.68 Hz, 2H, $C_{2”}H$ and $C_{6”}H$), 7.84 (d, *J* = 0.92 Hz, 1H, C_2H), 7.91 (d, *J* = 0.92 Hz, 1H, C_3H), 8.04 (d, *J* = 8.28 Hz, 2H, $C_{2’}H$ and $C_{6’}H$), 8.25 (d, *J* = 8.28 Hz, 2H, $C_{3’}H$ and $C_{5’}H$), 8.60 (s, 1H,

C_5H), 8.88 (d, J = 8.68 Hz, 2H, $C_{3''}H$ and $C_{5''}H$), 10.10 (s, 1H, CHO); ^{13}C NMR ($CDCl_3$, 100 MHz): δ 114.82, 115.41, 126.71, 128.77, 130.46, 131.16, 134.28, 135.84, 136.31, 137.05, 137.39, 138.72, 142.29, 147.91 (ArC), 191.94 (CHO); Mass (EI): m/z 334 (M^++1).

Spectral data 2”-(8-(4’-chlorophenyl)imidazo[1,2-*a*]pyrazin-6-yl)phenol (21): Yellow solid;

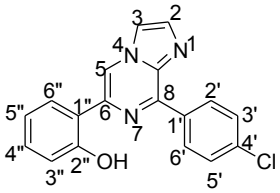

Yield: 68%; mp 172-174 ^oC; ^1H NMR ($CDCl_3$, 400 MHz): δ 6.97- 6.93 (m, 1H, $C_{5''}H$), 7.06-7.04 (dd, ^2J = 8.24 Hz, ^3J = 0.92 Hz, 1H, $C_{6''}H$), 7.34-7.30 (m, 1H, $C_{4''}H$), 7.56 (d, J = 8.72 Hz, 2H, $C_{2'}H$ and $C_{6'}H$), 7.64-7.62 (dd, ^2J = 8.24 Hz, ^3J = 1.62 Hz, 1H, $C_{3'}H$), 7.87 (d, J = 0.92 Hz, 1H, C_2H), 7.95 (d, J = 0.92 Hz, 1H, C_3H), 8.59 (s, 1H, C_5H), 8.61 (d, J = 8.68 Hz, 2H, $C_{3'}H$ and $C_{5'}H$); ^{13}C NMR ($CDCl_3$, 100 MHz): δ 113.77, 115.14, 117.45, 118.77, 119.73, 125.05, 129.17, 130.95, 131.15, 133.12, 136.72, 137.59, 137.76, 139.30, 146.44, 158.07 (ArC); Mass (EI): m/z 322 (M^++1).

Spectral data 8-(4’-chlorophenyl)-6-(furan-2”-yl)imidazo[1,2-*a*]pyrazine (22): White

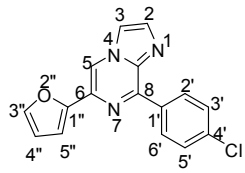

solid; Yield: 72%; mp 159-161 ^oC; ^1H NMR ($CDCl_3$, 400 MHz): δ 6.58-6.56 (dd, ^2J = 3.2 Hz, ^3J = 1.84 Hz, 1H, $C_{4''}H$), 7.12 (d, J = 2.72 Hz, 1H, $C_{5''}H$), 7.54-7.51 (m, 3H, $C_{3''}H$, $C_{2'}H$ and $C_{6'}H$), 7.76 (d, J = 1.4 Hz, 1H, C_2H), 7.84 (d, J = 1.36 Hz, 1H, C_3H), 8.43 (s, 1H, C_5H), 8.80 (d, (J = 6.88 Hz, 2H, $C_{3'}H$ and $C_{5'}H$); ^{13}C NMR ($CDCl_3$, 100 MHz): 108.72, 112.14, 112.49, 114.73, 128.68, 131.14, 132.08, 134.28, 135.38, 136.83, 138.50, 142.78, 148.06, 151.58 (ArC); Mass (EI): m/z 296 (M^++1).

Spectral data 8-(4’-chlorophenyl)-6-(4”-fluorophenyl)imidazo[1,2-*a*]pyrazine (23):

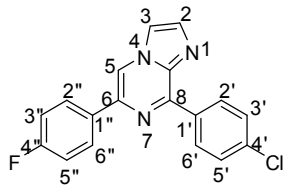

White solid; Yield: 70%; mp 134-135 ^oC; ^1H NMR ($CDCl_3$, 400 MHz): δ 7.19 (t, J = 8.72 Hz, 2H, $C_{2''}H$ and $C_{6''}H$), 7.52 (d, J = 8.72 Hz, 2H, $C_{2'}H$ and $C_{6'}H$), 7.77 (d, J = 1.36 Hz, 1H, C_2H), 7.85 (d, J = 0.92 Hz, 1H, C_3H), 8.03-7.99 (dd, ^2J = 9.16 Hz, ^3J = 5.26 Hz, 2H, $C_{3''}H$ and $C_{5''}H$), 8.39 (s, 1H, C_5H), 8.84 (d, J = 8.68 Hz, 2H, $C_{3'}H$ and $C_{5'}H$); ^{13}C NMR ($CDCl_3$, 100 MHz): 113.68, 114.33, 115.67, 115.89, 127.81, 127.89, 128.47, 130.92, 132.45, 134.28, 135.27, 136.59, 137.78, 138.34, 147.17, 161.92, 164.39 (ArC); Mass (EI): m/z 324 (M^++1).

Spectral data 8-(4’-chlorophenyl)-6-(4”-methoxyphenyl)imidazo[1,2-*a*]pyrazine (24): White

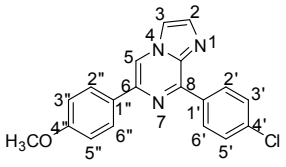

solid; Yield: 74%; mp 115-117 ^{o}C; ^{1}H NMR ($CDCl_3$, 400 MHz): δ 3.88 (s, 3H, OCH_3), 7.03 (d, J = 8.68 Hz, 2H, $C_{2'}H$ and $C_{6'}H$), 7.52 (d, J = 8.72 Hz, 2H, $C_{2''}H$ and $C_{6''}H$), 7.75 (d, J = 1.4 Hz, 1H, C_2H), 7.83 (d, J = 1.36 Hz, 1H, C_3H), 7.97 (2H, d, J = 8.68 Hz, $C_{3'}H$ and $C_{5'}H$), 8.36 (s, 1 H, C_5H), 8.85 (d, J = 8.28 Hz, 2H, $C_{3''}H$ and $C_{5''}H$); ^{13}C NMR ($CDCl_3$, 100 MHz): 108.72, 112.14, 112.49, 114.73, 128.68, 131.14, 132.08, 134.28, 135.38, 136.83, 138.50, 142.78, 148.06, 151.58 (ArC); Mass (EI): m/z 336 (M^++1).

Spectral data 4'-(6-(thiophen-2"-yl)imidazo[1,2-*a*]pyrazin-8-yl)benzaldehyde (25): Green

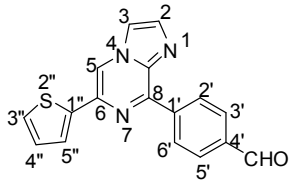

solid; Yield: 52%; mp 165-167 ^{o}C; ^{1}H NMR ($CDCl_3$, 400 MHz): δ 7.14 (t, J = 4.36 Hz, 1H, $C_{4''}H$), 7.42-7.40 (dd, ^{2}J = 5.04 Hz, ^{3}J = 1.36 Hz, 1H, $C_{5''}H$), 7.59-7.57 (dd, ^{2}J = 3.64 Hz, ^{3}J = 0.92 Hz, 1H, $C_{3''}H$), 7.77 (d, J = 0.92 Hz, 1H, C_2H), 7.86 (d, J = 0.8 Hz, 1H, C_3H), 8.05 (d, J = 8.24 Hz, 2H, $C_{2'}H$ and $C_{6'}H$), 8.43 (s, 1H, C_5H), 9.03 (d, J = 8.24 Hz, 2H, $C_{3'}H$ and $C_{5'}H$), 10.12 (s, 1H, CHO); ^{13}C NMR ($CDCl_3$, 100 MHz): δ 112.92, 114.56, 123.56, 126.96, 128.26, 129.70, 130.41, 135.14, 135.86, 137.30, 138.76, 141.19, 141.31, 147.20 (ArC), 192.36 (CHO); Mass (EI): m/z 306 (M^++1).

Spectral data 4"-(8-(4'-methoxyphenyl)imidazo[1,2-*a*]pyrazin-6-yl)benzaldehyde (26): Off

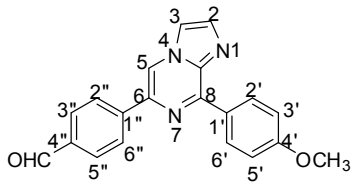

white solid; Yield: 85%; mp 190-192 ^{o}C; ^{1}H NMR ($CDCl_3$, 400 MHz): δ 3.92 (s, 3H, OCH_3), 7.11 (d, J = 9.16 Hz, 2H, $C_{2'}H$ and $C_{6'}H$), 7.80 (d, J = 0.92 Hz, 1H, C_2H), 7.88 (d, J = 0.92 Hz, 1H, C_3H), 8.03 (d, J = 8.72 Hz, 2H, $C_{2''}H$ and $C_{6''}H$), 8.27 (d, J = 8.28 Hz, 2H, $C_{3''}H$ and $C_{5''}H$), 8.54 (s, 1H, C_5H), 8.90 (d, J = 9.16 Hz, 2H, $C_{3'}H$ and $C_{5'}H$), 10.10 (s, 1H, CHO); ^{13}C NMR ($CDCl_3$, 100 MHz): δ 55.37 (OCH_3), 113.75, 114.47, 114.51, 126.48, 128.44, 130.21, 131.37, 135.27, 136.00, 137.64, 138.59, 142.48, 148.46, 161.68 (ArC), 191.84 (CHO); Mass (EI): m/z 330 (M^++1).

Spectral data 2"-(8-(4'-methoxyphenyl)imidazo[1,2-*a*]pyrazin-6-yl)phenol (27): Yellow

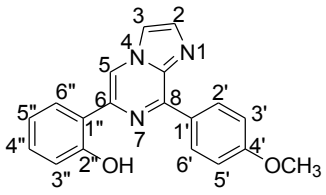

solid; Yield: 75%; mp 125-127 ^{o}C; ^{1}H NMR ($CDCl_3$, 400 MHz): δ 3.92 (s, 3H, OCH_3), 6.97-6.93 (m, 1H, $C_{5''}H$), 7.07-7.05 (dd, ^{2}J = 8.28 Hz, ^{3}J = 0.92 Hz, 1H, $C_{6''}H$), 7.11 (d, J = 9.16 Hz, 2H, $C_{2'}H$ and $C_{6'}H$), 7.34-7.30 (m, 1H, $C_{4''}H$), 7.66-7.63 (dd, ^{2}J = 7.80 Hz, ^{3}J = 1.60 Hz,

1H, $C_{3''}H$), 7.84 (d, *J* = 0.92 Hz, 1H, C_2H), 7.93 (d, *J* = 0.92 Hz, 1H, C_3H), 8.54 (s, 1H, C_5H), 8.66 (d, *J* = 9.16 Hz, 2H, $C_{3'}H$ and $C_{5'}H$); ^{13}C NMR ($CDCl_3$, 100 MHz): δ 55.40 (OCH_3), 112.66, 114.12, 114.82, 117.43, 118.48, 119.34, 124.77, 127.09, 130.71, 131.21, 136.05, 137.60, 138.89, 146.85, 158.09, 161.97 (ArC); Mass (EI): m/z 318 (M^++1).

Spectral data 6-(4”-fluorophenyl)-8-(4’-methoxyphenyl)imidazo[1,2-*a*]pyrazine (28):

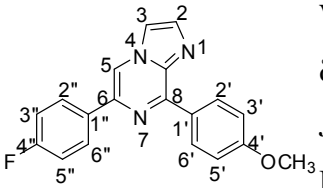

White solid; Yield: 68%; mp 108-110 ^oC; ^1H NMR ($CDCl_3$, 400 MHz): δ 3.91 (s, 3H, OCH_3), 7.09 (d, *J* = 9.16 Hz, 2H, $C_{2'}H$ and $C_{6'}H$), 7.19 (t, *J* = 8.46 Hz, 2H, $C_{2''}H$ and $C_{6''}H$), 7.75 (s, 1H, C_2H), 7.84 (d, *J* = 0.92 Hz, 1H, C_3H), 8.05-8.02 (dd, ^2J = 8.72 Hz, ^3J = 5.50 Hz, 2H, $C_{3''}H$ and $C_{5''}H$), 8.36 (s, 1H, C_5H), 8.87 (d, *J* = 9.16 Hz, 2H, $C_{3'}H$ and $C_{5'}H$); ^{13}C NMR ($CDCl_3$, 100 MHz): δ 55.37 (OCH_3), 112.92, 113.71, 114.20, 115.62, 115.83, 127.87, 127.94, 128.67, 131.30, 132.86, 132.89, 134.97, 137.81, 138.50, 148.22, 161.52, 161.88, 164.34 (ArC); Mass (EI): m/z 320 (M^++1).

Spectral data 6-(4”-chlorophenyl)-8-(4’-methoxyphenyl)imidazo[1,2-*a*]pyrazine (29): White

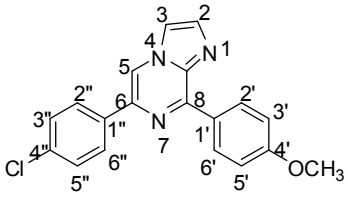

solid; Yield: 76%; mp 119-121 ^oC; ^1H NMR ($CDCl_3$, 400 MHz): δ 3.91 (s, 3H, OCH_3), 7.09 (d, *J* = 9.16 Hz, 2H, $C_{2'}H$ and $C_{6'}H$), 7.46 (d, *J* = 8.68 Hz, 2H, $C_{2''}H$ and $C_{6''}H$), 7.74 (d, *J* = 1.36 Hz, 1H, C_2H), 7.84 (d, *J* = 0.92 Hz, 1H, C_3H), 7.99 (d, *J* = 8.68 Hz, 2H, $C_{3''}H$ and $C_{5''}H$), 8.37 (s, 1H, C_5H), 8.86 (d, 2H, *J* = 9.16 Hz, $C_{3'}H$ and $C_{5'}H$); ^{13}C NMR ($CDCl_3$, 100 MHz): δ 55.35 (OCH_3), 113.15, 113.69, 114.26, 127.32, 128.59, 128.91, 137.29, 134.44, 135.00, 135.17, 137.46, 138.50, 148.20, 161.53 (ArC), Mass (EI): m/z 336 (M^++1).

Spectral data 8-(4’-methoxyphenyl)-6-(thiophen-2”-yl)imidazo[1,2-*a*]pyrazine (30): White

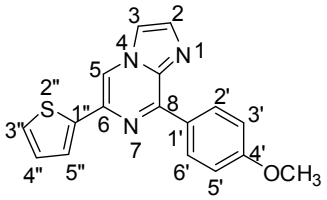

solid; Yield: 70%; mp 120-122 ^oC; ^1H NMR ($CDCl_3$, 400 MHz): δ 3.91 (s, 3H, OCH_3), 7.09 (d, *J* = 9.20 Hz, 2H, $C_{2'}H$ and $C_{6'}H$), 7.15 - 7.13 (dd, ^2J = 5.04 Hz, ^3J = 3.68 Hz, 1H, $C_{4''}H$), 7.40-7.39 (dd, ^2J = 5.04 Hz, ^3J = 0.92 Hz, 1H, $C_{5''}H$), 7.58-7.57 (dd, ^2J = 3.68 Hz, ^3J = 0.92 Hz, 1H, $C_{3''}H$), 7.72 (d, *J* = 1.36 Hz, 1H, C_2H), 7.85 (d, *J* = 0.92 Hz, 1H, C_3H), 8.35 (s, 1H, C_5H), 8.87 (d, *J* = 9.16 Hz, 2H, $C_{3'}H$ and $C_{5'}H$); ^{13}C NMR ($CDCl_3$, 100 MHz): δ 55.38 (OCH_3), 113.74, 114.42, 114.16, 123.01, 126.45, 127.99, 128.40, 131.43, 134.76, 135.04, 138.54, 141.94,

148.32, 161.23 (ArC); Mass (EI): m/z 308 (M^++1).

2.7.6. *In vitro* anticancer screening assay

The *in vitro* anticancer screening at NCI was a two-stage process, beginning with the evaluation of all compounds against the 60 cell lines at a single dose of 10 μM. The output from the single dose screen was reported as a mean graph and was available for analysis by the COMPARE program. Compounds which exhibited significant growth inhibition were evaluated against the 60 cell panel at five concentration levels. The human tumor cell lines of the cancer screening panel were grown in RPMI 1640 medium containing 5% fetal bovine serum and 2 mM L-glutamine. For a typical screening experiment, cells were inoculated into 96 well microtiter plates in 100 mL at plating densities ranging from 5000 to 40,000 cells/well depending on the doubling time of individual cell lines. After cell inoculation, the microtiter plates were incubated at 37^o C, 5% CO_2, 95% air and 100% relative humidity for 24 h prior to addition of experimental drugs. After 24 h, two plates of each cell line were fixed in situ with TCA, to represent a measurement of the cell population for each cell line at the time of drug addition (Tz). Experimental drugs were solubilized in dimethyl sulfoxide at 400 fold the desired final maximum test concentration and stored frozen prior to use. At the time of drug addition, an aliquot of frozen concentrate was thawed and diluted to twice the desired final maximum test concentration with complete medium containing 50 μg/ml gentamicin. Additional four, 10-fold or ½ log serial dilutions were made to provide a total of five drug concentrations plus control. Aliquots of 100 μL of these different drug dilutions were added to the appropriate microtiter wells already containing 100 μL of medium, resulting in the required final drug concentrations.

Following drug addition, the plates were incubated for an additional 48 h at 37 ^{o}C, 5% CO_2, 95% air, and 100% relative humidity. For adherent cells, the assay was terminated by the addition of cold TCA. Cells were fixed *in situ* by the gentle addition of 50 μL of cold 50% (w/v) TCA (final concentration, 10% TCA) and incubated for 60 min at 4 ^{o}C. The supernatant was discarded, and the plates were washed five times with tap water and air dried. Sulforhodamine B (SRB) solution (100 μl) at 0.4% (w/v) in 1% acetic acid was added to each well, and plates were incubated for 10 min at room temperature. After staining, unbound dye was removed by washing five times with 1% acetic acid and the plates were air dried. Bound stain was subsequently solubilized with 10 mM trizma base, and the absorbance was read on an automated plate reader at a wavelength of 515 nm. For suspension cells, the methodology was the same except that the

assay was terminated by fixing settled cells at the bottom of the wells by gently adding 50 μL of 80% TCA (final concentration, 16% TCA). Using the seven absorbance measurements [time zero, (Tz), control growth, (C), and test growth in the presence of drug at the five concentration levels (Ti)], the percentage growth was calculated at each of the drug concentrations levels. Percentage growth inhibition was calculated as:

$[(Ti - Tz)/(C-Tz)] \times 100$ for concentrations for which $Ti >= Tz$

$[(Ti – Tz)/Tz] \times 100$ for concentrations for which $Ti < Tz$:

Three dose response parameters were calculated for each experimental agent. Growth inhibition of 50% (GI_{50}) was calculated from $[(Ti-Tz)/(C-Tz)] \times 100 = 50$, which was the drug concentration resulting in a 50% reduction in the net protein increase (as measured by SRB staining) in control cells during the drug incubation. The drug concentration resulting in total growth inhibition (TGI) was calculated from $Ti = Tz$. The LC_{50} (concentration of drug resulting in a 50% reduction in the measured protein at the end of the drug treatment as compared to that at the beginning) indicating a net loss of cells following treatment was calculated from $[(Ti-Tz) / Tz] \times 100 = -50$.

CHAPTER 3

IMIDAZO[1,2-*a*]PYRAZINE-COUMARIN HYBRIDS

3.1. INTRODUCTION

Heterocyclic moieties play an important role in pharmaceutical, veterinary and agrochemicals.[109] Among various heterocycles, imidazo[1,2-*a*]pyrazine, is a well known privileged fused heterocyclic motif and has attracted its importance in search for anticancer agents by various modifications at different positions of the core to improve their biological profile.[93,110] The imidazo[1,2-*a*]pyrazine exhibited prominent anticancer activity through inhibition of Aurora kinase,[89] phosphoinositide-3-kinase,[9] breast tumor kinase/protein tyrosine kinase 6,[10] check point kinase,[14] spleen tyrosine kinase,[111] topoisomerase-II[13] and cyclin dependent kinase [7] (Figure 1). Coumarin is also a biologically active heterocyclic moiety possessing anticancer,[112] anti HIV,[113] antituberculosis,[114] antihypercholestrolemic activities[115] etc. It is a decade of molecular hybridization to obtain a more active pharmacophore in a single biological molecule by joining the two heterocyclic pharmacophores.[116] Concept of hybridization led to a revolution in the field of drug design and development to obtain a hybrid drug with improved characteristics and minimize side effects as compared to parent molecules. Therefore, hybrids of coumarin with various heterocyclic moieties viz., coumarin-benzimidazole,[117] coumarin-benzothiazole[118] and coumarin-chalcone[119] (Figure 2) have been reported in the literature, with great biological significance as anticancer agents.

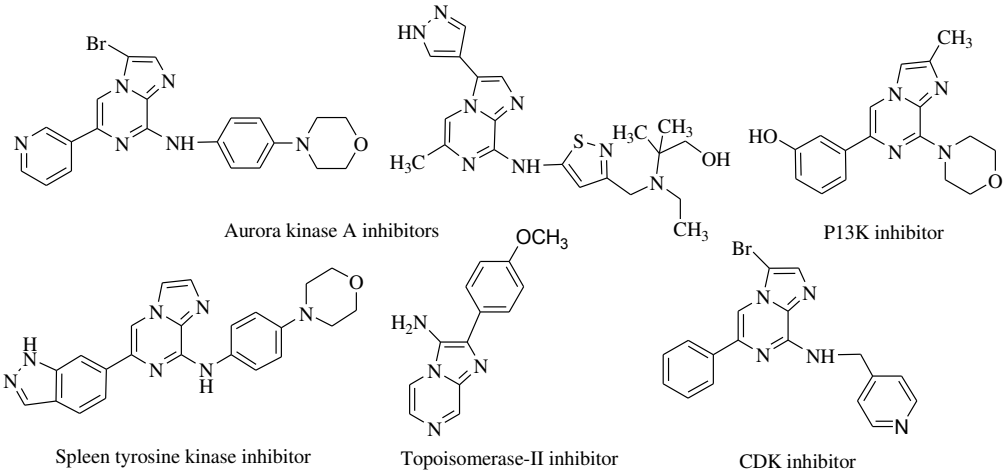

Figure 1 Imidazo[1,2-*a*]pyrazines based anticancer agents

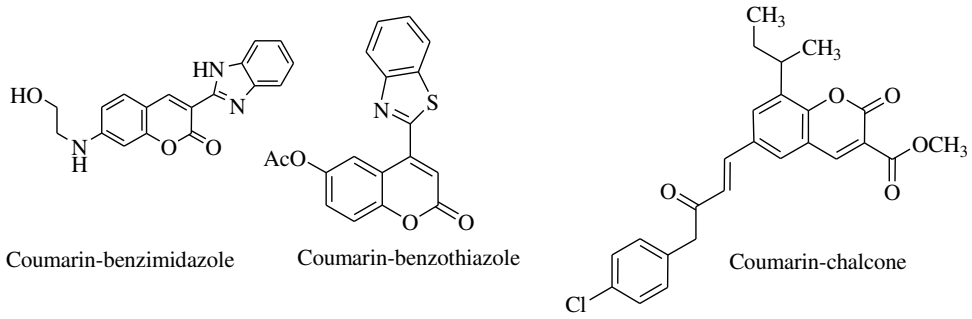

Figure 2 Coumarin based hybrids as anticancer agents

3.2. OBJECTIVE

To the best of my knowledge, no reports for anticancer activity of imidazo[1,2-*a*]pyrazine with biologically active coumarin moiety have been known in literature till now. In view of the previous rationale for new structural leads with potential chemotherapeutic activities using molecular hybridization, in the present study, a new series of hybrid using imidazo[1,2-*a*]pyrazine and coumarin has been synthesized. These compounds have further been approached for Suzuki-Miyaura cross coupling reaction for monoarylation at C6 position, and symmetrical/unsymmetrical diarylation at C3 and C6 positions. These compounds were further screened for their *in vitro* anticancer activity on a panel of 60 human cancer cell lines viz., leukaemia, non small cell lung, colon, CNS, melanoma, ovarian, renal, prostate and breast. Molecular docking studies have also been performed to support the effective binding of compound at the active site of the enzyme.

3.3. CHEMISTRY

2-Aminopyrazine **1** was treated with *N*-bromosuccinimide (NBS) in DMSO and water (9:1) at room temperature for 6 h to give 2-amino-3,5-dibromopyrazine **2** in 90% yield followed by cyclization with 50% aq. chloroacetaldehyde in isopropyl alcohol at 110 ^{o}C for 12 h to obtain 6,8-dibromoimidazo[1,2-*a*]pyrazine **3** in 80% yield. Bromination was done with compound **3** in the presence of NBS in acetonitrile (ACN) at room temperature for 2 h to afford 3,6,8-tribromoimidazo[1,2-*a*]pyrazine **4**[120] in 90% yield. 3,6,8-Tribromoimidazo[1,2-*a*]pyrazine **4** was then stirred with 7-hydroxy-4-methylcoumarin **5** in the presence of K_2CO_3 and DMF at room temperature for 12 h to afford 7'-(3,6-dibromoimidazo[1,2-*a*]pyrazin-8-yloxy)-4'-methyl-2*H*-chromen-2'-one **6** in 85% yield (Scheme 1).

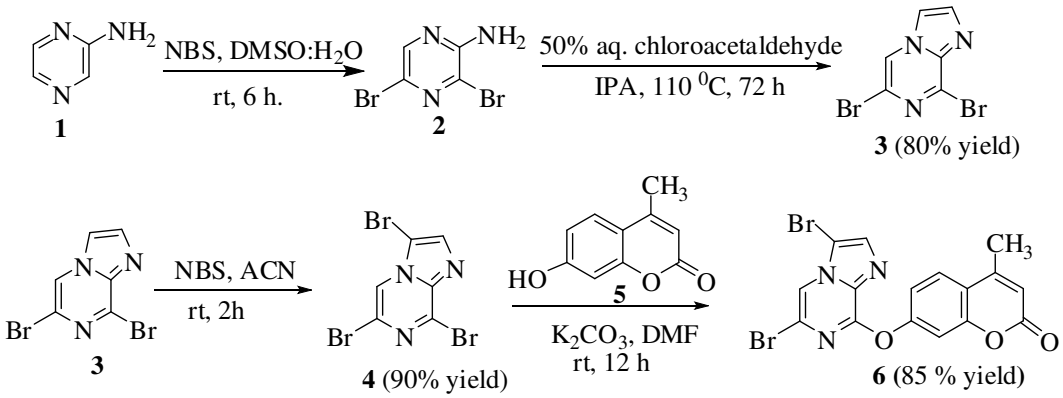

Scheme 1 Synthesis of imidazo[1,2-*a*]pyrazine-coumarin hybrid

Palladium catalyzed Suzuki-Miyaura cross coupling of compound **6** with 2-methoxyphenyl boronic acid (1 eq.) in the presence of K_2CO_3 (1 eq.) and 5 mol% of $Pd(PPh_3)_4$ in DME:H_2O (9:1) under inert atmosphere afforded C6-monoarylated **7a** and C3, C6 diarylated **7b** products in 61% and 33% yields, respectively (Table 1, entry 1). Similarly, compound **6** was also treated with 2-furan boronic acid under same reaction conditions to give compounds **8a** and **8b** in 48% and 25% yields, respectively (Table 1, entry 2). Reaction of compound **6** with 4-chlorophenyl boronic acid afforded C6 monoarylated product **9a** and C3, C6 diarylated product **9b** in 40% and 42% yields (GCMS), respectively. These two compounds could not be separated through column chromatography and used as such without purification (Table 1, entry 3). However, reactions of **6** with other aryl boronic acids under the same reaction conditions gave only C3, C6 diarylated products **10b-19b** with 54-74% yields (Table 1, entries 4-13). Monoarylated products with these boronic acids could not be separated as these were formed only in traces, i.e. < 5% (determined by GCMS). Reaction of compound **6** with naphthalene-1-boronic acid could not give a successful attempt. This might be due to steric crowding of the bulky naphthyl ring.

Table 1 Reactions of 3,6-dibromoimidazo[1,2-*a*]pyrazine-coumarin hybrid **6** with aryl boronic acids

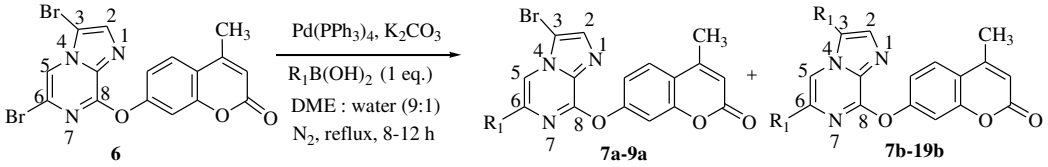

Entry	Time (h)	R_1	Products [#]	
1	8	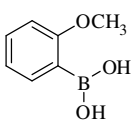	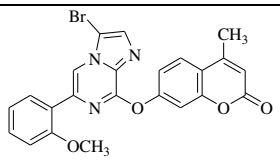 **7a** (61)	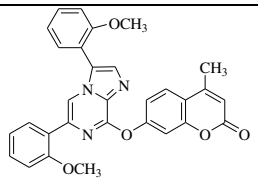 **7b** (33)
2	11	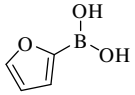	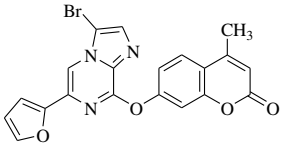 **8a** (48)	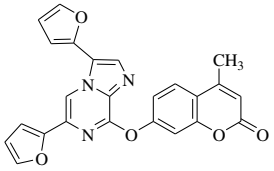 **8b** (25)
3	10	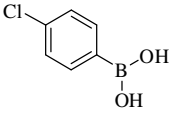	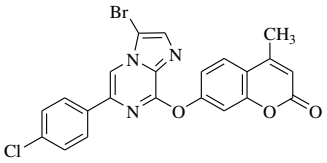 **9a** (40)*	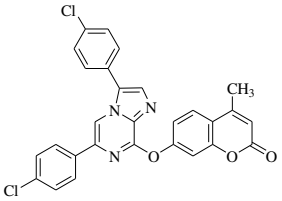 **9b** (42)
4	10	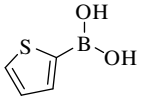	-----	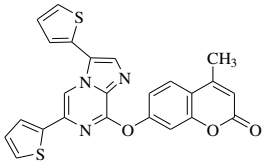 **10b** (66)
5	9	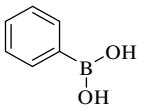	-----	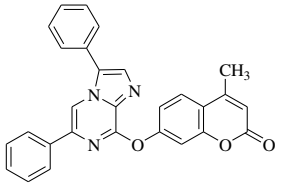 **11b** (74)
6	12	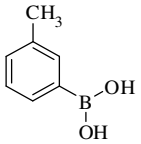	-----	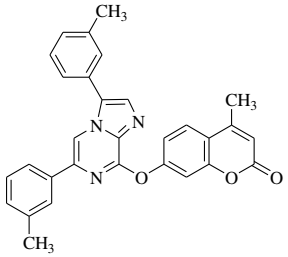 **12b** (70)

7	12	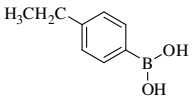	-----	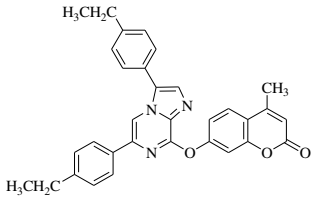 **13b** (69)
8	9	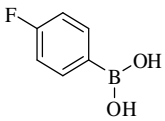	-----	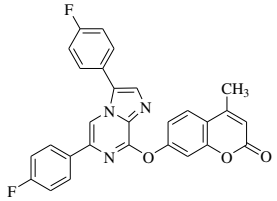 **14b** (72)
9	12	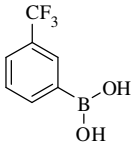	-----	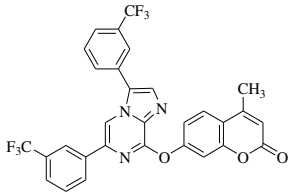 **15b** (60)
10	8	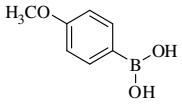	-----	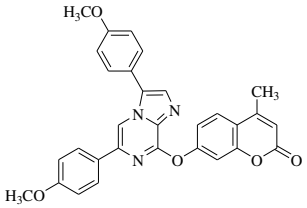 **16b** (73)
11	10	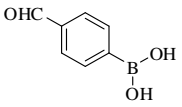	-----	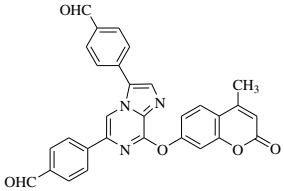 **17b** (70)
12	11	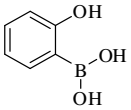	-----	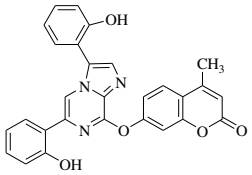 **18b** (68)
13	12	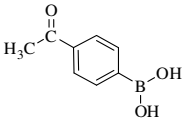	-----	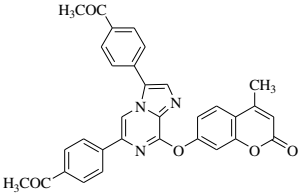 **19b** (54)

[#] isolated yields, --,*GC-MS yields (< 5%)

Subsequently use of monoarylated product has been implemented for unsymmetrical diarylation via cross coupling reaction at C3 position. Monoarylated imidazo[1,2-*a*]pyrazine-coumarin hybrid **7a** was further refluxed with variety of aryl boronic acids (1.0 eq.) in the presence of 5 mol% of $Pd(PPh_3)_4$, K_2CO_3 (1.1 eq.) in DME:H_2O (9:1) for 6-8 h to give C3, C6 unsymmetrical diarylated imidazo[1,2-*a*]pyrazine-coumarin hybrids **20**-**29** in 52-75% yields (Table 2). However, Suzuki reaction of mixture of monoarylated and symmetrical diarylated compounds (**9a** and **9b)** with 2-thiophene boronic acid under the same reaction conditions afforded C3, C6 symmetrical and unsymmetrical disubstituted imidazo[1,2-*a*]pyrazine-coumarin hybrids **9b** and **30** in 42% and 61% yields, respectively. All the synthesized compounds have been well characterized by ^1H and ^{13}C NMR as well as mass spectrometry.

Table 2 Reactions of monoarylated-3-bromoimidazo[1,2-*a*]pyrazine-coumarin hybrids **7a** and **9a** with different aryl boronic acids

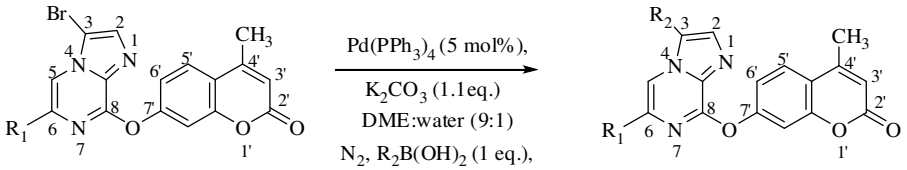

7a, R_1 = 2-methoxy phenyl
9a, R_1 = 4-chloro phenyl

20-30

Entry	Starting Material	$R_2B(OH)_2$	Product	Time (h)	Yield (%)[#]	mp (^oC)
1	**7a**	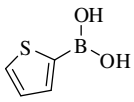	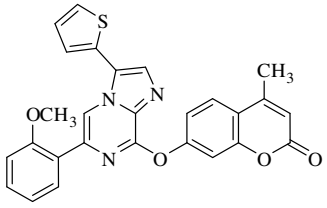	6	**20** (64)	221-223
2	**7a**	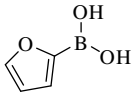	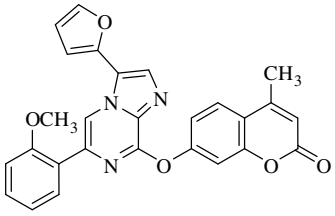	7	**21** (52)	204-205

3	**7a**	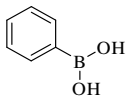	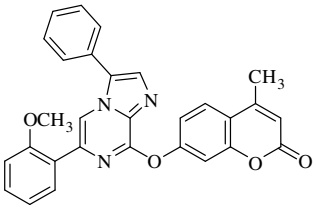	6	**22** (69)	194-195
4	**7a**	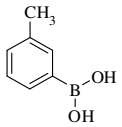	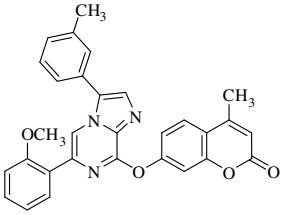	8	**23** (72)	202-203
5	**7a**	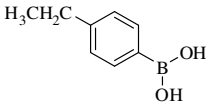	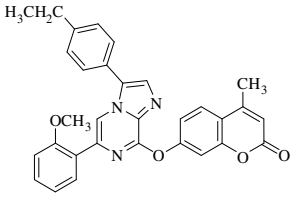	8	**24** (55)	179-180
6	**7a**	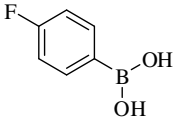	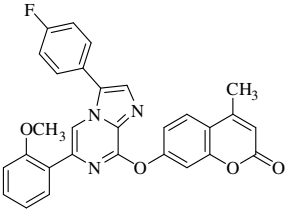	7	**25** (75)	235-237
7	**7a**	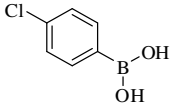	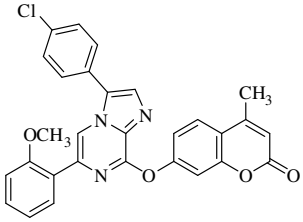	7	**26** (65)	243-245
8	**7a**	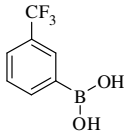	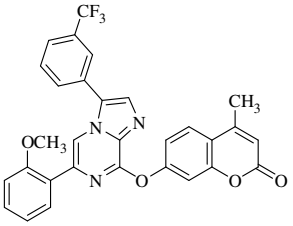	8	**27** (55)	204-206
9	**7a**	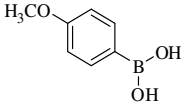	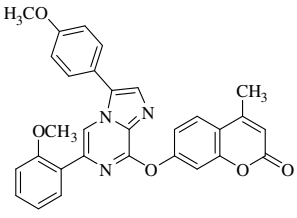	7	**28** (64)	239-241

10	**7a**	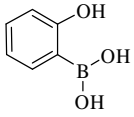	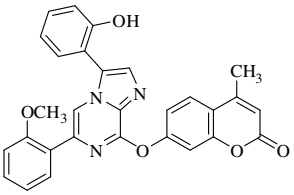	8	**29** (53)	>300
11	**9a**	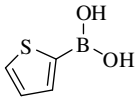	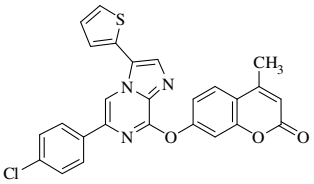	8	**30** (61)	187-189

[#].isolated yield

The assigned regiochemistry of monoarylation at C6 position and unsymmetrical diarylation at C3 and C6 positions of imidazo[1,2-*a*]pyrazine-coumarin hybrid was confirmed by considering 2D NOE difference experiments. Singlet of C5H of imidazo[1,2-*a*]pyrazine **7a** showed positive NOE signal with protons of methoxy group of 2-methoxyphenyl ring while negative NOE signal of singlet of C2H of imidazo[1,2-*a*]pyrazine with protons of methoxy group of 2-methoxyphenyl ring was observed, indicating the monoarylation primarily at C6 position (Figure 3). On the other hand, singlets of C2H and C5H of imidazo[1,2-*a*]pyrazine ring in compound **28** showed positive NOE signals with C2"'H and C6"'H of 4-methoxyphenyl ring present at C3 position. Due to negative NOE signal of singlet of C2H of imidazo[1,2-*a*]pyrazine with methoxy protons of 2-methoxy phenyl ring (at C6 position) and positive NOE signal with 4-methoxy phenyl ring (at C3 position), confirmed the second arylation at C3 position of imidazo[1,2-*a*]pyrazine **28** (Figure 3).

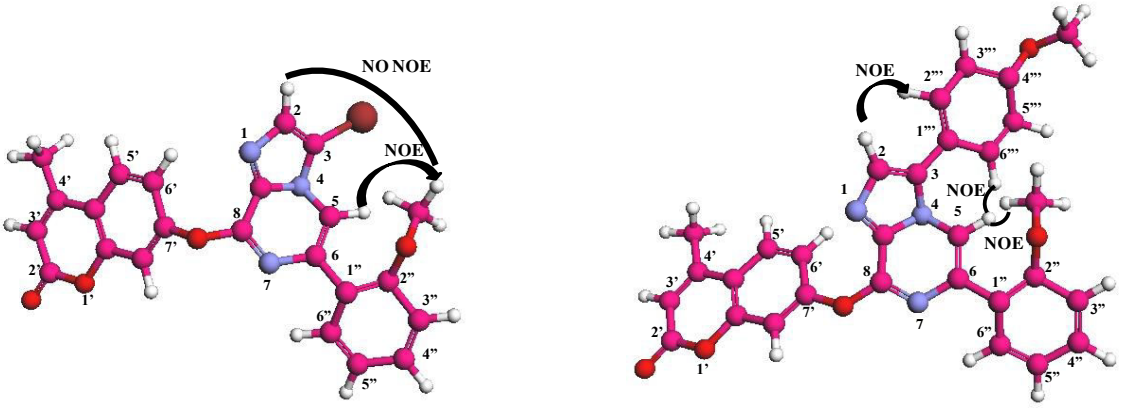

Figure 3 2D NOEs ^{1}H, ^{1}H correlations used for structural assignments of compounds **7a** and **28**

3.4. *IN VITRO* EVALUATION ON CANCER CELL LINES

Compounds **6**, **7a**, **9b**, **10b**, **11b**, **16b**, **28** and **30** were submitted to NCI, USA to test their *in vitro* anticancer activities against a panel of 60 human cancer cell lines at a single dose concentration of 10 μM. Compound **6** with bromo at the C3 and C6 positions showed growth inhibition against the renal cancer cell line 786-0 with a GI value of 71.02% and breast cancer cell lines MCF-7 and MDA-MB-231/ATCC with respective GI values of 77.75% and 70.43%. But monoarylation with 2-methoxy phenyl at the C6 position **7a** displayed poor anticancer activity. Amongst the symmetrical diarylated compounds, 4-chlorophenyl ring at both C3 and C6 positions **9b** showed no significant growth inhibition against cancer cell lines while 2-thiophene moiety at C3 and C6 positions **10b** showed excellent inhibition against non small cell lung cancer cell line HOP-92 with a GI value of 92.29% (Table 3). Replacement with six membered phenyl rings at C3 and C6 positions **11b** exhibited excellent anticancer activity against renal cancer cell line A-498 with GI value of 90.12% while moderate activity was observed against renal cancer RXF-393 and non small cell lung cancer cell line HOP-92 with respective GI values of 71.67% and 77.65%. Substitution with 4-methoxy groups at phenyl rings at C3 and C6 positions of imidazo[1,2-*a*]pyrazine **16b** displayed a broad spectrum of anticancer activity towards various cancer cell lines viz., breast cancer cell line MDA-MB-231/ATCC, melanoma cell line LOX IMVI, CNS cancer cell line SNB-75, non small cell lung cancer cell line A549/ATCC and prostate cancer cell line PC-3 with GI values of 93.71%, 91.98%, 85.69%, 83.52% and 82.27%, respectively. Compound **16b** also displayed good inhibition with other cancer cell lines viz., non small cell lung cancer cell line NCI-H460 (GI = 73.64%), colon cancer cell line HT29 (GI = 74.56%), CNS cancer cell lines U251 (GI = 77.45%) and SF-295 (GI = 76.68%), melanoma cancer cell lines MALME-3M (GI = 73.25%), SK-MEL-5 (GI = 71.37%) and UACC-257 (GI = 70.84%), ovarian cancer cell lines OVCAR-8 (GI = 73.68%), NCI/ADR-RES (GI = 70.09%), renal cancer cell line SN12C (GI = 75.49%), prostate cancer cell line DU-145 (GI = 70.53%) and breast cancer cell line BT-549 (GI = 0.80%) (Table 3, Figure 4). Compound **16b** exhibited more than 70% growth inhibition for most of the tumor cell lines and was much better than 5-fluorouracil (positive control) in tested derivatives. It showed higher activity than 5-fluorouracil (5-FU) in non-small cell lung cancer cells (A549/ATCC, HOP-62, NCI-H23 and NCI-H460), colon cancer cells (HCT-116 and HT-29), melanoma (LOX IMVI, MALME-3M, MDA-MB-435, SK-MEL-5 and UACC-257), prostate cancer (PC-3 and DU-145)

and breast cancer cells (MCF-7, MDA-MB-231/ATCC and BT-549). In the series of unsymmetrical compounds, imidazo[1,2-*a*]pyrazine with 4-methoxy phenyl at C3 and 2-methoxy phenyl at C6 position **28** displayed poor anticancer activity while substitution with 2-thiophene at C3 position and 4-chlorophenyl at C6 position **30**, increases the activity with more selectivity towards the melanoma cancer cell line MALME-3M with a GI value of 77.82% (Table 3).

Table 3 Percentage (%) growth inhibition (GI) of compounds **6**, **7a**, **9b, 10b**, **11b**, **16b**, **28** and **30** over the full panel of 60 tumor cell lines at concentration of 10 µM.

Cell line type	Cell line name	6	7a	9b	10b	11b	16b	28	30
Leukemia	CCRF-CEM	-	-	19.41	-	22.39	-	-	14.72
	HL-60(TB)	**69.19**	-	13.22	32.40	14.82	NT	-	32.62
	K-562	-	-	14.92	18.35	38.24	NT	-	47.06
	MOLT-4	12.54	-	25.52	21.25	41.55	NT	-	20.34
	RPMI-8226	-	-	-	29.69	48.96	36.31	-	17.02
	SR	30.60	-	49.13	**54.39**	45.46	NT	-	27.81
Non-Small Cell Lung Cancer	A549/ATCC	22.21	13.25	-	41.45	43.86	**83.52**	-	-
	EKVX	24.43	24.04	-	35.95	33.20	49.84	-	-
	HOP-62	48.29	22.74	-	40.98	31.25	**59.14**	-	-
	HOP-92	**62.81**	-	-	**92.29**	**77.65**	**-13.56**	11.79	15.61
	NCI-H226	46.40	27.46	-	16.99	**55.35**	29.28	-	-
	NCI-H23	36.05	25.40	21.91	43.37	37.56	**66.97**	-	28.24
	NCI-H322M	23.24	18.07	-	10.57	14.03	18.02	-	11.91
	NCI-H460	26.12	-	-	49.53	36.05	**73.64**	-	-
	NCI-H522	45.23	36.87	-	25.35	**52.85**	**60.39**	-	-
Colon Cancer	COLO 205	-	-	-	25.05	29.50	43.89	-	11.30
	HCC-2998	-	11.61	-	21.86	18.95	22.91	-	-
	HCT-116	44.49	20.47	-	41.34	**60.66**	**66.14**	-	18.23
	HCT-15	-	-	36.21	27.11	31.38	36.61	-	29.83
	HT29	-	-	52.34	**53.36**	46.79	**74.56**	-	49.09
	KM12	21.08	-	18.81	40.37	24.49	**57.01**	-	23.63
	SW-620	-	-	33.27	43.33	11.72	**60.98**	-	13.73
CNS Cancer	SF-268	43.44	22.13	-	23.75	35.64	34.29	-	14.33
	SF-295	-	11.75	-	**52.52**	45.77	**76.68**	-	-
	SF-539	**52.78**	18.31	-	40.04	45.41	**-21.15**	-	-
	SNB-19	25.37	-	NT	NT	35.56	NT	NT	-
	SNB-75	**-2.07**	68.32	-	**64.44**	**-1.39**	**85.69**	15.18	-
	U251	**52.35**	17.29	11.95	**52.46**	32.65	**77.45**	-	19.30
Melanoma	LOX IMVI	25.67	24.60	15.63	**61.63**	43.60	**91.98**	-	21.46
	MALME-3M	**53.11**	24.30	**56.42**	**60.88**	**-9.77**	**73.25**	-	**77.82**
	M14	17.22	-	35.77	32.45	32.28	**61.41**	-	**61.10**
	MDA-MB-435	12.82	-	24.52	38.65	27.95	**62.77**	-	20.55
	SK-MEL-2	22.00	-	-	31.03	48.10	**50.58**	-	-
	SK-MEL-28	-	-	**61.69**	**76.09**	32.37	**-17.37**	-	40.28

	SK-MEL-5	**59.65**	13.41	15.59	**57.50**	**61.69**	**71.37**	-	30.47
	UACC-257	10.94	-	11.68	**51.80**	34.28	**70.84**	-	-
	UACC-62	14.79	-	-	28.89	18.62	49.89	-	-
Ovarian Cancer	IGROV1	22.57	26.28	-	20.77	16.32	29.38	-	-
	OVCAR-3	43.29	13.76	-	32.04	23.36	**53.41**	-	-
	OVCAR-4	**54.55**	-	14.41	45.94	39.32	**-18.64**	-	25.03
	OVCAR-5	-	-	-	-	---	12.00	-	-
	OVCAR-8	35.35	-	-	47.45	38.43	**73.68**	-	-
	NCI/ADR-RES	42.47	22.95	21.20	46.63	**54.62**	**70.09**	-	12.56
	SK-OV-3	14.52	13.64	-	-	36.88	-	-	-
Renal Cancer	786-0	**71.02**	-	NT	NT	32.72	NT	-	-
	A498	-	-	-	35.60	**90.12**	29.38	-	-
	ACHN	34.24	22.25	-	42.72	**51.39**	**53.41**	-	-
	CAKI-1	-	10.67	-	32.18	14.82	28.33	-	-
	RXF 393	**55.79**	11.01	29.51	36.41	**71.67**	**-20.76**	-	12.23
	SN12C	24.19	-	-	26.17	32.41	**75.49**	-	-
	TK-10	-	-	-	46.11	19.47	**64.26**	-	-
	UO-31	41.18	37.92	14.45	39.73	**59.18**	25.03	18.30	31.13
Prostate Cancer	PC-3	17.90	23.95	12.06	47.04	**60.82**	**82.27**	-	19.78
	DU-145	24.95	12.94	30.37	44.61	31.96	**70.53**	-	18.46
Breast Cancer	MCF7	**77.75**	24.89	26.92	40.08	49.54	**55.81**	-	44.11
	MDA-MB-231/ATCC	**70.43**	31.76	26.69	36.78	49.62	**93.71**	24.30	-
	HS 578T	30.14	15.90	12.25	32.35	41.43	42.41	-	-
	BT-549	-	-	10.59	**75.01**	17.35	**70.80**	-	-
	T-47D	46.34	22.05	-	45.27	**61.52**	**54.65**	-	15.70
	MDA-MB-468	**58.60**	30.06	15.17	45.34	**55.77**	**56.11**	-	17.46

50-60% inhibition, **60-70% inhibition**, **70-90% inhibition**, **90-100% growth inhibition**, **highly potent compounds**, NT: not tested

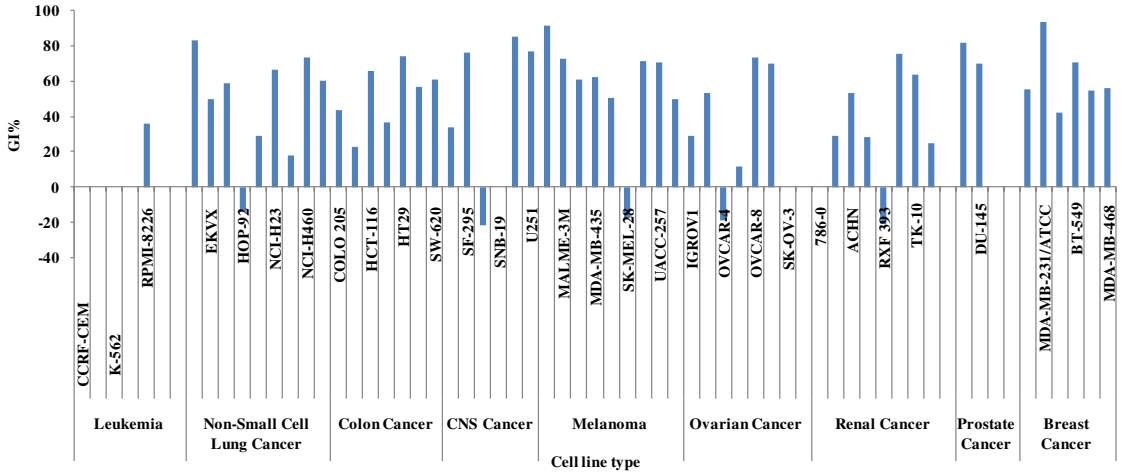

Figure 4 The percentages of growth inhibition of compound **16b** over the full panel of tumor cell lines.

3.5. *IN VITRO* EVALUATION ON NORMAL CELL LINES

Compound **16b** was also evaluated for toxicity to normal cell line Hek293 (human embryonic kidney) using MTT assay. It was observed that compound **16b** showed only 17%, 15%, 9%, 5% and 3% cytotoxicity to Hek293 cells at 10^{-4}, 10^{-5}, 10^{-6}, 10^{-7} and 10^{-8} M concentrations, respectively (Figure 5). Compound showed only 17% of toxicity to Hek293 cells even at 100 µM concentration. These data indicated that compound **16b** showed potent anticancer activity and low toxicity to normal cells.

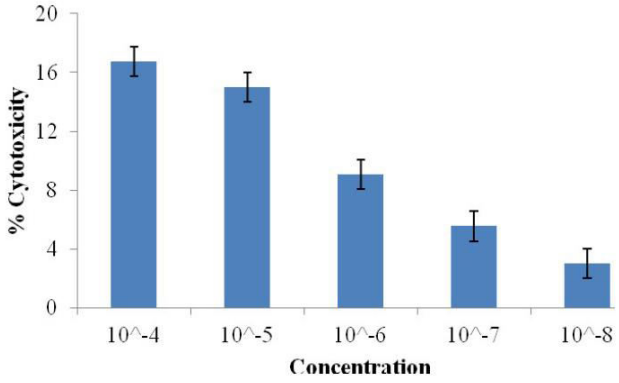

Figure 5 MTT assay of compound **16b** showing cytotoxicity on Normal Hek 293 cells

3.6. LIPOPHILICITY DETERMINATION BY SHAKE FLASK METHOD

The partition coefficient of the compounds was also studied in an octanol/water system for the determination of log P values by shake-flask method.[121] It was observed that compounds **11b** and **16b** showed higher log P values (Table 4), which suggested that the higher anti-tumor activity of these compounds was related to the lipophilicity. Thus, lipophilicity is a crucial factor for the activity of the synthesized compounds.

Table 4 Experimental determined lipophilicity

Compounds	P	Log P
6	239.88	2.38
7a	489.77	2.69
9b	371.53	2.57
10b	467.73	2.67
11b	2511.88	3.40
16b	758.57	2.88

28	257.03	2.41
30	380.19	2.58

P—partition coefficient; log P—logarithm of the partition coefficient.

3.7. STRUCTURE-ACTIVITY RELATIONSHIP (SAR) STUDIES

Structure–activity correlation, based on the number of cancer cell lines that were inhibited by each compound revealed that nature of substituents at C3- and C6-positions of imidazo[1,2-*a*]pyrazine affected the biological activity. Compounds **10b**, **11b** and **16b** showed comparatively higher activity than **6**, **7a**, **9b**, **28** and **30**, suggesting that there is much difference in antitumor activity with different substitutions of phenyl rings. The antitumor results indicated that compound **6** with a coumarin moiety at C8 position and bromo at C3 and C6 positions displayed only moderate anticancer activity. The anticancer activity has been slightly increased with substitution of 2-thiophene rings at C3 and C6 positions, as in the case of compound **10b**. Higher activity has been achieved with substitution of phenyl rings **11b** and 4-methoxyphenyl rings 1**6b** at C3 and C6 positions. On the other hand, substitution with 4-chlorophenyl at C6 position and 2-thiophene at C3 position, as in case of compound **30**, decreased the activity. It has been revealed that symmetrical diarylated imidazo[1,2-*a*]pyrazine–coumarin hybrids **11b** and **16b** showed higher activity than unsymmetrical diarylated hybrids **28** and **30**. These studies indicated that substitution of coumarin heterocycle with various phenyl derivatives on imidazo[1,2-*a*]pyrazine gave highly potent anticancer activity towards 60 human cancer cell lines. Overall, **16b** has been found to be the most effective member of this series of compounds and showed broad spectrum of activity against melanoma cancer cell lines.

3.8. MOLECULAR DOCKING STUDIES

Preliminary anticancer screening showed that compound **16b** has been found to be the most active member of imidazo[1,2-*a*]pyrazine-coumarin hybrids and showed excellent inhibition against melanoma cell lines than other cancer cell lines. So, in order to observe the molecular interactions of compound in the active site of enzyme for melanoma cancer, docking experiment was performed. The crystal coordinates of enzyme used in melanoma was downloaded from protein data bank (www.rcsb.org)[122] (PDB code: 3OG7).[123] Compound **16b** showed H-bonding interaction of N1 (d = 2.93 Å), N4 (d = 2.72 Å) and N7 (d = 1.75 Å) atoms of imidazo[1,2-

a]pyrazine with G518 amino acid residue of the coil of enzyme. N7 atom of the pyrazine ring of imidazo[1,2-*a*]pyrazine also showed H-bonding interaction with M517 (d = 2.17 Å) amino acid residue of enzyme. Oxygen atom of the 4-methoxy phenyl at C6 position of imidazo[1,2-*a*]pyrazine showed H-bonding interaction with R781 amino acid residue of enzyme (d = 2.85 Å). Carbonyl group of coumarin ring interacts with W531 amino acid residue of β-strand of enzyme with d = 2.56 Å. Oxygen atom and carbonyl group of coumarin ring also showed H-bonding interactions with Q530 amino acid residues of β-strand of enzyme (d = 1.77 Å and d = 2.31 Å). Therefore, docking of compound **16b** in the active site of this enzyme indicated the probable mode of action for anticancer activities (Figure 6).

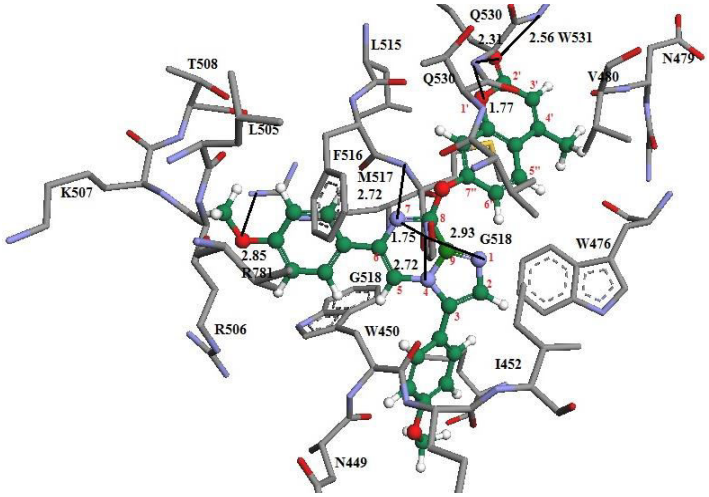

Figure 6 Docking of compound **16b** in the active site of 3OG7. H-bonds of compound **16b** with different amino acid residues are visible. Carbon atoms are given in green colour.

3.9. CONCLUSION

In summary, imidazo[1,2-*a*]pyrazine-coumarin hybrid has been synthesized by nucleophilic substitution reaction at C8 position from easily accessible 3,6,8-tribromoimidazo[1,2-*a*]pyrazine and 7-hydroxy-4-methylcoumarin. This compound was further functionalized at C6 position for monoarylation and C3, C6 positions for symmetrical diarylations using palladium catalyzed C-C coupling. Subsequent use of monoarylated products has been implemented for synthesis of unsymmetrical diarylated imidazo[1,2-*a*]pyrazine-coumarin hybrids in moderate to good yields. Evaluation of selected compounds for anticancer activity revealed that symmetrical diarylated hybrids **11b** and **16b** showed broad spectrum of anticancer activity towards most of the cancer cell lines. These compounds also have good lipophilicity that qualifies them to have good

pharmacokinetic and drug bioavailability. Molecular docking study has also further supported the inhibitory activity of **16b** that helped in understanding the interactions between the ligand and enzyme active sites.

3.10. EXPERIMENTAL SECTION

All commercially available compounds (Avra, Spectrochem, Aldrich, Merck etc.) were used without purification. Unless otherwise noted, all reactions were performed in oven-dried glassware. Final reactions were carried out in an oil bath using Microwave Vials (10-15 ml). Melting points were determined in open capillaries and were uncorrected. ^{1}H and ^{13}C NMR spectra were performed on Jeol ECS 400 NMR spectrometer, which was operated at 400 MHz for ^{1}H nuclei and 100 MHz for ^{13}C nuclei, using $CDCl_3$ and trifluoroacetic acid (TFA) as solvents. Chemical shifts are reported in parts per million (ppm) with TMS as internal reference and *J* values are given in hertz. 2D NOE studies were performed on same instrument. Mass Spectra of the synthesized compounds were recorded at Water Micromass-Q-T of Micro. Reactions were monitored by thin layer chromatography (TLC) with silica plate coated with silica gel HF-254 and column chromatography was performed with silica gel 60-120/100-200 mesh. Chloroform/ethyl acetate and chloroform/methanol were adopted solvent systems.

3.10.1. Synthesis of 2-amino-3,5-dibromopyrazine (2)

N-Bromosuccinimide (14.95 g, 83.99 mmol) was added over 50 min to a mixture of 2-aminopyrazine **1** (3.80 g, 40 mmol) in DMSO: H_2O (9:1) below 15 ^{o}C. Mixture was then stirred for 6 h at room temperature. After completion of reaction, mixture was then extracted with water and ethyl acetate. Ethyl acetate layer was separated, dried over sodium sulphate, filtered and concentrated in vacuum. Crude product was purified by column chromatography using hexane: ethyl acetate (9:1) as eluents.

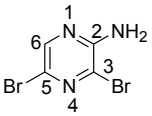

Spectral data 2-amino-3,5-dibromopyrazine (2): White solid; Yield: 90%; mp 115-116 ^{o}C; ^{1}H NMR ($CDCl_3$, 400 MHz): δ 5.12 (bs, 1H, NH_2), 8.04 (s, 1H, C_6H); ^{13}C NMR ($CDCl_3$, 100 MHz): δ 123.5, 123.9, 143.1, 151.8.

3.10.2. Synthesis of 6,8-dibromo-imidazo[1,2-*a*]pyrazine (3)

To 2-amino-3,5-dibromopyrazine **2** (5.0 g, 19.8 mmol) in 100 ml of isopropyl alcohol (IPA), 50% aqueous solution of chloroacetaldehyde (99 mmol) was added dropwise. The reaction mixture was refluxed at 110 ^{o}C for 72 h. After the completion of the reaction, cooled the reaction

mixture to room temperature and then extracted with water and chloroform. Chloroform layer was separated, dried over sodium sulphate, filtered and concentrated in vacuum to get the crude product. The product was purified by column chromatography using hexane: ethyl acetate (6:4) as eluents.

Spectral data of 6,8-dibromoimidazo[1,2-*a*]pyrazine (3): White solid; Yield: 80%; mp 163-

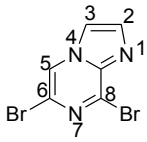

165 ^{o}C; ^{1}H NMR ($CDCl_3$, 400 MHz): δ 7.80 (d, J = 0.92 Hz, 1H, C_2H), 7.86 (d, = 1.36 Hz, 1H, C_3H), 8.29 (s, 1H, C_5H); ^{13}C NMR ($CDCl_3$, 400 MHz): δ 115. 119.3, 119.9, 137.0, 137.4, 142.5.

3.10.3. Synthesis of 3,6,8-tribromoimidazo[1,2-*a*]pyrazine (4)

N-Bromosuccinimide (6.29 g, 35.34 mmol) was added to 6,8-dibromoimidazo[1,2-*a*]pyrazine **3** (10 g, 36 mmol) in acetonitrile and stirred at room temperature for 2 h. After completion of reaction (indicated by TLC), mixture was then extracted with water and chloroform. Chloroform layer was dried over sodium sulphate and concentrated in vacuum. Crude product was purified by column chromatography using hexane: ethyl acetate (8.5:1.5) as eluents.

Spectral data of 3,6,8-tribromoimidazo[1,2-*a*]pyrazine (4): White solid; Yield: 90%; mp

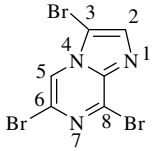

162-164 ^{o}C; ^{1}H NMR ($CDCl_3$, 400 MHz): δ 7.84 (s, 1H, C_2H), 8.22 (s, 1H, C_5H); ^{13}C NMR ($CDCl_3$, 400 MHz): δ 116.12, 119.28, 120.97, 137.03, 137.39, 142.54.

3.10.4. Synthesis of imidazo[1,2-*a*]pyrazine-coumarin hybrid (6)

To the solution of 3,6,8-tribromoimidazo[1,2-*a*]pyrazine **4** (10 g, 28.09 mmol) in 50 ml dry DMF, 7-hydroxy-4-methylcoumarin **5** (4.94 g, 28.09 mmol) and K_2CO_3 (3.87 g, 28.09 mmol) were added and allowed to stir at room temperature for 12 h. After completion of reaction, the reaction mixture was poured into crushed ice. The crude solid was filtered through and dried in vacuum. The solid was recrystallized from hot ethanol to obtain pure white solid of compound **6**.

Spectral data of 7'-(3,6-dibromoimidazo[1,2-*a*]pyrazin-8-yloxy)-4'-methyl-2*H*-chromen-

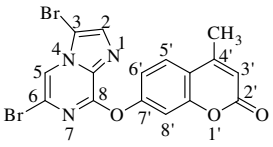

2'-one (6): Off white solid; Yield: 85%; mp 280-282 ^{o}C; ^{1}H NMR ($CDCl_3$+TFA, 400 MHz): δ 2.48 (d, J = 1.36 Hz, 3H, CH_3), 6.32 (d, J = 0.92 Hz, 1H, C3'H) 7.32 (dd, ^{2}J = 8.68 Hz, ^{3}J = 2.74 Hz, 1H, C5'H), 7.43 (d, J = 2.32 Hz, 1H, C8'H), 7.71 (d, J = 8.68 Hz, 1H, C6'H), 7.86 (s, 1H, C2H), 8.08 (s, 1H, C5H); ^{13}C NMR ($CDCl_3$+TFA, 100 MHz): δ 18.7 (CH_3), 100.6, 110.1, 114.0, 114.3, 118.2, 118.3, 122.2, 126.2, 130.2, 131.7, 149.4, 153.5, 153.7, 154.3 (ArC), 162.9 (C=O); MS

(EI): m/z 451.9 (M^++1); Anal. Calcd for $C_{16}H_9Br_2N_3O_3$: C, 42.60; H, 2.01; N, 9.32. Found: C, 42.72; H, 2.08; N, 9.12.

3.10.5. General procedure for synthesis of monoarylated (7a, 8a) and symmetrical hybrids (7b-19b)

To a solution of 3,6-dibromoimidazo[1,2-*a*]pyrazine-coumarin hybrid **6** (0.46 g, 1.0 mmol) in mixture of 1,2-DME : water (9:1) in a sealed tube, boronic acid (1 eq.) and K_2CO_3 (0.150 g, 1.0 mmol) were added under inert atmosphere. Then, $Pd(PPh_3)_4$ (5mol%) was added with nitrogen purging and refluxed the reaction mixture for 8-12 h. Completion of reaction was determined by TLC. The mixture was extracted with chloroform and water. Chloroform layer was dried using sodium sulphate to obtain crude product which was further purified by column chromatography using chloroform: ethylacetate / chloroform: methanol as eluents.

Spectral data of 7'-(3-bromo-6-(2-methoxyphenyl)imidazo[1,2-*a*]pyrazin-8-yloxy)-4'-methyl-2*H*-chromen-2'-one (7a): White solid; Yield: 61%; mp 239-240 ^oC; ^1H NMR ($CDCl_3$, 400 MHz): δ 2.49 (s, 3H, CH_3), 3.99 (s, 3H, OCH_3), 6.30 (s, 1H, C3'H), 6.97-7.02 (m, 2H, ArH), 7.31-7.38 (m, 2H, ArH), 7.48 (d, *J* = 2.32 Hz, 1H, C8'H), 7.68 (d, *J* = 8.72 Hz, 1H, ArH), 7.76-7.79 (m, 2H, ArH), 8.74 (s, 1H, C5H); ^{13}C NMR ($CDCl_3$, 100 MHz): δ 18.7 (CH_3), 55.6 (OCH_3), 99.1, 110.3, 111.2, 114.1, 114.3, 117.3, 118.1, 121.0, 123.6, 125.2, 129.9, 130.1, 132.6, 133.7, 134.9, 150.8, 152.1, 154.1, 155.0, 156.7 (ArC), 160.7 (C=O); MS (EI): m/z 480.1 (M^++2); Anal. Calcd for $C_{23}H_{16}BrN_3O_4$: C, 57.76; H, 3.37; N, 8.79. Found: C, 57.50; H, 3.22; N, 8.68.

Spectral data of 7'-(3,6-bis(2-methoxyphenyl)imidazo[1,2-*a*]pyrazin-8-yloxy)-4'-methyl-2*H*-chromen-2'-one (7b): White solid; Yield: 33%; mp 204-205 ^oC; ^1H NMR ($CDCl_3$, 400 MHz): δ 2.48 (d, *J* = 0.92 Hz, 3H, CH_3), 3.85 (s, 3H, OCH_3), 3.86 (s, 3H, OCH_3), 6.29 (d, *J* = 1.40 Hz, 1H, C3'H), 6.93-6.99 (m, 2H, ArH), 7.10-7.16 (m, 2H, ArH), 7.28-7.30 (m, 1H, ArH), 7.42 (dd, ^2J = 8.68 Hz, ^3J = 2.28 Hz, 1H, C5'H), 7.48-7.52 (m, 2H, ArH), 7.54 (d, *J* = 2.28 Hz, 1H, C8'H), 7.68 (d, *J* = 8.72 Hz, 1H, ArH), 7.79 (dd, ^2J = 7.76 Hz, ^3J = 1.82 Hz, 1H, ArH), 7.82 (s, 1H, C2H), 8.49 (s, 1H, C5H); ^{13}C NMR ($CDCl_3$, 100 MHz): δ 18.7 (CH_3), 55.5 (OCH_3), 110.2, 111.1, 111.2, 113.9, 116.0, 116.8, 117.0, 118.1, 120.9, 121.0,

124.4, 125.2, 126.5, 129.4, 130.1, 130.9, 131.4, 132.3, 134.5, 150.9, 152.2, 154.2, 155.5, 156.7, 157.0 (ArC), 160.9 (C=O); MS (EI): m/z 506.2 (M^++1); Anal. Calcd for: C_{30} $H_{23}N_3O_5$: C, 71.28; H, 4.59; N, 8.31. Found: C, 71.41; H, 4.37; N, 8.22.

Spectral data of 7'-(3-bromo-6-(furan-2-yl)imidazo[1,2-*a*]pyrazin-8-yloxy)-4'-methyl-2*H*-

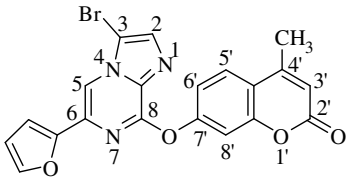

chromen-2'-one (8a): White solid; Yield: 48%; mp 225-226 ^oC; ^1H NMR ($CDCl_3$, 400 MHz): δ 2.50 (d, *J* = 1.40 Hz, 3H, CH_3), 6.32 (d, *J* = 1.36 Hz, 1H, C3'H), 6.45 (q, *J* = 1.60 Hz, 1H, ArH), 6.69 (d, *J* = 3.20 Hz, 1H, ArH), 7.37 (dd, ^2J = 8.72 Hz, ^3J = 2.28 Hz, 1H, C5'H), 7.47 (d, *J* = 0.92 Hz, 1H, ArH), 7.51 (d, *J* = 2.28 Hz, 1H, C8'H), 7.69 (d, *J* = 8.72 Hz, 1H, ArH), 7.75 (s, 1H, C2H), 8.20 (s, 1H, C5H); ^{13}C NMR ($CDCl_3$, 100 MHz): δ 18.8 (CH_3), 99.6, 107.9, 109.7, 110.4, 112.0, 114.3, 117.5, 118.1, 125.2, 130.1, 132.6, 135.0, 143.1, 150.2, 151.7, 152.1, 154.1, 154.7 (ArC), 160.7 (C=O); MS (EI): m/z 440.1 (M^++2); Anal. Calcd for $C_{20}H_{12}BrN_3O_4$: C, 54.81; H, 2.76; N, 9.59. Found: C, 54.76; H, 2.69; N, 9.73.

Spectral data of 7'-(3,6-di(furan-2-yl)imidazo[1,2-*a*]pyrazin-8-yloxy)-4'-methyl-2*H*-

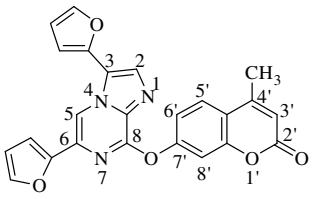

chromen-2'-one (8b): Off White solid; Yield: 25%; mp 192-194 ^oC; ^1H NMR ($CDCl_3$, 400 MHz): δ 2.50 (s, 3H, CH_3), 6.31 (s, 1H, C3'H), 6.46 (q, *J* = 1.82 Hz, 1H, ArH), 6.64 (q, *J* = 1.82 Hz, 1H, ArH), 6.69 (d, *J* = 3.20 Hz, 1H, ArH), 6.81 (d, *J* = 3.68 Hz, 1H, ArH), 7.40 (dd, ^2J = 8.72 Hz, ^3J = 2.28 Hz, 1H, C5'H), 7.46 (s, 1H, ArH), 7.53 (d, *J* = 2.28 Hz, 1H, C8'H), 7.68-7.70 (m, 2H, ArH), 7.96 (s, 1H, C2H), 8.66 (s, 1H, C5H); ^{13}C NMR ($CDCl_3$, 100 MHz): δ 18.8 (CH_3), 108.4, 109.3, 109.4, 110.4, 111.7, 111.9, 114.2, 117.4, 118.2, 121.2, 125.2, 129.9, 132.0, 132.9, 142.8, 143.1, 143.2, 150.5, 152.0, 152.1, 154.1, 154.9 (ArC), 160.8 (C=O); MS (EI): m/z 426.2 (M^++1); Anal. Calcd for C_{24} $H_{15}N_3O_5$: C, 67.76; H, 3.55; N, 9.88. Found: C, 67.59; H, 3.63; N, 9.70.

Spectral data of 7'-(3,6-bis(4-chlorophenyl)imidazo[1,2-a]pyrazin-8-yloxy)-4'-methyl-2H-

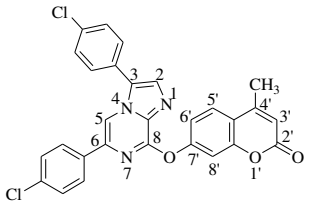

chromen-2'-one (9b): White solid; Yield: 42%; mp 245-247 ^oC; ^1H NMR ($CDCl_3$ + TFA, 400 MHz): δ 2.55 (d, *J* = 0.88 Hz, 3H, CH_3), 6.43 (d, *J* = 0.92 Hz, 1H, C3'H), 7.40-7.43 (m, 3H, ArH), 7.53 (d, *J* = 2.32 Hz, 1H, C8'H), 7.58-7.63 (m, 4H, ArH), 7.69 (d, *J* = 8.72 Hz,

2H, ArH), 7.81 (d, *J* = 8.68 Hz, 1H, ArH), 8.17 (s, 1H, C2H), 8.33 (s, 1H, C5H); ^{13}C NMR ($CDCl_3$ + TFA, 100 MHz): δ 18.8 (CH_3), 108.6, 110.2, 114.4, 118.1, 118.5, 122.2, 124.7, 126.2, 126.9, 127.7, 129.3, 129.5, 130.3, 130.6, 131.6, 136.9, 138.0, 141.3, 149.5, 153.4, 153.6, 153.7 (ArC), 162.1 (C=O); MS (EI): m/z 514.1 (M^++1); Anal. Calcd for $C_{28}H_{17}Cl_2N_3O_3$: C, 65.38; H, 3.33; N, 8.17. Found: C, 65.48; H, 3.50; N, 8.20.

Spectral data of 7'-(3,6-di(thiophen-2-yl)imidazo[1,2-*a*]pyrazin-8-yloxy)-4'-methyl-2*H*-chromen-2'-one (10b): Light green solid; Yield: 66%; mp 191-192 ^{o}C; ^{1}H NMR ($CDCl_3$, 400 MHz): δ 2.50 (d, *J* = 0.88 Hz, 3H, CH_3), 6.32 (d, *J* = 1.36 Hz, 1H, C3'H), 7.03-7.05 (m, 1H, ArH), 7.27-7.31 (m, 2H, ArH), 7.39 (dd, ^{2}J = 3.68 Hz, ^{3}J = 1.36 Hz, 1H, ArH), 7.40-7.44 (m, 2H, ArH), 7.55-7.58 (m, 2H, ArH), 7.71 (d, *J* = 8.72 Hz, 1H, ArH), 7.88 (s, 1H, C2H), 8.40 (s, 1H, C5H); ^{13}C NMR ($CDCl_3$, 100 MHz): δ 18.8 (CH_3), 108.0, 110.5, 114.2, 117.4, 118.2, 123.1, 124.0, 125.2, 126.7, 127.1, 127.3, 128.0, 128.2, 132.5, 133.1, 134.6, 140.2, 151.7, 152.1, 154.1, 154.8 (ArC), 160.8 (C=O); MS (EI): m/z 458.1 (M^++1); Anal. Calcd for $C_{24}H_{15}N_3O_3S_2$: C, 63.00; H, 3.30; N, 9.18; S, 14.02. Found: C, 63.28; H, 3.19; N, 9.26; S, 13.93.

Spectral data of 7'-(3,6-diphenylimidazo[1,2-*a*]pyrazin-8-yloxy)-4'-methyl-2*H*-chromen-2'-one (11b): White solid; Yield: 74%; mp 204-206 ^{o}C; ^{1}H NMR ($CDCl_3$, 400 MHz): δ 2.50 (d, *J* = 0.68 Hz, 3H, CH_3), 6.32 (d, *J* = 0.88 Hz, 1H, C3'H), 7.34-7.43 (m, 4H, ArH), 7.51-7.56 (m, 2H, ArH), 7.59-7.66 (m, 4H, ArH), 7.69-7.72 (m, 3H, ArH), 7.86 (s, 1H, C2H), 8.40, (s, 1H, C5H); ^{13}C NMR ($CDCl_3$, 100 MHz): δ 18.5 (CH_3), 109.4, 110.5, 114.2, 117.4, 118.3 125.3, 125.9, 128.0, 128.2, 128.8, 129.2, 129.4, 129.5, 132.6, 133.8, 135.6, 136.9, 152.2, 154.2, 155.1 (ArC), 160.8 (C=O); MS (EI): m/z 446.1 (M^++1); Anal. Calcd for $C_{28}H_{19}N_3O_3$: C, 75.49; H, 4.30; N, 9.43. Found: C, 75.28; H, 4.39; N, 9.58.

Spectral data of 7'-(3,6-di-*m*-tolylimidazo[1,2-*a*]pyrazin-8-yloxy)-4'-methyl-2*H*-chromen-2'-one (12b): White solid; Yield: 70%; mp 198-199 ^{o}C; ^{1}H NMR ($CDCl_3$, 400 MHz): δ 2.36 (s, 3H, CH_3), 2.50 (s, 6H, CH_3), 6.31 (d, *J* = 0.92 Hz, 1H, C3'H), 7.16 (d, *J* = 7.76 Hz, 1H, ArH), 7.30 (d, *J* = 2.76 Hz, 1H, ArH), 7.35 (d, *J* = 7.80 Hz, 1H, ArH), 7.41-7.45 (m, 3H, ArH), 7.49-7.53 (m, 4H, ArH), 7.70 (d, *J* = 8.72 Hz, 1H, ArH), 7.83 (s, 1H,

C2H), 8.37 (s, 1H, C5H); ^{13}C NMR ($CDCl_3$, 100 MHz): δ 18.8 (CH_3), 21.5 (CH_3), 109.6, 110.4, 114.1, 117.3, 118.2, 123.3, 125.1, 125.2, 126.5, 127.9, 128.8, 129.0, 129.4, 129.5, 129.6, 130.0, 132.5, 133.8, 135.6, 137.0, 138.4, 139.5, 152.0, 152.2, 154.2, 155.2 (ArC), 160.8 (C=O); MS (EI): m/z 474.2 (M^++1); Anal. Calcd for: $C_{30}H_{23}N_3O_3$: C, 76.09; H, 4.90; N, 8.87. Found: C, 76.42; H, 4.88; N, 8.76.

Spectral data of 7'-(3,6-bis(4-ethylphenyl)imidazo[1,2-*a*]pyrazin-8-yloxy)-4'-methyl-2*H*-

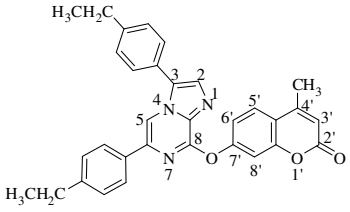

chromen-2'-one (13b): White solid; Yield: 69%; mp 179-181 ^{o}C; ^{1}H NMR ($CDCl_3$, 400 MHz): δ 1.22 (t, *J* = 7.56 Hz, 3H, CH_3), 1.34 (t, *J* = 7.80 Hz, 3H, CH_3), 2.49 (d, *J* = 0.68 Hz, 3H, CH_3), 2.64 (q, *J* = 7.64 Hz, 2H, CH_2), 2.78 (q, *J* = 7.64 Hz, 2H, CH_2), 6.31 (d, *J* = 1.40 Hz, 1H, C3'H), 7.21 (d, *J* = 8.24 Hz, 2H, ArH), 7.40-7.44 (m, 3H, ArH), 7.52 (d, *J* = 1.80 Hz, 1H, C8'H), 7.55 (d, *J* = 8.24 Hz, 2H, ArH), 7.62 (d, *J* = 8.24 Hz, 2H, ArH), 7.70 (d, *J* = 8.72 Hz, 1H, ArH), 7.81 (s, 1H, C2H), 8.36 (s, 1H, C5H); ^{13}C NMR ($CDCl_3$,100 MHz): δ 15.4 (CH_3), 15.5 (CH_3), 18.8 (CH_3), 28.5 (CH_2), 28.7 (CH_2), 109.0, 110.5, 114.1, 117.3, 118.3, 125.2, 125.3, 125.9, 128.1, 128.3, 129.0, 129.3, 132.4, 133.1, 133.5, 136.9, 145.1, 145.5, 152.0, 152.2, 154.2, 155.2 (ArC), 160.8 (C=O); MS (EI): m/z 502.2 (M^++1); Anal. Calcd for $C_{33}H_{27}N_3O_3$: C, 76.63; H, 5.43; N, 8.38. Found: C, 76.82; H, 5.57; N, 8.45.

Spectral data of 7'-(3,6-bis(4-fluorophenyl)imidazo[1,2-*a*]pyrazin-8-yloxy)-4'-methyl-2*H*-

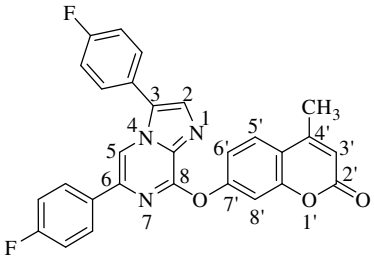

chromen-2'-one (14b): White solid; Yield: 72%; mp 240-242 ^{o}C; ^{1}H NMR ($CDCl_3$, 400 MHz): δ 2.51 (d, *J* = 1.40 Hz, 3H, CH_3), 6.32 (d, *J* = 1.36 Hz, 1H, C3'H), 7.04-7.09 (m, 2H, ArH), 7.29-7.34 (m, 2H, ArH), 7.41 (dd, ^2J = 8.72 Hz, ^3J = 2.28 Hz, 1H, C5'H), 7.48 (d, *J* = 2.28 Hz, 1H, C8'H), 7.59-7.62 (m, 2H, ArH), 7.65-7.69 (m, 2H, ArH), 7.72 (d, *J* = 8.72 Hz, 1H, ArH), 7.83 (s, 1H, C2H), 8.24 (s, 1H, C5H); ^{13}C NMR ($CDCl_3$, 100 MHz): δ 18.8 (CH_3), 108.8, 110.5, 114.3, 115.7, 115.9, 116.7, 116.9, 117.5, 118.2, 123.9, 125.4, 127.7, 127.8, 128.4, 130.2, 130.3, 131.6, 132.4, 133.8, 136.3, 152.1, 152.2, 154.2, 154.9 (ArC), 160.7 (C=O), 161.9, 162.0, 164.4, 164.5 (ArC); MS (EI): m/z 482.2 (M^++1); Anal. Calcd for $C_{28}H_{17}F_2N_3O_3$: C, 69.85; H, 3.56; N, 8.73. Found: C, 69.56; H, 3.65; N, 8.99.

Spectral data of 7'-(3,6-bis(3-(trifluoromethyl)phenyl)imidazo[1,2-*a*]pyrazin-8-yloxy)-4'-

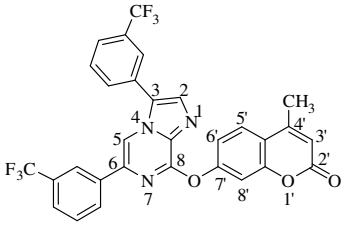

methyl -2*H*-chromen-2'-one (15b): White solid; Yield: 60%; mp 195-196 ^{o}C; ^{1}H NMR ($CDCl_3$, 400 MHz): δ 2.51 (d, *J* = 0.92 Hz, 3H, CH_3), 6.33 (d, *J* = 1.40 Hz, 1H, C3'H), 7.43 (dd, ^{2}J = 8.24 Hz, ^{3}J = 2.52 Hz, 1H, C5'H), 7.48 (d, *J* = 2.28 Hz, 1H, C8'H), 7.52 (t, *J* = 7.78 Hz, 1H, ArH), 7.60 (d, *J* = 7.80 Hz, 1H, ArH), 7.73 (d, *J* = 8.72 Hz, 1H, ArH), 7.76-7.82 (m, 2H, ArH), 7.84 (s, 1H, ArH), 7.86-7.87 (m, 1H, ArH), 7.90 (d, *J* = 1.84 Hz, 1H, ArH), 7.92 (s, 1H, ArH), 7.94 (s, 1H, C2H), 8.36 (s, 1H, C5H); ^{13}C NMR ($CDCl_3$, 100 MHz): δ 18.8 (CH_3), 109.4, 110.5, 114.4, 117.7, 118.3, 122.2, 122.4, 122.6, 122.7, 125.2, 125.3, 125.4, 125.6, 125.7, 126.1, 128.1, 128.6, 129.1, 129.5, 130.3, 131.1, 131.3, 131.4, 132.1, 132.4, 132.7, 132.9, 134.5, 136.0, 136.1, 152.0, 152.5, 154.2, 154.7 (ArC), 160.6 (C=O); MS (EI): m/z 582.2 (M^{+}+1); Anal. Calcd for: $C_{30}H_{17}F_6N_3O_3$: C, 61.97; H, 2.95; N, 7.23. Found: C, 62.13; H, 2.82; N, 7.03.

Spectral data of 7'-(3,6-bis(4-methoxyphenyl)imidazo[1,2-*a*]pyrazin-8-yloxy)-4'-methyl-2*H*-chromen-2'-one (16b): White solid; Yield: 73%; mp 224-226 ^{o}C; ^{1}H NMR ($CDCl_3$, 400 MHz): δ 2.50 (d, *J* = 0.92 Hz, 3H, CH_3), 3.81 (s, 3H, OCH_3), 3.92 (s, 3H, OCH_3), 6.31 (d, *J* = 1.36 Hz, 1H, C3'H), 6.90 (d, *J* = 8.68 Hz, 2H, ArH), 7.12 (d, *J* = 9.16 Hz, 2H, ArH), 7.42 (dd, ^{2}J = 8.72 Hz, ^{3}J = 2.28 Hz, 1H, C5'H), 7.52 (d, *J* = 2.28 Hz, 1H, C8'H), 7.54 (d, *J* = 8.72 Hz, 2H, ArH), 7.63 (d, *J* = 8.72 Hz, 2H, ArH), 7.70 (d, *J* = 8.72 Hz, 1H, ArH), 7.77 (s, 1H, C2H), 8.25 (s, 1H, C5H); ^{13}C NMR ($CDCl_3$, 100 MHz): δ 18.8 (CH_3), 55.3 (OCH_3), 55.4 (OCH_3), 108.2, 110.4, 114.1, 114.2, 114.9, 117.3, 118.3, 120.2, 125.2, 127.2, 128.3, 129.1, 129.7, 132.1, 133.3, 136.6, 151.9, 152.2, 154.2, 155.2, 160.1, 160.2 (ArC), 160.8 (C=O); MS (EI): m/z 506.3 (M^{+}+1); Anal. Calcd for $C_{30}H_{23}N_3O_5$: C, 71.28; H, 4.59; N, 8.31. Found: C, 71.03; H, 4.48; N, 8.18.

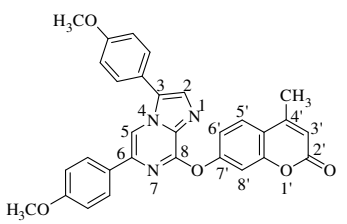

Spectral data of 4,4'-(8-(4'-methyl-2'-oxo-2*H*-chromen-7'-yloxy)imidazo[1,2-*a*]pyrazine-3,6-diyl) dibenzaldehyde (17b): White solid; Yield: 70%; mp >300 ^{o}C; ^{1}H NMR ($CDCl_3$ + TFA, 400 MHz): δ 2.56 (s, 3H, CH_3), 6.45 (d, *J* = 0.92 Hz, 1H, C3'H), 7.46 (dd, ^{2}J = 8.68 Hz, ^{3}J = 2.28 Hz, 1H, C5'H), 7.60 (d, *J* = 2.28 Hz, 1H, C8'H), 7.83 (d, *J* = 8.68 Hz, 1H, ArH), 7.87-7.90 (m, 4H, ArH), 7.97 (d, *J* = 8.24 Hz, 2H, ArH), 8.22-8.26 (m, 3H, ArH), 8.52 (s, 1H, C5H), 10.02 (s, 1H, CHO), 10.18 (s, 1H, CHO); ^{13}C NMR ($CDCl_3$ + TFA, 100 MHz): δ

18.9 (CH_3), 109.9, 110.3, 114.4, 118.2, 118.5, 126.2, 127.1, 128.5, 129.4, 130.1, 130.7, 131.3, 136.9, 137.6, 139.2, 140.4, 150.2, 153.6, 153.7, 153.8 (ArC), 162.5 (C=O), 191.6 (CHO), 192.4 (CHO); MS (EI): m/z 501.2 (M^++1); Anal. Calcd for $C_{30}H_{19}N_3O_5$: C, 71.85; H, 3.82; N, 8.38. Found: C, 71.69; H, 3.66; N, 8.19.

Spectral data of 7'-(3,6-bis(2-hydroxyphenyl)imidazo[1,2-*a*]pyrazin-8-yloxy)-4'-methyl-2*H*-chromen-2'-one (18b): White solid; Yield: 68%; mp >300 ^oC; ^1H NMR ($CDCl_3$ + TFA, 400 MHz): δ 2.58 (d, *J* = 0.92 Hz, 3H, CH_3), 6.52 (d, *J* = 1.40 Hz, 1H, C3'H), 6.86-6.95 (m, 2H, ArH), 7.14-7.23 (m, 2H, ArH), 7.28-7.32 (m, 1H, ArH), 7.40 (dd, ^2J = 8.72 Hz, ^3J = 2.28 Hz, 1H, ArH), 7.43-7.46 (m, 2H, ArH), 7.53 (dd, ^2J = 8.24 Hz, ^3J = 1.36 Hz, 1H, ArH), 7.56-7.60 (m, 1H, ArH), 7.88 (d, *J* = 8.68 Hz, 1H, ArH), 8.15 (s, 1H, C2H), 8.37 (s, 1H, C5H); ^{13}C NMR ($CDCl_3$ + TFA, 100 MHz): δ 18.8 (CH_3), 109.8, 110.4, 111.7, 114.4, 116.0, 117.0, 118.6, 119.3, 121.2, 122.0, 124.1, 124.8, 126.7, 127.2, 128.9, 131.6, 132.9, 133.9, 141.1, 148.2, 152.9, 153.7, 154.2, 155.1, 155.7 (ArC), 163.7 (C=O); MS (EI): m/z 478.2 (M^++1); Anal. Calcd for: $C_{28}H_{19}N_3O_5$: C, 70.43; H, 4.01; N, 8.80. Found: C, 70.61; H, 3.89; N, 8.63

Spectral data of 1,1'-(4,4'-(8-(4'-methyl-2'-oxo-2*H*-chromen-7'-yloxy)imidazo[1,2-*a*]pyrazin-3,6-diyl)bis(4,1-phenylene)diethanone (19b): White solid; Yield: 54%; mp >300 ^oC; ^1H NMR ($CDCl_3$ + TFA, 400 MHz): δ 2.55 (d, *J* = 0.92 Hz, 3H, CH_3), 2.64 (s, 3H, CH_3), 2.75 (s, 3H, CH_3), 6.42 (d, *J* = 1.40 Hz, 1H, C3'H), 7.44 (dd, ^2J = 8.72 Hz, ^3J = 2.28 Hz, 1H, C5'H), 7.62 (d, *J* = 2.28 Hz, 1H, C8'H), 7.79 (d, *J* = 8.24 Hz, 3H, ArH), 7.83 (d, *J* = 8.72 Hz, 2H, ArH), 8.03 (d, *J* = 8.72 Hz, 2H, ArH), 8.18 (s, 1H, C2H), 8.27 (d, *J* = 8.28 Hz, 2H, ArH), 8.49 (s, 1H, C5H); ^{13}C NMR ($CDCl_3$ + TFA, 100 MHz): δ 18.9 (CH_3), 26.6 (CH_3), 26.7 (CH_3), 109.7, 110.2, 114.4, 118.1, 118.4, 126.2, 126.6, 127.5, 128.6, 128.7, 129.0, 129.2, 129.3, 129.4, 130.0, 137.7, 138.1, 138.5, 140.1, 150.2, 153.5, 153.6, 153.7 (ArC), 162.2 (C=O), 198.1 (C=O), 199.0 (C=O); MS (EI): m/z 530.2 (M^++1); Anal. Calcd for $C_{32}H_{23}N_3O_5$: C, 72.58; H, 4.38; N, 7.94. Found: C, 72.71; H, 4.22; N, 7.84.

3.10.6. General procedure for synthesis of unsymmetrical hybrids (20-30)

Monoarylated imidazo[1,2-*a*]pyrazine-coumarin hybrid was dissolved in a mixture of 1,2-DME : water (9:1) in a sealed tube. Boronic acid (1 eq.) and K_2CO_3 (1.1 eq.) were added and purged the

reaction mixture with nitrogen. Then, $Pd(PPh_3)_4$ (5mol%) was added with nitrogen purging, sealed the vial and refluxed for 6-8 h. Completion of reaction was determined by TLC. The mixture was extracted with chloroform and water. Chloroform layer was dried over sodium sulphate to obtain crude product which was further purified by column chromatography using chloroform: ethylacetate / chloroform: methanol as eluents.

Spectral data of 7'-(6-(2-methoxyphenyl)-3-(thiophen-2-yl)imidazo[1,2-*a*]pyrazin-8-yloxy)-4'-methyl-2*H*-chromen-2'-one (20): Off White solid; Yield: 64%; mp 221-223 ^oC; ^1H NMR ($CDCl_3$, 400 MHz): δ 2.49 (d, J = 1.36 Hz, 3H, CH_3), 3.96 (s, 3H, OCH_3), 6.30 (d, J = 0.92 Hz, 1H, C3'H), 6.98-7.01 (m, 2H, ArH), 7.28-7.34 (m, 2H, ArH), 7.41 (dd, ^2J = 8.72 Hz, ^3J = 2.28 Hz, 1H, C5'H), 7.44 (dd, ^2J = 3.64 Hz, ^3J = 0.92 Hz, 1H, ArH), 7.51 (d, J = 2.28 Hz, 1H, C8'H), 7.55 (dd, ^2J = 5.04 Hz, ^3J = 0.92 Hz, 1H, ArH), 7.69 (d, J = 8.72 Hz, 1H, ArH), 7.82 (dd, ^2J = 8.24 Hz, ^3J = 1.60 Hz, 1H, ArH), 7.91 (s, 1H, C2H), 9.12 (s, 1H, C5H); ^{13}C NMR ($CDCl_3$, 100 MHz): δ 18.8 (CH_3), 55.7 (OCH_3), 110.3, 111.2, 114.1, 114.7, 117.2, 118.2, 121.1, 123.1, 123.9, 125.2, 126.5, 126.7, 128.0, 128.9, 129.7, 130.1, 132.5, 133.5, 134.2, 151.2, 152.2, 154.2, 155.3, 156.7 (ArC), 160.8 (C=O); MS (EI): m/z 482.1 (M^++1); Anal. Calcd for $C_{27}H_{19}N_3O_4S$: C, 67.35; H, 3.98; N, 8.73; S, 6.66. Found: C, 67.63; H, 4.10; N, 8.61; S, 6.51.

Spectral data of 7'-(3-(furan-2-yl)-6-(2-methoxyphenyl)imidazo[1,2-*a*]pyrazin-8-yloxy)-4'-methyl-2*H*-chromen-2'-one (21): Off White solid; Yield: 52%; mp 204-205 ^oC; ^1H NMR ($CDCl_3$, 400 MHz): δ 2.49 (s, 3H, CH_3), 3.99 (s, 3H, OCH_3), 6.30 (d, J = 1.36 Hz, 1H, C3'H), 6.64 (q, J = 1.62 Hz, 1H, ArH), 6.78 (d, J = 3.68 Hz, 1H, ArH), 6.98-7.02 (m, 2H, ArH), 7.30-7.35 (m, 1H, ArH), 7.41 (dd, ^2J = 8.72 Hz, ^3J = 2.32 Hz, 1H, C5'H), 7.52 (d, J = 2.32 Hz, 1H, C8'H), 7.64 (d, J = 1.84 Hz, 1H, ArH), 7.68 (d, J = 8.68 Hz, 1H, ArH), 7.81 (dd, ^2J = 7.80 Hz, ^3J = 1.84 Hz, 1H, ArH), 7.99 (s, 1H, C2H), 9.19 (s, 1H, C5H); ^{13}C NMR ($CDCl_3$, 100 MHz): δ 18.8 (CH_3), 55.7 (OCH_3), 107.7, 110.3, 111.3, 111.7, 114.1, 115.7, 117.2, 118.2, 120.9, 121.1, 124.1, 125.2, 129.7, 130.2, 132.1, 133.0, 133.6, 142.7, 143.6, 151.1, 152.2, 154.2, 155.3, 156.8 (ArC), 160.8 (C=O); MS (EI): m/z 466.1 (M^++1); Anal. Calcd for $C_{27}H_{19}N_3O_5$: C, 69.67; H, 4.11; N, 9.03. Found: C, 69.85; H, 4.01; N, 9.18.

Spectral data of 7'-(6-(2-methoxyphenyl)-3-phenylimidazo[1,2-*a*]pyrazin-8-ylxy)-4'-methyl-

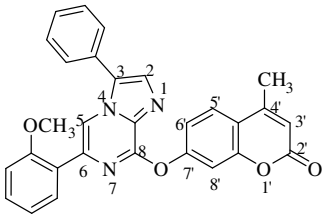

2*H*-chromen-2'-one (22): White solid; Yield: 69%; mp 194-195 ^{o}C; ^{1}H NMR ($CDCl_3$, 400 MHz): δ 2.49 (d, *J* = 1.40 Hz, 3H, CH_3), 3.90 (s, 3H, OCH_3), 6.29 (d, *J* = 0.92 Hz, 1H, C3'H), 6.95-7.00 (m, 2H, ArH), 7.28-7.32 (m, 1H, ArH), 7.42 (dd, ^{2}J = 8.72 Hz, ^{3}J = 2.28 Hz, 1H, C5'H), 7.48-7.50 (m, 1H, ArH), 7.52 (d, *J* = 2.28 Hz, 1H, C8'H), 7.59 (t, *J* = 7.58 Hz, 2H, ArH), 7.67-7.70 (m, 3H, ArH), 7.81 (dd, ^{2}J = 7.80 Hz, ^{3}J = 1.82 Hz, 1H, ArH), 7.86 (s, 1H, C2H), 8.99 (s, 1H, C5H); ^{13}C NMR ($CDCl_3$, 100 MHz): δ 18.7 (CH_3), 55.6 (OCH_3), 110.3, 111.2, 114.0, 114.3, 117.2, 118.2, 121.1, 124.1, 125.2, 128.0, 128.3, 128.9, 129.2, 129.3, 129.6, 130.1, 132.5, 133.2, 133.6, 151.4, 152.1, 154.3, 155.4, 156.7 (ArC), 160.8 (C=O); MS (EI): m/z 476.2 (M^{+}+1); Anal. Calcd for $C_{29}H_{21}N_3O_4$: C, 73.25; H, 4.45; N, 8.84. Found: C, 73.49; H, 4.62; N, 8.99.

Spectral data of 7'-(6-(2-methoxyphenyl)-3-*m*-tolylimidazo[1,2-*a*]pyrazin-8-yloxy)-4'-methyl-2*H*-chromen-2'-one (23):

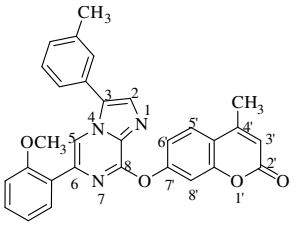

White solid; Yield: 72%; mp 202-203 ^{o}C; ^{1}H NMR ($CDCl_3$, 400 MHz): δ 2.49 (d, *J* = 1.36 Hz, 3H, CH_3), 2.50 (s, 3H, CH_3), 3.92 (s, 3H, OCH_3), 6.30 (d, *J* = 1.36 Hz, 1H, C3'H), 6.96-7.00 (m, 2H, ArH), 7.28-7.32 (m, 2H, ArH), 7.42 (dd, ^{2}J = 8.72 Hz, ^{3}J = 2.28 Hz, 1H, C5'H), 7.48 (d, *J* = 5.48 Hz, 2H, ArH), 7.50 (s, 1H, ArH), 7.52 (d, *J* = 2.28 Hz, 1H, C8'H), 7.69 (d, *J* = 8.72 Hz, 1H, ArH), 7.81 (dd, ^{2}J = 7.32 Hz, ^{3}J = 1.60 Hz, 1H, ArH), 7.85 (s, 1H, C2H), 9.00 (s, 1H, C5H); ^{13}C NMR ($CDCl_3$, 100 MHz): δ 18.8 (CH_3), 21.5 (CH_3), 55.5 (OCH_3), 110.3, 111.1, 114.0, 114.4, 117.2, 118.2, 121.1, 124.1, 125.0, 125.2, 128.2, 128.5, 129.1, 129.3, 129.6, 129.7, 130.1, 132.4, 132.9, 133.6, 139.1, 151.3, 152.2, 154.2, 155.4, 156.6 (ArC), 160.9 (C=O); MS (EI): m/z 490.2 (M^{+}+1); Anal. Calcd for $C_{30}H_{23}N_3O_4$: C, 73.61; H, 4.74; N, 8.58. Found: C, 73.72; H, 4.82; N, 8.33.

Spectral data of 7'-(3-(4-ethylphenyl)-6-(2-methoxyphenyl)imidazo[1,2-*a*]pyrazin-8-yloxy)-4'-methyl-2*H*-chromen-2'-one (24):

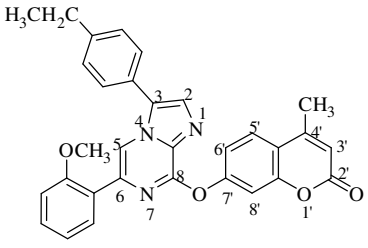

Off White solid; Yield: 55%; mp 179-180 ^{o}C; ^{1}H NMR ($CDCl_3$, 400 MHz): δ 1.33 (t, *J* = 7.56 Hz, 3H, CH_3), 2.48 (d, *J* = 0.92 Hz, 3H, CH_3), 2.77 (q, *J* = 7.56 Hz, 2H, CH_2), 3.91 (s, 3H, OCH_3), 6.29 (d, *J* = 1.20 Hz, 1H, C3'H), 6.95-7.00 (m, 2H, ArH), 7.27-7.31 (m, 1H, ArH), 7.39-7.42 (m, 3H, ArH), 7.52 (d, *J* = 2.28 Hz, 1H, C8'H), 7.59 (d, *J* = 8.24 Hz, 2H, ArH), 7.68 (d, *J* = 8.72 Hz, 1H, ArH), 7.77-7.82 (m, 1H, ArH), 7.83 (s, 1H, C2H), 8.97 (s, 1H, C5H);

^{13}C NMR ($CDCl_3$, 100 MHz): δ 15.4 (CH_3), 18.8 (CH_3), 28.7 (CH_2), 55.6 (OCH_3), 110.3, 111.1, 114.0, 114.4, 117.2, 118.2, 121.1, 124.5, 125.2, 127.9, 128.7, 130.1, 130.9, 131.4, 132.3, 133.0, 133.4, 134.5, 151.3, 152.2, 154.2, 155.4, 156.7 (ArC), 160.9 (C=O); MS (EI): m/z 504.2 (M^++1); Anal. Calcd for $C_{31}H_{25}N_3O_4$: C, 73.94; H, 5.00; N, 8.34; Found: C, 74.16; H, 4.89; N, 8.17.

Spectral data of 7'-(3-(4-fluorophenyl)-6-(2-methoxyphenyl)imidazo[1,2-*a*]pyrazin-8-yloxy)-4'-methyl-2*H*-chromen-2'-one (25): White solid; Yield: 75%; mp 235-237 ^{o}C; ^{1}H NMR ($CDCl_3$, 400 MHz): δ 2.49 (d, *J* = 1.36 Hz, 3H, CH_3), 3.90 (s, 3H, OCH_3), 6.30 (d, *J* = 0.92 Hz, 1H, C3'H), 6.96-7.01 (m, 2H, ArH), 7.27-7.33 (m, 3H, ArH), 7.42 (dd, ^2J = 8.72 Hz, ^3J = 2.28 Hz, 1H, C5'H), 7.52 (d, *J* = 2.32 Hz, 1H, C8'H), 7.63-7.66 (m, 2H, ArH), 7.69 (d, *J* = 8.72 Hz, 1H, ArH), 7.81 (dd, ^2J = 7.80 Hz, ^3J = 1.84 Hz, 1H, ArH), 7.83 (s, 1H, C2H), 8.89 (s, 1H, C5H); ^{13}C NMR ($CDCl_3$, 100 MHz): δ 18.8 (CH_3), 55.6 (OCH_3), 110.3, 111.1, 114.0, 114.1, 116.4, 116.6, 117.2, 118.2, 121.1, 123.9, 124.4, 125.2, 128.1, 129.7, 130.0, 130.1, 132.5, 133.2, 133.6, 151.4, 152.2, 154.2, 155.3, 156.6, 160.8 (C=O), 161.7, 164.1 (ArC); MS (EI): m/z 494.2 (M^++1); Anal. Calcd for $C_{29}H_{20}FN_3O_4$: C, 70.58; H, 4.08; N, 8.51. Found: C, 70.69; H, 3.97; N, 8.32.

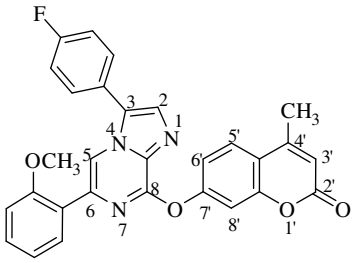

Spectral data of 7'-(3-(4-chlorophenyl)-6-(2-methoxyphenyl)imidazo[1,2-*a*]pyrazin-8-yloxy)-4'-methyl-2*H*-chromen-2'-one (26): White solid; Yield: 65%; mp 243-245 ^{o}C; ^{1}H NMR ($CDCl_3$, 400 MHz): δ 2.49 (d, *J* = 1.36 Hz, 3H, CH_3), 3.92 (s, 3H, OCH_3), 6.30 (d, *J* = 1.40 Hz, 1H, C3'H), 6.97-7.01 (m, 2H, ArH), 7.29-7.33 (m, 1H, ArH), 7.41 (dd, ^2J = 8.68 Hz, ^3J = 2.28 Hz, 1H, C5'H), 7.51 (d, *J* = 2.28 Hz, 1H, C8'H), 7.55-7.58 (m, 2H, ArH), 7.60-7.63 (m, 2H, ArH), 7.69 (d, *J* = 8.72 Hz, 1H, ArH), 7.81 (dd, ^2J = 7.76 Hz, ^3J = 1.82 Hz, 1H, ArH), 7.85 (s, 1H, C2H), 8.92 (s, 1H, C5H); ^{13}C NMR ($CDCl_3$, 100 MHz): δ 18.8 (CH_3), 55.7 (OCH_3), 110.3, 111.2, 114.0, 114.1, 117.3, 118.2, 121.2, 123.9, 125.2, 126.8, 128.0, 129.2, 129.6, 129.7, 130.1, 132.6, 133.4, 133.8, 134.9, 151.4, 152.2, 154.2, 155.3, 156.6 (ArC), 160.8 (C=O); MS (EI): m/z 510.1 (M^++1); Anal. Calcd for $C_{29}H_{20}ClN_3O_4$: C, 68.30; H, 3.95; N, 8.24. Found: C, 68.61; H, 4.06; N, 8.16.

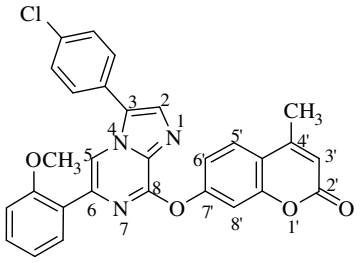

Spectral data of 7'-(6-(2-methoxyphenyl)-3-(3-(trifluoromethyl)phenyl)imidazo[1,2-

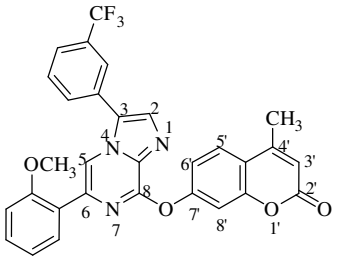

***a*]pyrazin-8-yloxy)-4'-methyl-2*H*-chromen-2'-one (27):** White solid; Yield: 55%; mp 204-206 ^{o}C; ^{1}H NMR ($CDCl_3$, 400 MHz): δ 2.49 (d, J = 0.92 Hz, 3H, CH_3), 3.92 (s, 3H, OCH_3), 6.31 (d, J = 0.68 Hz, 1H, C3'H), 6.97-7.00 (m, 2H, ArH), 7.28-7.33 (m, 1H, ArH), 7.42 (dd, ^{2}J = 8.68 Hz, ^{3}J = 2.30 Hz, 1H, C5'H), 7.50 (d, J = 2.28 Hz, 1H, C8'H), 7.70 (d, J = 8.68 Hz, 1H, ArH), 7.73-7.78 (m, 2H ArH), 7.84 (dd, ^{2}J = 8.24 Hz, ^{3}J = 1.84 Hz, 1H, ArH), 7.86 (d, J = 7.32 Hz, 1H, ArH), 7.92 (s, 1H, ArH), 7.98 (s, 1H, C2H), 9.01 (s, 1H, C5H); ^{13}C NMR ($CDCl_3$, 100 MHz): δ 18.8 (CH_3), 55.4 (OCH_3), 110.3, 111.1, 113.9, 114.1, 117.3, 118.2, 121.1, 123.6, 124.1, 124.2, 125.1, 125.3, 125.5, 125.6, 127.6, 129.3, 129.8, 130.0, 131.5, 131.6, 131.9, 132.9, 133.5, 134.2, 151.5, 152.1, 154.2, 155.2, 156.7 (ArC), 160.8 (C=O); MS (EI): m/z 544.2 (M^{+}+1); Anal. Calcd for $C_{30}H_{20}F_3N_3O_4$: C, 66.30; H, 3.71; N, 7.73. Found: C, 66.03; H, 3.60; N, 7.66.

Spectral data of 7'-(6-(2-methoxyphenyl)-3-(4-methoxyphenyl)imidazo[1,2-*a*]pyrazin-8-yloxy)-4'-methyl-2*H*-chromen-2'-one (28): White solid; Yield: 64%; mp 239-241 ^{o}C; ^{1}H NMR ($CDCl_3$, 400 MHz): δ 2.49 (d, J = 1.40 Hz, 3H, CH_3), 3.90 (s, 3H, OCH_3), 3.92 (s, 3H, OCH_3), 6.30 (d, J = 0.92 Hz, 1H, C3'H), 6.95-7.00 (m, 2H, ArH), 7.11 (d, J = 9.16 Hz, 2H, ArH), 7.28-7.32 (m, 1H, ArH), 7.42 (dd, ^{2}J = 8.72 Hz, ^{3}J = 2.30 Hz, 1H, C5'H), 7.52 (d, J = 2.28 Hz, 1H, C8'H), 7.59 (d, J = 8.68 Hz, 2H, ArH), 7.68 (d, J = 8.72 Hz, 1H, ArH), 7.78-7.80 (m, 2H, ArH, C2H), 8.91 (s, 1H, C5H); ^{13}C NMR ($CDCl_3$, 100 MHz): δ 18.7 (CH_3), 55.4 (OCH_3), 55.6 (OCH_3), 110.2, 111.1, 114.0, 114.2, 114.6, 117.1, 118.2, 120.5, 121.1, 124.1, 125.2, 129.0, 129.4, 129.5, 130.0, 132.2, 132.9, 133.1, 151.3, 152.2, 154.2, 155.4, 156.6, 160.0 (ArC), 160.8 (C=O); MS (EI): m/z 506.2 (M^{+}+1); Anal. Calcd for $C_{30}H_{23}N_3O_5$: C, 71.28; H, 4.59; N, 8.31. Found: C, 71.46; H, 4.70; N, 8.18.

Spectral data of 7'-(3-(2-hydroxyphenyl)-6-(2-methoxyphenyl)imidazo[1,2-*a*]pyrazin-8-yloxy)-4'-methyl-2*H*-chromen-2'-one (29): 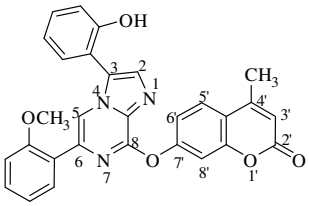

White solid; Yield: 53%; mp >300 ^{o}C; ^{1}H NMR ($CDCl_3$ + TFA, 400 MHz): δ 2.58 (d, *J* = 0.92 Hz, 3H, CH_3), 3.85 (s, 3H, OCH_3), 6.51 (s, 1H, C3'H), 6.98-7.01 (m, 2H, ArH), 7.13-7.20 (m, 2H, ArH), 7.37-7.41 (m, 1H, ArH), 7.46 (d, *J* = 7.76 Hz, 2H, ArH), 7.53--7.58 (m, 2H, ArH), 7.72 (dd, ^{2}J = 8.24 Hz, ^{3}J = 1.60 Hz, 1H, ArH), 7.85 (d, *J* = 8.72 Hz, 1H, ArH), 8.10 (s, 1H, C2H), 8.86 (s, 1H, C5H); ^{13}C NMR ($CDCl_3$+TFA, 100 MHz): δ 18.9 (CH_3), 55.6 (OCH_3), 111.2, 111.6, 113.6, 115.4, 116.8, 118.4, 118.8, 121.4, 121.7, 123.2, 125.1, 126.5, 128.0, 130.2, 131.2, 131.8, 133.6, 139.1, 147.3, 153.4, 153.9, 154.4, 155.9, 157.1 (ArC), 164.6 (C=O); MS (EI): m/z 492.2 (M^{+}+1); Anal. Calcd for $C_{29}H_{21}N_3O_5$: C, 70.87; H, 4.31; N, 8.55. Found: C, 70.77; H, 4.28; N, 8.70.

Spectral data of 7'-(6-(4-chlorophenyl)-3-(thiophen-2-yl)imidazo[1,2-*a*]pyrazin-8-yloxy)-4'-methyl-2*H*-chromen-2'-one (30): 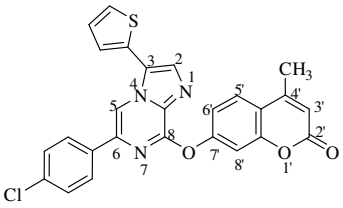

White solid; Yield: 61%; mp 187-189 ^{o}C; ^{1}H NMR ($CDCl_3$, 400 MHz): δ 2.52 (d, *J* = 0.92 Hz, 3H, CH_3), 6.32 (d, *J* = 1.40 Hz, 1H, C3'H), 7.28-7.30 (m, 1H, ArH), 7.33-7.40 (m, 3H, ArH), 7.42 (dd, ^{2}J = 3.68 Hz, ^{3}J = 1.38 Hz, 1H, ArH), 7.47 (d, *J* = 2.28 Hz, 1H, C8'H), 7.57-7.58 (m, 1H, ArH), 7.66 (d, *J* = 8.72 Hz, 2H, ArH), 7.71 (d, *J* = 8.72 Hz, 1H, ArH), 7.90 (s, 1H, C2H), 8.47 (s, 1H, C5H); ^{13}C NMR ($CDCl_3$, 100 MHz): δ 18.8 (CH_3), 109.7, 110.5, 114.3, 117.5, 118.2, 123.1, 125.3, 127.2, 127.3, 127.3, 128.2, 129.0, 129.4, 129.9, 132.6, 133.9, 134.7, 134.8, 136.1, 152.1, 154.2, 154.9 (ArC), 160.7 (C=O); MS (EI): m/z 486.1 (M^{+}+1); Anal. Calcd for $C_{20}H_{16}ClN_3O_3S$: C, 64.26; H, 3.32; N, 8.65; S, 6.60. Found: C, 64.41; H, 3.24; N, 8.78; S, 6.43.

3.10.7. MTT ASSAY PROTOCOL

Hek293 (Human embryonic kidney)cells, DMEM with 50 mM glutamine, 10% FBS, 100 u/ml pencillin and 100 mg/ml streptomycin. The test was performed against Hek293 (Human embryonic kidney) cells. Cells were seeded in 96 well plates at the density of $1x10^{-5}$ cells/well in DMEM media supplemented with 10% FBS cells. Cells were incubated at 37^{o} C in 5% CO_2 incubator. Cells were treated with compound **16b** at five concentrations (10^{-4}, 10^{-5}, 10^{-6}, 10^{-7}, 10^{-8}) for 24 h at 37 ^{o}C. 10 µl of MTT (prepared in 1* PBS buffer) from 5mg/ml stock was added in each well and incubated at 37^{o}C for 4 h in dark. The formazan crystals were dissolved using 100 µl of DMSO. Further, the amount of formazan crystal formation was measured as difference in

absorbance by Bio-Red ELISA plate reader at 570 nm and 690 nm reference wavelength. The relative cell toxicity (%) related to control wells containing culture medium without test material was calculated by using formula:

$$\% \text{ Cell Toxicity} = 100 - \frac{\text{OD (Compound treated wells)}}{\text{OD (Untreated Wells)}} \text{ X } 100$$

3.10.8. SHAKE-FLASK METHOD

Partition coefficient for the target compounds was determined at room temperature using n-octanol–phosphate buffer (0.15 M, pH = 7.4). The experiments were performed in the system phosphate buffer: n-octanol at different volumes (30: 1, 50: 1). The stock solutions of the entire compounds were prepared in dimethylsulfoxide (spectroscopy grade) at concentration of 5×10^{-4} M. All solutions were pipette into glass vials; phosphate buffer and stock solution (125 µL, 250 µL) were added with a micropipette. The wavelength chosen according to the λ_{max} of the compounds i.e., 307, 315, 287, 323, 283, 290, 272, and 294 for **6**, **7a**, **9b**, **10b**, **11b**, **16b**, **28** and **30** respectively. Initial absorbance (A_i) of stock solution in the buffer phase was recorded for each compound followed by n-Octanol was added into each vial. The phases were shaken together on a mechanical shaker (METREX, Cat No. MRS-50H) for 45 minutes, centrifuged (REMI R-24) at 2500 rpm for 30 min to afford complete phase separation, and n-octanol phase was removed. Absorbance of the buffer phase was measured spectrophotometrically using a CHAMPION UV-500 spectrophotometer.

P values were calculated from the following equation:-

$$P = \frac{A_i - A_f}{A_f} \times \frac{V_w}{V_o}$$

Where A_i and A_f represent the absorbance of compounds in the aqueous phase before and after partitioning, respectively. V_w and V_o represent the volume of the aqueous and organic phases used in the octanol/buffer system.

3.10.9. MOLECULAR MODELLING (DOCKING)

Coordinates from the X-ray crystal structure of (PDB ID: 3OG7) were taken from the RCSB Protein Data Bank. Compounds were constructed with the builder toolkit of the software package ArgusLab 4.0.1 (www.arguslab.com) and energy minimized using the semiempirical quantum

mechanical method PM3. The monomeric structure of the enzyme was chosen, and the active site was defined around the ligand. The molecule to be docked in the enzyme active site was inserted into the work space carrying the structure of the enzyme. The docking program implements an efficient grid-based docking algorithm, which approximates an exhaustive search within the free volume of the binding site cavity. The conformational space was surveyed by the geometry optimization of the flexible ligand (rings are treated as rigid) in combination with the incremental construction of the ligand torsions. Thus, docking occurred between the flexible ligand parts of the compound and enzyme. The ligand orientation was determined by a shape scoring function based on A score and the final positions were ranked by lowest interaction energy values. Hydrogen bond between the compound and enzyme were explored by distance measurements.

CHAPTER 4

4.1. IMIDAZO[1,2-*a*]PYRAZINE-TRIAZOLE-COUMARIN CONJUGATES

4.1.1. INTRODUCTION

Energy transfer (ET) cassettes involve the absorption of photon of light by one of the chromophores, resulting in energy transfer. Donor molecule returned to ground state along with raising the acceptor to excited state.[124] Energy transfer process can take place in two different ways; (i) through bond energy transfer (TBET),[125] and (ii) through space energy transfer (Fluorescence resonance energy transfer, FRET).[126] Energy transfer through both pathways involves use of a donor and an acceptor linked through, conjugated spacer in case of TBET and non-conjugated spacer in case of FRET. Energy transfer through TBET does not require the criterion of spectral overlap between the absorption of the acceptor and emission of the donor. On the other hand, FRET phenomenon requires the criterion of spectral overlap between absorption spectra of acceptor and emission spectra of donor. It can also afford simultaneous recording ratio signals of two emission intensities at different wavelengths, which could provide a built-in correction for the environmental effects and supply a facile method for visualizing complex biological processes at the molecular level, such as nucleic acid regulation, DNA detection, protein labelling, and other biomarkers. Consequently, studying the construction of energy donor–acceptor architectures, or "energy transfer cassettes" is very interesting and significant to many chemists, biologists, environmentalists, and medical scientists.

4.1.2. OBJECTIVE

"Click reactions" and "Suzuki-Miyaura cross couplings" have been proved to be the powerful tools to construct the heterocyclic molecular frameworks. Herein, we have reported the first sequential functionalization at C-8 and C-6 positions of imidazo[1,2-*a*]pyrazine by implementing "click" and "Suzuki-Miyaura cross coupling" reactions respectively. These have been leading to energy transfer cassettes along with the determination of photophysical characterization of the synthesized compounds by depicting the quantum yields. We have introduced various electron donating substituents viz., methyl, ethyl, hydroxy, methoxy as well as electron withdrawing substituents viz., formyl, acetyl to the donor part of the cassette, thereby determining the overall quantum yield and energy transfer efficiency (ETE). The effect of spacer length between donor

and acceptor has also been studied to predict the energy transfer efficiency. To the best of our knowledge, this is first report for coupling of imidazo[1,2-*a*]pyrazine based donors with coumarin acceptors in way that facilitate energy transfer through space.

4.1.3. CHEMISTRY

To synthesize these energy transfer cassettes, our study was initiated with the easily available starting material 2-bromoethylamine hydrobromide **1** which was refluxed with sodium azide in water for 12 h followed by stirring with sodium hydroxide at room temperature to give 2-azidoethanamine **2**.[127] The azide has limited thermal stability but they could be stored in ether or hexane for longer period of time at low temperature in pure state. To obtain the first precursor, we have treated 6,8-dibromoimidazo[1,2-*a*]pyrazine **3** (obtained from bromination of 2-aminopyrazine followed by cyclization with 50% aqueous chloroacetaldehyde) with 2-azidoethanamine **2** in the presence of diisopropylethylamine (DIPEA) in acetonitrile at reflux temperature for 24 h to obtain *N*-(2-azidoethyl)-6-bromoimidazo[1,2-*a*]pyrazin-8-amine **4** in 72% yield (Scheme 1).

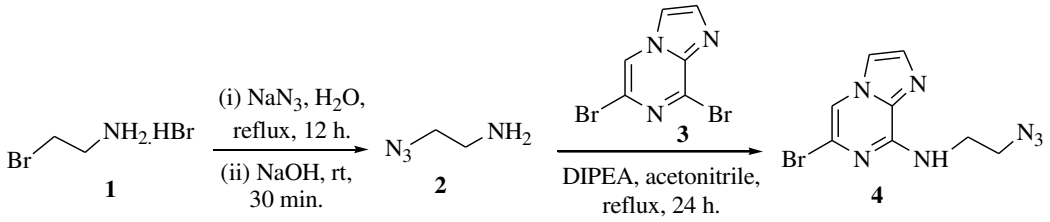

Scheme 1 Synthesis of *N*-(2-azidoethyl)-6-bromoimidazo[1,2-*a*]pyrazin-8-amine (**4**)

Second precursor 4-methyl-7-(prop-2-ynyloxy)-2*H*-chromen-2-one **6** was obtained in 81% yield by the reaction of 7-hydroxy-4-methyl-2*H*-chromen-2-one **5** with 2 equivalents of 80% solution of propargyl bromide in the presence of potassium carbonate and acetone at room temperature for 12 h (Scheme 2).

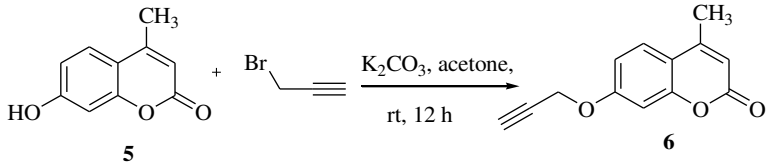

Scheme 2 Synthesis of 4-methyl-7-(prop-2-ynyloxy)-2*H*-chromen-2-one (**6**)

With both the precursors in hand, copper-catalyzed azide alkyne cycloaddition (CuAAC) reaction of imidazo[1,2-*a*]pyrazine **4** and coumarin **6** was performed. To explore the feasibility of [2+3] cycloaddition of azide alkyne reaction, various catalysts and solvents (Table 1) were screened according to the existing literature. Among the various catalysts ($CuSO_4.5H_2O$, CuBr, CuI and $CuCl_2$), $CuSO_4.5H_2O$ showed the highest efficiency in the presence of sodium ascorbate at room temperature (Table 1, entry 8). Several solvents were also tested; ethanol and water mixture was proved to be the most effective solvent (Table 1, entries 4,8,12). Increasing the temperature of the reaction did not lead to any further improvements in the yield (Table 1, entries 13,14). No improvement in efficiency observed when the loading of $CuSO_4$ was increased from 5-15 mol% (Table 1, entries 15,16).

Table 1 Optimization of click reactions

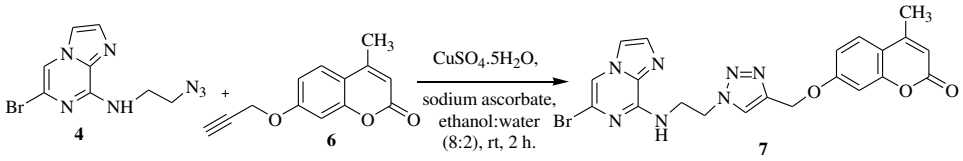

4 **6** **7**

Entry	Cu (5 mol%)	Sodium ascorbate	Solvent	Temp.	Yield (%)
1	CuBr	10 mol%	Butanol:H_2O	rt	50%
2	CuI	10 mol%	Butanol:H_2O	rt	52%
3	$CuCl_2$	10 mol%	Butanol:H_2O	rt	52%
4	$CuSO_4.5H_2O$	10 mol%	Butanol:H_2O	rt	61%
5	CuBr	10 mol%	Ethanol:H_2O	rt	20%
6	CuI	10 mol%	Ethanol:H_2O	rt	60%
7	$CuCl_2$	10 mol%	Ethanol:H_2O	rt	30%
8	**$CuSO_4.5H_2O$**	**10 mol%**	**Ethanol:H_2O**	rt	**91%**
9	CuBr	10 mol%	H_2O	rt	< 5%
10	CuI	10 mol%	H_2O	rt	15%
11	$CuCl_2$	10 mol%	H_2O	rt	20%
12	$CuSO_4.5H_2O$	10 mol%	H_2O	rt	49%
13	$CuSO_4.5H_2O$	10 mol%	Ethanol:H_2O	60 ^oC	79%
14	$CuSO_4.5H_2O$	10 mol%	Ethanol:H_2O	80 ^oC	78%
15	$CuSO_4.5H_2O$ (10 mol%)	10 mol%	Ethanol:H_2O	rt	81%
16	$CuSO_4.5H_2O$ (15 mol%)	10 mol%	Ethanol:H_2O	Rt	83%

With the optimized reaction conditions, compound **4** was treated with 4-methyl-7-(prop-2-ynyloxy)-2*H*-chromen-2-one **6** in the presence of 5 mol% of $CuSO_4.5H_2O$ and 10 mol% of sodium ascorbate in ethanol:water (8:2) at room temperature for 2h to give 1,4-disubstituted triazole **7** in 91% yield. However, when the reaction was typically carried out in heating without using any catalyst, mixtures of 1,4- (**7**) and 1,5-disubstituted (**8**) triazole derivatives in the ratio of 2:1 were obtained (Scheme 3). It has been observed that thermal [2+3] dipolar cycloaddition of alkyne to azide is not a regiospecific reaction.[128] Strong Nuclear Overhauser effect (NOE) was observed between the H-5' triazole proton and protons of substituted alkyl groups present at N-1' and C-4' positions in compound **7**, suggesting that the triazole proton and alkyl groups are in close proximity, confirmed the formation of 1,4-disubstituted triazole. NOE spectrum of 1,5-disubstituted triazole **8** showed no correlation between the singlet of triazole at C-4' position and triplet of substituted alkyl group present at N-1' position. The expected NOE correlation of triazole protons at C-4' and C-5' alkyl group was observed (Scheme 3).

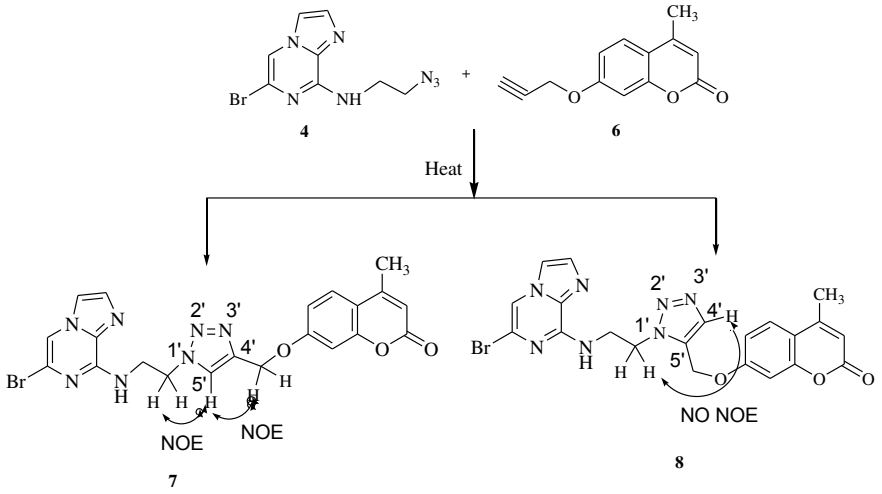

Scheme 3 Thermal [2+3] cycloaddition reaction of **4** and **6**

1,4-Disubstituted triazole **7** was further used for the synthesis of library of compounds with Suzuki-Miyaura cross coupling reactions at C-6 position of imidazo[1,2-*a*]pyrazine. To identify the optimal reaction conditions, various reported Pd-catalysts, along with different combinations of bases and organic solvents were examined in the reaction of imidazo[1,2-*a*]pyrazine **7** with thiophen-2-yl boronic acid. Previous study[129] showed that base was a key reaction parameter, so different bases (Cs_2CO_3, K_2CO_3, and DIPEA) and solvents (CH_3CN:H_2O, dioxane:H_2O and DME:H_2O) were reviewed first. Both affected the product yields as K_2CO_3 and dioxane:water gave best results.

Table 2 Optimization of Suzuki-Miyaura cross coupling reaction

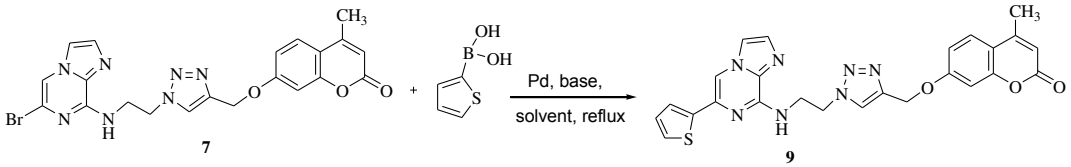

7 9

Entry	Time (h)	Catalyst	Base	Solvent	Yield (%)
1	12	$Pd(PPh_3)_2Cl_2$	Cs_2CO_3	MeCN:H_2O	38%
2	12	$Pd_2(dba)_3$	Cs_2CO_3	MeCN:H_2O	19%
3	8	$Pd(PPh_3)_4$	Cs_2CO_3	MeCN:H_2O	33%
4	8	[$PdCl_2$(*dppf*)]DCM	Cs_2CO_3	MeCN:H_2O	35%
5	10	$Pd(PPh_3)_2Cl_2$	K_2CO_3	MeCN:H_2O	28%
6	12	$Pd_2(dba)_3$	K_2CO_3	MeCN:H_2O	25%
7	12	$Pd(PPh_3)_4$	K_2CO_3	MeCN:H_2O	27%
8	18	[$PdCl_2$(*dppf*)]DCM	K_2CO_3	MeCN:H_2O	27%
9	19	$Pd(PPh_3)_2Cl_2$	DIPEA	MeCN:H_2O	15%
10	18	$Pd_2(dba)_3$	DIPEA	MeCN:H_2O	15%
11	12	$Pd(PPh_3)_4$	DIPEA	MeCN:H_2O	20%
12	19	[$PdCl_2$(*dppf*)]DCM	DIPEA	MeCN:H_2O	15%
13	10	$Pd(PPh_3)_2Cl_2$	Cs_2CO_3	Dioxane:H_2O	51%
14	10	$Pd_2(dba)_3$	Cs_2CO_3	Dioxane:H_2O	32%
15	15	$Pd(PPh_3)_4$	Cs_2CO_3	Dioxane:H_2O	55%
16	14	[$PdCl_2$(*dppf*)]DCM	Cs_2CO_3	Dioxane:H_2O	55%
17	14	$Pd(PPh_3)_2Cl_2$	K_2CO_3	Dioxane:H_2O	58%
18	15	$Pd_2(dba)_3$	K_2CO_3	Dioxane:H_2O	53%
19	**12**	**$Pd(PPh_3)_4$**	**K_2CO_3**	**Dioxane:H_2O**	73%
20	12	[$PdCl_2$(*dppf*)]DCM	K_2CO_3	Dioxane:H_2O	70%
21	12	$Pd(PPh_3)_2Cl_2$	DIPEA	Dioxane:H_2O	42%
22	20	$Pd_2(dba)_3$	DIPEA	Dioxane:H_2O	12%
23	12	$Pd(PPh_3)_4$	DIPEA	Dioxane:H_2O	22%
24	12	[$PdCl_2$(*dppf*)]DCM	DIPEA	Dioxane:H_2O	27%
25	8	$Pd(PPh_3)_2Cl_2$	Cs_2CO_3	DME:H_2O	45%
26	12	$Pd_2(dba)_3$	Cs_2CO_3	DME:H_2O	10%
27	11	$Pd(PPh_3)_4$	Cs_2CO_3	DME:H_2O	32%
28	10	[$PdCl_2$(*dppf*)]DCM	Cs_2CO_3	DME:H_2O	33%

29	10	$Pd(PPh_3)_2Cl_2$	K_2CO_3	DME:H_2O	41%
30	9	$Pd_2(dba)_3$	K_2CO_3	DME:H_2O	9%
31	12	$Pd(PPh_3)_4$	K_2CO_3	DME:H_2O	68%
32	12	[$PdCl_2$(*dppf*)]DCM	K_2CO_3	DME:H_2O	65%
33	12	$Pd(PPh_3)_2Cl_2$	DIPEA	DME:H_2O	15%
34	12	$Pd_2(dba)_3$	DIPEA	DME:H_2O	<5%
35	12	$Pd(PPh_3)_4$	DIPEA	DME:H_2O	12%
36	12	[$PdCl_2$(*dppf*)]DCM	DIPEA	DME:H_2O	15%

With identification of base and solvent, several Pd catalysts were screened (Table 2). Using [$Pd(PPh_3)_4$] as the catalyst, **9** was obtained in 73% yield (Table 2, entry 19), while [$Pd(PPh_3)_2Cl_2$], [$Pd(dba)_3$] and [$PdCl_2$(*dppf*)].DCM declined the yields of desired products (Table 2, entries 17, 18, 20). The best yield was obtained when the model reaction was catalyzed with 5 mol% [$Pd(PPh_3)_4$] and using 1.0 equivalent of thiophen-2-yl boronic acid, 1.0 equivalent of K_2CO_3 in dioxane:water (9:1) at reflux temperature for 6-8 hrs in a sealed tube (Table 2, entry 19). With these optimized reaction conditions, the scope of the reaction was further examined with various aryl boronic acids (Table 3). Suzuki reactions with imidazo[1,2-*a*]pyrazine **7** proceeded well to give the desired products irrespective of the substitution on the phenyl ring. It has been observed that the five member rings were well compatible with optimized conditions, affording the corresponding products in moderate yields (**9-11**, 58-75% yields). Both electron withdrawing substituents viz., fluoro (**13**), chloro (**14**), bromo (**15**), trifluorormethyl (**16**) and acetyl (**24**) as well as electron donating substituents such as methyl (**17**), ethyl (**18**) and methoxy (**21** and **22**) were also compatible with the protocol, providing the arylated imidazo[1,2-*a*]pyrazine in moderate to good yields. The change in directing groups from ortho to para or vice versa did not affect the reactivity. However, with 2-hydroxyphenyl substrate, the reactivity decreased significantly, and the arylated products **20** was obtained in only 53% yield (Table 3, entry 12).

After the screening of 2-azidoethanamine linker, another alkyl chain 3-azidopropanamine was investigated. 3-Bromopropylamine hydrobromide **25** was first reacted with sodium azide to give **26** followed by substitution at C-8 position of 6,8-dibromoimidazo[1,2-*a*]pyrazine **3** to give **27** in 65% yield. Compound **27** was then coupled with coumarin **6** via. copper-catalyzed azide-alkyne cycloaddition reaction to give **28** in 82% yield (Scheme 4).

Table 3 Suzuki-Miyaura cross coupling of ethyl triazole bridged imidazo[1,2-*a*]pyrazine-coumarin conjugates

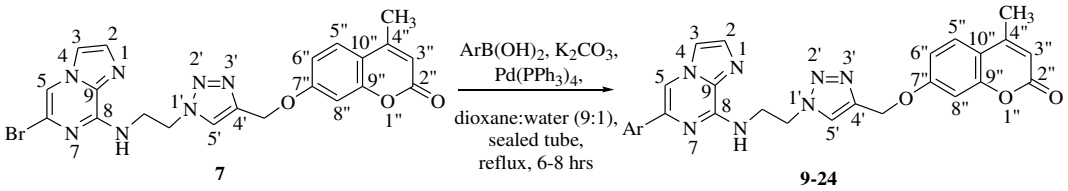

7 **9-24**

Entry	Time (h)	$ArB(OH)_2$	Product	Compound (%)
1	8	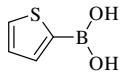	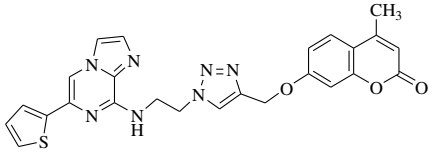	**9** (73)
2	8	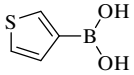	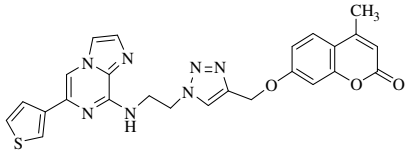	**10** (75)
3	8	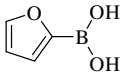	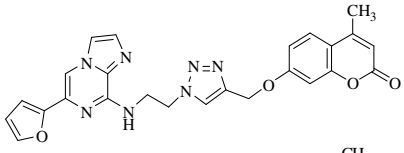	**11** (58)
4	6	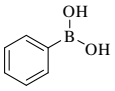	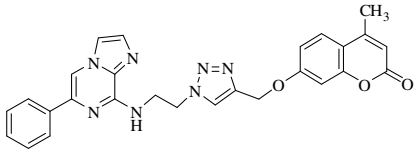	**12** (71)
/				
5	7	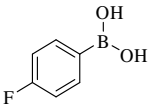	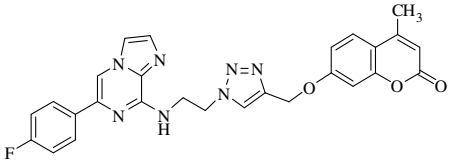	**13** (80)
6	7	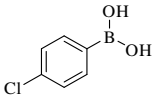	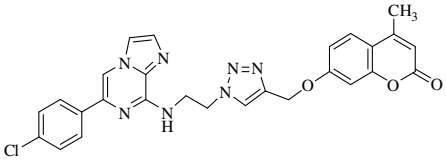	**14** (82)
7	7	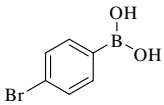	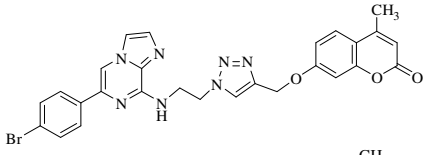	**15** (64)
8	6	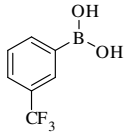	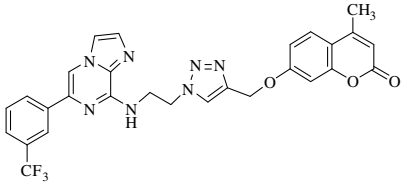	**16** (71)

9	6	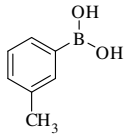	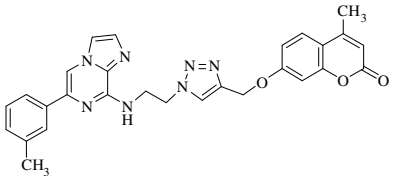	**17** (65)
10	6	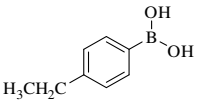	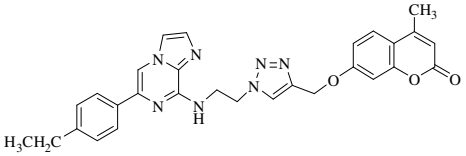	**18** (66)
11	8	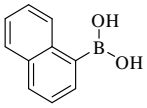	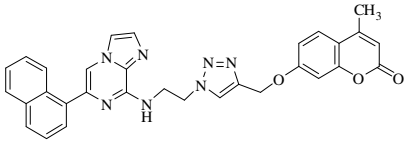	**19** (74)
12	8	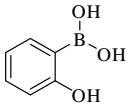	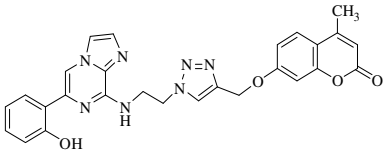	**20** (53)
13	7	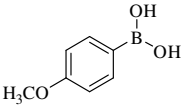	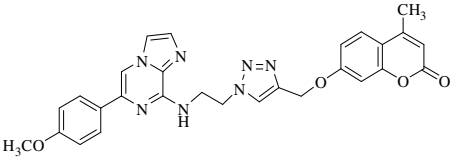	**21** (90)
14	6	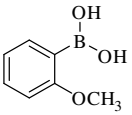	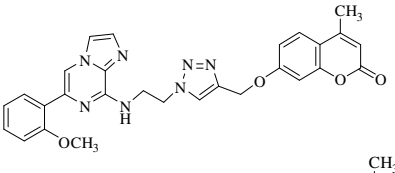	**22** (91)
15	6	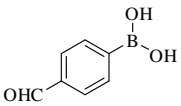	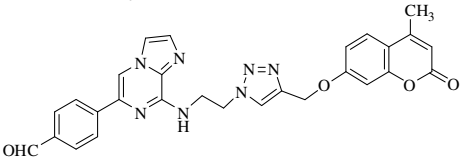	**23** (92)
16	8	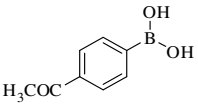	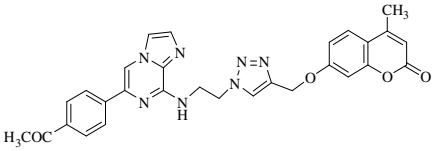	**24** (90)

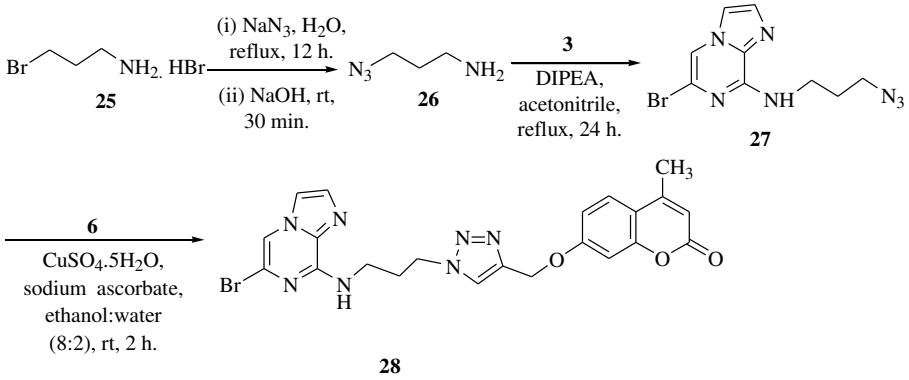

25 **26** **27** **28**

Scheme 4 Synthesis of propyl triazole bridged imidazo[1,2-pyrazine-coumarin conjugate (**28**)

Compound **28** was further coupled with various aryl boronic acids via Suzuki-Miyaura cross coupling reaction using $Pd(PPh_3)_4$, K_2CO_3 and dioxane:water at reflux temperature for 6-8 h to obtain compounds **29-38** in 56-90% yields (Table 4).

Table 4 Suzuki-Miyaura coupling of propyl triazole bridged imidazo[1,2-*a*]pyrazine-coumarin conjugates

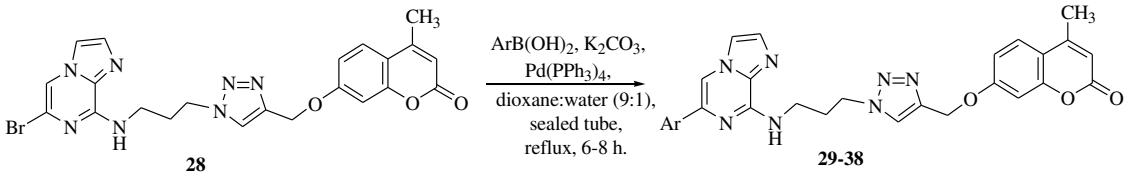

28 **29-38**

Entry	Time (h)	$ArB(OH)_2$	Product	Compound (%)
1	8	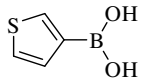	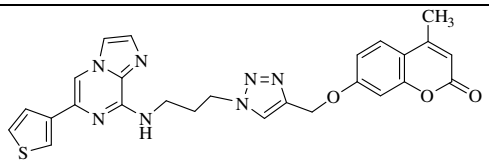	**29** (72)
2	8	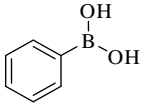	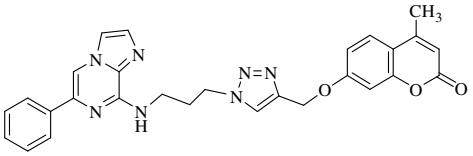	**30** (70)
3	8	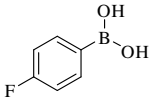	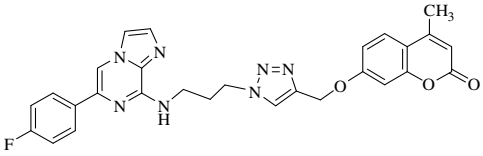	**31** (76)
4	6	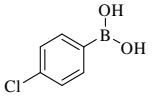	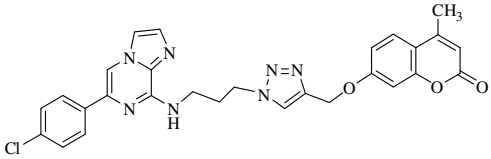	**32** (70)
5	7	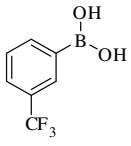	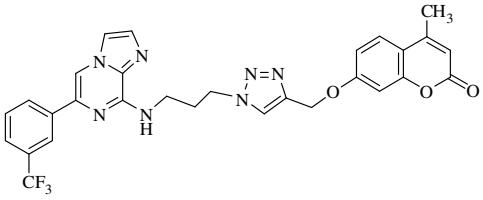	**33** (80)
6	7	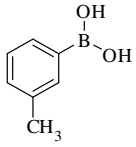	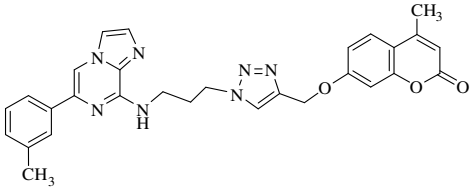	**34** (81)

7	7	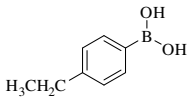	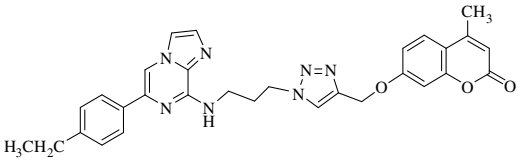	**35** (56)
8	6	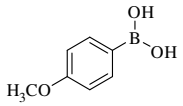	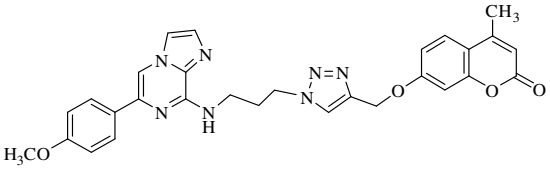	**36** (76)
9	6	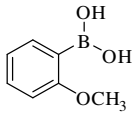	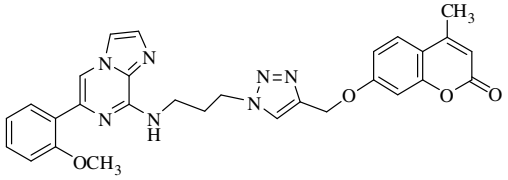	**37** (68)
10	6	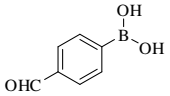	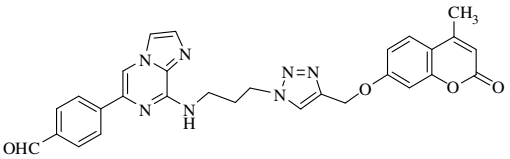	**38** (90)

4.1.4. PHOTOPHYSICAL PROPERTIES

UV-visible and fluorescence spectroscopic measurements (Figures 1 and 2) were recorded for the molecules to test the cassettes, based on the quantification of their efficiencies. Molar absorptivities (€) and quantum yields (Φ_f) for all 28 compounds were determined in acetonitrile. All the derivatives have similar absorption maxima (between 312 to 319 nm). However, compounds **23**, **24** and **38** containing electron withdrawing groups such as formyl and acetyl attached to phenyl ring exhibited two absorption peaks at 275 nm and 317 nm. Similar emission maxima were observed for all derivatives (between 375 to 390 nm). However, emission maxima to longer wavelength (red shift) i.e. from 415 nm to 500 nm were observed for compounds **15**, **19**, **23**, **24** and **38**. Compounds **17**, **18**, **20**, **21** and **22** containing the electron donating groups have lower quantum yields (Φ_f = 0.016 to 0.36) in comparison to compounds **23** and **24** (Φ_f = 0.40 to 0.48) with electron withdrawing 4-formyl and 4-acetyl attached to phenyl ring at C-6 position of imidazo[1,2-*a*]pyrazine. Similar pattern of quantum yield was observed in case of propyl chain in which the electron withdrawing group in **38** showed the highest quantum yield (Φ_f = 0.47). However, on increasing the linker length from ethyl to propyl, a slightly decrease in quantum yield was observed (Tables 5 and 6). Overall, it was inferred that compounds with

electron donating groups showed lower quantum yields in comparison to compounds with electron withdrawing groups. Increase in linker length also resulted in similar or decrease in quantum yields. Energy transfer efficiencies (ETE) based upon the fluorescence quantum yields have also been determined. The efficiency of the energy transfer (ηEET) was evaluated using the equation[130] $\eta EET = 1 - \Phi_{F(\text{donor in dyad})}/\Phi_{F(\text{free donor})}$. Here, $\Phi_{F(\text{donor in dyad})}$ is the fluorescence quantum yield of the donor part in dyad and $\Phi_{F(\text{free donor})}$ is the fluorescence quantum yield of the donor when not connected to the acceptor.

Compound **7** and **28** with bromo at C-6 position of imidazo[1,2-*a*]pyrazine (at the donor part) acted as good energy transfer cassette with ETE values of 73.9% and 76% respectively. Introduction of electron donating groups such as methyl (**17** and **34**) and ethyl (**18** and **35**) also showed comparable ETE (67.3% and 71.7%). While, substitution with halogen to phenyl ring on donor part of the cassettes (**13**, **14**, **15**, **16, 31**, **32** and **33)** displayed low ETE (15.2-69.5%). Presence of electron donating group *viz*., methoxy in compounds **21**, **22** and **36** showed 56.5%, 65.2% and 65.2% ETE respectively. But, the presence of 2-hydroxyphenyl (**20**) to donor moiety

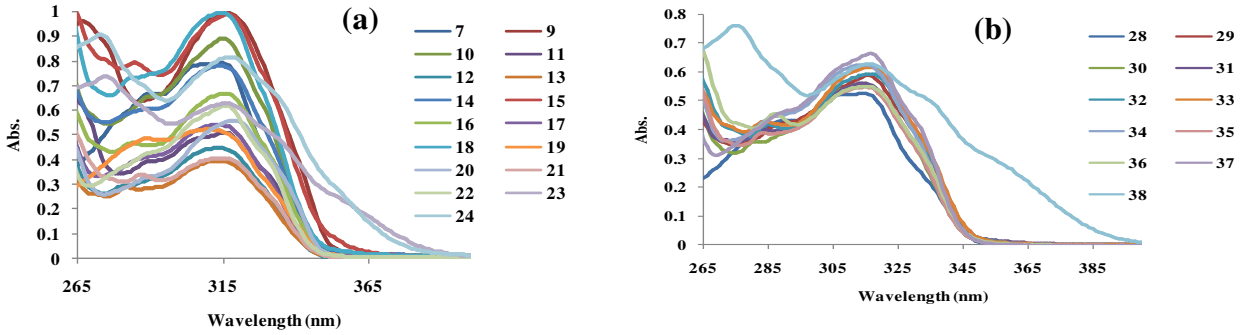

Figure 1 Absorption spectra of (**a**) compounds **7-24** and **(b)** compounds **28-38.**

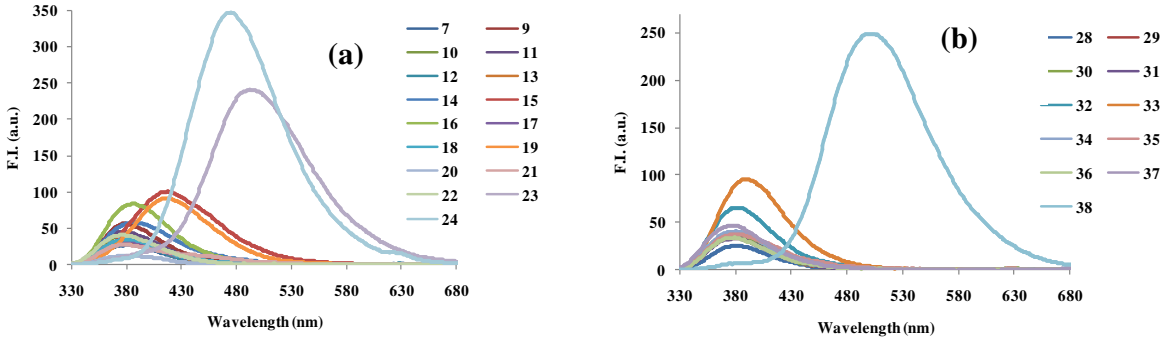

Figure 2 Emission spectra of (**a**) compounds **7-24** and **(b)** compounds **28-38**

Table 5 Photophysical characterizations of absorption and fluorescence properties of compounds 7, **9-24** in acetonitrile

Compd.	λ_{max}^{abs} (nm)	λ_{max}^{emi} (nm)	€	Φ_f	ETE (%)
7	315	380	39600	0.12	73.9
9	315	375	49700	0.22	52.1
10	316	375	44600	0.24	47.8
11	316	377	25350	0.20	56.5
12	315	377	22400	0.15	67.3
13	312	378	19850	0.18	60.8
14	315	385	39050	0.30	34.7
15	317	415	49250	0.34	17.3
16	316	385	33400	0.32	15.2
17	314	378	26950	0.15	67.3
18	315	378	49800	0.13	71.7
19	312	415	26150	0.36	N.D
20	319	378	28000	0.016	96.5
21	314	375	20350	0.20	56.5
22	316	375	30900	0.16	65.2
23	275, 317	495	31400	0.48	N.D
24	275, 317	475	40800	0.40	N.D

N.D: Not determined

showed significant energy transfer efficiency (96.5%). Presence of naphthyl group (**19)** and electron withdrawing 4-formyl (**23** and **38)** and 4-acetyl (**24)** groups to aromatic ring did not show any energy transfer. Thus, compound **20** showed maximum energy transfer efficiency of 96.5% which indicated that this compound behave as a energy transfer cassette to transfer energy from imidazo[1,2-*a*]pyrazine donor to coumarin acceptor. Thus, emission spectra of the imidazo[1,2-*a*]pyrazine (donor) and absorption spectra of the coumarin (acceptor) showed significant spectral overlap for the energy transfer (Figure 3). The energy transfer cassettes of imidazo[1,2-a]pyrazine-coumarin conjugates were also compared with different known molecular hybrids. It has been observed that compound **20** (ETE = 96.5%) showed better or comparable results with fluorescin-coumarin cassettes for detection of phosphodiesterase I

activity (ETE = 94%),[131] fluorescin-coumarin cassettes for ATP complexes (ETE = 76% and 83%),[132] and Bodipy with phenanthroline and terpyridine cassettes for light harvesting system (ETE = 82%) [133] and Bodipy-cyanine based cassettes (ETE = 43-90%).[134]

Table 6 Photophysical characterizations of absorption and fluorescence properties of compounds **28-38** in acetonitrile

Compd.	λ_{max}^{abs} (nm)	λ_{max}^{emi} (nm)	€	Φ_f	ETE (%)
28	315	380	26250	0.11	76.0
29	316	376	29450	0.11	76.0
30	314	375	27900	0.13	71.7
31	315	380	28050	0.14	69.5
32	317	380	29700	0.27	41.3
33	316	390	30850	0.35	15.2
34	315	378	31300	0.13	71.7
35	312	377	27400	0.15	67.3
36	315	375	27550	0.16	65.2
37	317	380	33250	0.17	0.5
38	275, 317	500	31400	0.47	N.D

N.D: Not determined

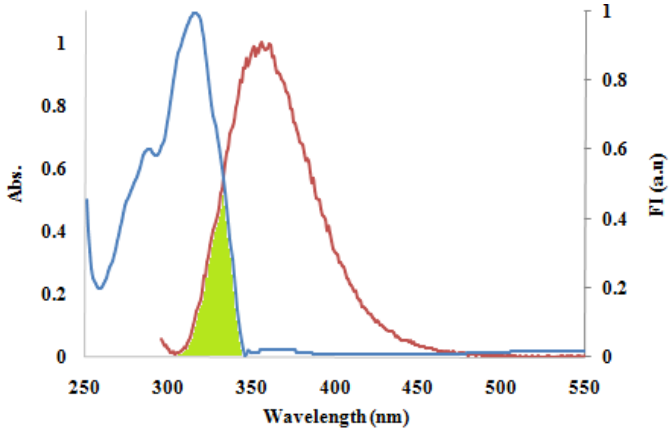

Figure 3 Spectra overlap of emission of the imidazo[1,2-*a*]pyrazine (donor) and absorption spectra of the coumarin (acceptor).

4.1.5. CONCLUSION

Here, we have reported the first examples of new structural strategy to improve the ETE efficiency in molecular hybrids involving the imidazo[1,2-*a*]pyrazine as a key linking the acting

chromophore. This design consists of imidazo[1,2-*a*]pyrazine-coumarin conjugates with variable spacer linker (ethyl and propyl chain) via click reaction at C-8 position and Suzuki-Miyaura cross coupling reaction at C-6 position of imidazo[1,2-*a*]pyrazine. The goal of this simple design was to keep the conformational motion of the involved donor-acceptor chromophores restricted, and tightly fixed to ensure an efficient ETE via FRET. Another important goal was the straight-forward synthetic access to these conjugate cassettes from imidazo[1,2-*a*]pyrazine and acceptor-based coumarins, which assures an excellent potential for developing future smarter hybrid cassettes for valuable fluorescence applications (bioimaging, chemosensing, optoelectronics etc.). We are convinced that herein communicated new structural design to boost the ETE, has great potential for inspiring the future development of molecular cassettes on the basis of molecular hybridization.

4.1.6. EXPERIMENTAL SECTION

4.1.6.1. General Chemistry

All commercially available compounds (Avra, Spectrochem, Aldrich, Merck etc.) were used without further purification. Final reactions were carried out in an oil bath using Microwave Vials (10-15 ml). Melting points were determined in open capillaries and were uncorrected. ^{1}H and ^{13}C NMR spectra were performed on Jeol ECS 400 NMR spectrometer, which was operated at 400 MHz for ^{1}H nuclei and 100 MHz for ^{13}C nuclei, using $CDCl_3$, DMSO-d_6 and trifluoroacetic acid (TFA) as solvents. Chemical shifts are reported in parts per million (ppm) with TMS as internal reference and *J* values are given in hertz. 2D NOE studies were performed on same instrument. Mass Spectra of the synthesized compounds were recorded at Water Micromass-Q-T of Micro. Reactions were monitored by thin layer chromatography (TLC) with silica plate coated with silica gel HF-254 and column chromatography was performed with silica gel 60-120/100-200 mesh. Ethylacetate and methanol were adopted solvent systems.

4.1.6.2. Synthesis of 2-azidoethanamine (2): 2-Bromoethyamine hydrobromide **1** (1 g, 4.90 mmol) was dissolved in distilled water with stirring. Sodium azide was added (0.90 g, 13.84 mmol) carefully to this solution in succession with continuous stirring. The reaction mixture was refluxed for 12 h. After completion of reaction, reaction mixture was cooled to room temperature and was quenched by addition of sodium hydroxide (0.7 g, 17.5 mmol) and further stirred for 30

min at room temperature. Thereafter, mixture was extracted with diethyl ether and dried over sodium sulphate to obtain ether extract and stored at low temperature. The ether extract being volatile in nature, was used as such for next reaction.

4.1.6.3. Synthesis of *N*-(2-azidoethyl)-6-bromoimidazo[1,2-*a*]pyrazin-8-amine (4): To the ether extract containing 2-azidoethanamine **2** was added solution of 6,8-dibromoimidazo[1,2-*a*]pyrazine **3** (0.5 g, 1.80 mmol) in acetonitrile in the presence of diisopropylethylamine (DIPEA). The reaction mixture was refluxed for 24 h. After completion of reaction, the mixture was extracted with chloroform and water. Organic layer was separated, dried over sodium sulphate, filtered and concentrated under vacuum. The crude mixture was then purified by silica gel chromatography 60-120 mesh using hexane : ethyl acetate (8:2) as eluents.

Spectral data of *N*-(2-azidoethyl)-6-bromoimidazo[1,2-*a*]pyrazin-8-amine (4): light

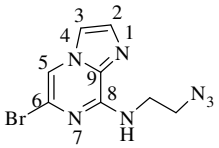

orange solid; yield: 72%; mp 66-68 ^{o}C; ^{1}H NMR ($CDCl_3$, 400 MHz): δ 3.59 (t, *J* = 5.74 Hz, 2H, N<u>CH$_2$</u>), 3.74 (q, *J* = 5.81 Hz, 2H, NH<u>CH$_2$</u>), 7.29 (t, *J* = 5.04 Hz, 1H, NH), 7.47 (d, *J* = 0.92 Hz, 1H, H-2), 7.54 (d, *J* = 0.92 Hz, 1H, H-3), 7.60 (s, 1H, H-5); ^{13}C NMR ($CDCl_3$, 100 MHz): δ 39.9 (NH<u>CH$_2$</u>), 50.0 (N<u>CH$_2$</u>), 109.3, 114.7, 122.5, 131.9, 132.3, 147.2 (ArC); MS (ESI): m/z 284.1 (M^++2); Anal. Calcd for $C_8H_8BrN_7$: C, 34.06; H, 2.86; N, 34.76. Found: C, 34.10; H, 2.81; N, 34.70.

4.1.6.4. Synthesis of 4-methyl-7-(prop-2-ynyloxy)-2*H*-chromen-2-one (6): To 7-hydroxy-4-methyl-2*H*-chromen-2-one **5** (1 g, 5.15 mmol) was added 80% solution of propargyl bromide in toluene (1.33 g, 11.30 mmol) in the presence of potassium carbonate (0.7 g, 5.15 mmol) and acetone. The mixture was stirred at room temperature for 12 h. Completion of reaction was monitored by TLC. Reaction was quenched by addition of ice cold water. The solid product was filtered on vacuum pump to obtain off white solid.

Spectral data of 4-methyl-7-(prop-2-ynyloxy)-2*H*-chromen-2-one (6): Off white solid; Yield:

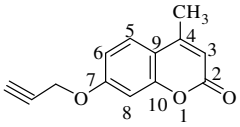

81%; mp 102-104 ^{o}C; ^{1}H NMR ($CDCl_3$, 400 MHz): δ 2.41 (d, *J* = 1.36 Hz, 3H, CH_3), 2.59 (t, *J* = 2.52 Hz, 1H, CH), 4.77 (d, *J* = 2.32 Hz, 2H, OCH_2), 6.16 (d, *J* = 1.36 Hz, 1H, ArH), 6.92-6.95 (m, 2H, ArH), 7.53 (d, *J* = 9.16 Hz, 1H, ArH); ^{13}C NMR ($CDCl_3$, 100 MHz): δ 18.6 (CH_3), 56.0 (OCH_2), 76.4 (alkyne CH, C), 102.0, 112.3, 112.6, 114.1, 125.5, 152.4, 154.9, 160.2 (ArC), 161.1 (C=O); MS (ESI): m/z 216.2 (M^++2).

4.1.6.5. Synthesis of 7-((1-(2-(6-bromoimidazo[1,2-*a*]pyrazin-8-ylamino)ethyl)-1*H*-1,2,3-triazol-4-yl)methoxy)-4-methyl-2*H*-chromen-2-one (7): To the stirred solution of 4-methyl-7-(prop-2-ynyloxy)-2*H*-chromen-2-one **6** (1g, 4.67 mmol) and *N*-(2-azidoethyl)-6-bromoimidazo[1,2-*a*]pyrazin-8-amine **4** (1.31 g, 4.67 mmol) in ethanol:water (8:2), copper sulphate pentahydrate (5 mol%) and sodium ascorbate (10 mol%) was added and stirred at room temperature for 2 h. After completion of reaction, water was added and extracted with chloroform. Organic layer was dried over sodium sulphate, filtered and concentrated in vacuum to obtain off white solid.

Spectral data of 7-((1-(2-(6-bromoimidazo[1,2-*a*]pyrazin-8-ylamino)ethyl)-1*H*-1,2,3-triazol-4-yl)methoxy)-4-methyl-2*H*-chromen-2-one (7): off white solid; yield: 91%; mp156-158 ^{o}C;

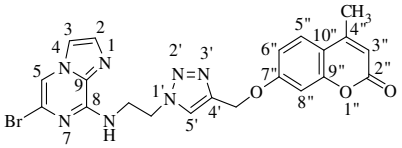

^{1}H NMR ($CDCl_3$, 400 MHz): δ 2.40 (d, *J* = 1.36 Hz, 3H,CH_3), 4.13 (q, *J* = 5.80 Hz, 2H, NH$\underline{CH_2}$), 4.73 (t, *J* = 5.94 Hz, 2H, N$\underline{CH_2}$), 5.24 (s, 2H, O$\underline{CH_2}$), 6.15 (d, *J* = 0.92 Hz, 1H, ArH), 6.82 (t, *J* = 5.72 Hz, 1H, NH), 6.90 (d, *J* = 2.76 Hz, 1H, ArH), 6.93-6.96 (dd, ^{2}J = 9.16 Hz, ^{3}J = 2.52 Hz, 1H, ArH), 7.47 (s, 2H, ArH), 7.50 (d, *J* = 9.16 Hz, 1H, ArH), 7.62 (s, 1H, ArH), 7.73 (s, 1H, ArH); ^{13}C NMR ($CDCl_3$, 100 MHz): δ 18.7 (CH_3), 40.8 (NH$\underline{CH_2}$), 49.3 (N$\underline{CH_2}$), 62.1 (OCH_2), 102.0, 110.1, 112.2, 112.3, 114.9, 122.3, 123.7, 125.6, 131.8, 132.8, 143.0, 147.1, 152.5, 155.0, 161.0 (ArC), 161.2 (C=O); MS (ESI): m/z 498.3 (M^{+}+2); Anal. Calcd for $C_{21}H_{18}BrN_7O_3$: C, 50.82; H, 3.66; N, 19.75. Found: C, 50.79; H, 3.60; N, 19.81.

4.1.6.6. General procedure for synthesis of 6-arylated-7-((1-(2-(6-bromoimidazo[1,2-*a*]pyrazin-8-ylamino)ethyl)-1*H*-1,2,3-triazol-4-yl)methoxy)-4-methyl-2*H*-chromen-2-one (9-24): To a solution of **7** (0.10 g, 0.201 mmol) in 1,4-dioxane: water (9:1) in a sealed tube, boronic acid (0.201 mmol) and K_2CO_3 (0.027 g, 0.201 mmol) were added under inert atmosphere. $Pd(PPh_3)_4$ (5mol%) was added with continued nitrogen purging and refluxed the reaction mixture for 6-8 h. Completion of reaction was determined by TLC. The mixture was extracted with chloroform and water. Organic layer was dried over sodium sulphate to obtain crude product which was further purified by column chromatography using ethylacetate: methanol as eluents.

Spectral data of 4-methyl-7-((1-(2-(6-(thiophen-2-yl)imidazo[1,2-*a*]pyrazin-8-ylamino)ethyl)-1*H*-1,2,3-triazol-4-yl)methoxy)-2*H*-chromen-2-one (9): greenish solid; yield:

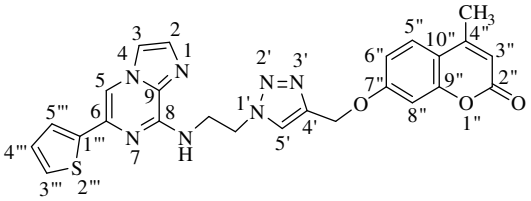

73%; mp 180-182 ^{o}C; ^{1}H NMR ($CDCl_3$, 400 MHz): δ 2.38 (s, 3H, CH_3), 4.17 (q, J = 5.96 Hz, 2H, NH$\underline{CH_2}$), 4.82 (t, J = 5.74 Hz, 2H, N$\underline{CH_2}$), 5.15 (s, 2H, O$\underline{CH_2}$), 6.13 (d, J = 0.68 Hz, 1H, ArH), 6.74 (t, J = 5.16 Hz, 1H, NH), 6.83 (d, J = 2.28 Hz, 1H, ArH), 6.88-6.90 (dd, ^{2}J = 8.72 Hz, ^{3}J = 2.30 Hz, 1H, ArH), 7.09-7.11 (m, 1H, ArH), 7.34 (d, J = 5.04 Hz, 1H, ArH), 7.43-7.47 (m, 2H, ArH), 7.48 (s, 1H, ArH), 7.54 (s, 1H, ArH), 7.74 (s, 1H, ArH), 7.88 (s, 1H, ArH); ^{13}C NMR ($CDCl_3$, 100 MHz): δ 18.6 (CH_3), 41.1 (NH$\underline{CH_2}$), 49.2 (N$\underline{CH_2}$), 62.1 (OCH_2), 102.0, 105.3, 112.1, 112.3, 113.9, 115.3, 122.5, 123.8, 125.6, 126.0, 127.9, 131.9, 132.1, 134.1, 142.2, 142.8, 147.2, 152.4, 155.0, 161.0 (ArC), 161.2 (C=O); MS (ESI): m/z 500.4 (M^{+}+1); Anal. Calcd for $C_{25}H_{21}N_7O_3S$: C, 60.11; H, 4.24; N, 19.63; S, 6.42. Found: C, 60.38; H, 4.09; N, 19.75; S, 6.33.

Spectral data of 4-methyl-7-((1-(2-(6-(thiophen-3-yl)imidazo[1,2-*a*]pyrazin-8-ylamino)ethyl)-1*H*-1,2,3-triazol-4-yl)methoxy)-2*H*-chromen-2-one (10): off white solid;

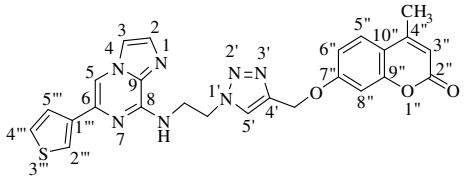

yield: 75%; mp 182-184 ^{o}C; ^{1}H NMR ($CDCl_3$, 400 MHz): δ 2.38 (d, J = 0.68 Hz, 3H,CH_3), 4.19 (q, J = 5.80 Hz, 2H, NH$\underline{CH_2}$), 4.81 (t, J = 5.72 Hz, 2H, N$\underline{CH_2}$), 5.14 (s, 2H, O$\underline{CH_2}$), 6.13 (d, J = 1.36 Hz, 1H, ArH), 6.64 (t, J = 5.96 Hz, 1H, NH), 6.82 (d, J = 2.76 Hz, 1H, ArH), 6.87-6.89 (dd, ^{2}J = 8.72 Hz, ^{3}J = 2.28 Hz, 1H, ArH), 7.39-7.41 (dd, ^{2}J = 5.04 Hz, ^{3}J = 3.24 Hz, 1H, ArH), 7.44-7.47 (m, 3H, H-2, ArH), 7.54 (d, J = 0.88 Hz, 1H, ArH), 7.68 (s, 1H, ArH), 7.80-7.81 (dd, ^{2}J = 3.20 Hz, ^{3}J = 1.14 Hz, 1H, ArH), 7.82 (s, 1H, ArH); ^{13}C ($CDCl_3$, 100 MHz): δ 18.6 (CH_3), 40.9 (NH$\underline{CH_2}$), 49.5 (N$\underline{CH_2}$), 62.0 (OCH_2), 102.0, 106.7, 112.1, 112.2, 113.9, 115.2, 122.3, 123.7, 124.7, 125.6, 126.5, 128.5, 132.3, 134.7, 139.2, 142.8, 147.4, 152.4, 155.0, 161.0 (ArC), 161.2 (C=O); MS (ESI): m/z 500.4 (M^{+}+1); Anal. Calcd for $C_{25}H_{21}N_7O_3S$: C, 60.11; H, 4.24; N, 19.63; S, 6.42. Found: C, 59.99; H, 4.11; N, 19.50; S, 6.53.

Spectral data of 7-((1-(2-(6-(furan-2-yl)imidazo[1,2-*a*]pyrazin-8-ylamino)ethyl)-1*H*-1,2,3-triazol-4-yl)methoxy)-4-methyl-2*H*-chromen-2-one (11): light pink solid; yield: 58%; mp 99-

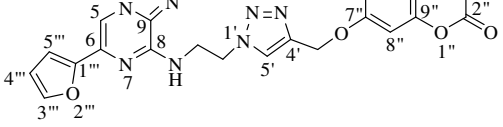

101 ^{o}C; ^{1}H NMR ($CDCl_3$, 400 MHz): δ 2.38 (d, J = 0.72 Hz, 3H, CH_3), 4.16 (q, J = 5.84 Hz, 2H, NH$\underline{CH_2}$), 4.78 (t, J = 5.72 Hz, 2H, N$\underline{CH_2}$), 5.15 (s, 2H, O$\underline{CH_2}$), 6.13 (d, J = 0.68 Hz, 1H, ArH), 6.51-6.52 (dd,^{2}J = 3.20

Hz, ^3J = 1.84 Hz, 1H, ArH), 6.70 (t, J = 5.72 Hz, 1H, NH), 6.84 (d, J = 2.72 Hz, 1H, ArH), 6.87-6.90 (m, 2H, ArH), 7.45-7.47 (m, 3H, ArH), 7.54 (d, J = 1.36 Hz, 1H, ArH), 7.69 (s, 1H, ArH), 7.89 (s, 1H, ArH); ^{13}C NMR ($CDCl_3$, 100 MHz): δ 18.6 (CH_3), 40.9 (NH<u>CH_2</u>), 49.4 (N<u>CH_2</u>), 62.0 (OCH_2), 101.9, 105.6, 107.8, 111.7, 112.1, 112.2, 113.9, 115.5, 123.7, 125.6, 131.0, 132.1, 132.3, 142.3, 142.8, 147.5, 152.0, 152.4, 155.0, 161.0 (ArC), 161.2 (C=O); MS (ESI): m/z 484.4 (M^++1); Anal. Calcd for $C_{25}H_{21}N_7O_4$: C, 62.11; H, 4.38; N, 20.28. Found: C, 61.90; H, 4.44; N, 20.12.

Spectral data of 4-methyl-7-((1-(2-(6-phenylimidazo[1,2-*a*]pyrazin-8-ylamino)ethyl)-1*H*-1,2,3-triazol-4-yl)methoxy)-2*H*-chromen-2-one (12): light orange solid; yield: 71%; mp 176-178 °C; ^{1}H NMR ($CDCl_3$, 400 MHz): δ 2.36 (s, 3H, CH_3), 4.20 (q, J = 5.81 Hz, 2H, NH<u>CH_2</u>), 4.80 (t, J = 5.72 Hz, 2H, N<u>CH_2</u>), 5.10 (s, 2H, O<u>CH_2</u>), 6.12 (s, 1H, ArH), 6.80 (d, J = 2.28 Hz, 1H, ArH), 6.84-6.87 (dd, ^2J = 8.72 Hz, ^3J = 2.28 Hz, 1H, ArH), 6.91 (t, J = 4.88 Hz, 1H, NH), 7.36-7.47 (m, 5H, ArH), 7.56 (s, 1H, ArH), 7.69 (s, 1H, ArH), 7.88 (s, 1H, ArH), 7.90 (s, 2H, ArH); ^{13}C ($CDCl_3$, 100 MHz): δ 18.6 (CH_3), 40.9 (NH<u>CH_2</u>), 49.5 (N<u>CH_2</u>), 62.0 (OCH_2), 101.9, 107.0, 112.1, 112.2, 113.8, 115.3, 123.8, 125.5, 125.8 , 128.4 , 128.7 , 132.3 , 136.9, 138.1, 142.8, 147.3, 152.4, 154.9, 160.9 (ArC), 161.2 (C=O); MS (ESI): m/z 494.5 (M^++1); Anal. Calcd for $C_{27}H_{23}N_7O_3$: C, 65.71; H, 4.70; N, 19.87. Found: C, 65.82; H, 4.76; N, 19.77.

Spectral data of 7-((1-(2-(6-(4-fluorophenyl)imidazo[1,2-*a*]pyrazin-8-ylamino)ethyl)-1*H*-1,2,3-triazol-4-yl)methoxy)-4-methyl-2*H*-chromen-2-one (13): white solid; yield: 80%; mp 250-252 °C; ^{1}H NMR ($CDCl_3$+ TFA, 400 MHz): δ 2.47 (d, J = 0.92 Hz, 3H,CH_3), 4.37 (t, J = 5.04 Hz, 2H, NH<u>CH_2</u>), 4.89 (t, J = 5.50 Hz, 2H, N<u>CH_2</u>), 5.14 (s, 2H, O<u>CH_2</u>), 6.31 (d, J = 1.36 Hz, 1H, ArH), 6.76 (d, J = 2.28 Hz, 1H, ArH), 6.94-6.97 (dd, ^2J = 9.16 Hz, ^3J = 2.50 Hz, 1H, ArH), 7.17 (t, J = 8.48 Hz, 2H, ArH), 7.59 (d, J = 8.72 Hz, 1H, ArH), 7.79-7.83 (m, 3H, ArH), 7.95 (d, J = 1.84 Hz, 1H, ArH), 7.99 (s, 1H, ArH), 8.06 (s, 1H, ArH); ^{13}C NMR (DMSO-d_6, 100 MHz): δ 18.1 (CH_3), 40.8 (NH<u>CH_2</u>), 48.7 (N<u>CH_2</u>), 61.6 (OCH_2), 101.5, 111.3, 112.5, 113.3, 115.2, 115.4, 116.0, 125.2, 126.4, 127.5, 127.6, 131.8, 132.2, 133.6, 133.7, 135.4, 141.8, 147.4, 153.4, 154.6, 160.2, 160.8 (ArC), 161.0 (C=O), 163.3 (ArC); MS (ESI): m/z 512.5 (M^++1); Anal. Calcd for $C_{27}H_{22}FN_7O_3$:

C, 63.40; H, 4.34; N, 19.17. Found: C, 63.18; H, 4.28; N, 19.02.

Spectral data of 7-((1-(2-(6-(4-chlorophenyl)imidazo[1,2-*a*]pyrazin-8-ylamino)ethyl)-1*H*-1,2,3-triazol-4-yl)methoxy)-4-methyl-2*H*-chromen-2-one (14): creamish solid; yield: 82%;

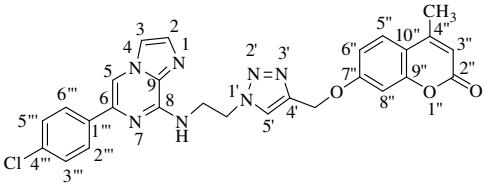

mp 127-129 ^{o}C; ^{1}H NMR ($CDCl_3$, 400 MHz): δ 2.37 (d, 3H, CH_3), 4.22 (q, *J* = 5.18 Hz, 2H, NH$\underline{CH_2}$), 4.81 (t, *J* = 5.74 Hz, 2H, N$\underline{CH_2}$), 5.13 (s, 2H, O$\underline{CH_2}$), 6.13 (d, *J* = 0.92 Hz, 1H, ArH), 6.81-6.83 (m, 1H, ArH), 6.87-6.89 (dd, ^{2}J = 8.68 Hz, ^{3}J = 2.30 Hz, 1H, ArH), 7.39-7.42 (m, 1H, ArH), 7.45 (d, *J* = 8.24 Hz, 2H, ArH), 7.46 (s, 1H, ArH), 7.50 (s, 1H, ArH), 7.57 (s, 1H, NH), 7.70 (s, 1H, ArH), 7.81 (d, *J* = 8.72 Hz, 1H, ArH), 7.89 (d, *J* = 8.24 Hz, 2H, ArH); ^{13}C NMR ($CDCl_3$, 100 MHz): δ 18.6 (CH_3), 40.9 (NH$\underline{CH_2}$), 49.6 (N$\underline{CH_2}$), 62.0 (OCH_2), 102.0, 107.0, 112.2, 113.9, 123.8, 125.6, 125.9, 127.1, 128.7, 132.2, 134.2, 135.4, 136.9, 137.2, 138.2, 142.9, 147.3, 152.5, 154.9, 160.9 (ArC), 161.2 (C=O); MS (ESI): m/z 528.9 (M^{+}+1); Anal. Calcd for $C_{27}H_{22}ClN_7O_3$: C, 61.42; H, 4.20; N, 18.57. Found: C, 61.55; H, 4.04; N, 18.66.

Spectral data of 7-((1-(2-(6-(4-bromophenyl)imidazo[1,2-*a*]pyrazin-8-ylamino)ethyl)-1*H*-1,2,3-triazol-4-yl)methoxy)-4-methyl-2*H*-chromen-2-one (15): off white solid; yield: 64%;

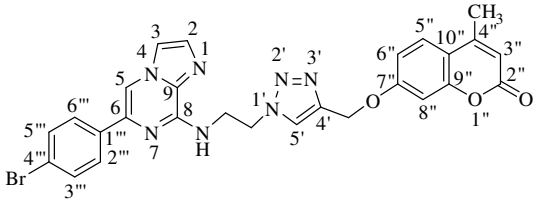

mp 138-140 ^{o}C; ^{1}H NMR ($CDCl_3$, 400 MHz): δ 2.37 (d, *J* = 0.92 Hz, 3H,CH_3), 4.21 (q, *J* = 5.80 Hz, 2H, NH$\underline{CH_2}$), 4.79 (t, *J* = 5.72 Hz, 2H, N$\underline{CH_2}$), 5.12 (s, 2H, O$\underline{CH_2}$), 6.13 (d, *J* = 0.68 Hz, 1H, ArH), 6.71 (t, *J* = 5.72 Hz, 1H, NH), 6.81 (d, *J* = 2.28 Hz, 1H, ArH), 6.85-6.88 (dd, ^{2}J = 8.72 Hz, ^{3}J = 2.76 Hz, 1H, ArH), 7.40-7.45 (m, 3H, ArH), 7.54-7.58 (m, 2H, ArH), 7.67 (s, 1H, ArH), 7.75 (d, *J* = 8.00 Hz, 2H, ArH), 7.90-7.97 (s, 1H, ArH); ^{13}C ($CDCl_3$, 100 MHz): δ 18.6 (CH_3), 40.9 (NH$\underline{CH_2}$), 49.5 (N$\underline{CH_2}$), 62.0 (OCH_2), 101.9, 107.0, 112.1, 113.9, 115.4, 122.4, 123.7, 125.6, 126.3, 127.4, 128.4, 131.7, 132.5, 135.9, 137.0, 142.8, 147.3, 152.4, 154.9, 160.9 (ArC), 161.1 (C=O); MS (ESI): m/z 573.4 (M^{+}+1); Anal. Calcd for $C_{27}H_{22}BrN_7O_3$: C, 56.65; H, 3.87; N, 17.13. Found: C, 56.92; H, 3.71; N, 17.09.

Spectral data of 4-methyl-7-((1-(2-(6-(3-(trifluoromethyl)phenyl)imidazo[1,2-*a*]pyrazin-8-ylamino)ethyl)-1*H*-1,2,3-triazol-4-yl)methoxy)-2*H*-chromen-2-one (16): white solid;

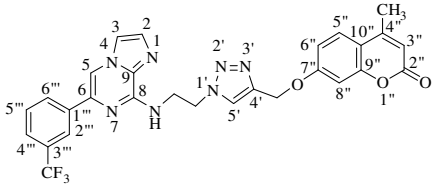

yield:71%; mp 220-122 ^{o}C; ^{1}H NMR ($CDCl_3$+ TFA, 400 MHz): δ 2.41 (d, *J* = 1.36 Hz, 3H, CH_3), 4.35 (d, *J* = 3.64 Hz, 2H, NH$\underline{CH_2}$), 4.86 (t, *J* = 5.72 Hz, 2H, N$\underline{CH_2}$), 5.09 (s, 2H, O$\underline{CH_2}$), 6.21 (d, *J* = 1.36 Hz, 1H, ArH), 6.70 (d, *J* = 2.28 Hz, 1H, ArH), 6.88-6.91 (dd, ^{2}J = 8.72 Hz, ^{3}J = 2.30 Hz, 1H, ArH), 7.51 (d, *J* = 9.48 Hz, 1H, ArH), 7.63 (t, *J* = 7.80 Hz, 1H, ArH), 7.71 (d, *J* = 7.76 Hz, 1H, ArH), 7.85 (d, *J* = 1.84 Hz, 1H, ArH), 7.96 (s, 2H, ArH), 8.06 (d, *J* = 9.6 Hz, 2H, ArH), 8.10 (s, 1H, ArH), 8.89 (s, 1H, NH); ^{13}C NMR ($CDCl_3$+ TFA, 100 MHz): δ 18.7 (CH_3), 40.8 (NH$\underline{CH_2}$), 49.8 (N$\underline{CH_2}$), 60.8 (OCH_2), 101.8, 106.3, 111.6, 112.9, 114.2, 122.4, 123.0, 124.2, 124.4, 125.1, 125.9, 126.0, 126.6, 126.7, 129.6, 129.7, 131.3, 131.6, 135.2, 142.1, 142.5, 144.1, 154.3, 154.5, 160.8 (ArC), 163.0 (C=O); MS (ESI): m/z 562.5 (M^{+}+1); Anal. Calcd for $C_{28}H_{22}F_3N_7O_3$: C, 59.89; H, 3.95; N, 17.46. Found: C, 60.10; H, 4.01; N, 17.39.

Spectral data of 4-methyl-7-((1-(2-(6-*m*-tolylimidazo[1,2-*a*]pyrazin-8-ylamino)ethyl)-1*H*-1,2,3-triazol-4-yl)methoxy)-2*H*-chromen-2-one (17): creamish solid; yield: 65%; mp 122-124

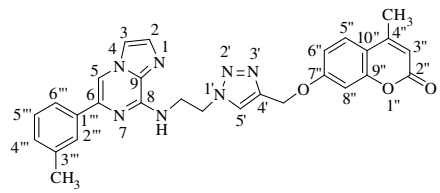

^{o}C; ^{1}H NMR ($CDCl_3$, 400 MHz): δ 2.37 (d, *J* = 1.40 Hz, 3H,CH_3), 2.44 (s, 3H, CH_3), 4.22 (q, *J* = 5.80 Hz, 2H, NH$\underline{CH_2}$), 4.81 (t, *J* = 5.74 Hz, 2H, N$\underline{CH_2}$), 5.13 (s, 2H, O$\underline{CH_2}$), 6.13 (d, *J* = 0.92 Hz, 1H, ArH), 6.73 (s, 1H, NH), 6,82 (d, *J* = 2.28 Hz, 1H, ArH), 6.86-6.89 (dd, ^{2}J = 8.68 Hz, ^{3}J = 2.76 Hz, 1H, ArH), 7.20 (d, *J* = 7.32 Hz, 1H, ArH), 7.35 (t, *J* = 7.76 Hz, 1H, ArH), 7.45 (d, *J* = 8.72 Hz, 1H, ArH), 7.49 (d, *J* = 0.92 Hz, 1H, ArH), 7.56 (d, *J* = 0.92 Hz, 1H, ArH), 7.68-7.70 (m, 3H, ArH), 7.89 (s, 1H, ArH); ^{13}C NMR ($CDCl_3$, 100 MHz): δ 18.6 (CH_3), 21.6 (CH_3), 40.9 (NH$\underline{CH_2}$), 49.5 (N$\underline{CH_2}$), 62.0 (OCH_2), 102.0, 107.0, 112.1, 112.2, 113.9, 115.2, 123.1, 123.8, 125.6, 126.6, 128.6, 129.2, 132.2, 136.9, 138.3, 138.3, 142.8, 147.2, 152.5, 154.9, 161.0 (ArC), 161.2 (C=O); MS (ESI): m/z 508.5 (M^{+}+1); Anal. Calcd for $C_{28}H_{25}N_7O_3$: C, 66.26; H, 4.96; N, 19.32. Found: C, 66.42; H, 4.85; N, 19.39.

Spectral data of 7-((1-(2-(6-(4-ethylphenyl)imidazo[1,2-*a*]pyrazin-8-ylamino)ethyl)-1*H*-1,2,3-triazol-4-yl)methoxy)-4-methyl-2*H*-chromen-2-one (18): creamish solid; yield: 66%;

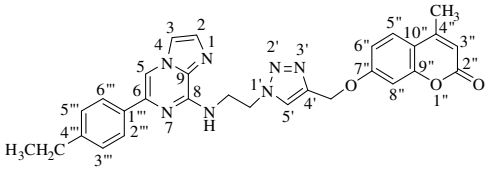

mp155-157 ^{o}C; ^{1}H NMR ($CDCl_3$, 400 MHz): δ 1.27 (t, *J* = 7.56 Hz, 3H,CH_3), 2.38 (d, *J* = 1.36 Hz, 3H,CH_3), 2.70 (q, *J* = 7.64 Hz, 2H, CH_2), 4.21 (q, *J* = 5.81 Hz, 2H,

NH$\underline{CH_2}$), 4.81 (t, *J* = 5.72 Hz, 2H, N$\underline{CH_2}$), 5.14 (s, 2H, O$\underline{CH_2}$), 6.14 (d, *J* = 0.72 Hz, 1H, ArH), 6.77 (t, *J* = 5.72 Hz, 1H, NH), 6.83 (d, *J* = 2.52 Hz, 1H, ArH), 6.88-6.91 (dd, ^2J = 9.16 Hz, ^3J = 2.54 Hz, 1H, ArH), 7.29 (d, *J* = 8.24 Hz, 2H, ArH), 7.46 (d, *J* = 9.16 Hz, 1H, ArH), 7.49 (d, *J* = 1.40 Hz, 1H, ArH), 7.55 (d, *J* = 0.92 Hz, 1H, ArH), 7.70 (s, 1H, ArH), 7.81 (d, *J* = 8.24 Hz, 2H, ArH), 7.87 (s, 1H, ArH); ^{13}C NMR ($CDCl_3$, 100 MHz): δ 15.5 (CH_3), 18.6 (CH_3), 28.6 (CH_2), 40.9 (NH$\underline{CH_2}$), 49.5 (N$\underline{CH_2}$), 62.0 (OCH_2), 102.0, 106.5, 112.1, 112.9, 113.9, 115.2, 123.8, 125.6, 125.9, 128.2, 132.0, 134.4, 138.4, 142.8, 144.8, 147.2, 152.4, 155.0, 161.0 (ArC), 161.2 (C=O); MS (ESI): m/z 522.5 (M^++1); Anal. Calcd for $C_{29}H_{27}N_7O_3$: C, 66.78; H, 5.22; N, 18.80. Found: C, 66.91; H, 5.28; N, 18.91.

Spectral data of 4-methyl-7-((1-(2-(6-(naphthalen-1-yl)imidazo[1,2-*a*]pyrazin-8-ylamino) ethyl)-1*H*-1,2,3-triazol-4-yl)methoxy)-2*H*-chromen-2-one (19): light orange solid; yield:

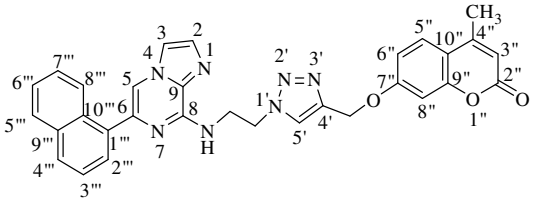

74%; mp 165-167 °C; ^{1}H NMR ($CDCl_3$, 400 MHz): δ 2.34 (d, *J* = 1.36 Hz, 3H, CH_3), 4.09 (q, *J* = 5.80 Hz, 2H, NH$\underline{CH_2}$), 4.69 (t, *J* = 5.74 Hz, 2H, N$\underline{CH_2}$), 5.05 (s, 2H, O$\underline{CH_2}$), 6.12 (d, *J* = 0.68 Hz, 1H, ArH), 6.80 (d, *J* = 2.28 Hz, 1H, ArH), 6.84-6.87 (dd, ^2J = 9.16 Hz, ^3J = 2.54 Hz, 1H, ArH), 6.97 (t, *J* = 5.26 Hz, 1H, NH), 7.42 (d, *J* = 8.72 Hz, 1H, ArH), 7.45-7.60 (m, 6H, ArH), 7.61 (s, 1H, ArH), 7.71 (s, 1H, ArH), 7.90 (s, 1H, ArH), 7.92 (d, *J* = 1.36 Hz, 1H, ArH), 8.18-8.20 (m, 1H, ArH); ^{13}C NMR ($CDCl_3$, 100 MHz): δ 18.6 (CH_3), 40.9 (NH$\underline{CH_2}$), 49.5 (N$\underline{CH_2}$), 61.9 (OCH_2), 101.9, 110.4, 112.0, 112.2, 113.8, 115.1, 123.7, 125.2, 125.5, 125.8, 125.9, 126.1, 127.1, 128.4, 128.9, 131.5, 131.9, 132.2, 133.8, 135.6, 139.5, 142.7, 147.2, 152.5, 154.9, 160.9 (ArC), 161.2 (C=O); MS (ESI): m/z 544.5 (M^++1); Anal. Calcd for $C_{31}H_{25}N_7O_3$: C, 68.50; H, 4.64; N, 18.04. Found: C, 68.19; H, 4.72; N, 17.98.

Spectral data of 7-((1-(2-(6-(2-hydroxyphenyl)imidazo[1,2-*a*]pyrazin-8-ylamino)ethyl)-1*H*-1,2,3-triazol-4-yl)methoxy)-4-methyl-2*H*-chromen-2-one (20): off white solid; yield: 53%; mp

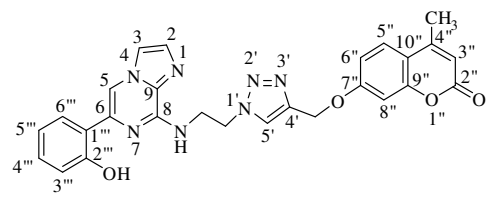

249-251 °C; ^{1}H NMR (DMSO-d_6, 400 MHz): δ 2.38 (d, *J* = 0.88 Hz, 3H,CH_3), 3.94 (d, *J* = 5.52 Hz, 2H, NH$\underline{CH_2}$), 4.74 (t, *J* = 5.74 Hz, 2H, N$\underline{CH_2}$), 5.18 (s, 2H, O$\underline{CH_2}$), 6.21 (d, *J* = 0.92 Hz, 1H, ArH), 6.86-6.90 (m, 2H, ArH), 6.96-6.99 (dd, ^2J = 8.68 Hz, ^3J = 2.76 Hz, 1H, ArH), 7.09 (d, *J* = 2.32 Hz, 1H, ArH),

7.17-7.21 (m, 1H, ArH), 7.56 (d, *J* = 0.92 Hz, 1H, ArH), 7.66 (d, *J* = 8.72 Hz, 1H, ArH), 7.81-7.84 (dd, ^{2}J = 8.24 Hz, ^{3}J = 1.62 Hz, 1H, ArH), 7.96 (s, 1H, ArH), 8.11 (t, *J* = 5.72 Hz, 1H, NH), 8.29 (s, 1H, ArH), 8.56 (s, 1H, ArH), 12.23 (s, 1H, OH); ^{13}C NMR (DMSO-d_6, 100 MHz): δ 18.1 (CH_3), 40.8 (NH<u>CH_2</u>), 48.27 (N<u>CH_2</u>), 61.6 (OCH_2), 101.5, 107.9, 111.3, 112.5, 113.5, 116.5, 117.2, 119.1, 119.8, 125.2, 126.4, 126.6, 129.4, 131.1, 132.5, 135.3, 141.8, 146.5, 153.4, 154.6, 156.7, 160.1 (ArC), 161.0 (C=O); MS (ESI): m/z 510.5 (M^{+}+1); Anal. Calcd for $C_{27}H_{23}N_7O_4$: C, 63.65; H, 4.55; N, 19.24. Found: C, 63.53; H, 4.44; N, 19.30.

Spectral data of 7-((1-(2-(6-(4-methoxyphenyl)imidazo[1,2-*a*]pyrazin-8-ylamino)ethyl)-1*H*-1,2,3-triazol-4-yl)methoxy)-4-methyl-2*H*-chromen-2-one (21): off white solid; yield: 90%;

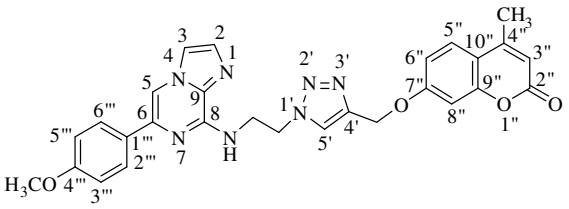

mp 172-174 °C; ^{1}H NMR ($CDCl_3$, 400 MHz): δ 2.37 (d, *J* = 0.88 Hz, 3H,CH_3), 3.86 (s, 3H, OCH_3), 4.20 (q, *J* = 5.28 Hz, 2H, NH<u>CH_2</u>), 4.80 (t, *J* = 5.50 Hz, 2H, N<u>CH_2</u>), 5.10 (s, 2H, O<u>CH_2</u>), 6.17 (d, *J* = 0.88 Hz, 1H, ArH), 6.81 (m, 2H, ArH, NH), 6.85-6.88 (dd, ^{2}J = 8.72 Hz, ^{3}J = 2.28 Hz, 1H, ArH), 6.98 (d, *J* = 9.16 Hz, 2H, ArH), 7.44 (d, *J* = 8.68 Hz, 2H, ArH), 7.54 (s,1H, ArH), 7.69 (s,1H, ArH), 7.81 (s, 1H, ArH), 7.82 (s, 1H, ArH), 7.83 (s, 1H, ArH); ^{13}C NMR ($CDCl_3$, 100 MHz): δ 18.6 (CH_3), 40.9 (NH<u>CH_2</u>), 49.6 (N<u>CH_2</u>), 52.3 (OCH_3), 62.0 (OCH_2), 101.9, 106.0, 112.1, 112.2, 113.9, 114.0, 115.1, 123.8, 125.6, 127.1 =, 129.5, 132.1, 138.0, 142.8, 147.2, 152.4, 154.9, 159.9, 161.0 (ArC), 161.2 (C=O); MS (ESI): m/z 524.5 (M^{+}+1); Anal. Calcd for $C_{28}H_{25}N_7O_4$: C, 64.24; H, 4.81; N, 18.73. Found: C, 64.56; H, 4.92; N, 18.90.

Spectral data of 7-((1-(2-(6-(2-methoxyphenyl)imidazo[1,2-*a*]pyrazin-8-ylamino)ethyl)-1*H*-1,2,3-triazol-4-yl)methoxy)-4-methyl-2*H*-chromen-2-one (22): creamish solid; yield: 91%; mp

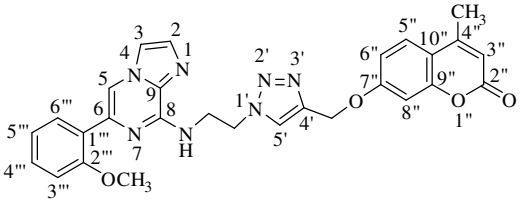

120-122 °C; ^{1}H NMR ($CDCl_3$, 400 MHz): δ 2.36 (d, *J* = 0.68 Hz, 3H, CH_3), 3.95 (s,3H, OCH_3), 4.16 (q, *J* = 5.65 Hz, 2H, NH<u>CH_2</u>), 4.80 (t, *J* = 5.50 Hz, 2H, N<u>CH_2</u>), 5.09 (s, 2H, O<u>CH_2</u>), 6.12 (d, *J* = 1.36 Hz, 1H, ArH), 6.80 (d, *J* = 2.32 Hz, 1H, ArH), 6.84 (d, *J* = 2.28 Hz, 1H, ArH), 6.86 (d, *J* = 2.32 Hz, 1H, ArH), 7.02 (d, *J* = 8.24 Hz, 1H, ArH), 7.08-7.12 (m, 1H, ArH), 7.33-7.37 (m, 1H, ArH), 7.42 (d, *J* = 8.72 Hz, 1H, ArH), 7.45 (s, 1H, NH), 7.55 (s, 1H, ArH), 7.67 (s, 1H, ArH), 8.10-8.12 (dd, ^{2}J = 7.80 Hz, ^{3}J = 1.84 Hz, 1H, ArH), 8.35 (s, 1H, ArH); ^{13}C NMR ($CDCl_3$, 100 MHz): δ 18.6 (CH_3), 41.0 (NH<u>CH_2</u>), 49.4 (N<u>CH_2</u>), 55.5 (OCH_3), 62.0 (OCH_2), 101.9, 111.2, 111.7, 112.0,

112.1, 113.8, 115.3, 120.9, 123.8, 125.4, 125.5, 129.2, 130.2, 132.2, 134.2, 142.7, 146.8, 152.4, 154.9, 156.7, 161.0 (ArC), 161.2 (C=O); MS (ESI): m/z 524.5 (M^++1); Anal. Calcd for $C_{28}H_{25}N_7O_4$: C, 64.24; H, 4.81; N, 18.73. Found: C, 64.11; H, 4.79; N, 18.86.

Spectral data of 4-(8-(2-(4-((4-methyl-2-oxo-2*H*-chromen-7-yloxy)methyl)-1*H*-1,2,3-triazol-1-yl)ethylamino)imidazo[1,2-*a*]pyrazin-6-yl)benzaldehyde (23): yellowish solid; yield: 92%;

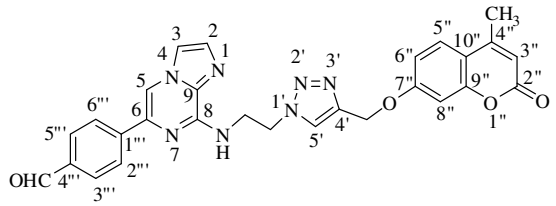

mp 212-214 ^oC; ^1H NMR ($CDCl_3$+ DMSO-d_6, 400 MHz): δ 2.37 (s, 3H, $\underline{CH_3}$), 4.04 (q, J = 5.96 Hz, 2H, NH$\underline{CH_2}$), 4.76 (t, J = 6.18 Hz, 2H, N$\underline{CH_2}$), 5.12 (s, 2H, O$\underline{CH_2}$), 6.19 (d, J = 1.36 Hz, 1H, ArH), 6.90-6.92 (dd, ^2J = 8.72 Hz, ^3J = 3.20 Hz, 1H, ArH), 7.02 (d, J = 2.28 Hz, 1H, ArH), 7.54 (s, 1H, ArH), 7.62 (d, J = 8.72 Hz, 1H, ArH), 7.88-7.90 (m, 2H, ArH), 7.95 (d, J = 8.24 Hz, 2H, ArH), 8.17 (d, J = 8.68 Hz, 2H, ArH), 8.30 (bs, 1H, NH), 8.59 (s, 1H, ArH), 9.99 (s, 1H, CHO); ^{13}C NMR ($CDCl_3$ + DMSO-d_6,100 MHz): δ 18.1 (CH_3), 40.4 (NH$\underline{CH_2}$), 48.8 (N$\underline{CH_2}$), 61.6 (OCH_2), 101.4, 108.9, 111.3, 112.5, 113.3, 116.4, 125.2, 126.0, 126.4, 129.8, 132.0, 132.4, 134.9, 135.4, 141.8, 143.0, 147.5, 153.4, 154.6, 160.2 (ArC), 160.9 (C=O), 192.6 (CHO); MS (ESI): m/z 522.5 (M^++1); Anal. Calcd for $C_{28}H_{23}N_7O_4$: C, 64.48; H, 4.45; N, 18.80. Found: C, 64.56; H, 4.40; N, 18.73.

Spectral data of 7-((1-(2-(6-(4-acetylphenyl)imidazo[1,2-*a*]pyrazin-8-ylamino)ethyl)-1*H*-1,2,3-triazol-4-yl)methoxy)-4-methyl-2*H*-chromen-2-one (24): creamish solid; yield: 90%;

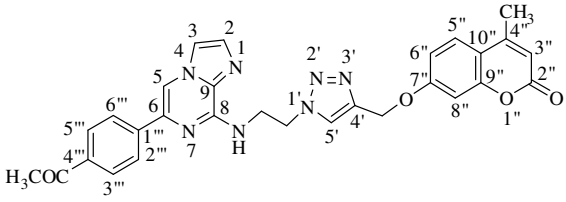

mp 235-237 ^oC; ^1H NMR ($CDCl_3$ + DMSO-d_6, 400 MHz): δ 2.41 (s, 3H, CH_3), 2.64 (s, 3H, CO$\underline{CH_3}$), 4.24 (q, J = 5.65 Hz, 2H, NH$\underline{CH_2}$), 4.84 (t, J = 5.72 Hz, 2H, N$\underline{CH_2}$), 5.14 (s, 2H, O$\underline{CH_2}$), 6.12 (s, 1H, ArH), 6.85-6.92 (m, 2H, ArH), 7.52 (m, 2H, ArH), 7.84-8.05 (m, 7H, ArH), 8.27 (s, 1H, ArH); ^{13}C NMR ($CDCl_3$ + DMSO-d_6, 100 MHz): δ 17.2 (CH_3), 25.3 (CH_3), 41.0 (NH$\underline{CH_2}$), 47.8 (N$\underline{CH_2}$), 60.4 (OCH_2), 100.2, 106.9, 110.3, 111.0, 112.2, 114.8, 123.3, 124.4, 124.5, 127.1, 129.6, 130.0, 134.8, 135.2, 140.1, 140.8, 145.7, 151.5, 153.4, 159.3 (ArC), 159.7 (C=O), 195.9 (C=O); MS (ESI): m/z 536.5 (M^++1); Anal. Calcd for $C_{29}H_{25}N_7O_4$: C, 65.04; H, 4.71; N, 18.31. Found: C, 64.90; H, 4.56; N, 18.28.

4.1.6.7. Synthesis of 3-azidopropanamine (26): 3-Bromopropylamine hydrobromide **25** (1 g, 4.56 mmol) was dissolved in distilled water with stirring. Sodium azide was added (0.95 g, 14.61

mmol) carefully in succession with continuous stirring. The reaction mixture was refluxed for 12 h. After completion of reaction, reaction mixture was cooled to room temperature and was quenched by addition of sodium hydroxide (0.7 g, 17.5 mmol) and further stirred for 30 min at room temperature. Thereafter, mixture was extracted with diethyl ether and dried over sodium sulphate, filteres to obtain ether extract and stored at low temperature. The ether extract being volatile in nature, was used as such for next reaction.

4.1.6.8. Synthesis of *N*-(3-azidopropyl)-6-bromoimidazo[1,2-*a*]pyrazin-8-amine (27): To the ether extract containing 3-azidopropanamine **26,** was added mixture of 6,8-dibromoimidazo[1,2-*a*]pyrazine **3** (0.5 g, 1.80 mmol) in acetonitrile in the presence of diisopropylethylamine. The reaction mixture was refluxed for 24 h. After completion of reaction, the mixture was extracted with chloroform and water. Organic layer was dried over anhydrous sodium sulphate, filtered and concentrated over vacuum. The crude mixture was then purified by silica gel chromatography 60-120 mesh using hexane : ethyl acetate (6:1) as eluents.

Spectral data of *N*-(3-azidopropyl)-6-bromoimidazo[1,2-*a*]pyrazin-8-amine (27): red solid;

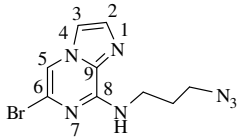

yield: 65%; mp 62-64 ^{o}C; ^{1}H NMR ($CDCl_3$, 400 MHz): δ 1.97 (m, 2H, CH_2), 3.44 (t, *J* = 6.64 Hz, 2H, N$\underline{CH_2}$), 3.69 (q, *J* = 6.56 Hz, 2H, NH$\underline{CH_2}$), 6.64 (bs, 1H, NH), 7.45 (d, *J* = 0.92 Hz, 1H, H-2), 7.48 (d, *J* = 1.36 Hz, 1H, H-3), 7.58 (s, 1H, H-5); ^{13}C NMR ($CDCl_3$, 100 MHz): δ 28.3 (CH_2), 38.1 (NH$\underline{CH_2}$), 49.0 (N$\underline{CH_2}$), 109.1, 114.7, 122.9, 132.0, 132.2, 147.5 (ArC); MS (ESI): m/z 297.0 (M^++1); Anal. Calcd for $C_9H_{10}BrN_7$: C, 36.50; H, 3.40; N, 33.11. Found: C, 36.54; H, 3.41; N, 33.13.

4.1.6.9. Synthesis of 7-((1-(3-(6-bromoimidazo[1,2-*a*]pyrazin-8-ylamino)propyl)-1*H*-1,2,3-triazol-4-yl)methoxy)-4-methyl-2*H*-chromen-2-one (28): To the stirred solution of 4-methyl-7-(prop-2-ynyloxy)-2*H*-chromen-2-one **6** (1g, 4.67 mmol) and *N*-(2-azidopropyl)-6-bromoimidazo[1,2-*a*]pyrazin-8-amine **27** (1.31 g, 4.67 mmol) in ethanol:water (8:2), copper sulphate pentahydrate (5 mol%) and sodium ascorbate (10 mol%) was added and stirred at room temperature for 2 h. After completion of reaction, water was added and extracted with chloroform. Organic layer was dried over sodium sulphate, filtered and concentrated in vacuum to obtain off white solid.

Spectral data of 7-((1-(3-(6-bromoimidazo[1,2-*a*]pyrazin-8-ylamino)propyl)-1*H*-1,2,3-triazol-4-yl)methoxy)-4-methyl-2*H*-chromen-2-one (28): white solid; yield: 82%; mp 155-157

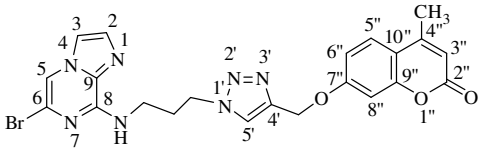

^{o}C; ^{1}H NMR (DMSO-d_6, 400 MHz): δ 2.18 (m, 2H, CH_2), 2.35 (s, 3H, CH_3), 3.43 (m, 2H, NH$\underline{CH_2}$), 4.45 (t, J = 6.88 Hz, 2H, N$\underline{CH_2}$), 5.24 (s, 2H, O$\underline{CH_2}$), 6.17 (d, J = 0.92 Hz, 1H, ArH), 6.98-7.00 (dd, ^{2}J = 8.72 Hz, ^{3}J = 2.52 Hz, 1H, ArH), 7.10 (d, J = 2.28 Hz, 1H, ArH), 7.49 (d, J = 0.68 Hz, 1H, ArH), 7.63 (d, J = 8.72 Hz, 1H, ArH), 7.81 (d, J = 0.92 Hz, 1H, ArH), 7.98 (s, 1H, ArH), 8.13 (t, J = 5.50 Hz, 1H, NH), 8.35 (s, 1H, ArH); ^{13}C NMR (DMSO-d_6, 100 MHz): δ 18.1 (CH_3), 29.2 (CH_2), 37.3 (NH$\underline{CH_2}$), 47.4 (N$\underline{CH_2}$), 61.7 (OCH_2), 101.5, 109.1, 111.2, 112.6, 113.3, 115.9, 121.8, 124.9, 126.4, 131.5, 132.1, 141.8, 147.5, 153.4, 154.6, 160.1 (ArC), 161.0 (C=O); MS (ESI): m/z 512.3 (M^{+}+2); Anal. Calcd for $C_{22}H_{20}BrN_7O_3$: C, 51.78; H, 3.95; N, 19.21. Found: C, 51.91; H, 3.88; N, 19.07.

4.1.6.10. General procedure for synthesis of 6-arylated-7-((1-(2-(6-bromoimidazo[1,2-*a*]pyrazin-8-ylamino)propyl)-1*H*-1,2,3-triazol-4-yl)methoxy)-4-methyl-2*H*-chromen-2-one (29-38): To a solution of 6-bromotriazole bridged imidazo[1,2-*a*]pyrazine-coumarin conjugate **28** (0.10 g, 0.196 mmol) in 1,4-dioxane: water (9:1) in a sealed tube, boronic acid (0.196 mmol) and K_2CO_3 (0.027 g, 0.196 mmol) were added under inert atmosphere. $Pd(PPh_3)_4$ (5mol%) was added with continued nitrogen purging and refluxed the reaction mixture for 6-8 h. Completion of reaction was determined by TLC. The mixture was extracted with chloroform and water. Organic layer was dried using sodium sulphate to obtain crude product which was further purified by column chromatography using ethylacetate: methanol as eluents.

Spectral data of 4-methyl-7-((1-(3-(6-(thiophen-3-yl)imidazo[1,2-*a*]pyrazin-8-ylamino)propyl)-1*H*-1,2,3-triazol-4-yl)methoxy)-2*H*-chromen-2-one (29): reddish brown

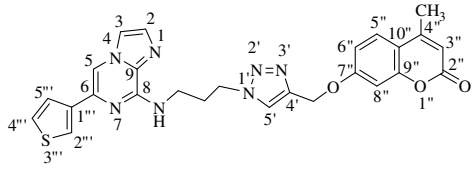

solid; yield: 72%; mp 170-172 ^{o}C; ^{1}H NMR ($CDCl_3$, 400 MHz): δ 2.37-2.43 (m, 5H, CH_3, CH_2), 3.79 (q, J = 6.41 Hz, 2H, NH$\underline{CH_2}$), 4.54 (t, J = 6.64 Hz, 2H, N$\underline{CH_2}$), 5.18 (s, 2H, O$\underline{CH_2}$), 6.15 (d, J = 1.36 Hz, 1H, ArH), 6.40 (s, 1H, NH), 6.86 (d, J = 2.32 Hz, 1H, ArH), 6.91-6.94 (dd, ^{2}J = 8.72 Hz, ^{3}J= 2.28 Hz, 1H, ArH), 7.35-7.37 (m, 1H, ArH), 7.44-7.45 (dd, ^{2}J = 5.04 Hz, ^{3}J = 1.36 Hz, 1H, ArH), 7.48 (s, 1H, ArH), 7.51 (d, J = 0.92 Hz, 1H, ArH), 7.54 (d, J = 0.88 Hz, 1H, ArH), 7.77-7.78 (m, 2H, ArH), 7.81 (s, 1H, ArH); ^{13}C NMR ($CDCl_3$, 100 MHz): δ 18.6 (CH_3), 30.2 (CH_2), 37.0 (NH$\underline{CH_2}$), 47.7 (N$\underline{CH_2}$), 62.1 (OCH_2), 101.9, 106.2, 112.1, 112.4, 113.9, 115.2, 122.4, 123.7, 124.8, 125.6, 126.5, 131.9, 133.2, 135.0, 139.3, 142.7, 147.8, 152.4, 155.0, 161.1 (ArC), 161.2 (C=O); MS (ESI): m/z 514.5

(M^++1); Anal. Calcd for $C_{26}H_{23}N_7O_3S$: C, 60.81; H, 4.51; N, 19.09;S, 6.24. Found: C, 60.76; H, 4.43; N, 19.28; S, 6.08.

Spectral data of 4-methyl-7-((1-(3-(6-phenylimidazo[1,2-*a*]pyrazin-8-ylamino)propyl)-1*H*-1,2,3-triazol-4-yl)methoxy)-2*H*-chromen-2-one (30): creamish solid; yield: 70%; mp 154-156

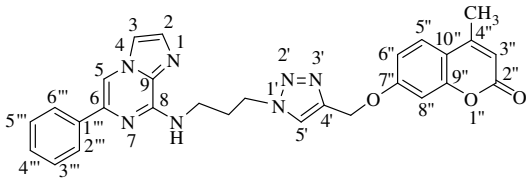

°C; ^{1}H NMR ($CDCl_3$, 400 MHz): δ 2.37-2.43 (m, 5H, CH_3, CH_2), 3.82 (q, *J* = 6.27 Hz, 2H, NH$\underline{CH_2}$), 4.54 (t, *J* = 6.88 Hz, 2H, N$\underline{CH_2}$), 5.09 (s, 2H, O$\underline{CH_2}$), 6.14 (d, *J* = 1.40 Hz, 1H, ArH), 6.40 (t, *J* = 5.96 Hz, 1H, NH), 6.83 (d, *J* = 2.32 Hz, 1H, ArH), 6.89-6.91 (dd, ^2J = 8.72 Hz, ^3J = 2.28 Hz, 1H, ArH), 7.32-7.36 (m, 1H, ArH), 7.43 (t, *J* = 7.22 Hz, 2H, ArH), 7.48 (d, *J* = 8.72 Hz, 1H, ArH), 7.52 (s, 1H, ArH), 7.57 (d, *J* = 0.92 Hz, 1H, ArH), 7.78 (s, 1H, ArH), 7.87 (s, 1H, ArH), 7.89 (d, *J* = 1.40 Hz, 2H, ArH); ^{13}C NMR ($CDCl_3$, 100 MHz): δ 18.6 (CH_3), 30.3 (CH_2), 37.1 (NH$\underline{CH_2}$), 47.7 (N$\underline{CH_2}$), 61.9 (OCH_2), 101.9, 106.6, 112.1, 112.4, 113.9, 115.2, 123.8, 125.6, 126.0, 128.3, 128.6, 132.1, 132.4, 137.1, 138.3, 142.6, 147.8, 152.5, 155.0, 161.0 (ArC), 161.2 (C=O); MS (ESI): m/z 508.5 (M^++1); Anal. Calcd for $C_{28}H_{25}N_7O_3$: C, 66.26; H, 4.96; N, 19.32. Found: C, 66.41; H, 5.03; N, 19.19.

Spectral data of 7-((1-(3-(6-(4-fluorophenyl)imidazo[1,2-*a*]pyrazin-8-ylamino)propyl)-1*H*-1,2,3-triazol-4-yl)methoxy)-4-methyl-2*H*-chromen-2-one (31): brown solid; yield: 76%; mp

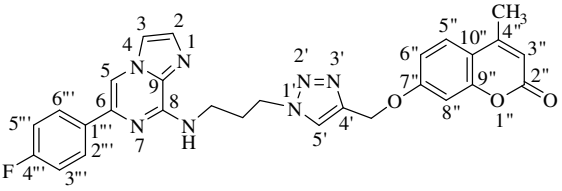

185-187 °C; ^{1}H NMR ($CDCl_3$+ TFA, 400 MHz): δ 2.39 (d, *J* = 1.40 Hz, 3H, CH_3), 2.47 (m, 2H, CH_2), 3.80 (d, *J* = 4.12 Hz, 2H, NH$\underline{CH_2}$), 4.59 (t, *J* = 6.88 Hz, 2H, N$\underline{CH_2}$), 5.21 (s, 2H, O$\underline{CH_2}$), 6.13 (d, *J* = 1.36 Hz, 1H, ArH), 6.87 (d, *J* = 2.76 Hz, 1H, ArH), 6.94-6.96 (dd, ^2J = 8.72 Hz, ^3J = 2.30 Hz, 1H, ArH), 7.16 (t, *J* = 8.70 Hz, 2H, ArH), 7.50 (d, *J* = 8.68 Hz, 1H, ArH), 7.77 (d, *J* = 1.84 Hz, 1H, ArH), 7.78 (d, *J* = 1.84 Hz, 1H, ArH), 7.86-7.90 (m, 2H, ArH), 7.96 (s, 1H, ArH), 8.04 (s, 1H, ArH), 9.25 (s, 1H, NH); ^{13}C NMR (DMSO-d_6, 100 MHz): δ 18.1 (CH_3), 29.5 (CH_2), 37.2 (NH$\underline{CH_2}$) 47.6 (N$\underline{CH_2}$), 61.7 (OCH_2), 101.5, 106.4, 111.3, 112.5, 113.3, 115.2, 115.4, 115.9, 125.0, 126.4, 127.4, 127.5, 131.9, 132.0, 133.7, 133.7, 135.5, 141.8, 147.6, 153.3, 154.6, 160.1, 160.8 (ArC), 161.0 (C=O), 163.2 (ArC); MS (ESI): m/z 526.5 (M^++1); Anal. Calcd for $C_{28}H_{24}FN_7O_3$: C, 63.99; H, 4.60; N, 18.66. Found: C, 63.71; H, 4.52; N, 18.79.

Spectral data of 7-((1-(3-(6-(4-chlorophenyl)imidazo[1,2-*a*]pyrazin-8-ylamino)propyl)-1*H*-

1,2,3-triazol-4-yl)methoxy)-4-methyl-2*H*-chromen-2-one (32): creamish solid; yield: 70%;

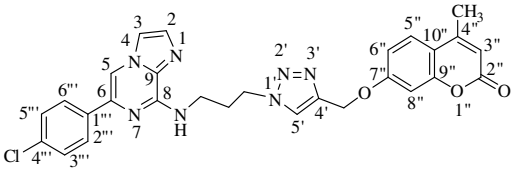

mp 188-190 ^{o}C; ^{1}H NMR ($CDCl_3$, 400 MHz): δ 2.43-2.44 (m, 5H, CH_3, CH_2), 3.80 (q, *J* = 6.25 Hz, 2H, NH$\underline{CH_2}$), 4.54 (t, *J* = 6.66 Hz, 2H, N$\underline{CH_2}$), 5.15 (s, 2H, O$\underline{CH_2}$), 6.15 (d, *J* = 0.92 Hz, 1H, ArH), 6.35 (t, *J* = 5.28 Hz, 1H, NH), 6.85 (d, *J* = 2.76 Hz, 1H, ArH), 6.90-6.93 (dd, ^{2}J = 8.68 Hz, ^{3}J = 2.74 Hz, 1H, ArH), 7.38 (d, *J* = 8.68 Hz, 2H, ArH), 7.50 (d, *J* = 9.16 Hz, 1H, ArH), 7.53 (s, 1H, ArH), 7.57 (s, 1H, ArH), 7.74 (s, 1H, ArH), 7.82 (d, *J* = 8.72 Hz, 2H, ArH), 7.88 (s, 1H, ArH); ^{13}C NMR ($CDCl_3$, 100 MHz): δ 18.6 (CH_3), 30.2 (CH_2), 37.1 (NH$\underline{CH_2}$), 47.8 (N$\underline{CH_2}$), 62.0 (OCH_2), 102.0, 106.6, 112.1, 112.2, 113.9, 115.3, 123.5, 125.6, 127.1, 128.8, 132.3, 132.4, 134.1, 135.6, 137.2, 142.8, 147.8, 152.5, 155.0, 161.0 (ArC), 161.2 (C=O); MS (ESI): m/z 542.9 (M^{+}+1); Anal. Calcd for $C_{28}H_{24}ClN_7O_3$: C, 62.05; H, 4.46; N, 18.09. Found: C, 61.91; H, 4.32; N, 18.23.

Spectral data of 4-methyl-7-((1-(3-(6-(3-(trifluoromethyl)phenyl)imidazo[1,2-*a*]pyrazin-8-ylamino)propyl)-1*H*-1,2,3-triazol-4-yl)methoxy)-2*H*-chromen-2-one (33): creamish solid;

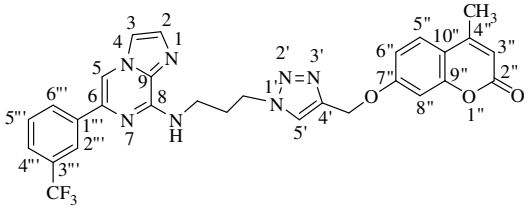

yield: 80%; mp 181-183 ^{o}C; ^{1}H NMR ($CDCl_3$ + TFA, 400 MHz): δ 2.40 (d, *J* = 0.92 Hz, 3H, CH_3), 2.51 (m, 2H, CH_2), 3.84 (bs, 2H, NH$\underline{CH_2}$), 4.63 (t, *J* = 6.64 Hz, 2H, N$\underline{CH_2}$), 5.23 (s, 2H, O$\underline{CH_2}$), 6.13 (d, *J* = 1.36 Hz, 1H, ArH), 6.83 (d, *J* = 2.28 Hz, 1H, ArH), 6.92-6.95 (dd, ^{2}J = 8.68 Hz, ^{3}J = 2.52 Hz, 1H, ArH), 7.52 (d, *J* = 8.68 Hz, 1H, ArH), 7.63 (t, *J* = 7.80 Hz, 1H, ArH), 7.71 (d, *J* = 7.80 Hz, 1H, ArH), 7.85 (d, *J* = 1.80 Hz, 1H, ArH), 7.90 (d, *J* = 1.80 Hz, 1H, ArH), 8.07 (s, 1H, ArH), 8.11-8.12 (m, 3H, ArH), 8.97 (s, 1H, NH); ^{13}C NMR ($CDCl_3$ + TFA,, 100 MHz): δ 18.6 (CH_3), 28.6 (CH_2), 38.2 (NH$\underline{CH_2}$), 48.6 (N$\underline{CH_2}$), 61.3 (OCH_2), 101.9, 105.6, 111.9, 112.6, 114.1, 116.2, 119.7, 122.4, 122.9, 124.0, 124.5, 125.1, 125.8, 126.2, 126.5, 129.6, 129.7, 131.2, 131.5, 135.7, 142.2, 142.4, 144.4, 153.3, 154.7, 160.9 (ArC), 162.0 (C=O); MS (ESI): m/z 576.5 (M^{+}+1); Anal. Calcd for $C_{29}H_{24}F_3N_7O_3$: C, 60.52; H, 4.20; N, 17.04. Found: C, 60.88; H, 4.05; N, 17.19.

Spectral data of 4-methyl-7-((1-(3-(6-*m*-tolylimidazo[1,2-*a*]pyrazin-8-ylamino)propyl)-1*H*-1,2,3-triazol-4-yl)methoxy)-2*H*-chromen-2-one (34): brown solid; yield: 81%; mp 95-

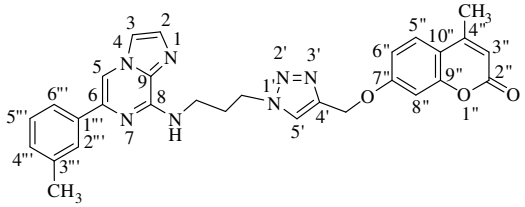

97 °C; ^{1}H NMR ($CDCl_3$, 400 MHz): δ 2.37-2.44 (m, 7H, CH_3, CH_3, CH_2), 3.83 (q, *J* = 6.25 Hz, 2H, NH$\underline{CH_2}$), 4.54 (t, *J* = 6.64 Hz, 2H, N$\underline{CH_2}$), 5.09 (s, 2H, O$\underline{CH_2}$), 6.15 (d, *J* = 0.92 Hz, 1H, ArH), 6.36 (t, *J* = 5.72 Hz, 1H, NH), 6.83 (d, *J* = 2.28 Hz, 1H, ArH), 6.88-6.91 (dd, ^2J =8.68 Hz, ^3J = 2.30 Hz, 1H, ArH), 7.17 (d, *J* = 7.36 Hz, 1H, ArH), 7.32 (d, *J* = 7.56 Hz, 1H, ArH), 7.49 (d, *J* = 8.72 Hz, 1H, ArH), 7.53 (d, *J* = 0.88 Hz, 1H, ArH), 7.56 (d, *J* = 1.36 Hz, 1H, ArH), 7.67-7.69 (m, 2H, ArH), 7.78 (s, 1H, ArH), 7.88 (s, 1H, ArH); ^{13}C NMR ($CDCl_3$, 100 MHz): δ 18.6 (CH_3), 21.6 (CH_3), 30.3 (CH_2), 37.1 (NH$\underline{CH_2}$), 47.7 (N$\underline{CH_2}$), 61.9 (OCH_2), 101.9, 106.6, 112.1, 112.4, 113.9, 115.2, 123.2, 123.8, 125.6, 126.6, 128.6, 129.1, 132.1, 132.4, 137.1, 138.3, 138.5, 142.6, 147.8, 152.5, 155.0, 161.1 (ArC), 161.2 (C=O); MS (ESI): m/z 522.6 (M^++1); Anal. Calcd for $C_{29}H_{27}N_7O_3$: C, 66.78; H, 5.22; N, 18.80. Found: C, 66.62; H, 5.34; N, 18.91.

Spectral data of 7-((1-(3-(6-(4-ethylphenyl)imidazo[1,2-*a*]pyrazin-8-ylamino)propyl)-1*H*-1,2,3-triazol-4-yl)methoxy)-4-methyl-2*H*-chromen-2-one (35): creamish solid; yield: 56%; mp

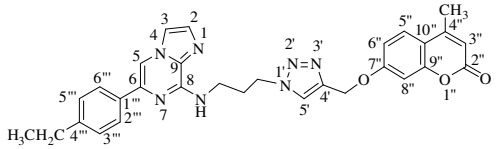

100-102 °C; ^{1}H NMR ($CDCl_3$, 400 MHz): δ 1.23 (t, *J* = 7.56 Hz, 3H, CH_3), 2.35-2.42 (m, 5H, CH_3, CH_2), 2.65 (q, *J* = 7.64 Hz, 2H, CH_2), 3.81 (q, *J* = 6.10 Hz, 2H, NH$\underline{CH_2}$), 4.54 (t, *J* = 6.64 Hz, 2H, N$\underline{CH_2}$), 5.15 (s, 2H, O$\underline{CH_2}$), 6.14 (d, *J* = 1.36 Hz, 1H, ArH), 6.41 (s, 1H, NH), 6.84 (d, *J* = 2.76 Hz, 1H, ArH), 6.89-6.92 (dd, ^2J = 9.16 Hz, ^3J = 2.52 Hz, 1H, ArH), 7.25 (m, 2H, ArH), 7.48 (d, *J* = 8.68 Hz, 1H, ArH), 7.52 (s, 1H, ArH), 7.56 (s, 1H, ArH), 7.79 (d, *J* = 2.76 Hz, 2H, ArH), 7.81 (s, 1H, ArH), 7.86 (s, 1H, ArH); ^{13}C NMR ($CDCl_3$, 100 MHz): δ 15.5 (CH_3), 18.6 (CH_3), 28.5 (CH_2), 30.3 (CH_2), 37.1 (NH$\underline{CH_2}$), 47/.8 (N$\underline{CH_2}$), 62.0 (OCH_2), 101.9, 106.2, 112.1, 112.4, 113.9, 115.2, 123.8, 125.6, 125.9, 128.2, 131.9, 132.3, 134.5, 138.5, 142.6, 144.7, 147.7, 152.4, 155.0, 161.1 (ArC), 161.2 (C=O); MS (ESI): m/z 536.5 (M^++1); Anal. Calcd for $C_{30}H_{29}N_7O_3$: C, 67.27; H, 5.46; N, 18.31. Found: C, 67.10; H, 5.51; N, 18.19.

Spectral data of 7-((1-(3-(6-(4-methoxyphenyl)imidazo[1,2-*a*]pyrazin-8-ylamino)propyl)-1*H*-1,2,3-triazol-4-yl)methoxy)-4-methyl-2*H*-chromen-2-one (36): brownish solid; yield: 76%;

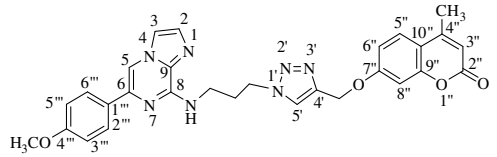

mp 118-120 °C; ^{1}H NMR ($CDCl_3$, 400 MHz): δ 2.37-2.44 (m, 5H, CH_3, CH_2), 3.79-3.83 (m, 5H, NH$\underline{CH_2}$, OCH_3), 4.54 (t, *J* = 6.64 Hz, 2H, N$\underline{CH_2}$), 5.12 (s, 2H,

O$\underline{CH_2}$), 6.14 (d, *J* = 1.40 Hz, 1H, ArH), 6.64 (t, *J* = 5.96 Hz, 1H, NH), 6.84 (d, *J* = 2.76 Hz, 1H, ArH), 6.89-6.92 (dd, ^2J = 9.20 Hz, ^3J = 2.52 Hz, 1H, ArH), 6.95 (d, *J* = 8.72 Hz, 2H, ArH), 7.47 (s, 1H, ArH), 7.50 (d, *J* = 1.36 Hz, 1H, ArH), 7.54 (d, *J* = 1.36 Hz, 1H, ArH), 7.80 (d, *J* = 1.40 Hz, 2H, ArH), 7.81 (s, 1H, ArH), 7.83 (s, 1H, ArH); ^{13}C NMR ($CDCl_3$, 100 MHz): δ 18.6 (CH_3), 30.2 (CH_2), 37.0 (NH$\underline{CH_2}$), 47.7 (N$\underline{CH_2}$), 55.3 (OCH_3), 62.0 (OCH_2), 101.9, 105.5, 112.1, 112.4, 113.9, 114.0, 115.1, 123.8, 125.6, 127.2, 129.6, 131.7, 132.1, 138.3, 142.6, 147.7, 152.4, 155.0, 159.8, 161.1 (ArC), 161.2 (C=O); MS (ESI): m/z 538.5 (M^++1); Anal. Calcd for $C_{29}H_{27}N_7O_4$: C, 64.79; H, 5.06; N, 18.24. Found: C, 64.63; H, 4.91; N, 18.36.

Spectral data of 7-((1-(3-(6-(2-methoxyphenyl)imidazo[1,2-*a*]pyrazin-8-ylamino)propyl)-1*H*-1,2,3-triazol-4-yl)methoxy)-4-methyl-2*H*-chromen-2-one (37): brown solid; yield:

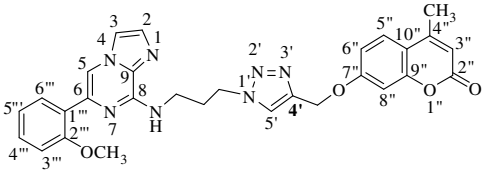

68%; mp 162-164 ^{o}C; ^{1}H NMR ($CDCl_3$, 400 MHz): δ 2.35-2.42 (m, 5H, CH_3, CH_2), 3.79 (q, *J* = 6.12 Hz, 2H, NH$\underline{CH_2}$), 3.92 (s, 3H, OCH_3), 4.54 (t, *J* = 6.64 Hz, 2H, N$\underline{CH_2}$), 5.05 (s, 2H, O$\underline{CH_2}$), 6.14(d, *J* = 0.92 Hz, 1H, ArH), 6.55 (bs, 1H, NH), 6.84 (d, *J* = 2.28 Hz, 1H, ArH), 6.89-6.92 (dd,^2J = 8.72 Hz, ^3J = 2.54 Hz, 1H, ArH), 6.99 (d, *J* = 8.24 Hz, 1H, ArH), 7.04-7.08 (m, 1H, ArH), 7.28-7.33 (m, 1H, ArH), 7.49 (d, *J* = 8.72 Hz, 1H, ArH), 7.53 (d, *J* = 0.92 Hz, 1H, ArH), 7.56 (d, *J* = 1.40 Hz, 1H, ArH), 7.87 (s, 1H, ArH), 8.04-8.06 (dd, ^2J = 7.80 Hz, ^3J = 1.84 Hz, 1H, ArH), 8.28 (s, 1H, ArH); ^{13}C NMR ($CDCl_3$, 100 MHz): δ 18.6 (CH_3), 30.4 (CH_2), 37.1 (NH$\underline{CH_2}$), 47.7 (N$\underline{CH_2}$), 55.5 (OCH_3), 61.9 (OCH_2), 101.9, 111.1, 111.2, 112.1, 112.4, 113.8, 115.3, 120.9, 124.1, 125.4, 125.5, 129.3, 130.4, 131.4, 131.8, 134.8, 142.4, 147.2, 152.5, 155.0, 156.8, 161.1 (ArC), 161.2 (C=O); MS (ESI): m/z 538.5 (M^++1); Anal. Calcd for $C_{29}H_{27}N_7O_4$: C, 64.79; H, 5.06; N, 18.24. Found: C, 64.52; H, 4.92; N, 18.08.

Spectral data of 4-(8-(3-(4-((4-methyl-2-oxo-2*H*-chromen-7-yloxy)methyl)-1*H*-1,2,3-triazol-1-yl)propylamino)imidazo[1,2-*a*]pyrazin-6-yl)benzaldehyde (38): brownish solid;

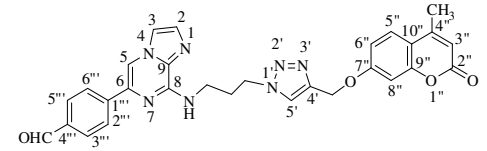

yield: 90%; mp 194-196 ^{o}C; ^{1}H NMR ($CDCl_3$ + DMSO-d_6, 400 MHz): δ 2.40-2.45 (m, 5H, CH_3, CH_2), 3.80 (q, *J* = 6.10 Hz, 2H, NH$\underline{CH_2}$), 4.58 (t, *J* = 6.64 Hz, 2H, N$\underline{CH_2}$), 5.17 (s, 2H, O$\underline{CH_2}$), 6.12 (s, 1H, ArH), 6.86 (d, *J* = 2.28 Hz, 1H, ArH), 6.90-6.93 (dd, ^2J = 8.72 Hz, ^3J = 2.28 Hz, 1H, ArH), 7.05 (t, *J* = 5.04 Hz, 1H, NH), 7.52 (d, *J* = 6.40 Hz, 2H, ArH), 7.67 (s, 1H, ArH), 7.92 (d, *J* = 8.24 Hz, 2H, ArH), 7.94 (s, 1H, ArH), 8.10 (d, *J* = 8.28

Hz, 2H, ArH), 8.14 (s, 1H, ArH), 9.98 (s, 1H, CHO); ^{13}C NMR ($CDCl_3$ + DMSO-d_6, 100 MHz): 18.0 (CH_3), 29.3 (CH_2), 36.4 (NH<u>CH_2</u>), 47.2 (N<u>CH_2</u>), 61.4 (OCH_2), 101.2, 107.5, 111.3, 111.7, 113.2, 115.1, 123.4, 125.2, 125.6, 129.3, 131.7, 132.0, 135.0, 135.8, 141.9, 142.7, 147.4, 152.1, 154.3, 160.4 (ArC), 160.5 (C=O), 191.2 (CHO); MS (ESI): m/z 536.5 (M^++1); Anal. Calcd for $C_{29}H_{25}N_7O_4$: C, 65.04; H, 4.71; N, 18.31. Found: C, 64.89; H, 4.58; N, 18.25.

4.1.6.11. Photophysical measurements

All photophysical measurements were performed in acetonitrile. Absorption spectra were measured with a UV-2500, Shimadzu spectrophotometer. Fluorescent measurements were performed with a Carry Eclipse spectrophotometer. The quantum yields of the imidazo[1,2-*a*]pyrazine analogues were determined relative to anthracene.

4.1.6.12. Fluorescence quantum yield

The fluorescence quantum yield Φ_{fs} for all compounds was determined at room temperature in analytical grade CH_3CN using anthracene (Φ_{fr} = 0.22) in acetonitrile as the standard. The quantum yield was calculated by using eqn--1, in which Φ_{fs} is the radiative quantum yield of the sample, Φ_{fr} is the radiative quantum yield of reference, A_s and A_r are the absorbance of the sample and the reference, respectively, D_s and D_r are the areas of emission for the sample and reference respectively, L_s and L_r are the lengths of the absorption cells, and N_s and N_r are the refractive indices of the respective sample and reference solutions (pure solvents were assumed).

$$\Phi_{fs} = \Phi_{fr} \times \frac{1-10^{-A_r L_r}}{1-10^{-A_s L_s}} \times \frac{N_s^2}{N_r^2} \times \frac{D_s}{D_r} \qquad \text{--------1}$$

4.2. IMIDAZO[1,2-*a*]PYRAZINE-TRIAZOLE-BENZIMIDAZOLE CONJUGATES

4.2.1. INTRODUCTION

Phosphate-containing anionic species[135] are ubiquitous in biological systems and play important mediatory roles in signal transduction pathways, and also in carrying genetic information.[136] For example, anions such as pyrophosphate ion (PPi) is involved in energy transduction in organisms, and controlling metabolic processes via participation in enzymatic reactions.[137] Various important biochemical reactions like DNA polymerization, synthesis of cyclic AMP (second messenger) and formation of the activated intermediates (aminoacyl-tRNA) in protein synthesis are catalyzed by DNA polymerase, adenylate cyclase and aminoacyl-tRNA synthetase, respectively, whereas the hydrolysis of ATP with concomitant release of PPi is at the heart of biochemical pathways.[138] Therefore, several research groups have focused on the detection of this biological anion. But, the design of fluorescent chemosensors for detection of biologically important anion remains a challenge. This is due to lack of a general design principle in translating anion-binding event to a large fluorescent signal response.[139] Moreover, most of the developed phosphate anion sensors are based on transition metal complexes where the cavity formed by the metal ion with the receptor provides a cooperative binding site for phosphate derivative.[140] In this context, Zn(II) complexes are frequently used.[141] but other metal ions like Tb(III),[142] Cd(II),[143] Mn(II),[144] Cu(II)[145] and Eu(III)[146] have also been employed. Some of these sensors display remarkable selectivity and sensitivity. However, considerable synthetic efforts are required for their preparation. Moreover, sensing molecules for detection of PPi are limited in literature and the potential for the development of this PPi sensor is at the primitive stage for bioanalytical application. Until now, very few sensors for detection of PPi, displaying high selectivity and reliability in the absence of any metal ions were reported.[147] To the best of our knowledge, examples of chemosensors based on imidazo[1,2-*a*]pyrazine and benzimidazole platforms have not been reported so far.

Moreover, fluorescence resonance energy transfer (FRET) are generally designed as fluorescence sensor to adopt the photophysical changes produced on complexation.[148] Recently FRET based probes[149] have actively been used in cell physiology, optical therapy and selective as well as specific sensing towards the target analytes.[150]

4.2.2. OBJECTIVE

Keeping above points in consideration, we have designed and synthesized imidazo[1,2-*a*]pyrazine-benzimidazole conjugates for FRET based ratiometric determination of pyrophosphate (PPi). Despite of great research, there is no report available for synthesis of FRET based probes for ratiometric detection of pyrophosphate. Herein, we have synthesized these conjugates by implementing click reaction and Suzuki-Miyaura cross coupling at respective C-8 and C-6 positions of imidazo[1,2-*a*]pyrazine.

4.2.3. CHEMISTRY

Compound **4** was synthesized according to the procedure mentioned in section 4.1.3 (Scheme 1). Reaction of 2-(3-nitrophenyl)-1*H*-benzo[*d*]imidazole **5** with 2 eq. of 80% solution of propargyl bromide, in the presence of potassium carbonate and DMF at room temperature for 12 h to obtain 2-(3-nitrophenyl)-1-(prop-2-ynyl)-1*H*-benzo[*d*]imidazole **6** in 95% yield (Scheme 5).

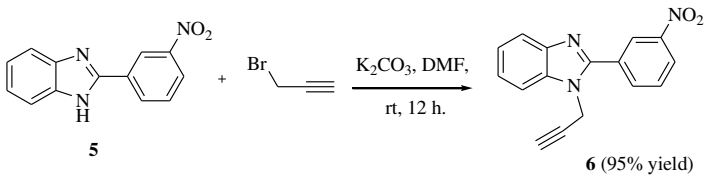

Scheme 5 Synthesis of *N*-propargylated benzimidazole

Keeping both the precursors i.e. azide and alkyne, copper catalyzed azide-alkyne cyloaddition (CuAAC) reaction was performed by reacting azide **4** and alkyne **6** in the presence of 5 mol% of $CuSO_4.5H_2O$ as catalyst and 10 mol% of sodium ascorbate as reducing agent in ethanol:water (8:2) at room temperature for 2 h to afford triazole linked imidazo[1,2-*a*]pyrazine-benzimidazole conjugate **7** in 81% yield (Scheme 6).

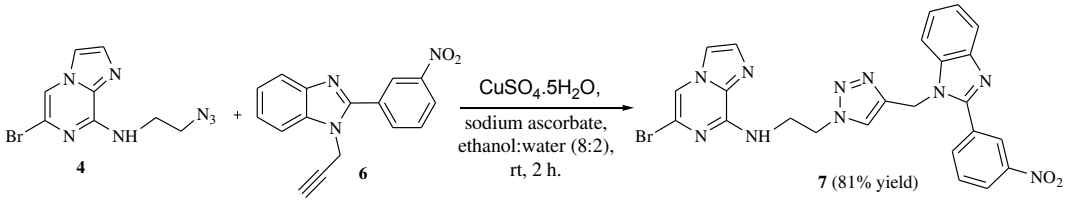

Scheme 6 Synthesis of triazole based imidazo[1,2-*a*]pyrazine-benzimidazole conjugates.

However, a mixture of 1,4-disubstituted triazole **7** and 1,5-disubstituted triazole **8** in 2:1 ratio was obtained on reaction of azide **4** and alkyne **6** in heating without the use of any catalyst. It has been observed that thermal [2+3] dipolar cycloaddition of alkyne to azide is not a regiospecific

reaction. NOESY experiment was carried out to confirm the formation of 1,4 and 1,5-disubstituted products. Positive NOE was observed between the protons of triazole H-5' and alkyl groups at N-1' and C-4' positions in compound **7**, suggesting that the triazole proton and both alkyl groups are in close proximity, thereby confirmed the formation of 1,4-disubstituted triazole. On the other hand, No NOE signals was observed between the C-4' proton of triazole and alkyl group at N-1' position in 1,5-disubstituted triazole **8**. However, positive NOE signal was observed between triazole proton C-4' and C-5' substituted alkyl group (Figure 4).

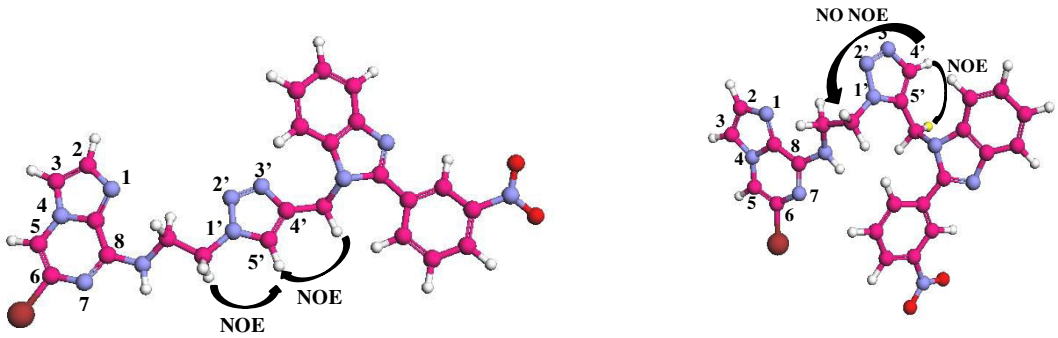

Figure 4 2D NOE experiments of 1,4-disubstituted triazole **7** and 1,5-disubstituted triazole **8**

Conjugate **7** was further reacted with variety of aryl boronic acids through Suzuki-Miyaura cross coupling at C-6 position of imidazo[1,2-*a*]pyrazine using $Pd(PPh_3)_4$ (5 mol%), K_2CO_3 (1 equiv.) in 1,4-dioxane:H_2O (9:1), providing library of arylated compounds **9-24** (Table 7). Various electron donating and electron withdrawing groups were introduced on aryl group of imidazo[1,2-*a*]pyrazine. The reactions were well tolerated with five member ring viz., thiophen-2-boronic acid (**9**), thiophene-3-boronic acid (**10**) and furan-2-boronic acid (**11**). Substitution with electron withdrawing groups such as 4-fluorophenyl (**13**), 4-chlorophenyl (**14**), 4-bromophenyl (**15**), 3-trifluoromethylphenyl (**16**), 4-formylphenyl (**23**) and 4-acetylphenyl (**24**) gave good yields of products while electron donating groups, 3-methylphenyl (**17**) and 2-methoxy phenyl (**22**) were obtained in moderate yields.

Table 7 Suzuki-Miyaura coupling of ethyl triazole bridged imidazo[1,2-*a*]pyrazine-benzimidazole conjugates.

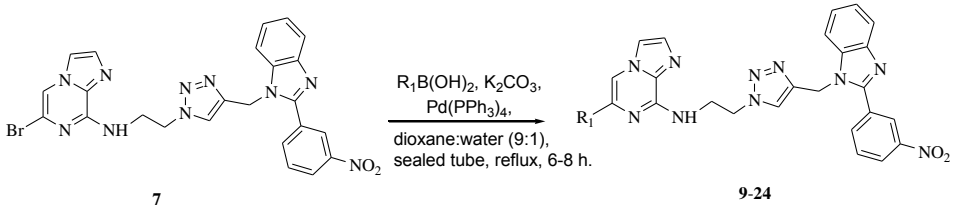

7 9-24

Entry	Time (h)	$R_1B(OH)_2$	Product	Compound (%)
1	8	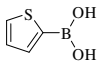	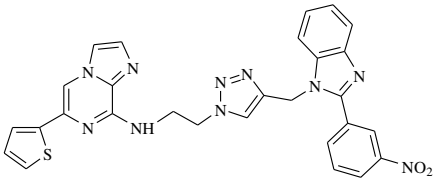	**9** (73)
2	8	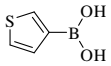	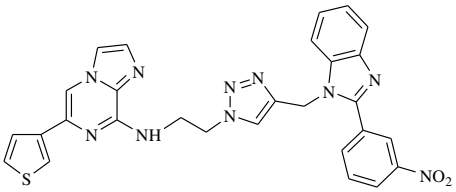	**10** (81)
3	8	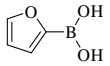	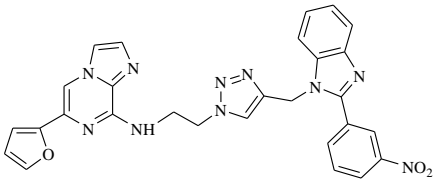	**11** (62)
4	6	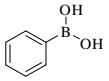	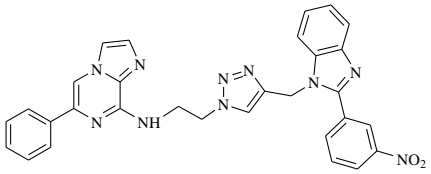	**12** (80)
5	7	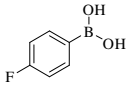	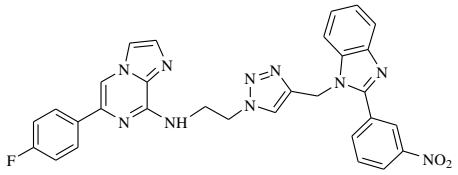	**13** (73)
6	7	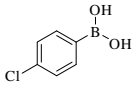	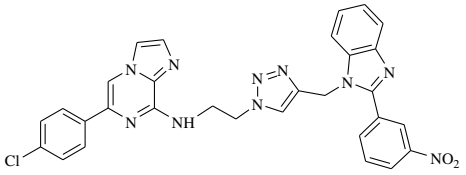	**14** (79)
7	7	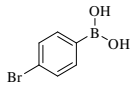	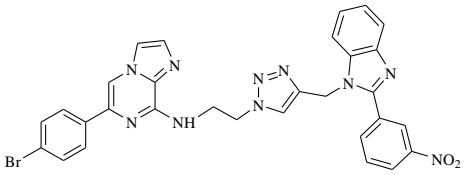	**15** (84)
8	6	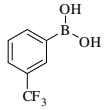	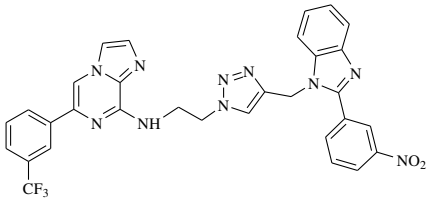	**16** (69)

9	6	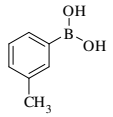	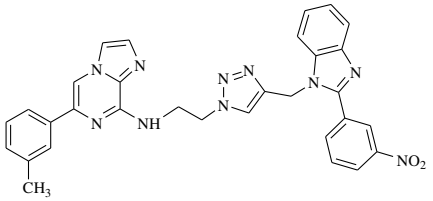	**17** (61)
10	6	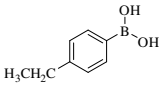	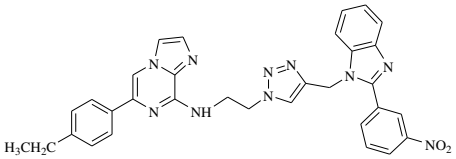	**18** (77)
11	8	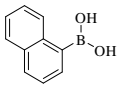	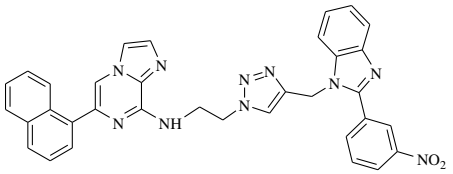	**19** (55)
12	8	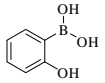	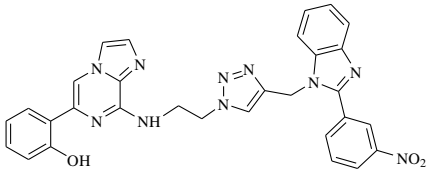	**20** (43)
13	7	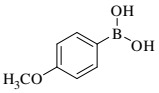	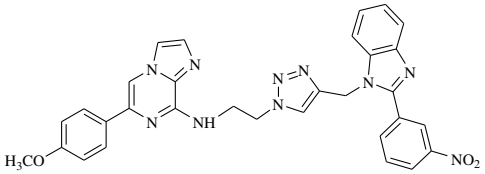	**21** (91)
14	6	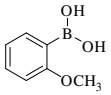	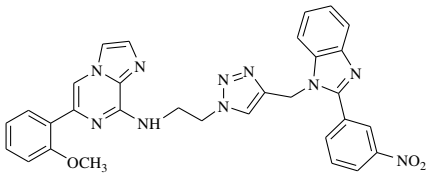	**22** (58)
15	6	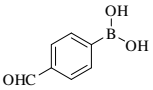	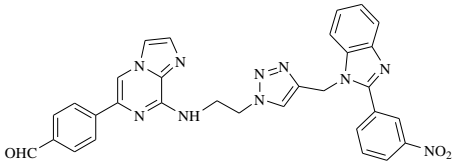	**23** (88)
16	8	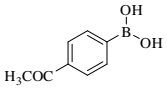	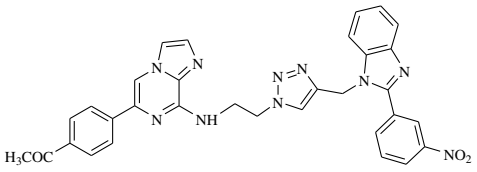	**24** (71)

After the screening of 2-azidoethanamine, reaction with another alkyl chain, 3-azidopropanamine was investigated as described above in section 4.1.3. (Scheme 4). Copper catalyzed azide-alkyne cycloaddition of **27** with **6** gave compound **28** in 85% yield. Subsequent

reaction of **28** with variety of aryl boronic acids via Suzuki-Miyaura coupling reaction, to obtain compounds **29-38** in 53-83% yields (Scheme 7, Table 8).

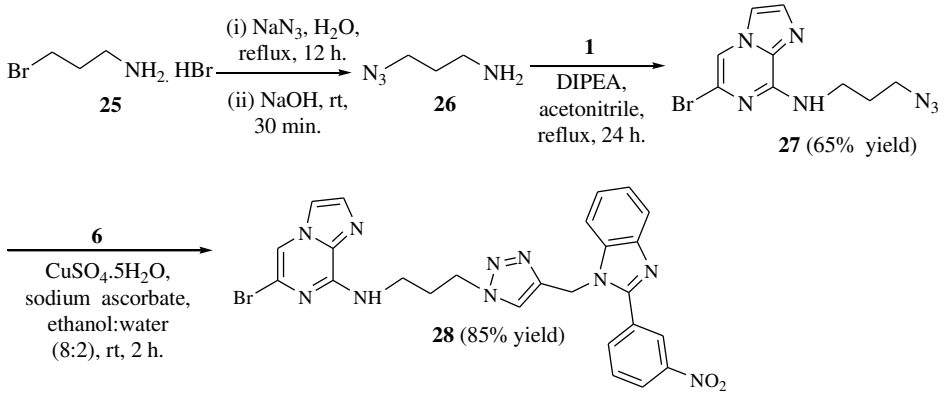

Scheme 7 Synthesis of triazole based imidazo[1,2-*a*]pyrazine-benzimidazole conjugate

Table 8 Suzuki-Miyaura coupling of propyl triazole bridged imidazo[1,2-*a*]pyrazine-benzimidazole conjugates

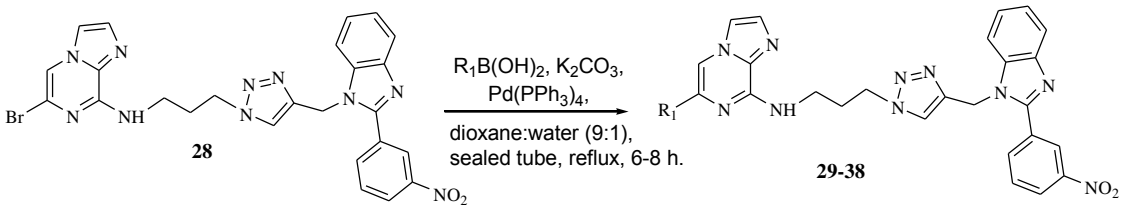

Entry	Time (h)	$R_1B(OH)_2$	Product	Compound (%)
1	6	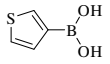	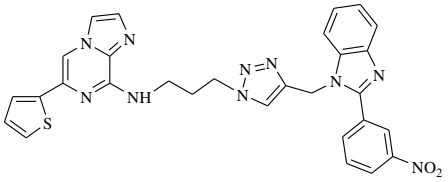	**29** (68)
2	8	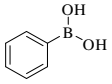	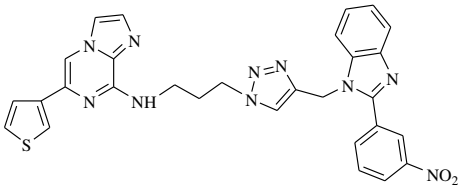	**30** (67)
3	8	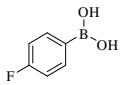	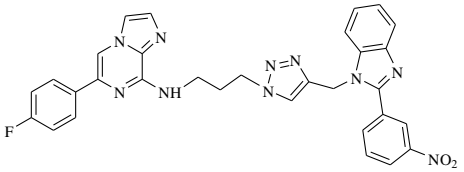	**31** (76)
4	8	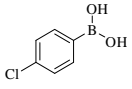	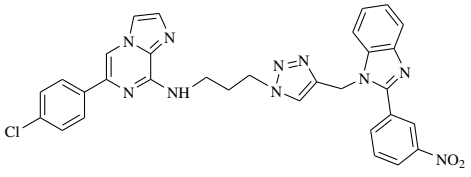	**32** (78)

5	6	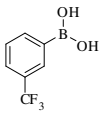	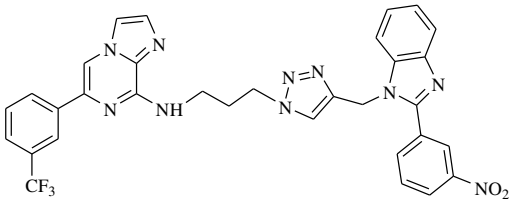	**33** (53)
6	7	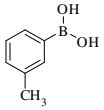	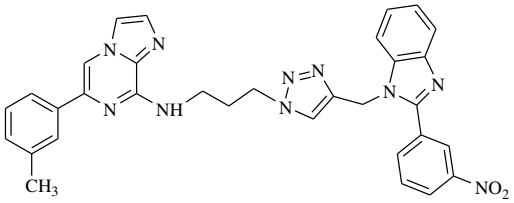	**34** (57)
7	7	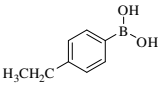	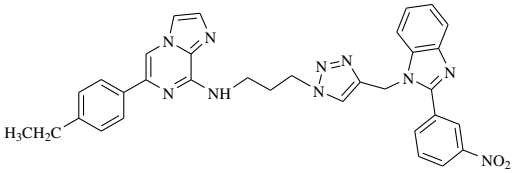	**35** (62)
8	8	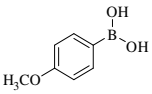	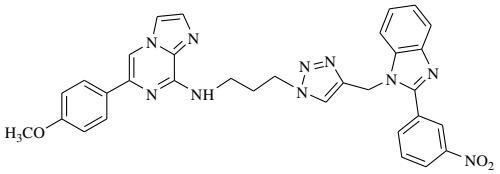	**36** (81)
9	6	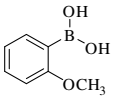	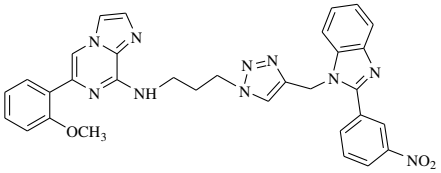	**37** (83)
10	6	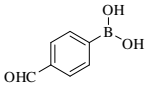	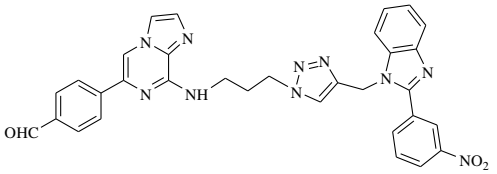	**38** (80)

4.2.4. PHOTOPHYSICAL PROPERTIES

Compounds **7**, **9-24** and **28-38** were further studied for their photophysical properties. Quantum yields of all compounds were calculated with respect to anthracene in acetonitrile. It was revealed that presence of electron withdrawing groups viz., 4-formyl phenyl (**23** and **38**) and 4-acetyl phenyl (**24**) gave excellent quantum yields (0.90, 0.92 and 0.85 respectively). In case of halogen containing compounds, the most electron withdrawing group such as 3-(trifluoromethyl)phenyl moiety in **16** and **33** gave good quantum yield (0.53 and 0.62 respectively) in comparison to other halogenated compounds **13** (0.14), **14** (0.38)**, 15** (0.38). On increasing linker length from ethyl to propyl as exemplified by compounds **16** and **23** with **33** and **38**, increase in quantum yields was observed (Tables 9, 10). FRET efficiencies (η) based

upon the fluorescence quantum yields have also been determined using the equation[151] $\eta = 1 - \Phi_{F(\text{donor in dyad})}/\Phi_{F(\text{free donor})}$. Where, $\Phi_{F(\text{donor in dyad})}$ is the fluorescence quantum yield of the donor part in dyad and $\Phi_{F(\text{free donor})}$ is the fluorescence quantum yield of the donor when not connected to the acceptor. It revealed that in most of the cases, presence of electron donating substituents showed lower FRET efficiencies in comparison to electron withdrawing

substituents. However, the maximum FRET efficiency (92%) from donor part of dyad to acceptor was displayed by compound **20** having 2-hydroxyphenyl substituent attached to the acceptor part. Imidazo[1,2-*a*]pyrazine acts as an acceptor and showed absorption band at 360 nm. There is a significant spectral overlap between absorption spectra of the imidazo[1,2-*a*]pyrazine (acceptor) and emission spectra of the benzimidazole (donor) (Figure 5). Dyad **20** (Φ_f = 0.080) showed the emission band at 365 nm. Upon addition of PPi to dyad **20**, red shift of 65 nm from 365 nm to 430 nm is observed particularly due to fluorescence resonance energy transfer (FRET). It signifies that donor benzimidazole transfers its energy to acceptor imidazo[1,2-*a*]pyrazine (430 nm) with red shift upon addition of PPi resulting FRET on (Energy transfer efficiency = 92%).

Table 9: Photophysical properties of compounds **7**, **9-24**

Entry	Product (%)[a]	λ_{max}^{abs} (nm)	λ_{max}^{emi} (nm)	€	Φ_f	FRET efficiency (η)
1	**7**	287	375	36600	0.22	85.3
2	**9**	286	420	42250	0.19	87.3
3	**10**	288	366	46250	0.13	91.3
4	**11**	288	375	36200	0.26	82.6
5	**12**	291, 280	408	53800	0.52	65.3
6	**13**	282	365	47250	0.14	90.6
7	**14**	284	380	56050	0.38	72.6
8	**15**	283	380	50450	0.38	74.6
9	**16**	283	395	50400	0.53	64.6
10	**17**	285	406	50250	0.32	62.6
11	**18**	283	385	57700	0.28	81.3
12	**19**	285	420	55050	0.11	25.3
13	**20**	286	365	26600	0.95	92.0
14	**21**	286, 258	373	66950	0.15	90.0
15	**22**	289	407	37550	0.48	45.3
16	**23**	340, 274	496	47300	0.90	ND
17	**24**	340, 272	475	59750	0.85	ND

ND: not determined

Table 10: Photophysical properties of compounds **28-38**

Entry	Product (%)[a]	λ_{max}^{abs} (nm)	λ_{max}^{emi} (nm)	€	Φ_f	FRET efficiency (η)[d]
1	**28**	287	365	28100	0.15	90.3
2	**29**	287	368	30300	0.28	81.3
3	**30**	288	405	30400	0.70	53.3
4	**31**	282	370	28350	0.14	90.6
5	**32**	284	390	32550	0.41	74.6
6	**33**	283	392	17800	0.62	18.6
7	**34**	284	372	22750	0.56	78.6
8	**35**	283	371	37000	0.36	76.0
9	**36**	286, 258	372	31800	0.43	71.3
10	**37**	289	370	34950	0.82	71.0
11	**38**	341, 274	505	31250	0.92	ND

ND: not determined

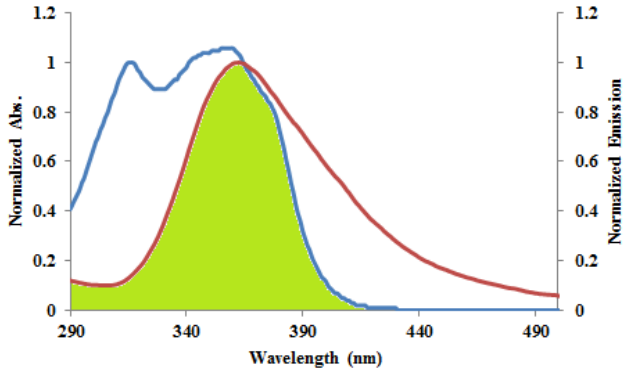

Figure 5 Spectral overlap between absorption spectra of the imidazopyrazine (acceptor) and emission spectra of the benzimdazole (donor)

Further insight and quantitative evaluation of the sensing capability of compounds **7**, **9-24** and **28-38** (20 µM, CH_3CN) with pyrophosphate was obtained from UV-visible and fluorescence quenching experiments. It was surprising that only compound **20** with 2-hydroxylphenyl ring at C6 position of imidazo[1,2-*a*]pyrazine, showed significant change with pyrophosphate indicating that 2-hydroxyphenyl moiety is responsible for binding with PPi. As shown in figure 6a, compound **20** showed an absorption band centered at 286 nm. Upon addition of increasing amount of PPi (0.2 µM to 900 µM), we observed the decrease of the band at 286 nm with a concomitant appearance of new band at 340 nm that could be attributed either to the

deprotonation, observed in the ^{1}H NMR titration or to an interaction *via* hydrogen bonding. The association constant for binding of compound **20** with PPi has been found to be 4.69×10^3 M^{-1} determined by Benesi–Hildebrand equation.[152] Lowest detection limit was found to be 0.1 µM. The behaviour of compound **20** towards PPi was then studied by spectrofluorimetric titrations in CH_3CN. Compound **20** showed an emission band at 365 nm when excited at 280 nm. As shown in figure 6b, upon addition of increasing amount of PPi (20 µM to 1000 µM), a quenching of the emission band of the receptor was accompanied by the formation of a new band at 430 nm. This new band could probably originate from the intramolecular interaction in the excited state of the hydroxyphenyl and benzimidazole moieties. This interaction could be favoured by the presence of the coordinated PPi. The association constant for binding of compound **20** with PPi was 2×10^4 M^{-1} and the lowest detection limit was found to be 20 µM.

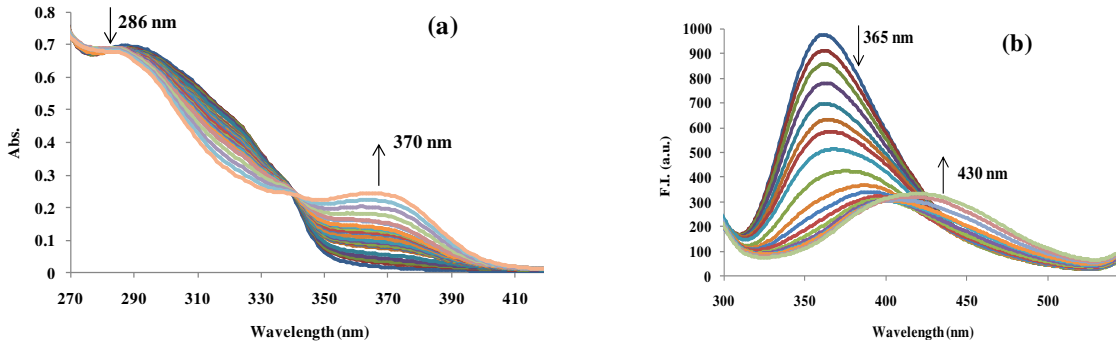

Figure 6 (a) Changes in UV-visible of **20** (20 µM in CH_3CN) upon addition of tris(tetrabutyl ammonium) hydrogen pyrophosphate (0.2 µM to 900 µM). (b) Changes in fluorescence emission intensity of **20** (20 µM in CH_3CN) upon the addition of pyrophosphate (20 µM to 1000 µM).

In an effort to gain more detailed information of the interaction between compound **20** and PPi, ^{1}H NMR titration study was carried out in CD_3CN (Figure 7). The proton signal at δ 8.1 ppm was attributed to the 2-hydroxyphenyl proton H_a and signal at δ 6.8 ppm is due to the overlapping triplet and doublet from the characteristic protons H_b and H_d of hydroxyphenyl along with NH_c. The addition of 0.5 equivalents of PPi caused deprotonation of both OH and NH_c at δ 12.7 and δ 6.8, respectively. On the other hand, proton H_a adjacent to the hydroxyl group broadened and shifted downfield by δ 0.9 ppm (δ 8.1-9.0 ppm) until the end of the titration experiment (over one equivalents of PPi added). The large shifting as well as broadening of signal might be due to hydrogen bonding of compound with pyrophosphate. The signal of the other proton H_b is separated out and shifted upfield by 0.3 ppm (δ 6.8-6.5 ppm) upon addition of

pyrophosphate ion. Moreover, two double doublets at δ 8.2 and 8.3 ppm of benzimidazole are also approaching towards each other. This interesting behaviour of compound **20** could be explained by considering the important contribution given by the benzimidazole and 2-hydroxylphenyl in assisting the interaction of the receptor and pyrophosphate anion. The proposed mechanism for the binding of pyrophosphate with compound **20** has been shown in Figure 8. It has been shown that 2-hydroxyphenyl, imidazopyrazine and benzimdazole moieties are interacting with pyrophosphate anion. On the basis of ^{1}H NMR studies, the proposed binding mode for compound **20** with PPi is shown in Figure 8.

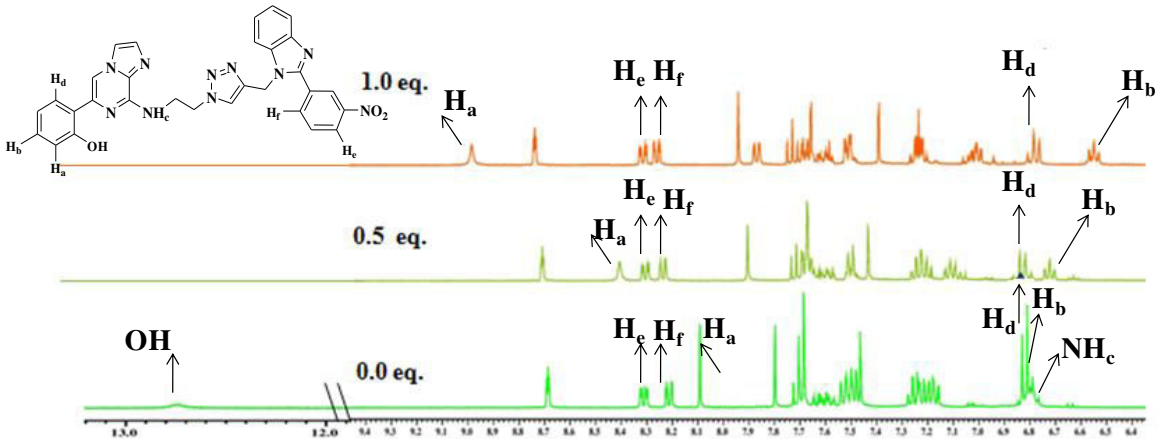

Figure 7 ^{1}H NMR stack plot of a CD_3CN solution of compound **20** (5 mM) upon addition of tris(tetrabutylammonium) hydrogen pyrophosphate (0.5-1.0 eq.).

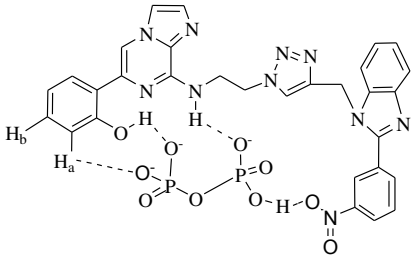

Figure 8 Suggested binding structure for **20** with PPi

4.2.5. CONCLUSION

We have synthesized a new series of imidazo[1,2-*a*]pyrazine-benzimidazole conjugates based on click reaction and Suzuki-Miyaura coupling reaction. We have demonstrated that while simply changing the substituents in the acceptor part of conjugate, a ratiometric detection of pyrophosphate was observed in CH_3CN. In particular, in case of receptor bearing 2-

hydroxyphenyl group at C-6 position of imidazo[1,2-*a*]pyrazine (**20**), binding is achieved thanks to the uncommon interaction of an aromatic CH from fluorophore with PPi guest.

4.2.6. EXPERIMENTAL SECTION

4.2.6.1. Synthesis of 2-(3-nitrophenyl)-1-(prop-2-ynyl)-1*H*-benzo[*d*]imidazole (6): To 2-(3-nitrophenyl)-1*H*-benzo[*d*]imidazole **5** (1 g, 4.08 mmol) was added 80% solution of propargyl bromide in toluene (1.055 g, 8.40 mmol) in the presence of potassium carbonate (0.56 g, 4.08 mmol) and DMF. The mixture was stirred at room temperature for 12 h. Completion of reaction was monitored by TLC. Reaction was quenched by addition of ice cold water. The solid product was filtered to obtain pure off white solid.

Spectral data of 2-(3-nitrophenyl)-1-(prop-2-ynyl)-1*H*-benzo[*d*]imidazole (6): off white

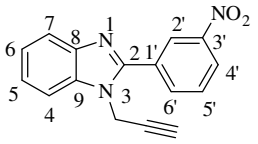

solid; yield: 95%; mp 128-130 ^{o}C; ^{1}H NMR ($CDCl_3$, 400 MHz): δ 2.56 (t, *J* = 2.52 Hz, 1H, alkyne CH), 4.97 (d, *J* = 2.28 Hz, 2H, NCH_2), 7.37-7.45 (m, 2H, ArH), 7.57-7.59 (m, 1H, ArH), 7.77 (t, *J* = 8.02 Hz, 1H, ArH), 7.86-7.88 (m, 1H, ArH), 8.24- 8.27 (dt, ^{2}J = 6.40 Hz, ^{3}J = 1.36 Hz, 1H, ArH), 8.39-8.42 (ddd, ^{2}J = 8.24 Hz, ^{3}J = 2.28 Hz, ^{4}J = 0.92, 1H, ArH), 8.82 (t, *J* = 2.06 Hz, 1H, ArH); ^{13}C NMR ($CDCl_3$, 100 MHz): δ 34.6 (NCH_2), 74.5 (alkyne CH, C), 109.9, 120.1, 123.2, 123.8, 124.0, 124.4, 129.9, 131.1, 134.8, 135.2, 142.5, 148.2, 150.2 (ArC); MS (ESI): m/z 278.2 (M^{+}+1).

4.2.6.2. Synthesis of 6-bromo-*N*-(2-(4-((2-(3-nitrophenyl)-1*H*-benzo[*d*]imidazol-1-yl)methyl)-1*H*-1,2,3-triazol-1-yl)ethyl)imidazo[1,2-*a*]pyrazin-8-amine (7): To a stirred solution of 2-(3-nitrophenyl)-1-(prop-2-ynyl)-1*H*-benzo[*d*]imidazole **6** (1.00 g, 3.6 mmol) and *N*-(2-azidoethyl)-6-bromoimidazo[1,2-*a*]pyrazin-8-amine **4** (1.00 g, 3.6 mmol) in 50 ml ethanol:water (8:2), copper sulphate pentahydrate (5 mol%) and sodium ascorbate (10 mol%) were added and stirred at room temperature for 2 h. After completion of reaction, water was added and extracted with chloroform. Chloroform layer was dried over anhydrous sodium sulphate, filtered and concentrated in vacuum to obtain pure yellow solid.

Spectral data of 6-bromo-*N*-(2-(4-((2-(3-nitrophenyl)-1*H*-benzo[*d*]imidazol-1-yl)methyl)-1*H*-1,2,3-triazol-1-yl)ethyl)imidazo[1,2-*a*]pyrazin-8-amine (7): yellow solid; yield: 81%; mp

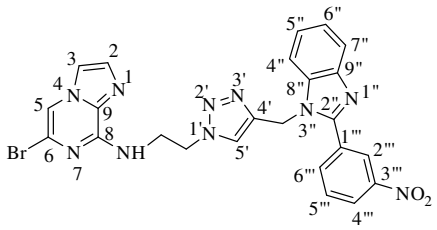

230-232 ^{o}C; ^{1}H NMR (DMSO-d_6, 400 MHz): δ 3.79 (q, J = 5.04 Hz, 2H, NHC<u>H</u>$_2$), 4.59 (t, J = 5.74 Hz, 2H, NC<u>H</u>$_2$), 5.51 (s, 2H, NC<u>H</u>$_2$), 7.17-7.24 (m, 2H, ArH), 7.45 (s, 1H, ArH), 7.57 (d, J = 7.32 Hz, 1H, ArH), 7.68 (d, J = 7.36 Hz, 1H, ArH), 7.78 (d, J = 0.92 Hz, 1H, ArH), 7.81 (d, J = 7.80 Hz, 1H, ArH), 7.96 (s, 1H, ArH), 8.03 (t, J = 5.72 Hz, 1H, NH), 8.17 (s, 1H, ArH), 8.34- 8.38 (m, 2H, ArH), 8.75 (t, J = 1.60 Hz, 1H, ArH); ^{13}C NMR (DMSO-d_6, 100 MHz): δ 40.4 (NH<u>C</u>H$_2$), 48.5 (2xN<u>C</u>H$_2$), 109.6, 111.3, 115.9, 119.4, 121.5, 122.5, 123.1, 124.2, 124.4, 130.4, 131.3, 131.5, 132.3, 135.6, 135.7, 142.1, 142.4, 147.3, 147.9 (ArC); MS (ESI): m/z 560.3 (M^++1); Anal. Calcd for $C_{24}H_{19}BrN_{10}O_2$: C, 51.53; H, 3.42; N, 25.04. Found: C, 51.40; H, 3.29; N, 24.94.

4.2.6.3. General procedure for synthesis of 6-arylated-*N*-(2-(4-((2-(3-nitrophenyl)-1*H*-benzo[*d*]imidazol-1-yl)methyl)-1*H*-1,2,3-triazol-1-yl)ethyl)imidazo[1,2-*a*]pyrazin-8-amine (9-24): To a solution of **7** (0.10 g, 0.178 mmol) in mixture of 1,4-dioxane : water (9:1) in a sealed tube, boronic acid (0.178 mmol) and K_2CO_3 (0.025 g, 0.178 mmol) were added under inert atmosphere. Then, [Pd(PPh$_3$)$_4$] (5mol%) was added with continued nitrogen purging. Sealed the tube and refluxed the reaction mixture for 6-8 h. Completion of reaction was determined by TLC. The mixture was extracted with chloroform and water. Organic layer was dried over sodium sulphate to obtain crude product which was further purified by column chromatography using ethylacetate: methanol as eluents.

Spectral data of *N*-(2-(4-((2-(3-nitrophenyl)-1*H*-benzo[*d*]imidazol-1-yl)methyl)-1*H*-1,2,3-triazol-1-yl)ethyl)-6-(thiophen-2-yl)imidazo[1,2-*a*]pyrazin-8-amine (9): brownish solid;

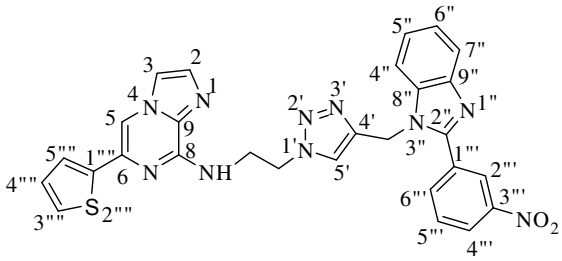

yield: 73%; mp 134-136 ^{o}C; ^{1}H NMR (CDCl$_3$, 400 MHz): δ 4.09 (q, J = 5.65 Hz, 2H, NHC<u>H</u>$_2$), 4.67 (t, J = 5.72 Hz, 2H, NC<u>H</u>$_2$), 5.37 (s, 2H, NC<u>H</u>$_2$), 6.44 (bs, 1H, NH), 7.37 (d, J = 7.76 Hz, 1H, ArH), 7.44 (s, 1H, ArH), 7.49 (d, J = 1.84 Hz, 1H, ArH), 7.51 (d, J = 7.80 Hz, 1H, ArH), 7.55 (s, 2H, ArH), 7.67-7.71 (m, 2H, ArH), 7.83 (d, J = 7.80 Hz, 1H, ArH), 7.89 (d, J = 8.24 Hz, 2H, ArH), 8.16 (d, J = 8.72 Hz, 1H, ArH), 8.22 (d, J = 7.80 Hz, 1H, ArH), 8.32-8.35 (m, 1H, ArH), 8.65 (s, 1H, ArH); ^{13}C NMR (CDCl$_3$, 100 MHz): δ 40.8 (NH<u>C</u>H$_2$), 40.9 (N<u>C</u>H$_2$), 49.6 (N<u>C</u>H$_2$), 110.4, 110.6, 115.1, 120.2, 122.8, 123.2, 123.8, 124.4, 125.27, 125.8, 125.9, 126.1, 127.1, 128.4, 128.9, 130.0, 131.6, 132.4, 133.8, 135.9, 139.4, 142.9 ,

147.1, 148.2, 150.9 (ArC); MS (ESI): m/z 563.6 (M^++1); Anal. Calcd for $C_{28}H_{22}N_{10}O_2S$: C, 59.78; H, 3.94; N, 24.90; S, 5.70. Found: C, 59.61; H, 3.83; N, 24.97; S, 5.66.

Spectral data of *N*-(2-(4-((2-(3-nitrophenyl)-1*H*-benzo[*d*]imidazol-1-yl)methyl)-1*H*-1,2,3-triazol-1-yl)ethyl)-6-(thiophen-3-yl)imidazo[1,2-*a*]pyrazin-8-amine (10): creamish solid;

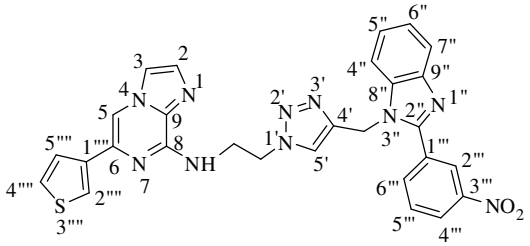

yield: 81%; mp 192-194 ^oC; ^1H NMR ($CDCl_3$, 400 MHz): δ 4.18 (q, *J* = 5.81 Hz, 2H, NHC<u>H</u>$_2$), 4.76 (t, *J* = 5.74 Hz, 2H, NC<u>H</u>$_2$), 5.39 (s, 2H, NC<u>H</u>$_2$), 6.40 (t, *J* = 6.18 Hz, 1H, NH), 7.19-7.23 (m, 1H, ArH), 7.28-7.33 (m, 3H, ArH), 7.37 (s, 1H, ArH), 7.41-7.44 (m, 2H, ArH), 7.55 (s, 1H, ArH), 7.63 (s, 1H, ArH), 7.67 (t, *J* = 7.90 Hz, 1H, ArH), 7.70 (dd, ^2J = 2.76 Hz, ^3J = 1.38 Hz, 1H, ArH), 7.81 (d, *J* = 8.24 Hz, 1H, ArH), 8.19-8.21 (dt, ^2J = 2.72 Hz, ^3J = 1.36 Hz, 1H, ArH), 8.31-8.34 (ddd, ^2J = 8.24 Hz, ^3J = 2.28 Hz, ^4J = 0.92 Hz, 1H, ArH), 8.62 (t, *J* = 1.82 Hz, 1H, ArH); ^{13}C NMR ($CDCl_3$, 100 MHz): δ 40.7 (NHC<u>H</u>$_2$), 40.7 (NC<u>H</u>$_2$), 49.9 (NC<u>H</u>$_2$), 106.6, 110.4, 115.2, 120.1, 122.3, 123.1, 123.1, 123.7, 124.4, 124.4, 124.6, 126.3, 130.0 , 131.3, 132.0, 132.2, 134.4, 135.4, 135.7, 138.9, 142.7, 142.8, 147.2, 148.2, 150.8 (ArC); MS (ESI): m/z 563.6 (M^++1); Anal. Calcd for $C_{28}H_{22}N_{10}O_2S$: C, 59.78; H, 3.94; N, 24.90; S, 5.70. Found: C, 60.01; H, 4.03; N, 24.82; S, 5.76.

Spectral data of 6-(furan-2-yl)-*N*-(2-(4-((2-(3-nitrophenyl)-1*H*-benzo[*d*]imidazol-1-yl)methyl)-1*H*-1,2,3-triazol-1-yl)ethyl)imidazo[1,2-*a*]pyrazin-8-amine (11): Grey coloured

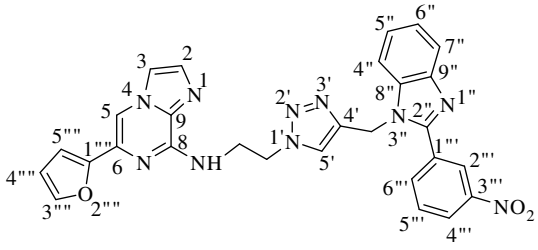

solid; yield: 62%; mp 122-124 ^oC; ^1H NMR ($CDCl_3$, 400 MHz): δ 4.15 (q, *J* = 5.80 Hz, 2H, NHC<u>H</u>$_2$), 4.75 (t, *J* = 5.72 Hz, 2H, NC<u>H</u>$_2$), 5.43 (s, 2H, NC<u>H</u>$_2$), 6.42 (dd, ^2J = 3.68 Hz, ^2J = 1.84 Hz, 1H, ArH), 6.47 (t, *J* = 5.96 Hz, 1H, NH), 6.78 (d, *J* = 3.24 Hz, 1H, ArH), 7.21-7.25 (m, 1H, ArH), 7.29-7.33 (m, 1H, ArH), 7.36 (t, *J* = 0.92 Hz, 1H, ArH), 7.39 (d, *J* = 1.36 Hz, 1H, ArH), 7.43 (s, 1H, ArH), 7.45 (d, *J* = 0.92 Hz, 1H, ArH), 7.55 (s, 1H, ArH), 7.68 (t, *J* = 8.02 Hz, 1H, ArH), 7.74 (s, 1H, ArH), 7.82 (d, *J* = 7.80 Hz, 1H, ArH), 8.20-8.22 (dt, ^2J = 2.28 Hz, ^3J = 0.92 Hz, 1H, ArH), 8.32-8.35 (ddd, ^2J = 8.20 Hz, ^3J = 2.32 Hz, ^4J = 1.40 Hz, 1H, ArH), 8.64 (t, *J* = 1.82 Hz, 1H, ArH); ^{13}C NMR ($CDCl_3$, 100 MHz): δ 40.7 (NHC<u>H</u>$_2$), 40.8 (NC<u>H</u>$_2$), 49.7 (NC<u>H</u>$_2$), 105.6, 107.8, 110.4, 111.6, 115.5, 120.2, 122.9, 123.1, 123.7, 124.4, 124.4 , 128.5, 130.0, 130.8, 131.4, 131.9, 132.1, 135.3, 142.2, 142.7, 142.8, 147.4, 148.2, 150.8, 151.8

(ArC); MS (ESI): m/z 547.5 (M^++1); Anal. Calcd for $C_{28}H_{22}N_{10}O_3$: C, 61.53; H, 4.06; N, 25.63. Found: C, 61.67; H, 4.09; N, 25.71.

Spectral data of *N*-(2-(4-((2-(3-nitrophenyl)-1*H*-benzo[*d*]imidazol-1-yl)methyl)-1*H*-1,2,3-triazol-1-yl)ethyl)-6-phenylimidazo[1,2-*a*]pyrazin-8-amine (12): yellow solid; yield: 80%; mp

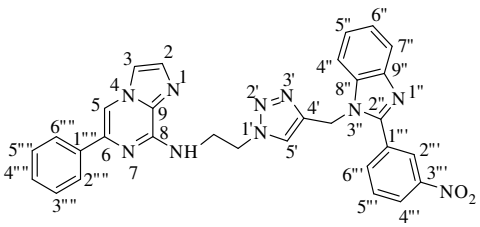

170-172 °C; ^{1}H NMR ($CDCl_3$, 400 MHz): δ 4.19 (q, *J* = 5.80 Hz, 2H, NH$\underline{CH_2}$), 4.77 (t, *J* = 5.74 Hz, 2H, N$\underline{CH_2}$), 5.39 (s, 2H, N$\underline{CH_2}$), 6.49 (t, *J* = 5.96 Hz, 1H, NH), 7.21-7.24 (m, 1H, ArH), 7.28-7.34 (m, 2H ArH), 7.37 (s, 1H, ArH), 7.39 (s, 2H, H-2, ArH), 7.43 (d, *J* = 8.0 Hz, 1H, ArH), 7.47 (d, *J* = 0.92 Hz, 1H, ArH), 7.53 (s, 1H, ArH), 7.65 (t, *J* = 8.02 Hz, 1H, ArH), 7.79 (s, 2H, ArH), 7.81 (d, *J* = 1.84 Hz, 2H, ArH), 8.18-8.19 (dt, ^2J = 2.28 Hz, ^3J = 1.40 Hz, 1H, ArH), 8.30-8.32 (ddd, ^2J = 8.24 Hz, ^3J = 2.28 Hz, ^4J = 0.92 Hz, 1H, ArH), 8.63 (t, *J* = 1.84 Hz, 1H, ArH); ^{13}C NMR ($CDCl_3$, 100 MHz): δ 40.7 (NH$\underline{CH_2}$), 40.8 (N$\underline{CH_2}$), 49.7 (N$\underline{CH_2}$), 107.0, 110.4, 115.2, 120.2, 123.0, 123.1, 123.8, 124.4, 125.8, 128.3, 128.6 , 129.9, 131.4, 132.1, 132.3, 135.3, 135.7, 136.8, 137.9, 142.8, 142.8, 147.2, 148.2, 150.9 (ArC); MS (ESI): m/z 557.6 (M^++1); Anal. Calcd for $C_{30}H_{24}N_{10}O_2$: C, 64.74; H, 4.35; N, 25.17. Found: C, 64.60; H, 4.29; N, 25.02.

Spectral data of 6-(4-fluorophenyl)-*N*-(2-(4-((2-(3-nitrophenyl)-1*H*-benzo[*d*]imidazol-1-yl)methyl)-1*H*-1,2,3-triazol-1-yl)ethyl)imidazo[1,2-*a*]pyrazin-8-amine (13): pale yellow

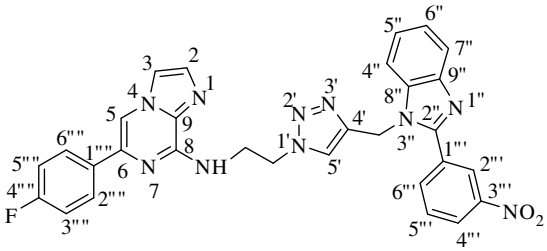

solid; yield: 73%; mp 182-184 °C; ^{1}H NMR ($CDCl_3$, 400 MHz): δ 4.20 (q, *J* = 5.80 Hz, 2H, NH$\underline{CH_2}$), 4.76 (t, *J* = 5.48 Hz, 2H, N$\underline{CH_2}$), 5.40 (s, 2H, N$\underline{CH_2}$), 6.42 (t, *J* = 5.96 Hz, 1H, NH), 7.04 (t, *J* = 8.70 Hz, 2H, ArH), 7.20-7.24 (m, 1H, ArH), 7.28-7.32 (m, 1H, ArH), 7.38 (d, *J* = 0.88 Hz, 1H, ArH), 7.42 (d, *J* = 0.92 Hz, 1H, ArH), 7.45 (d, *J* = 8.28 Hz, 1H, ArH), 7.56 (s, 1H, ArH), 7.64-7.68 (m, 2H, ArH), 7.72 (t, *J* = 5.04 Hz, 1H, ArH), 7.74 (d, *J* = 5.48 Hz, 1H, ArH), 7.80 (d, *J* = 8.28 Hz, 1H, ArH), 8.17-8.19 (dt, ^2J = 2.28 Hz, ^3J = 1.36 Hz, 1H, ArH), 8.31-8.34 (ddd, ^2J = 8.24 Hz, ^3J = 2.28 Hz, ^4J = 0.92 Hz, 1H, ArH), 8.57 (t, *J* = 2.04 Hz, 1H, ArH); ^{13}C NMR ($CDCl_3$, 100 MHz): δ 40.7 (NH$\underline{CH_2}$), 49.9 (2xN$\underline{CH_2}$), 106.6, 110.5, 115.3, 115.3, 115.5, 120.1, 123.0, 123.2, 123.7, 124.2, 124.4, 127.4, 127.5, 130.0, 131.3, 132.0, 132.4, 132.8, 135.4, 135.7, 136.9, 142.7, 142.8, 147.1, 148.2, 150.8, 161.6, 164.1 (ArC); MS (ESI): m/z 575.6 (M^++1); Anal. Calcd for $C_{30}H_{23}FN_{10}O_2$: C, 62.71; H, 4.03; N, 24.38.

Found: C, 62.56; H, 4.18; N, 24.51.

Spectral data of 6-(4-chlorophenyl)-*N*-(2-(4-((2-(3-nitrophenyl)-1*H*-benzo[*d*]imidazol-1-yl)methyl)-1*H*-1,2,3-triazol-1-yl)ethyl)imidazo[1,2-*a*]pyrazin-8-amine (14): creamish

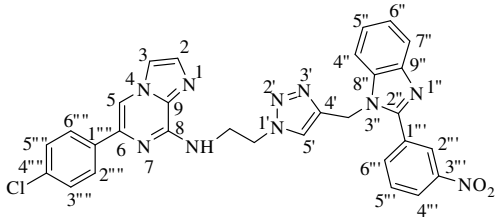

solid; yield: 79%; mp 192-194 ^{o}C; ^{1}H NMR ($CDCl_3$, 400 MHz): δ 4.19 (q, *J* = 5.65 Hz, 2H, NH$\underline{CH_2}$), 4.76 (t, *J* = 5.74 Hz, 2H, N$\underline{CH_2}$), 5.38 (s, 2H, N$\underline{CH_2}$), 6.47 (t, *J* = 6.18 Hz, 1H, NH), 7.18-7.22 (m, 1H, ArH), 7.27 (s, 1H, ArH), 7.30 (d, *J* = 8.72 Hz, 2H, ArH), 7.37 (d, *J* = 0.92 Hz, 1H, ArH), 7.40 (d, *J* = 0.92 Hz, 1H, ArH), 7.44 (d, *J* = 7.76 Hz, 1H, ArH), 7.58 (s, 1H, ArH), 7.63-7.66 (m, 2H, ArH), 7.68 (d, *J* = 3.68 Hz, 2H, ArH), 7.80 (d, *J* = 8.24 Hz, 1H, ArH), 8.16-8.18 (m, 1H, ArH), 8.30-8.33 (m, 1H, ArH), 8.56 (t, *J* = 1.82 Hz, 1H, ArH); ^{13}C NMR ($CDCl_3$, 100 MHz): δ 40.6 (NH$\underline{CH_2}$), 40.7 (N$\underline{CH_2}$), 49.9 (N$\underline{CH_2}$), 106.9, 110.4, 115.3, 120.1, 123.1, 123.2, 123.7, 124.2, 124.4, 126.9, 128.6, 129.9, 131.3, 132.0, 132.4, 134.1, 135.0, 135.4, 135.7, 136.6, 142.7, 142.8, 147.1, 148.1, 150.8 (ArC); MS (ESI): m/z 592.0 (M^{+}+1); Anal. Calcd for $C_{30}H_{23}ClN_{10}O_2$: C, 60.97; H, 3.92; N, 23.70. Found: C, 61.09; H, 3.99; N, 23.64.

Spectral data of 6-(4-bromophenyl)-*N*-(2-(4-((2-(3-nitrophenyl)-1*H*-benzo[*d*]imidazol-1-yl)methyl)-1*H*-1,2,3-triazol-1-yl)ethyl)imidazo[1,2-*a*]pyrazin-8-amine (15): brown solid;

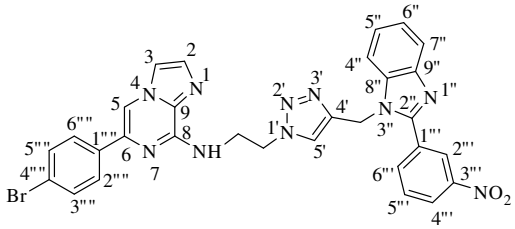

yield: 84%; mp 120-122 ^{o}C; ^{1}H NMR ($CDCl_3$, 400 MHz): δ 4.20 (q, *J* = 5.81 Hz, 2H, NH$\underline{CH_2}$), 4.76 (t, *J* = 5.50 Hz, 2H, N$\underline{CH_2}$), 5.38 (s, 2H, N$\underline{CH_2}$), 6.42 (t, *J* = 5.72 Hz, 1H, NH), 7.18-7.22 (m, 1H, ArH), 7.28-7.33 (m, 1H, ArH), 7.39 (d, *J* = 0.92 Hz, 1H, ArH), 7.41 (d, *J* = 0.92 Hz, 1H, ArH), 7.43 (s, 1H, ArH), 7.46 (d, *J* = 8.72 Hz, 2H, ArH), 7.57 (s, 1H, ArH), 7.61 (d, *J* = 8.24 Hz, 2H, ArH), 7.65-7.69 (m, 2H, ArH), 7.80 (d, *J* = 7.80 Hz, 1H, ArH), 8.16-8.19 (dt, ^{2}J = 2.72 Hz, ^{3}J = 1.36 Hz, 1H, ArH), 8.32-8.34 (ddd, ^{2}J = 8.24 Hz, ^{3}J = 2.32 Hz, ^{4}J = 0.92 Hz, 1H, ArH), 8.56 (t, *J* = 2.06 Hz, 1H, ArH); ^{13}C NMR ($CDCl_3$, 100 MHz): δ 40.7 (NH$\underline{CH_2}$), 50.0 (2xN$\underline{CH_2}$), 106.9, 110.4, 115.4, 120.1, 122.4, 123.1, 123.2, 123.7, 124.2, 124.4, 127.2, 128.4, 130.0, 131.3, 131.6, 131.9, 132.3, 135.4, 135.7, 136.7, 142.7, 142.8, 147.1, 148.1, 150.8 (ArC); MS (ESI): m/z 636.4 (M^{+}+1); Anal. Calcd for $C_{30}H_{23}BrN_{10}O_2$: C, 56.70; H, 3.65; N, 22.04. Found: C, 56.90; H, 3.53; N, 21.96.

Spectral data of *N*-(2-(4-((2-(3-nitrophenyl)-1H-benzo[*d*]imidazol-1-yl)methyl)-1*H*-1,2,3-triazol-1-yl)ethyl)-6-(3-(trifluoromethyl)phenyl)imidazo[1,2-*a*]pyrazin-8-amine (16): cream

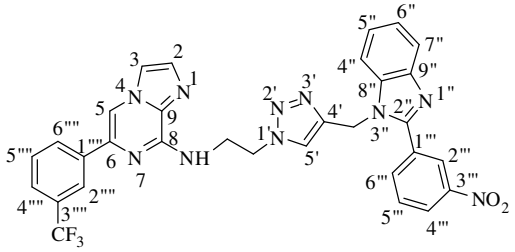

solid; yield: 69%; mp 183-185 ^{o}C; ^{1}H NMR ($CDCl_3$, 400 MHz): δ 4.21 (q, *J* = 5.80 Hz, 2H, NH$\underline{CH_2}$), 4.78 (t, *J* = 5.50 Hz, 2H, N$\underline{CH_2}$), 5.40 (s, 2H, N$\underline{CH_2}$), 6.47 (t, *J* = 5.96 Hz, 1H, NH), 7.19-7.23 (m, 1H, ArH), 7.27-7.31 (m, 1H, ArH), 7.39 (d, *J* = 0.92 Hz, 1H, ArH), 7.45-7.47 (m, 2H, ArH), 7.51 (d, *J* = 7.80 Hz, 1H, ArH), 7.56- 7.58 (m, 2H, ArH), 7.67 (t, *J* = 7.80 Hz, 1H, ArH), 7.79-7.80 (m, 2H, ArH), 7.96 (d, *J* = 7.80 Hz, 1H, ArH), 8.05 (s, 1H, ArH), 8.19-8.21 (dt, ^{2}J = 2.72 Hz, ^{3}J = 1.36 Hz, 1H, ArH), 8.30-8.33 (ddd, ^{2}J = 8.28 Hz, ^{3}J = 2.28 Hz, ^{4}J = 0.88 Hz, 1H, ArH), 8.57 (t, *J* = 1.82 Hz, 1H, ArH); ^{13}C NMR ($CDCl_3$, 100 MHz): δ 40.6 (NH$\underline{CH_2}$), 40.8 (N$\underline{CH_2}$), 49.7 (N$\underline{CH_2}$), 107.4, 110.5, 115.5, 120.1, 122.5, 122.7, 123.0, 123.2, 123.8, 124.2, 124.4, 124.8, 125.4, 128.9, 129.1, 130.0, 130.7, 131.0, 131.3, 131.9, 132.4, 135.4, 135.7, 136.5, 137.5, 142.6, 142.8, 147.2, 148.2, 150.8 ArC); MS (ESI): m/z 625.5 (M^{+}+1); Anal. Calcd for $C_{31}H_{23}F_3N_{10}O_2$: C, 59.61; H, 3.71; N, 22.43. Found: C, 59.42; H, 3.81; N, 22.57.

Spectral data of *N*-(2-(4-((2-(3-nitrophenyl)-1*H*-benzo[*d*]imidazol-1-yl)methyl)-1*H*-1,2,3-triazol-1-yl)ethyl)-6-*m*-tolylimidazo[1,2-*a*]pyrazin-8-amine (17): creamish solid; yield: 61%;

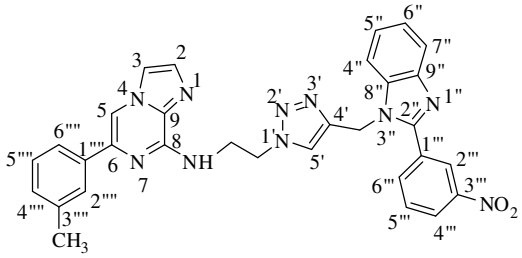

mp 154-156 ^{o}C; ^{1}H NMR ($CDCl_3$, 400 MHz): δ 2.39 (s, 3H, CH_3), 4.20 (q, *J* = 5.65 Hz, 2H, NH$\underline{CH_2}$), 4.78 (t, *J* = 5.72 Hz, 2H, N$\underline{CH_2}$), 5.40 (s, 2H, N$\underline{CH_2}$), 6.52 (t, *J* = 5.72 Hz, 1H, NH), 7.15 (d, *J* = 7.80 Hz, 1H, ArH), 7.21-7.25 (m, 1H, ArH), 7.28-7.32 (m, 2H, ArH), 7.39 (d, *J* = 0.92 Hz, 1H, ArH), 7.43 (d, *J* = 8.24 Hz, 1H, ArH), 7.47 (d, *J* = 0.92 Hz, 1H, ArH), 7.55 (s, 1H, ArH), 7.60-7.62 (m, 2H, ArH), 7.65 (t, *J* = 7.80 Hz, 1H, ArH), 7.78 (s, 1H, ArH), 7.80 (d, *J* = 7.76 Hz, 1H, ArH), 8.18-8.20 (dt, ^{2}J = 2.72 Hz, ^{3}J = 1.36 Hz, 1H, ArH), 8.30-8.32 (ddd, ^{2}J = 8.24 Hz, ^{3}J = 2.32 Hz, ^{4}J = 0.92 Hz, 1H, ArH), 8.63 (t, *J* = 1.82 Hz, 1H, ArH); ^{13}C NMR ($CDCl_3$, 100 MHz): δ 21.5 (CH_3), 40.7 (NH$\underline{CH_2}$), 40.8 (N$\underline{CH_2}$), 49.7 (N$\underline{CH_2}$), 106.9, 110.4, 115.2, 120.1, 123.0, 123.0, 123.1, 123.7, 124.4, 124.4, 126.4, 128.5, 129.1, 129.9, 131.3, 132.0, 132.1, 135.3, 135.6, 136.7, 138.1, 138.2, 142.7, 142.7, 147.0, 148.1, 150.8 (ArC); MS (ESI): m/z 571.6 (M^{+}+1); Anal. Calcd for $C_{31}H_{26}N_{10}O_2$: C, 65.25; H, 4.59; N, 24.55. Found: C, 65.43; H, 4.44; N, 24.67.

Spectral data of 6-(4-ethylphenyl)-*N*-(2-(4-((2-(3-nitrophenyl)-1*H*-benzo[*d*]imidazol-1-yl)methyl)-1*H*-1,2,3-triazol-1-yl)ethyl)imidazo[1,2-*a*]pyrazin-8-amine (18): creamish solid;

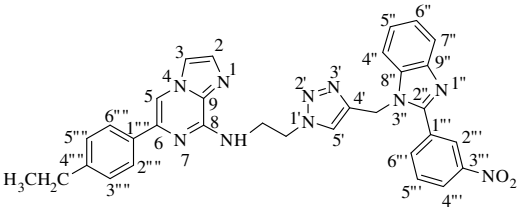

yield: 77%; mp 167-169 ^{o}C; ^{1}H NMR ($CDCl_3$, 400 MHz): δ 1.25 (t, *J* = 7.56 Hz, 3H, CH_3), 2.66 (q, *J* = 7.48 Hz, 2H, CH_2), 4.19 (q, *J* = 5.80 Hz, 2H, NH$\underline{CH_2}$), 4.77 (t, *J* = 5.50 Hz, 2H, N$\underline{CH_2}$), 5.40 (s, 2H, N$\underline{CH_2}$), 6.48 (t, *J* = 5.28 Hz, 1H, NH), 7.21-7.25 (m, 3H, ArH), 7.28-7.32 (m, 1H, ArH), 7.39 (s, 1H, ArH), 7.43 (d, *J* = 7.80 Hz, 1H, ArH), 7.46 (d, *J* = 0.92 Hz, 1H, ArH), 7.55 (s, 1H, ArH), 7.65 (t, *J* = 8.02 Hz, 1H, ArH), 7.71 (d, *J* = 8.24 Hz, 2H, ArH), 7.76 (s, 1H, ArH), 7.81 (d, *J* = 8.24 Hz, 1H, ArH), 8.17-8.20 (dt, ^{2}J = 2.76 Hz, ^{3}J = 1.40 Hz, 1H, ArH), 8.30-8.33 (ddd, ^{2}J = 8.24 Hz, ^{3}J = 2.28 Hz, ^{4}J = 0.92 Hz, 1H, ArH), 8.63 (t, *J* = 1.84 Hz, 1H, ArH); ^{13}C NMR ($CDCl_3$, 100 MHz): δ 15.4 (CH_3), 28.5 (CH_2), 40.6 (NH$\underline{CH_2}$), 40.8 (N$\underline{CH_2}$), 49.7 (N$\underline{CH_2}$), 106.5, 110.4, 115.1, 120.0, 123.1, 123.7, 124.3, 124.4, 125.7, 128.1, 129.9, 131.3, 132.0, 134.1, 135.3, 135.6, 137.9, 142.6, 144.6, 147.1, 148.1, 150.8 (ArC); MS (ESI): m/z 585.6 (M^{+}+1); Anal. Calcd for $C_{32}H_{28}N_{10}O_2$: C, 65.74; H, 4.83; N, 23.96. Found: C, 65.81; H, 4.79; N, 24.09.

Spectral data of 6-(naphthalen-1-yl)-*N*-(2-(4-((2-(3-nitrophenyl)-1*H*-benzo[*d*]imidazol-1-yl)methyl)-1*H*-1,2,3-triazol-1-yl)ethyl)imidazo[1,2-*a*]pyrazin-8-amine (19): brownish solid;

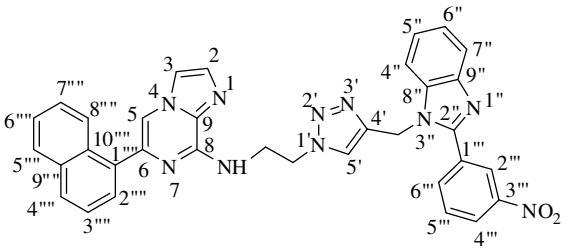

yield: 55%; mp 152-154 ^{o}C; ^{1}H NMR ($CDCl_3$, 400 MHz): δ 4.08 (q, *J* = 5.94 Hz, 2H, NH$\underline{CH_2}$), 4.67 (t, *J* = 5.74 Hz, 2H, N$\underline{CH_2}$), 5.36 (s, 2H, N$\underline{CH_2}$), 6.59 (t, *J* = 5.94 Hz, 1H, NH), 7.30-7.34 (m, 1H, ArH), 7.37 (d, *J* = 8.24 Hz, 1H, ArH), 7.40-7.44 (m, 1H, ArH), 7.45 (s, 1H, ArH), 7.47 (t, *J* = 1.38 Hz, 1H, ArH), 7.48 (d, *J* = 0.92 Hz, 2H, ArH), 7.51 (d, *J* = 7.76 Hz, 1H, ArH), 7.54 (d, *J* = 0.92 Hz, 2H, ArH), 7.69 (t, *J* = 3.90 Hz, 2H, ArH), 7.82 (d, *J* = 7.80 Hz, 1H, ArH), 7.89 (d, *J* = 8.24 Hz, 2H, ArH), 8.16 (m, 1H, ArH), 8.21-8.23 (dt, ^{2}J = 2.76 Hz, ^{3}J = 1.40 Hz, 1H, ArH), 8.31-8.34 (ddd, ^{2}J = 8.28 Hz, ^{3}J = 2.28 Hz, ^{4}J = 1.36 Hz, 1H, ArH), 8.65 (t, *J* = 1.84 Hz, 1H, ArH); ^{13}C NMR ($CDCl_3$, 100 MHz): δ 40.7 (NH$\underline{CH_2}$), 40.9 (N$\underline{CH_2}$), 49.6 (N$\underline{CH_2}$), 110.4, 110.5, 115.1, 120.2, 122.9, 123.1, 123.8, 124.4, 125.2, 125.7, 125.9 , 126.1, 127.1, 128.4, 128.9, 130.0, 131.4, 131.6, 131.9, 132.1, 132.3, 133.3, 135.3, 135.6, 135.7, 139.4, 142.8, 142.9, 147.1, 148.2, 150.9 (ArC); MS (ESI): m/z 607.6 (M^{+}+1); Anal. Calcd for $C_{34}H_{26}N_{10}O_2$: C, 67.32; H, 4.32; N, 23.09. Found: C, 67.45; H, 4.19; N, 23.27.

Spectral data of 3-(8-(2-(4-((2-(3-nitrophenyl)-1*H*-benzo[*d*]imidazol-1-yl)methyl)-1*H*-1,2,3-triazol-1-yl)ethylamino)imidazo[1,2-*a*]pyrazin-6-yl)phenol (20): brownish solid; yield: 43%;

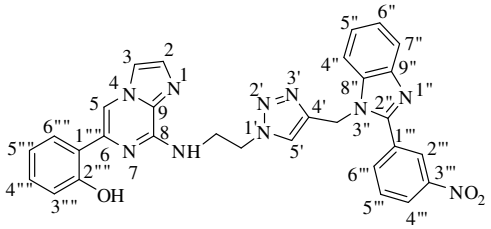

mp 131-133 ^{o}C; ^{1}H NMR ($CDCl_3$, 400 MHz): δ 4.10 (q, *J* = 6.10 Hz, 2H, NH$\underline{CH_2}$), 4.72 (t, *J* = 6.18 Hz, 2H, N$\underline{CH_2}$), 5.43 (s, 2H, N$\underline{CH_2}$), 6.84-6.88 (m, 2H, NH, ArH), 6.89 (d, *J* = 1.36 Hz, 1H, ArH), 6.91 (d, *J* = 0.92 Hz, 1H, ArH), 7.30-7.36 (m, 1H, ArH), 7.46 (d, *J* = 1.40 Hz, 1H, ArH), 7.47 (d, *J* = 0.88 Hz, 1H, ArH), 7.49-7.53 (m, 2H, ArH), 7.55 (d, *J* = 1.36 Hz, 1H, ArH), 7.71-7.72 (m, 2H, ArH), 7.83-7.84 (dd, ^{2}J = 6.40 Hz, ^{3}J = 1.60 Hz, 1H, ArH), 7.89 (s, 1H, ArH), 8.22-8.25 (dt, ^{2}J = 2.76 Hz, ^{3}J = 1.40 Hz, 1H, ArH), 8.33-8.36 (ddd, ^{2}J = 8.20 Hz, ^{3}J = 2.32 Hz, ^{4}J = 1.40 Hz, 1H, ArH), 8.67 (t, *J* = 2.06 Hz, 1H, ArH); ^{13}C NMR ($CDCl_3$, 100 MHz): δ 40.7 (NH$\underline{CH_2}$), 41.2 (N$\underline{CH_2}$), 49.0 (N$\underline{CH_2}$), 106.3, 110.4, 115.9, 117.8, 118.2, 119.5, 120.2, 123.1, 123.2, 123.9, 124.5, 125.0, 128.5, 130.0, 130.5, 131.0, 131.4, 132.9, 135.4, 135.7, 137.7, 142.8, 143.2, 146.0, 148.2, 150.9, 157.6 (ArC); MS (ESI): m/z 573.5 (M^{+}+1); Anal. Calcd for $C_{30}H_{24}N_{10}O_3$: C, 62.93; H, 4.22; N, 24.46. Found: C, 63.03; H, 4.11; N, 24.50.

Spectral data of 6-(4-methoxyphenyl)-*N*-(2-(4-((2-(3-nitrophenyl)-1*H*-benzo[*d*]imidazol-1-yl)methyl)-1*H*-1,2,3-triazol-1-yl)ethyl)imidazo[1,2-*a*]pyrazin-8-amine (21): pale yellow solid;

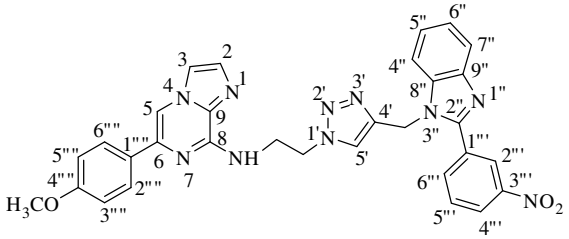

yield: 91%; mp 179-181 ^{o}C; ^{1}H NMR ($CDCl_3$, 400 MHz): δ 3.83 (s, 3H, OCH_3), 4.18 (q, *J* = 5.65 Hz, 2H, NH$\underline{CH_2}$), 4.76 (t, *J* = 5.50 Hz, 2H, N$\underline{CH_2}$), 5.39 (s, 2H, N$\underline{CH_2}$), 6.41 (t, *J* = 5.94 Hz, 1H, NH), 6.90 (d, *J* = 8.68 Hz, 2H, ArH), 7.19-7.23 (m, 1H, ArH), 7.28-7.31 (m, 1H, ArH), 7.37 (s, 1H, ArH), 7.41-7.43 (m, 2H, ArH), 7.54 (s, 1H, ArH), 7.65 (t, *J* = 8.02 Hz, 1H, ArH), 7.68 (s, 1H, ArH), 7.72 (d, *J* = 8.72 Hz, 2H, ArH), 7.80 (d, *J* = 8.24 Hz, 1H, ArH), 8.19 (d, *J* = 7.80 Hz, 1H, ArH), 8.30-8.32 (ddd, ^{2}J = 8.28 Hz, ^{3}J = 2.28 Hz, ^{4}J = 0.92 Hz, 1H, ArH), 8.62 (t, *J* = 1.82 Hz, 1H, ArH); ^{13}C NMR ($CDCl_3$, 100 MHz): δ 40.8 (NH$\underline{CH_2}$), 49.9 (2xN$\underline{CH_2}$), 55.3 (OCH_3), 106.0, 110.4, 113.9, 115.1, 120.1, 123.0, 123.1, 123.7, 124.4, 127.0, 129.3, 129.9, 131.4, 131.9, 132.2, 135.3, 135.7, 137.6, 142.8, 142.9, 147.0 , 148.2, 150.8, 159.8 (ArC); MS (ESI): m/z 587.6 (M^{+}+1); Anal. Calcd for $C_{31}H_{26}N_{10}O_3$: C, 63.47; H, 4.47; N, 23.88. Found: C, 63.60; H, 4.51; N, 23.99.

Spectral data of 6-(2-methoxyphenyl)-*N*-(2-(4-((2-(3-nitrophenyl)-1*H*-benzo[*d*]imidazol-1-

yl)methyl)-1*H*-1,2,3-triazol-1-yl)ethyl)imidazo[1,2-*a*]pyrazin-8-amine (22): creamish solid;

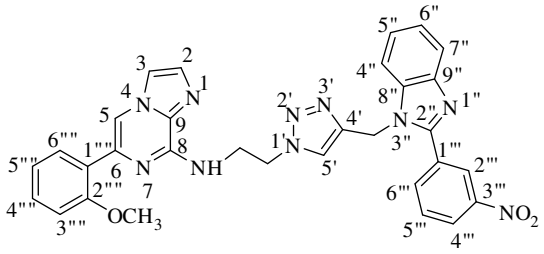

yield: 58%; mp 110-112 ^{o}C; ^{1}H NMR ($CDCl_3$, 400 MHz): δ 3.89 (s, 3H, OCH_3), 4.14 (q, J = 5.80 Hz, 2H, NH$\underline{CH_2}$), 4.75 (t, J = 5.74 Hz, 2H, N$\underline{CH_2}$), 5.39 (s, 2H, N$\underline{CH_2}$), 6.56 (t, J = 5.26 Hz, 1H, NH), 6.96 (d, J = 8.28 Hz, 1H, ArH), 7.00-7.04 (m, 1H, ArH), 7.21-7.25 (m, 1H, ArH), 7.27- 7.32 (m, 2H, ArH), 7.39 (s, 1H, ArH), 7.42 (d, J = 8.24 Hz, 1H, ArH), 7.49 (d, J = 0.92 Hz, 1H, ArH), 7.52 (s, 1H, ArH), 7.63 (t, J = 7.76 Hz, 1H, ArH), 7.80 (d, J = 7.80 Hz, 1H, ArH), 8.01-8.03 (dd, ^{2}J = 7.32 Hz, ^{3}J = 1.60 Hz, 1H, ArH), 8.18-8.20 (dt, ^{2}J = 2.72 Hz, ^{3}J = 1.36 Hz, 1H, ArH), 8.26 (s, 1H, ArH), 8.28-8.31 (ddd, ^{2}J = 8.24 Hz, ^{3}J = 2.32 Hz, ^{4}J = 0.92 Hz, 1H, ArH), 8.67 (t, J = 1.82 Hz, 1H, ArH); ^{13}C NMR ($CDCl_3$, 100 MHz): δ 40.6 (NH$\underline{CH_2}$), 40.9 (N$\underline{CH_2}$), 49.5 (N$\underline{CH_2}$), 55.4 (OCH_3), 110.4, 111.1, 111.7, 115.2, 120.1, 120.8, 123.0, 123.0, 123.7, 124.3, 124.4, 125.2, 129.1, 129.9, 130.1, 131.4, 131.9, 132.1, 134.1, 135.3, 135.6, 142.7, 142.7, 146.7, 148.1, 150.8, 156.6 (ArC); MS (ESI): m/z 587.6 (M^{+}+1); Anal. Calcd for $C_{31}H_{26}N_{10}O_3$: C, 63.47; H, 4.47; N, 23.88. Found: C, 63.59; H, 4.40; N, 23.96.

Spectral data of 4-(8-(2-(4-((2-(3-nitrophenyl)-1*H*-benzo[*d*]imidazol-1-yl)methyl)-1*H*-1,2,3-triazol-1-yl)ethylamino)imidazo[1,2-*a*]pyrazin-6-yl)benzaldehyde (23): yellow solid; yield:

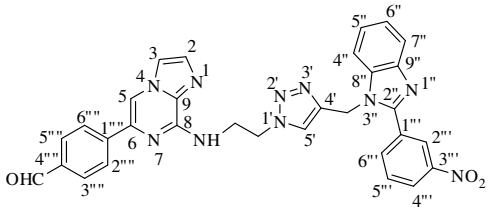

88%; mp 118-120 ^{o}C; ^{1}H NMR ($CDCl_3$, 400 MHz): δ 4.22 (q, J = 5.80 Hz, 2H, NH$\underline{CH_2}$), 4.78 (t, J = 5.50 Hz, 2H, N$\underline{CH_2}$), 5.38 (s, 2H, N$\underline{CH_2}$), 6.54 (t, J = 5.96 Hz, 1H, NH), 7.17-7.21 (m, 1H, ArH), 7.28-7.30 (m, 1H, ArH), 7.39 (d, J = 0.92 Hz, 1H, ArH), 7.43 (d, J = 0.92 Hz, 1H, ArH), 7.47 (d, J = 8.24 Hz, 1H, ArH), 7.61 (s, 1H, ArH), 7.65 (t, J = 8.02 Hz, 1H, ArH), 7.78 (d, J = 8.24 Hz, 1H, ArH), 7.81 (s, 1H, ArH), 7.84 (d, J = 8.72 Hz, 2H, ArH), 7.91 (d, J = 8.24 Hz, 2H, ArH), 8.17-8.19 (dt, ^{2}J = 1.84 Hz, ^{3}J = 0.92 Hz, 1H, ArH), 8.28-8.30 (ddd, ^{2}J = 8.68 Hz, ^{3}J = 1.84 Hz, ^{4}J = 0.92 Hz, 1H, ArH), 8.52 (t, J = 1.82 Hz, 1H, ArH), 9.99 (s, 1H, CHO); ^{13}C NMR ($CDCl_3$, 100 MHz): δ 40.6 (NH$\underline{CH_2}$), 40.7 (N$\underline{CH_2}$), 49.9 (N$\underline{CH_2}$), 108.3, 110.5, 115.5, 120.0, 123.1, 123.2, 123.7, 124.1, 124.4, 126.0, 129.9, 130.0, 131.2, 132.0, 132.1, 132.6, 135.4, 135.7, 136.2, 142.3, 142.6, 142.8, 147.2, 148.1, 150.7 (ArC), 191.7 (CHO); MS (ESI): m/z 585.6 (M^{+}+1); Anal. Calcd for $C_{31}H_{24}N_{10}O_3$: C, 63.69; H, 4.14; N, 23.96. Found: C, 63.76; H, 4.05; N, 24.10.

Spectral data of 1-(4-(8-(2-(4-((2-(3-nitrophenyl)-1*H*-benzo[*d*]imidazol-1-yl)methyl)-1*H*-

1,2,3-triazol-1-yl)ethylamino)imidazo[1,2-*a*]pyrazin-6-yl)phenyl)ethanone (24): yellowish

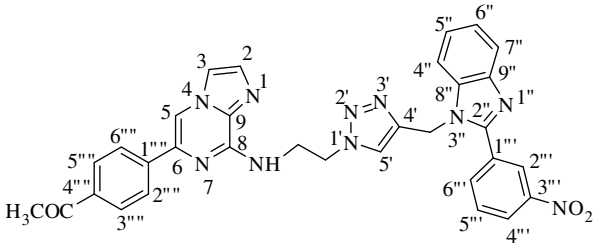

solid; yield: 71%; mp 119-121 ^{o}C; ^{1}H NMR ($CDCl_3$, 400 MHz): δ 2.62 (s, 3H, CO$\underline{CH_3}$), 4.22 (q, J = 5.65 Hz, 2H, NH$\underline{CH_2}$), 4.78 (t, J = 5.51 Hz, 2H, N$\underline{CH_2}$), 5.39 (s, 2H, N$\underline{CH_2}$), 6.54 (t, J = 5.96 Hz, 1H, NH), 7.17-7.21 (m, 1H, ArH), 7.29-7.31 (m, 1H, ArH), 7.40 (d, J = 0.92 Hz, 1H, ArH), 7.44 (d, J = 0.92 Hz, 1H, ArH), 7.46 (d, J = 8.24 Hz, 1H, ArH), 7.61 (s, 1H, ArH), 7.65 (t, J = 8.02 Hz, 1H, ArH), 7.78 (d, J = 7.32 Hz, 2H, ArH), 7.84 (d, J = 8.72 Hz, 2H, ArH), 7.94 (d, J = 8.68 Hz, 2H, ArH), 8.17-8.19 (dt, ^{2}J = 2.76 Hz, ^{3}J = 1.40 Hz, 1H, ArH), 8.29-8.32 (ddd, ^{2}J = 8.28 Hz, ^{3}J = 2.28 Hz, ^{4}J = 0.92 Hz, 1H, ArH), 8.54 (t, J = 1.84 Hz, 1H, ArH); ^{13}C NMR ($CDCl_3$, 100 MHz): δ 26.6 (CH_3), 40.7 (NH$\underline{CH_2}$), 40.7 (N$\underline{CH_2}$), 50.0 (N$\underline{CH_2}$), 108.0, 110.5, 115.5, 120.1, 123.1, 123.2, 123.7, 124.1, 124.4, 125.7, 128.6, 130.0, 131.3, 132.1, 132.5, 135.4, 135.7, 136.4, 136.5, 141.0, 142.7, 142.8, 147.2, 148.1, 150.7 (ArC), 197.6 (C=O); MS (ESI): m/z 599.6 (M^{+}+1); Anal. Calcd for $C_{32}H_{26}N_{10}O_3$: C, 64.21; H, 4.38; N, 23.40. Found: C, 64.11; H, 4.28; N, 23.49.

4.2.6.4. Synthesis of 6-bromo-*N*-(2-(4-((2-(3-nitrophenyl)-1*H*-benzo[*d*]imidazol-1-yl)methyl)-1*H*-1,2,3-triazol-1-yl)propyl)imidazo[1,2-*a*]pyrazin-8-amine (28): To the stirred solution of propargyl benzimidazole **6** (1 g, 3.6 mmol) and azide of imidazo[1,2-*a*]pyrazine **27** (1.07 g, 3.6 mmol) in ethanol:water (8:2), copper sulphate pentahydrate (5 mol%) and sodium ascorbate (10 mol%) was added and stirred at room temperature for 2 h. After completion of reaction, water was added and extracted with chloroform. Organic layer was dried over sodium sulphate and concentrated in vacuum to obtain creamish solid.

Spectral data of 6-bromo-*N*-(3-(4-((2-(3-nitrophenyl)-1*H*-benzo[*d*]imidazol-1-yl)methyl)-1*H*-1,2,3-triazol-1-yl)propyl)imidazo[1,2-*a*]pyrazin-8-amine (28): creamish solid; yield: 85%;

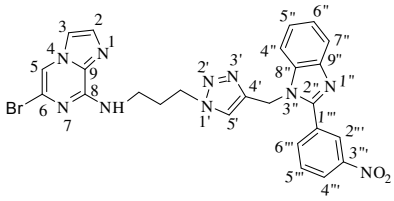

mp 174-176 ^{o}C; ^{1}H NMR (DMSO-d_6,400 MHz): δ 2.12 (m, 2H, CH_2), 3.38 (q, J = 6.10 Hz, 2H, NH$\underline{CH_2}$), 4.40 (t, J = 6.88 Hz, 2H, N$\underline{CH_2}$), 5.60 (s, 2H, N$\underline{CH_2}$), 7.24-7.31 (m, 2H, ArH), 7.48 (s, 1H, ArH), 7.67-7.69 (dd, ^{2}J = 5.96 Hz, ^{3}J = 2.30 Hz, 1H, ArH), 7.71-7.73 (dd, ^{2}J = 6.88 Hz, ^{3}J = 2.54 Hz, 1H, ArH), 7.81 (d, J = 0.92 Hz, 1H, ArH), 7.85 (t, J = 8.02 Hz, 1H, ArH), 7.98 (s, 1H, ArH), 8.10 (t, J = 5.50 Hz, 1H, NH), 8.29 (s, 1H, ArH), 8.36-8.38 (ddd, ^{2}J= 8.28 Hz, ^{3}J = 2.28 Hz, ^{4}J = 0.92, 1H, ArH), 8.42 (d, J = 7.80 Hz, 1H,

ArH), 8.79 (t, J = 1.82 Hz, 1H, ArH); ^{13}C NMR (DMSO-d_6, 100 MHz): δ 29.3 (CH_2), 37.2 (NH<u>CH_2</u>), 47.4 (N<u>CH_2</u>), 109.1, 110.3, 115.9, 119.4, 121.8, 122.5, 123.1, 123.8, 124.1, 124.4, 130.4, 131.5, 131.6, 132.1, 135.6, 135.8, 142.2, 142.4, 147.5, 147.9, 150.7 (ArC); MS (ESI): m/z 574.4 (M^++1); Anal. Calcd for $C_{25}H_{21}BrN_{10}O_2$: C, 52.37; H, 3.69; N, 24.43. Found: C, 52.45; H, 3.60; N, 24.41.

4.2.6.5. General procedure for synthesis of 6-arylated-*N*-(2-(4-((2-(3-nitrophenyl)-1*H*-benzo[*d*]imidazol-1-yl)methyl)-1*H*-1,2,3-triazol-1-yl)propyl)imidazo[1,2-*a*]pyrazin-8-amine (29-38): To a solution of **28** (0.10 g, 0.178 mmol) in a mixture of 1,4-dioxane: water (9:1) in a sealed tube, boronic acid (0.178 mmol) and K_2CO_3 (0.025 g, 0.178 mmol) were added under inert atmosphere. $Pd(PPh_3)_4$ (5mol%) was added with continued nitrogen purging and refluxed the reaction mixture for 6-8 h. Completion of reaction was determined by TLC. The mixture was extracted with chloroform and water. Organic layer was dried over sodium sulphate, filtered and concentrated to obtain crude product which was further purified by column chromatography using ethylacetate : methanol as eluents.

Spectral data of *N*-(3-(4-((2-(3-nitrophenyl)-1*H*-benzo[*d*]imidazol-1-yl)methyl)-1*H*-1,2,3-triazol-1-yl)propyl)-6-(thiophen-3-yl)imidazo[1,2-*a*]pyrazin-8-amine (29): Grey solid; yield:

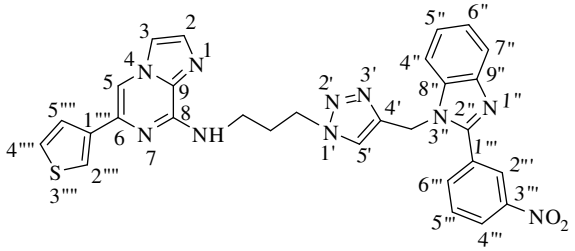

68%; mp 137-139 ^{o}C; ^{1}H NMR ($CDCl_3$, 400 MHz): δ 2.38 (m, 2H, CH_2), 3.75 (q, J = 6.11 Hz, 2H, NH<u>CH_2</u>), 4.50 (t, J = 6.86 Hz, 2H, N<u>CH_2</u>), 5.43 (s, 2H, N<u>CH_2</u>), 6.47 (t, J = 5.74 Hz, 1H, NH), 7.28-7.34 (m, 3H, ArH), 7.39-7.40 (dd, ^2J = 5.04 Hz, ^3J =1.40 Hz, 1H, ArH), 7.44 (s, 1H, ArH), 7.45-7.47 (m, 2H, ArH), 7.60 (s, 1H, ArH), 7.69 (t, J = 8.0 Hz, 1H, ArH), 7.71-7.73 (m, 2H, ArH), 7.82-7.84 (dd, ^2J = 6.88 Hz, ^3J = 1.82 Hz, 1H, ArH), 8.25-8.28 (dt, ^2J = 2.76 Hz, ^3J = 1.40 Hz, 1H, ArH), 8.31-8.34 (ddd, ^2J = 8.24 Hz, ^3J = 2.28 Hz, ^4J = 0.92 Hz, 1H, ArH), 8.66 (t, J = 1.84 Hz, 1H, ArH); ^{13}C NMR ($CDCl_3$, 100 MHz): δ 30.0 (CH_2), 37.2 (NH<u>CH_2</u>), 40.1 (N<u>CH_2</u>), 40.7 (N<u>CH_2</u>), 106.1, 110.5, 115.1, 120.2, 122.2, 122.6, 123.2, 123.5, 124.4, 124.5, 124.7, 126.4, 130.0, 131.5, 131.9, 132.2, 134.8, 135.4, 135.8, 139.4, 142.7, 142.8, 147.8, 148.1, 150.9 (ArC); MS (ESI): m/z 577.6 (M^++1); Anal. Calcd for $C_{29}H_{24}N_{10}O_2S$: C, 60.40; H, 4.20; N, 24.29; S, 5.56. Found: C, 60.31; H, 4.08; N, 24.50; S, 5.44.

Spectral data of *N*-(3-(4-((2-(3-nitrophenyl)-1*H*-benzo[*d*]imidazol-1-yl)methyl)-1*H*-1,2,3-triazol-1-yl)propyl)-6-phenylimidazo[1,2-*a*]pyrazin-8-amine (30): light yellow solid; yield:

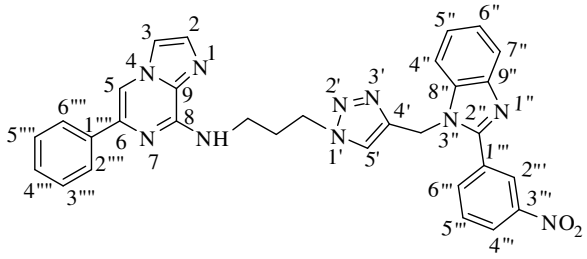

67%; mp 139-141 ^{o}C; ^{1}H NMR ($CDCl_3$, 400 MHz): δ 2.38 (m, 2H, CH_2), 3.79 (q, *J* = 6.10 Hz, 2H, NH$\underline{CH_2}$), 4.51 (t, *J* = 6.88 Hz, 2H, N$\underline{CH_2}$), 5.38 (s, 2H, N$\underline{CH_2}$), 6.33 (t, *J* = 5.96 Hz, 1H, NH), 7.29 (d, *J* = 0.92 Hz, 1H, ArH), 7.31 (d, *J* = 1.84 Hz, 1H, ArH), 7.39 (d, *J* = 8.24 Hz, 2H, ArH), 7.42 (t, *J* = 1.82 Hz, 1H, ArH), 7.44 (s, 1H, ArH), 7.48 (s, 1H, ArH), 7.52 (s, 1H, ArH), 7.61 (s, 1H, ArH), 7.69 (t, *J* = 8.02 Hz, 1H, ArH), 7.82 (s, 1H, ArH), 7.84 (d, *J* = 3.24 Hz, 2H, ArH), 7.86 (d, *J* = 1.36 Hz, 1H, ArH), 8.27 (d, *J* = 7.32 Hz, 1H, ArH), 8.32-8.34 (dd, ^{2}J = 8.24 Hz, ^{3}J = 2.28 Hz, 1H, ArH), 8.67 (t, *J* = 1.84 Hz, 1H, ArH); ^{13}C NMR ($CDCl_3$, 100 MHz): δ 30.2 (CH_2), 37.2 (NH$\underline{CH_2}$), 40.7 (N$\underline{CH_2}$), 48.0 (N$\underline{CH_2}$), 106.6, 110.5, 115.2, 120.2, 122.6, 123.2, 123.8, 124.4, 124.5, 125.9, 128.3, 128.6, 130.0, 131.6, 132.2, 132.4, 135.4, 135.8, 137.2, 138.2, 142.7, 142.8, 147.8, 148.2, 150.9 (ArC); MS (ESI): m/z 571.6 (M^{+}+1); Anal. Calcd for $C_{31}H_{26}N_{10}O_2$: C, 65.25; H, 4.59; N, 24.55. Found: C, 65.41; H, 4.40; N, 24.39.

Spectral data of 6-(4-fluorophenyl)-*N*-(3-(4-((2-(3-nitrophenyl)-1*H*-benzo[*d*]imidazol-1-yl)methyl)-1*H*-1,2,3-triazol-1-yl)propyl)imidazo[1,2-*a*]pyrazin-8-amine (31): pale yellow

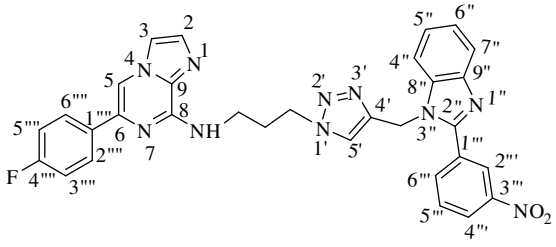

solid; yield: 76%; mp 110-112 ^{o}C; ^{1}H NMR ($CDCl_3$, 400 MHz): δ 2.38 (m, 2H, CH_2), 3.75 (q, *J* = 6.12 Hz, 2H, NH$\underline{CH_2}$), 4.51 (t, *J* = 6.66 Hz, 2H, N$\underline{CH_2}$), 5.42 (s, 2H, N$\underline{CH_2}$), 6.57 (t, *J* = 5.50 Hz, 1H, NH), 7.07 (t, *J* = 8.02 Hz, 2H, ArH), 7.27-7.34 (m, 2H, ArH),7.44 (s, 1H, ArH), 7.46- 7.47 (m, 2H, ArH), 7.58 (s, 1H, ArH), 7.69 (t, *J* = 7.90 Hz, 1H, ArH), 7.77 (s, 1H, ArH), 7.80-7.84 (m, 3H, ArH), 8.24-8.26 (dd, ^{2}J = 7.76 Hz, ^{3}J = 0.92 Hz, 1H, ArH), 8.30-8.33 (m, 1H, ArH), 8.65 (s, 1H, ArH); ^{13}C NMR ($CDCl_3$, 100 MHz): δ 29.9 (CH_2), 37.3 (NH$\underline{CH_2}$), 40.8 (N$\underline{CH_2}$), 48.1 (N$\underline{CH_2}$), 106.1, 110.5, 115.1, 115.4, 115.6, 120.2 , 122.4, 123.2, 123.8, 124.3, 124.5, 127.5, 127.6, 130.0, 131.4, 132.0, 132.2, 133.2, 135.4, 135.7, 137.4, 142.8, 142.9, 147.7, 148.1, 150.9, 161.6, 164.1 (ArC); MS (ESI): m/z 589.5 (M^{+}+1); Anal. Calcd for $C_{31}H_{25}FN_{10}O_2$: C, 63.26; H, 4.28; N, 23.80. Found: C, 63.06; H, 4.12; N, 23.99.

Spectral data of 6-(4-chlorophenyl)-*N*-(3-(4-((2-(3-nitrophenyl)-1*H*-benzo[*d*]imidazol-1-yl)methyl)-1*H*-1,2,3-triazol-1-yl)propyl)imidazo[1,2-*a*]pyrazin-8-amine (32): light brown

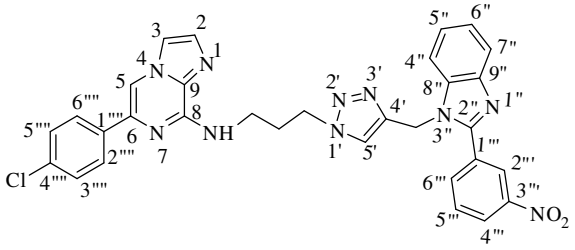

solid; yield: 78%; mp 112-114 ^{o}C; ^{1}H NMR ($CDCl_3$, 400 MHz): δ 2.39 (m, 2H, CH_2), 3.76 (q, J = 6.12 Hz, 2H, NH$\underline{CH_2}$), 4.52 (t, J = 6.88 Hz, 2H, N$\underline{CH_2}$), 5.44 (s, 2H, N$\underline{CH_2}$), 6.42 (t, J = 5.74 Hz, 1H, NH), 7.31 (d, J = 1.40 Hz, 1H, ArH), 7.33 (t, J = 1.60 Hz, 1H, ArH),7.36 (d, J = 8.72 Hz, 2H, ArH), 7.46 (d, J = 0.92 Hz, 1H, ArH), 7.49 (d, J = 1.36 Hz, 1H, ArH), 7.49-7.50 (m, 1H, ArH), 7.56 (s, 1H, ArH), 7.71 (t, J = 8.02 Hz, 1H, ArH), 7.78 (d, J = 8.68 Hz, 2H, ArH), 7.81 (s, 1H, ArH), 7.83-7.85 (dd, ^{2}J = 6.40 Hz, ^{3}J = 1.82 Hz, 1H, ArH), 8.25-8.27 (dt, ^{2}J = 2.76 Hz, ^{3}J = 1.40 Hz, 1H, ArH), 8.32-8.35 (ddd, ^{2}J = 8.24 Hz, ^{3}J = 2.28 Hz, ^{4}J = 0.92 Hz, 1H, ArH), 8.65 (t, J = 1.84 Hz, 1H, ArH); ^{13}C NMR ($CDCl_3$, 100 MHz): δ 29.9 (CH_2), 37.4 (NH$\underline{CH_2}$), 40.8 (N$\underline{CH_2}$), 48.2 (N$\underline{CH_2}$), 106.5, 110.5, 115.2, 120.3, 122.4, 123.2, 123.9, 124.4, 124.5, 126.3, 127.1, 128.7, 130.1, 131.5, 132.2, 134.1, 135.4, 135.6, 135.8, 137.2, 142.8, 142.9, 147.4, 148.2, 150.9 (ArC); MS (ESI): m/z 606.0 (M^{+}+1); Anal. Calcd for $C_{31}H_{25}ClN_{10}O_2$: C, 61.54; H, 4.16; N, 23.15. Found: C, 61.61; H, 4.20; N, 23.09.

Spectral data of *N*-(3-(4-((2-(3-nitrophenyl)-1*H*-benzo[*d*]imidazol-1-yl)methyl)-1*H*-1,2,3-triazol-1-yl)propyl)-6-(3-(trifluoromethyl)phenyl)imidazo[1,2-*a*]pyrazin-8-amine (33):

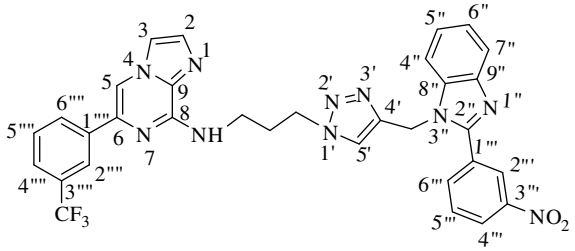

yellow solid; yield: 53%; mp 108-110 ^{o}C; ^{1}H NMR ($CDCl_3$, 400 MHz): δ 2.40 (m, 2H, CH_2), 3.76 (q, J = 6.10 Hz, 2H, NH$\underline{CH_2}$), 4.53 (t, J = 6.86 Hz, 2H, N$\underline{CH_2}$), 5.44 (s, 2H, N$\underline{CH_2}$), 6.60 (t, J = 5.94 Hz, 1H, NH), 7.28-7.35 (m, 2H, ArH), 7.48 (d, J = 1.36 Hz, 1H, ArH), 7.49-7.50 (m, 1H, ArH), 7.52 (d, J = 0.92 Hz, 1H, ArH), 7.52-7.60 (m, 3H, ArH), 7.69 (t, J = 8.02 Hz, 1H, ArH), 7.82-7.84 (m, 1H, ArH), 7.89 (s, 1H, ArH), 8.05 (d, J = 7.80 Hz, 1H, ArH), 8.10 (s, 1H, ArH), 8.24-8.26 (dt, ^{2}J = 2.28 Hz, ^{3}J = 0.88 Hz, 1H, ArH), 8.31-8.34 (ddd, ^{2}J = 8.24 Hz, ^{3}J = 2.28 Hz, ^{4}J = 0.92 Hz, 1H, ArH), 8.65 (t, J = 2.06 Hz, 1H, ArH); ^{13}C NMR ($CDCl_3$, 100 MHz): δ 29.9 (CH_2), 37.5 (NH$\underline{CH_2}$), 40.8 (N$\underline{CH_2}$), 48.2 (N$\underline{CH_2}$), 106.9, 110.5, 115.4, 120.2, 122.3, 122.5, 123.2, 123.9, 124.4, 124.5, 124.8, 125.4, 129.1, 129.3, 130.1, 130.7, 131.1, 131.5, 132.2, 132.3, 135.4, 135.8, 136.9, 138.0, 142.8, 142.9, 147.8, 148.2, 150.9 (ArC); MS (ESI): m/z 639.6 (M^{+}+1); Anal. Calcd for $C_{32}H_{25}F_3N_{10}O_2$: C, 60.18; H, 3.95; N, 21.93. Found: C, 60.26; H, 3.90; N, 21.85.

Spectral data of *N*-(3-(4-((2-(3-nitrophenyl)-1*H*-benzo[*d*]imidazol-1-yl)methyl)-1*H*-1,2,3-

triazol-1-yl)propyl)-6-*m*-tolylimidazo[1,2-*a*]pyrazin-8-amine (34): pale yellow solid; yield:

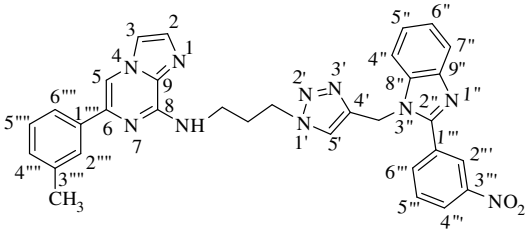

57%; mp 115-117 ^{o}C; ^{1}H NMR ($CDCl_3$, 400 MHz): δ 2.35-2.41 (m, 5H, CH_3, CH_2), 3.79 (q, *J* = 6.12 Hz, 2H, NH$\underline{CH_2}$), 4.51 (t, *J* = 6.88 Hz, 2H, N$\underline{CH_2}$), 5.37 (s, 2H, N$\underline{CH_2}$), 6.50 (t, *J* = 5.66 Hz, 1H, NH), 7.14 (d, *J* = 7.80 Hz, 1H, ArH), 7.28 (d, *J* = 0.92 Hz, 1H, ArH), 7.30 (t, *J* = 1.38 Hz, 1H, ArH), 7.32-7.34 (dd, ^{2}J = 7.32 Hz, ^{3}J = 1.36 Hz, 1H, ArH), 7.40-7.42 (dd, ^{2}J = 6.88 Hz, ^{3}J = 1.36 Hz, 1H, ArH), 7.47 (d, *J* = 0.88 Hz, 1H, ArH), 7.51 (d, *J* = 0.92 Hz, 1H, ArH), 7.64 (s, 2H, H-5', ArH), 7.67 (d, *J* = 3.20 Hz, 1H, ArH), 7.70 (d, *J* = 7.80 Hz, 1H, ArH), 7.82-7.84 (m, 2H, ArH), 8.26-8.29 (dt, ^{2}J = 2.76 Hz, ^{3}J = 1.40 Hz, 1H, ArH), 8.31-8.34 (ddd, ^{2}J = 8.28 Hz, ^{3}J = 2.28 Hz, ^{4}J = 1.36 Hz, 1H, ArH), 8.68 (t, *J* = 2.06 Hz, 1H, ArH); ^{13}C NMR ($CDCl_3$, 100 MHz): δ 21.5 (CH_3), 30.1 (CH_2), 37.9 (NH$\underline{CH_2}$), 40.6 (N$\underline{CH_2}$), 48.0 (N$\underline{CH_2}$), 106.5, 110.5, 115.1, 120.2, 122.7, 123.1, 123.2, 123.8, 124.4, 126.5, 128.5, 129.1, 130.0, 131.5, 131.9, 132.3, 135.4, 135.7, 137.1, 138.2, 142.6, 142.8, 147.7, 148.2, 150.9 (ArC); MS (ESI): m/z 585.6 (M^{+}+1); Anal. Calcd for $C_{32}H_{28}N_{10}O_2$: C, 65.74; H, 4.83; N, 23.96. Found: C, 65.90; H, 4.77; N, 24.02.

Spectral data of 6-(4-ethylphenyl)-*N*-(3-(4-((2-(3-nitrophenyl)-1*H*-benzo[*d*]imidazol-1-yl)methyl)-1*H*-1,2,3-triazol-1-yl)propyl)imidazo[1,2-*a*]pyrazin-8-amine (35): light yellow

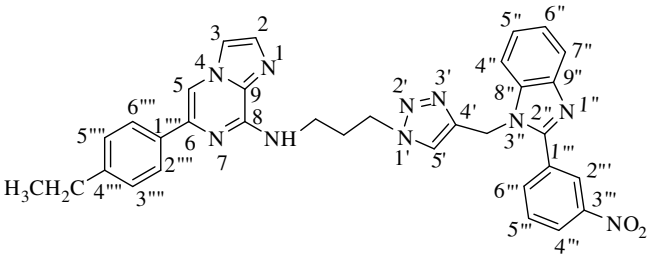

solid; yield: 62%; mp 104-106 ^{o}C; ^{1}H NMR ($CDCl_3$, 400 MHz): δ 1.20 (t, *J* = 7.56 Hz, 3H, CH_3), 2.38 (m, 2H, CH_2), 2.63 (q, *J* = 7.64 Hz, 1H, CH_2), 3.56 (q, *J* = 6.12 Hz, 2H, NH$\underline{CH_2}$), 4.50 (t, *J* = 6.64 Hz, 2H, N$\underline{CH_2}$), 5.38 (s, 2H, N$\underline{CH_2}$), 6.40 (t, *J* = 4.56 Hz, 1H, NH), 7.22 (d, *J* = 8.24 Hz, 2H, ArH), 7.28-7.34 (m, 2H, ArH), 7.43 (d, *J* = 7.32 Hz, 1H, ArH), 7.47 (s, 1H, ArH), 7.50 (s, 1H, ArH), 7.64 (s, 1H, ArH), 7.69 (t, *J* = 8.00 Hz, 1H, ArH), 7.76 (d, *J* = 8.24 Hz, 2H, ArH), 7.82 (d, *J* = 8.24 Hz, 2H, ArH), 8.28 (d, *J* = 7.80 Hz, 1H, ArH), 8.31-8.34 (dd, ^{2}J = 8.24 Hz, ^{3}J = 2.28 Hz, 1H, ArH), 8.67 (t, *J* = 1.84 Hz, 1H, ArH); ^{13}C NMR ($CDCl_3$, 100 MHz): δ 15.5 (CH_3), 28.5 (CH_2), 30.2 (CH_2), 37.2 (NH$\underline{CH_2}$), 40.7 (N$\underline{CH_2}$), 48.0 (N$\underline{CH_2}$), 106.1, 110.5, 115.1, 120.2, 122.7, 123.2, 123.8, 124.4, 125.9, 128.2, 130.0, 131.5, 131.9, 132.2, 134.5, 135.4, 135.7, 138.4, 142.6, 142.6, 142.8, 144.6, 147.7, 148.2, 150.9 (ArC); MS (ESI): m/z 599.6 (M^{+}+1); Anal. Calcd for

$C_{33}H_{30}N_{10}O_2$: C, 66.21; H, 5.05; N, 23.40. Found: C, 66.28; H, 4.92; N, 23.31.

Spectral data of 6-(4-methoxyphenyl)-*N*-(3-(4-((2-(3-nitrophenyl)-1*H*-benzo[*d*]imidazol-1-yl)methyl)-1*H*-1,2,3-triazol-1-yl)propyl)imidazo[1,2-*a*]pyrazin-8-amine (36): yellowish

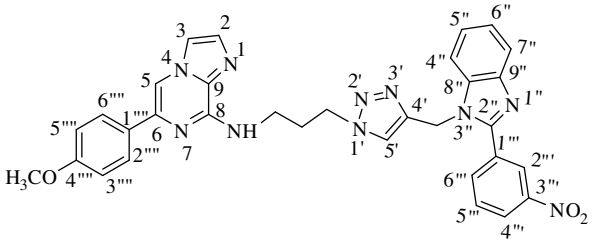

solid; yield: 81%; mp 111-113 ^{o}C; ^{1}H NMR ($CDCl_3$, 400 MHz): δ 2.39 (m, 2H, CH_2), 3.79-3.83 (m, 5H, NH$\underline{CH_2}$, OCH_3), 4.51 (t, *J* = 6.86 Hz, 2H, N$\underline{CH_2}$), 5.41 (s, 2H, N$\underline{CH_2}$), 6.52 (t, *J* = 5.96 Hz, 1H, NH), 6.93 (d, *J* = 9.16 Hz, 2H, ArH), 7.28-7.35 (m, 2H, ArH), 7.43-7.44 (m, 1H, ArH), 7.45 (d, *J* = 0.92 Hz, 1H, ArH), 7.49 (d, *J* = 0.92 Hz, 1H, ArH), 7.62 (s, 1H, ArH), 7.70 (t, *J* = 8.02 Hz, 1H, ArH), 7.76 (s, 1H, ArH), 7.78 (d, *J* = 8.72 Hz, 2H, ArH), 7.82-7.84 (dd, ^{2}J = 6.88 Hz, ^{3}J = 1.82 Hz, 1H, ArH), 8.26-8.28 (dt, ^{2}J = 1.36 Hz, ^{3}J = 0.44 Hz, 1H, ArH), 8.32-8.35 (ddd, ^{2}J = 8.12 Hz, ^{3}J = 2.40 Hz, ^{4}J = 0.92 Hz, 1H, ArH), 8.67 (t, *J* = 1.84 Hz, 1H, ArH); ^{13}C NMR ($CDCl_3$, 100 MHz): δ 30.1 (CH_2), 37.2 (NH$\underline{CH_2}$), 40.8 (N$\underline{CH_2}$), 48.1 (N$\underline{CH_2}$), 55.3 (OCH_3), 105.4, 110.5, 114.0, 115.0, 120.2, 122.6, 123.2, 123.8, 124.4, 124.5, 127.1, 129.6, 130.0, 131.5, 131.8, 132.1, 135.4, 135.8, 138.2, 142.7, 142.8, 147.6, 148.2, 150.9, 159.8 (ArC); MS (ESI): m/z 601.6 (M^{+}+1); Anal. Calcd for $C_{32}H_{28}N_{10}O_3$: C, 63.99; H, 4.70; N, 23.32. Found: C, 63.83; H, 4.77; N, 23.11.

Spectral data of 6-(2-methoxyphenyl)-*N*-(3-(4-((2-(3-nitrophenyl)-1*H*-benzo[*d*]imidazol-1-yl)methyl)-1*H*-1,2,3-triazol-1-yl)propyl)imidazo[1,2-*a*]pyrazin-8-amine (37): brownish

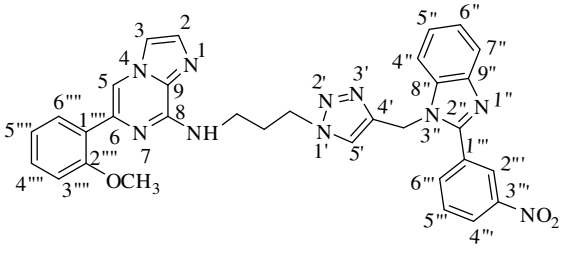

solid; yield: 83%; mp 138-140 ^{o}C; ^{1}H NMR ($CDCl_3$, 400 MHz): δ 2.35 (m, 2H, CH_2), 3.74 (q, *J* = 6.25 Hz, 2H, NH$\underline{CH_2}$), 3.90 (s, 3H, OCH_3), 4.49 (t, *J* = 6.64 Hz, 2H, N$\underline{CH_2}$), 5.33 (s, 2H, N$\underline{CH_2}$), 6.34 (t, *J* = 5.28 Hz, 1H, NH), 6.95 (d, *J* = 8.24 Hz, 1H, ArH), 7.03 (t, *J* = 7.56 Hz, 1H, ArH), 7.28-7.33 (m, 3H, ArH), 7.36 (d, *J* = 7.80 Hz, 1H, ArH), 7.48 (s, 1H, ArH), 7.53 (s, 1H, ArH), 7.69 (t, *J* = 8.02 Hz, 2H, ArH), 7.82 (d, *J* = 7.80 Hz, 1H, ArH), 8.03-8.06 (dd, ^{2}J = 7.32 Hz, ^{3}J = 1.60 Hz, 1H, ArH), 8.28 (s, 1H, ArH), 8.29-8.34 (m, 2H, ArH), 8.72 (t, *J* = 1.60 Hz, 1H, ArH); ^{13}C NMR ($CDCl_3$, 100 MHz): δ 30.3 (CH_2), 37.1 (NH$\underline{CH_2}$), 40.6 (N$\underline{CH_2}$), 47.9 (N$\underline{CH_2}$), 55.5 (OCH_3), 110.4, 111.1, 111.2, 115.2, 120.2, 120.8, 122.9, 123.1, 123.7, 124.4, 124.5, 125.6, 129.1, 129.9, 130.4, 131.5, 131.9, 132.2, 134.3, 135.4, 135.7, 142.5, 142.8, 147.4, 148.2, 150.9, 156.7 (ArC); MS (ESI): m/z 601.6 (M^{+}+1);

Anal. Calcd for $C_{32}H_{28}N_{10}O_3$: C, 63.99; H, 4.70; N, 23.32. Found: C, 64.10; H, 4.59; N, 23.22.

Spectral data of 4-(8-(3-(4-((2-(3-nitrophenyl)-1*H*-benzo[*d*]imidazol-1-yl)methyl)-1*H*-1,2,3-triazol-1-yl)propylamino)imidazo[1,2-*a*]pyrazin-6-yl)benzaldehyde (38): light orange

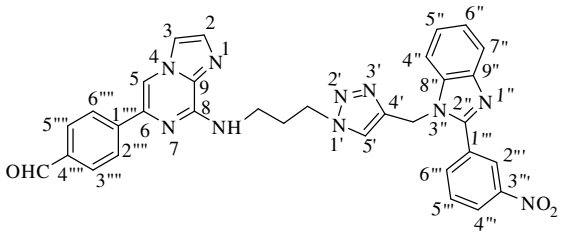

yield: 80%; mp 122-124 ^oC; ^1H NMR ($CDCl_3$, 400 MHz): δ 2.42 (m, 2H, CH_2), 3.79 (q, *J* = 6.27 Hz, 2H, NH$\underline{CH_2}$), 4.54 (t, *J* = 6.88 Hz, 2H, N$\underline{CH_2}$), 5.46 (s, 2H, N$\underline{CH_2}$), 6.51 (t, *J* = 5.96 Hz, 1H, NH), 7.31-7.34 (m, 2H, ArH), 7.48 (d, *J* = 1.36 Hz, 1H, ArH), 7.50 (d, *J* = 1.84 Hz, 1H, ArH), 7.53 (d, *J* = 0.92 Hz, 1H, ArH), 7.57 (s, 1H, ArH), 7.70 (t, *J* = 8.0 Hz, 1H, ArH), 7.83-7.85 (dd, ^2J = 6.40 Hz, ^3J = 2.08 Hz, 1H, ArH), 7.90 (d, *J* = 8.72 Hz, 2H, ArH), 7.95 (s, 1H, ArH), 8.03 (d, *J* = 8.24 Hz, 2H, ArH), 8.24-8.26 (dt, ^2J = 2.72 Hz, ^3J = 1.84 Hz, 1H, ArH), 8.32-8.34 (ddd, ^2J = 8.24 Hz, ^3J = 2.32 Hz, ^4J = 0.92 Hz, 1H, ArH), 8.63 (t, *J* = 2.06 Hz, 1H, ArH), 10.02 (s, 1H, CHO); ^{13}C NMR ($CDCl_3$, 100 MHz): δ 29.9 (CH_2), 37.5 (NH$\underline{CH_2}$), 40.8 (N$\underline{CH_2}$), 48.2 (N$\underline{CH_2}$), 107.9, 110.5, 115.4, 122.2, 122.3, 123.3, 123.9, 124.3, 124.5, 126.2, 130.0, 130.1, 131.5, 132.3, 132.4, 135.4, 135.8, 136.8, 142.8, 142.9, 142.9, 147.8, 148.1, 150.9 (ArC), 191.7 (CHO); MS (ESI): m/z 599.6 (M^++1); Anal. Calcd for $C_{32}H_{26}N_{10}O_3$: C, 64.21; H, 4.38; N, 23.40. Found: C, 64.43; H, 4.45; N, 23.45.

CHAPTER-5

PHOTOPHYSICAL AND DNA INTERACTION STUDIES OF NAPHTHALIMIDE DERIVATIVES

5.1. INTRODUCTION

The past decade has seen an ever increasing effort towards the development of small-molecular fluorescence probes for environmental and biological analyses, due to their simple design, synthesis and manipulation. There is need for a diverse set of probes capable of their fluorescence signal "turned on" in the presence of analytes in complex environments, so as to allow for analyte detection, imaging and quantification.[153] Diversity is required for both the mechanism of analyte activation of the probe to reveal its corresponding highly fluorescent reporter,[154] and the energy range over which the reporter provides a signal of analyte presence. However, some general issues remain for the majority of such probes like poor solubility and thus compromised sensitivity in a full aqueous environment due to the hydrophobicity of the fluorescence dyes and their cytotoxicity, inducing apoptosis or necrosis of cells.[155]

1,8-Naphthalimide derivatives[156] are dyes extensively employed in fluorogenic labeling and fluorescent chemosensors because of their high absorption coefficient, high fluorescence quantum yield and high photostability.[157] By virtue of these fascinating properties, the excellent examples of 1,8-naphthalimide-based fluorescent chemosensor applications in cell imaging have also been reported.[156-158] Amongst the metal ions, occurrence of aluminium in the earth crust is wide spread.[159] It find its application day to day life viz., aluminium foil, utensils, food and pharmaceuticals. Over dosage of aluminium in body resulted in various brain related disorders and cancer.[160-161] Amongst the anions, fluoride ion is an important anion having beneficial effects on dental health care and treatment of osteoporosis.[162] However, the acute dosage of fluoride ion resulted in severe side effects like thyroid activity and depression.[163] Therefore, to develop the fluoride based chemosensor, various analytical and spectroscopic techniques have been known.[164-165]

5.2. OBJECTIVE

In the present work, we have designed a new fluorescent probe based upon 1,8-naphthalimide moiety (tunable electronic system, good stability, and cell-permeable ability) and using

propylamine as a recognition moiety. We chose the skeleton of 1,8-naphthalimide because its derivatives usually produce a fluorescence response at longer wavelength,[166] which is beneficial for avoiding the influence of several variants, such as probe concentration and optical path length.[167] The detection mechanism is based on amine oxidation and β-elimination (*via* Schiff base hydrolysis)[168] to release the fluorophore (4-amino-*N*-propyl-1,8-naphthalimide) emission. The naphthalimide moiety is also useful for DNA intercalator as an anticancer agent. So, the synthesized moiety has also been used for interaction studies with calf thymus DNA.

5.3. CHEMISTRY

Probes **6** and **7** were synthesized in several steps as outlined in Scheme 1. Nitration of acenaphthene **1** with nitric acid in the presence of acetic acid gave 1,2-dihydro-5-nitroacenaphthylene **2** in 90% yield followed by oxidation in the presence of sodium dichromate and acetic acid to give 6-nitrobenzo[*de*]isochromene-1,3-dione **3** in 85% yield**.** Subsequent reaction with allyl amine in refluxing ethanol gave allylated nitro naphthalimide, 2-allyl-6-nitro-

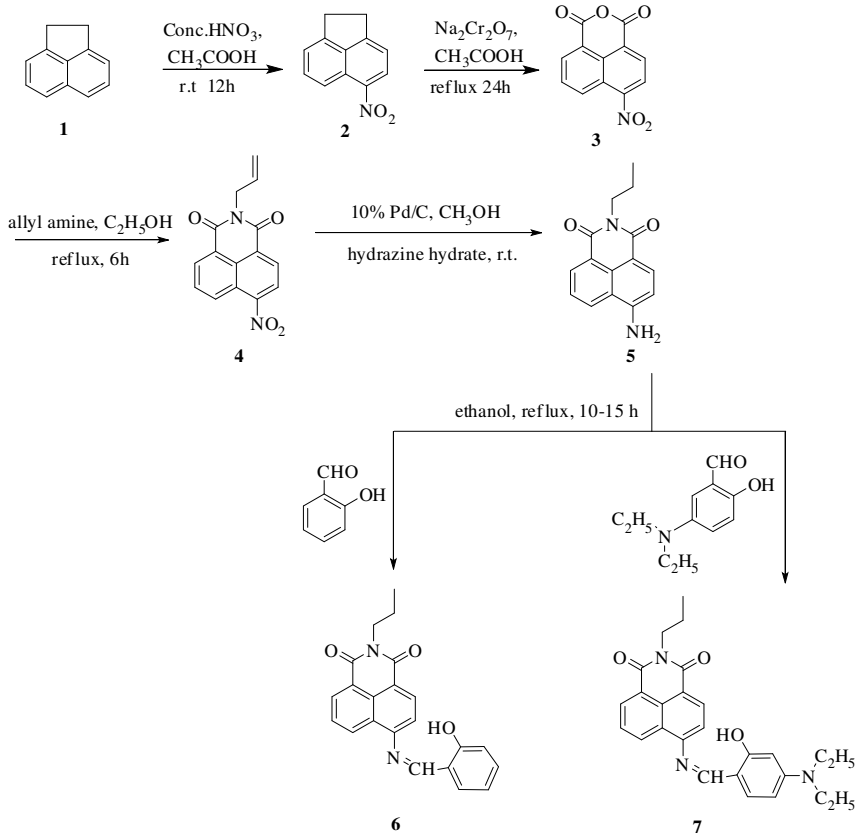

Scheme 1 Synthesis of naphthalimide schiff bases **6** and **7**

1*H*-benzo[*de*]isoquinoline-1,3(2*H*)-dione **4** in 90% yield. Reduction of **4** with palladium carbon in presence of catalytic amount of hydrazine hydrate in methanol gave reduced product, 6-amino-2-propyl-1*H*-benzo[*de*]isoquinoline-1,3(2*H*)-dione **5** in 78% yield. Final treatment of intermediate **5** with different aldehydes *viz.,* salicylaldehyde and 4-diethylaminosalicaldehyde in ethanol at room temperature for 10-15 h afforded corresponding Schiff base analogues **6** and **7** in 90% and 95% yields, respectively. Probes **6** and **7,** and intermediates were well characterized by ^{1}H and ^{13}C NMR as well as mass spectrometry (Scheme 1).

5.4. PHOTOPHYSICAL PROPERTIES OF PROBE 6

5.4.1. Photophysical properties towards metal ions

Absorption spectra of probe **6** (20 µM, CH_3OH) showed an absorption band centred at 380 nm. On addition of 1000 µM of different metal ions viz., Na^+, K^+, Ca^{2+}, Mg^{2+}, Li^+, Ba^{2+}, Co^{2+}, Ni^{2+}, Zn^{2+}, Hg^{2+}, Ag^+, Pb^{2+} and Al^{3+} as their perchlorate salts, a significant change in UV-visible spectra was observed with Al^{3+} ions while Hg^{2+} ions showed the sillier results albeit to the lesser extent (Figure 1a). Upon incremental addition of Al^{3+} to probe **6** (20 µM, CH_3OH), the absorption band at 380 nm underwent a gradual decrease in absorption intensity with concomitant appearance of new absorption band at 430 nm and an isobestic point at 415 nm (Figure 1b). A detectable colour change from pale yellow to bright yellow has also been observed (Figure 2a,b). Thus, probe **6** was used for ratiometric determination of Al^{3+} between 10 nM-6 µM with lowest detection limit of 10 nM. The association constant for binding of probe **6** with Al^{3+} was determined to be 4.4×10^5 M^{-1} through Benesi–Hildebrand equation. Interference

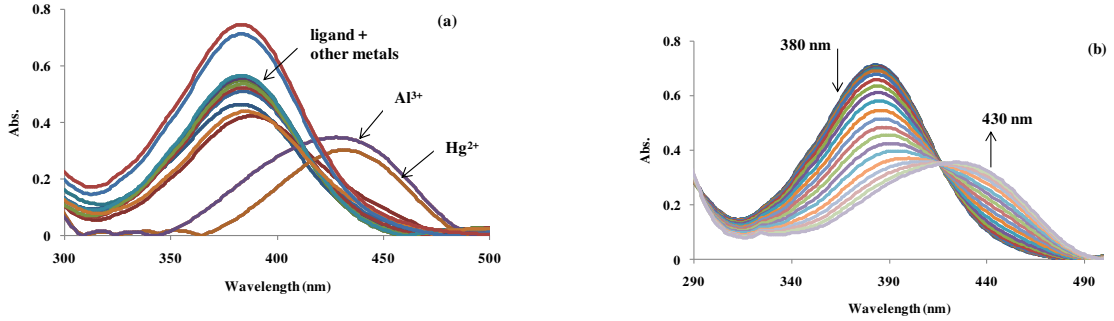

Figure 1: Absorption spectra of probe 6 (20 µM, CH_3OH) upon addition of (a) different metal ions and (b) increasing concentration of Al^{3+} ions

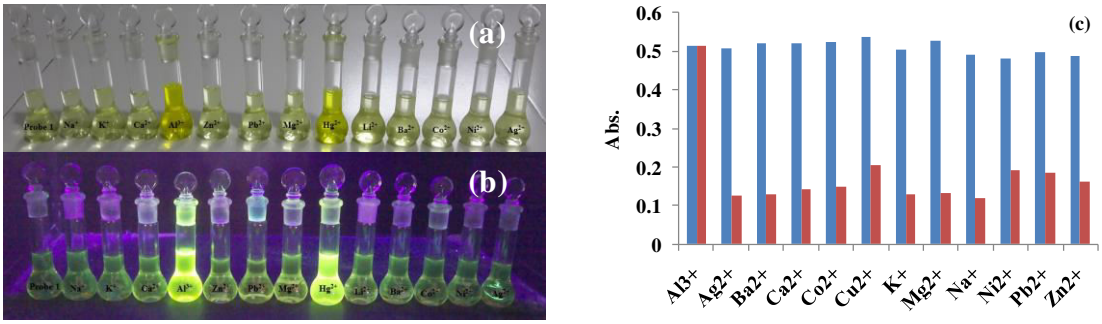

Figure 2: Colour changes; (a) visible and (b) under irradiation at 350 nm of probe **6** upon addition of various metal ions; (c) Red bars represent the selectivity of probe **6** upon addition of different metal ions in CH_3OH and the blue bars show the competitive selectivity of probe **6** in the presence of interfering metal ions (Al^{3+}).

studies of probe **6** were performed in the presence of 1 equiv. of Al^{3+} ions mixed with 1000 μM of other metal ions that showed no significant change in absorption spectrum with or without metal ions (Figure 2c).

Probe **6** (1 μM, CH_3OH, Φ = 0.16) upon excitation at 380 nm showed emission band at 530 nm. After addition of 5.0 equiv of metal ions such as Na^+, K^+, Ca^{2+}, Mg^{2+}, Li^+, Ba^{2+}, Co^{2+}, Ni^{2+}, Zn^{2+}, Hg^{2+}, Ag^+, Pb^{2+} and Al^{3+} under the established conditions. However, discernible changes in both emission color and spectral occurred only in the presence of Al^{3+} ions. Gratifyingly, other metal ions showed little or no interference to probe **6** (Figure 3a). Gradual addition of Al^{3+} to probe **6** showed abrupt fluorescent enhancement at 580 nm (Figure 3b). The quantum efficiency was enhanced from Φ = 0.16 (free probe) to Φ = 0.42 (probe **6**.Al^{3+}). However, no change was observed with other metal ions. Binding constant of probe **6** with Al^{3+} was found to be 6.89×10^6 M^{-1}. Lowest detection limit has been found to be 0.5 nM and probe **6** was able to detect 0.5 nM to 0.7 μM of Al^{3+}.

To further examine the sensing and selective ability of probe **6** toward Al^{3+}, competitive metal ion experiments were carried out. The sensing behaviour for Al^{3+} was hardly disturbed by the presence of other metal ions.

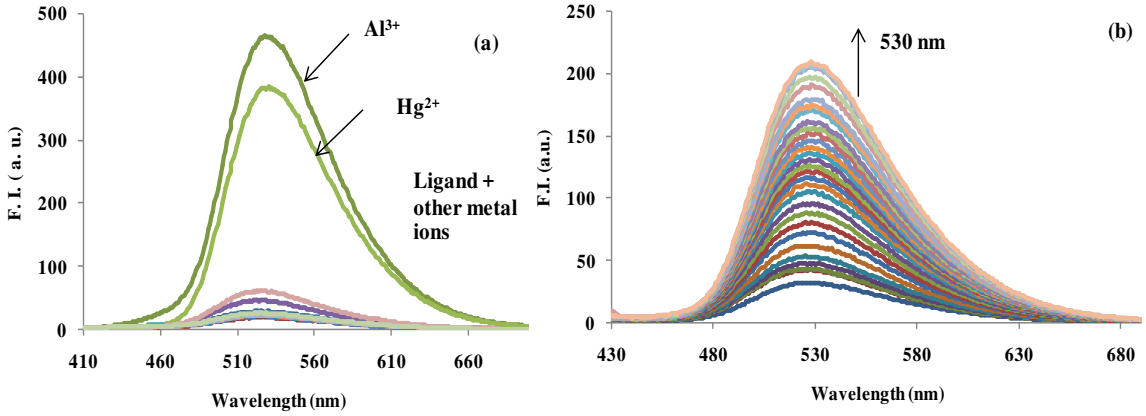

Figure 3: Emission spectra of probe **6** (1 μM, CH_3OH) upon addition of (a) different metal ions and (b) increasing concentration of Al^{3+} ions.

5.4.2. Photophysical properties towards anions

The sensing behaviour of probe **6** towards anions was determined using tetrabutylammonium salts of various anions viz., F^-, Cl^-, Br^-, I^-, AcO^-, NO_3^-, $H_2PO_4^-$, $HP_2O_7^-$, HSO_4^-, CN^-, SCN^- in CH_3OH. On addition of 50 equiv. of anions to probe **6** (20 μM, CH_3OH), no significant change in absorption spectrum was observed except the HSO_4^- (Figure 4a). Incremental addition of HSO_4^- ions to probe **6** resulted in decrease in absorption intensity at 380 nm with concomitant appearance of new absorption band at 430 nm with clear isobestic point at 420 nm (Figure 4b). The association constant on binding of **6** with HSO_4^- ions was found to be 5.2×10^4 M^{-1} having lowest detection limit of 2 μM. Ratiometric response on incremental addition of HSO_4^- ions showed the detection limit between 2 μM-180 μM and showed the 12-fold ratio change. Selectivity of probe **6** for HSO_4^- ions was confirmed by carrying out the competitive anion

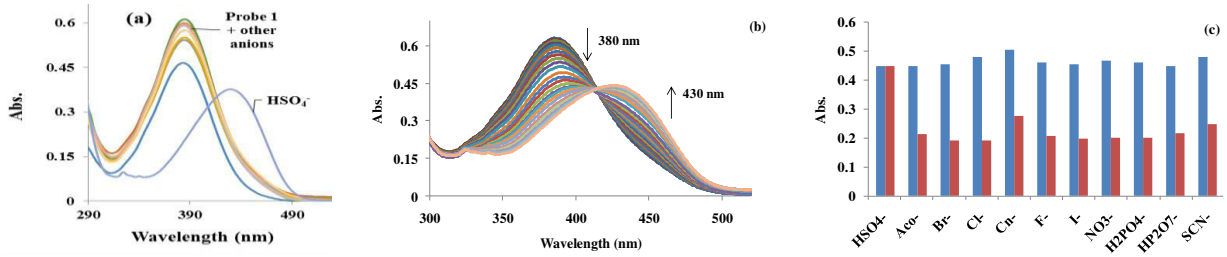

Figure 4: Absorption spectra of probe **6** (20 μM, CH_3OH) upon addition of (a) various anions and (b) increasing concentration of HSO_4^- ions; (c) Red bars represent the selectivity of probe **6** upon addition of different anions in CH_3OH and the blue bars show the competitive selectivity of probe **6** in the presence of interfering anions.

experiments. Therefore, addition of 10 equiv. of HSO_4^- ions to probe **1** mixed with various anions showed no significant change in absorption in the presence or absence of other anions (Figure 4c).

In case of addition of various anions to probe **6** (1 μM, CH_3OH), emission changes were observed only in the presence of HSO_4^- ions (Figure 5a). Gradual addition of HSO_4^- ions to probe **6** resulted in abrupt enhancement in fluorescence intensity at 530 nm and quantum efficiency was enhanced from $\Phi = 0.16$ (free probe) to $\Phi = 0.32$ (Figure 5b). Binding constant of probe **6** with HSO_4^- has been found to be 5.63×10^4 M^{-1} with lowest detection limit of 0.05 μM. On increasing the concentration of HSO_4^- ions from 0.05 μM to 40 μM, increase in fluorescent intensity was observed.

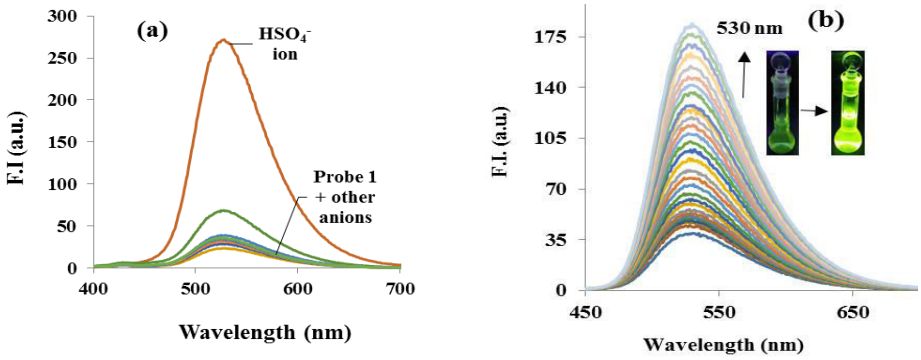

Figure 5: Emission spectra of probe **6** (1 μM, CH_3OH) upon addition of (a) different anions and (b) increasing concentration of HSO_4^- ions.

In order to understand the mode of interaction of probe **6** with Al^{3+} and HSO_4^-, ^1H NMR titrations were conducted in the presence of Al^{3+} and HSO_4^-. As shown in Figure 6, singlet at 8.9 ppm attributed to imine proton (-CH=N) of probe **6** disappeared on addition of 1.0 equiv. of Al^{3+} ions and a new singlet appeared at 9.9 ppm corresponding to CHO proton.

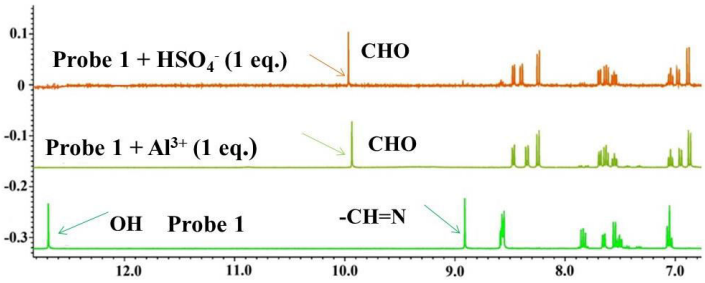

Figure 6 NMR titrations of probe **6** on addition of Al^{3+} and HSO_4^-

Similar changes in NMR signals were observed in the presence of HSO_4^- ions. NMR changes observed in the presence of Al^{3+} and HSO_4^-, indicated that a free amino compound **5** was generated by the Al^{3+}/HSO_4^- -triggered cleavage reaction (**Figure 6**). Owing to the specific reactivity of the Al^{3+}/HSO_4^- -catalyzed chemical reaction, probe **6** displayed a high sensitivity and selectivity toward these ions. A feasible mechanism of the cleavage reaction is shown in Scheme 2.

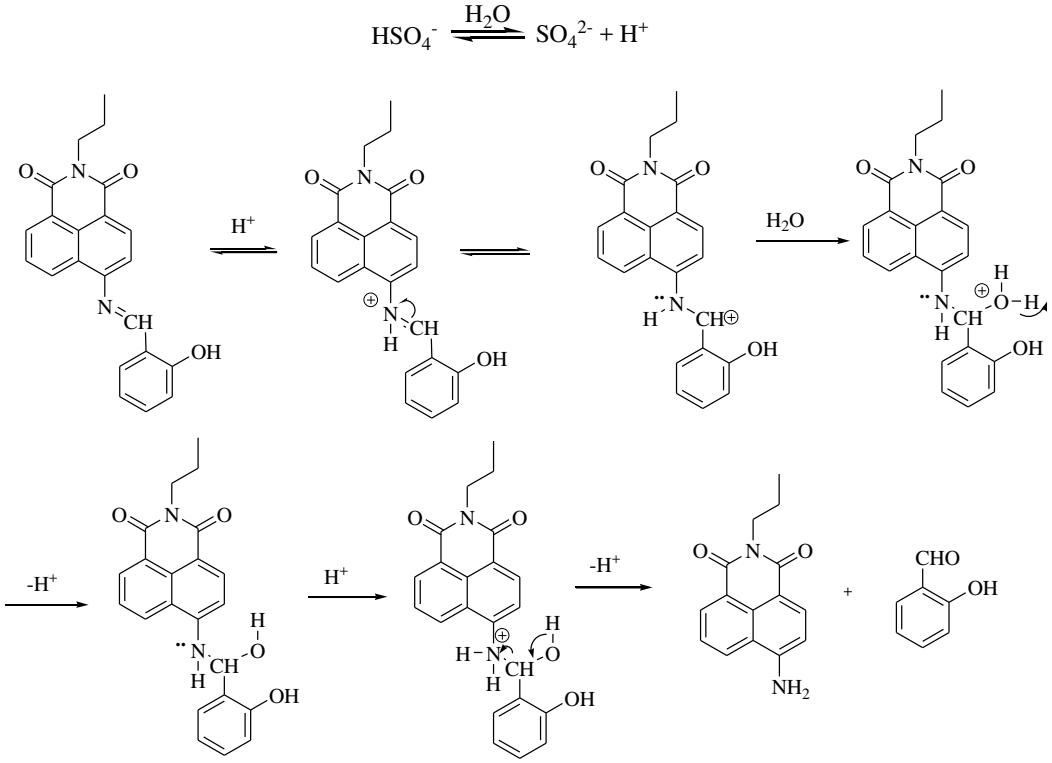

Scheme 2 Proposed mechanism of probe **6** binding with HSO_4^-

5.5. DNA binding studies

Gunnlaugsson *et. al.* reported several examples of DNA targeting binders, based on the use of 1,8-naphthalimide derivatives.[169-173] Such structures have tuneable electronic properties, and have been shown to exhibit good DNA binding affinity either through intercalation or groove binding. 4-Amino-1,8-naphthalimide derived Troger's base which possessed good water solubility at physiological *p*H and their two cationic amino terminus provided the strong electrostatic interaction/binding at the phosphate backbone of DNA.[170]

Thus, we envisaged that the naphthalimide moiety of probe **6** might significantly interact with the aromatic bases in DNA via intercalative stacking/H-bonding and/or electrostatic interaction.

Therefore, interaction studies of probe **6** with Ct-DNA were performed by spectroscopic means in aqueous phosphate buffer solution at *p*H 7.0. Thus, the absorption maxima of probe **6**, showed a negligible effect on the change in wavelength position and intensity on gradual addition of Ct-DNA.

Fluorescence titration experiment was also carried out with probe **6**. Thus, upon gradual addition of Ct-DNA, the emission intensity (λ_{em} = 530 nm) of the probe **6** was found to be significantly enhanced. The emission became saturated at 30 µM concentration of Ct-DNA (Figure 7a). This observation clearly indicated a well-defined binding of the probe **6** with Ct-DNA. The association constant of probe **6** with Ct-DNA was also determined by a Benesi-Hildebrand plot which was found to be 6.98 $\times 10^5$ M^{-1} towards the higher end as compared to amonafide (a well known DNA intercalative drug).

In order to prove the reversibility of probe **6** with DNA, an experiment was performed in the presence of competitive ethidium bromide (standard DNA intercalator). On addition of 0-20 µM solution of ethidium bromide to DNA.probe **6** complex, emission band at 530 nm quenched and new emission band formed at 630 nm due to the formation of EtBr-DNA complex (Figure 7b), confirmed the reversible binding of probe **6** to Ct-DNA through intercalation. The emission spectra of ethidium bromide bound to Ct-DNA in absence and presence of each complex have been recorded at [EtBr] = 10 µM, [DNA] = 10 µM. The emission intensities of EtBr bound to Ct-DNA at 630 nm enhanced with appearance of emission at 530 nm indicated that probe **6** cannot effectively displace EtBr from EtBr.DNA complex. It is generally agreed that strong emission enhancement accompanies intercalation of dye into double helix conformation of nucleic acids (Figure 7c).

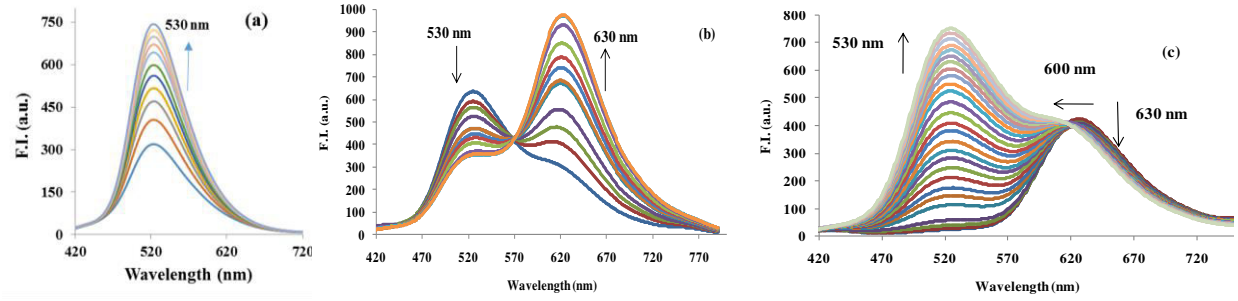

Figure 7: Effect of incremental addition of (a) Ct-DNA (4-70 µM) on emission spectra of probe **6** (20 µM, phosphate buffer, pH 7.0); (b) probe **6** on DNA.EtBr complex in phosphate buffer; (c) effect of incremental addition of probe **6** on EtBr:DNA complex

5.6. PHOTOPHYSICAL PROPERTIES OF PROBE 7

5.6.1. Photophysical properties towards metal ions

To examine the binding of probe **7** with metal ions, the UV-visible and emission studies of sensor **7** towards various metal ions viz., Ag^{2+}, Al^{3+}, Mg^{2+}, Ba^{2+}, Hg^{2+}, Pb^{2+}, Ni^{2+}, Zn^{2+}, Cu^{2+}, Ca^{2+}, Co^{2+}, K^{+} and Na^{+} were carried out in CH_3CN (Figure 8a). Binding of **7** with Al^{3+} as its perchlorate salt was examined by UV-visible spectroscopy. Probe **7** (20 µM, CH_3CN) showed two absorption bands at 340 nm and 460 nm. Addition of 50 eq. of Al^{3+} to probe **7** showed visible colour change from orange to yellow (Figure 9a,b) along with decrease in absorbance peak at 340 nm and enhancement at 460 nm. Whereas, addition of other metal ions did not show any significant change in absorption spectra. Therefore, UV-visible titration of **7** with Al^{3+} was carried out. Incremental addition of Al^{3+} (10-100 µM) to **7** in CH_3CN showed the decrease in absorption intensity at 340 nm with the simultaneous increase in absorption peak at 460 nm (Figure 8b). UV-visible response of ratiometric probe **7** with increasing concentrations of Al^{3+} (10-100 µM) was examined. From UV-visible studies, the association constants for probe-Al^{3+} in acetonitrile was determined by Benesi–Hildebrand equation and was found to be 4.72 $\times 10^3$ M^{-1} having lowest detection limit of 10 µM.

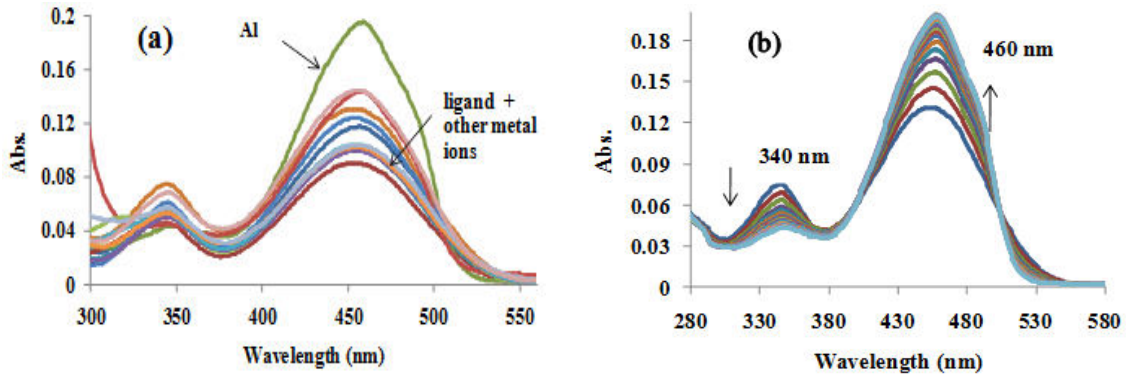

Figure 8: (a) Absorption spectra on addition of 50 eq. of different metal ions to probe **7** (20 µM, CH_3CN); (b) Changes in absorption spectra on addition of Al^{3+} (10-100 µM) to 20 µM of **7** in CH_3CN

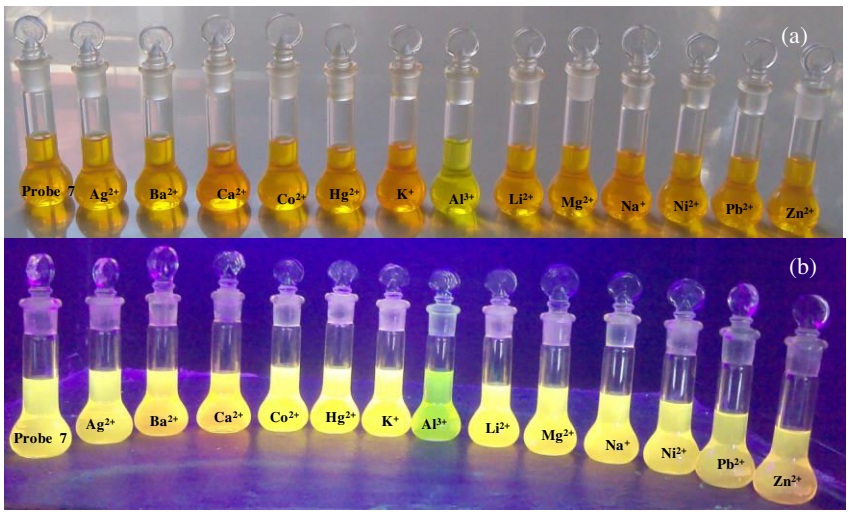

Figure 9: (a) Colour changes observed by naked eye on addition of 50 eq. of metal ions to probe **7** (20 µM); (b) Colour changes observed under UV lamp on addition of 50 eq. of metal ions to probe **7** (20 µM)

UV-visible spectroscopy is complementary part of fluorescence spectroscopy. Therefore, to interpret the more précised results, the recognition behaviour of naphthalimide based sensor on various metal ions was investigated by fluorescence studies. Probe **7** (20 µM) showed dual emission band, weak emission at 520 nm and strong emission at 610 nm when excited at 460 nm. On addition of 50 eq. of different metal ions viz., Ag^{2+}, Mg^{2+}, Ba^{2+}, Hg^{2+}, Pb^{2+}, Ni^{2+}, Zn^{2+}, Cu^{2+}, Ca^{2+}, Co^{2+}, K^{+} and Na^{+} to probe **7**, no significant change in fluorescence spectrum of different metal ligand complexes was observed. However, change was observed on addition of 50 eq. of Al^{3+} ions (Figure 10a). So, to investigate the sensing behaviour of **7** towards Al^{3+}, titration of **7** with increasing concentrations of Al^{3+} was performed. Incremental addition of Al^{3+} (1-25 µM) to probe **7**, resulted in decrease in fluorescence intensity at 610 nm with simultaneous increase in intensity at 520 nm (Figure 10b). This enhancement in fluorescence intensity at 520 nm is due to interaction of Al^{3+} ion with nitrogen and hydroxyl groups. Probe **7** showed the ratiometric change on addition of increasing concentrations of Al^{3+}. Job plot showed the 1:1 stoichiometric complex of probe **7** with Al^{3+} (Figure 10c). The selectivity of probe (20 µM) for Al^{3+} over different metal ions was investigated. Addition of 100 eq. of different metal ions; Ag^{2+}, Mg^{2+}, Ba^{2+}, Hg^{2+}, Pb^{2+}, Ni^{2+}, Zn^{2+}, Cu^{2+}, Ca^{2+}, Co^{2+}, K^{+} and Na^{+} to probe **7** showed no significant change in fluorescence intensity on comparison with other metal ions. So, practical applicability of ligand was determined by carrying out competitive experiments in the presence of 10 eq. of

Al^{3+} and 50 eq. of other metal ions, which showed no significant variation in fluorescence intensity on comparison of results with other metal ions (Figure 10d). From the emission studies, the association constant for **7**-Al^{3+} in acetonitrile has been determined by Benesi–Hildebrand equation and was found to be 8.90 $\times 10^4$ M^{-1}. The lowest detection limit was found to be 1 µM.

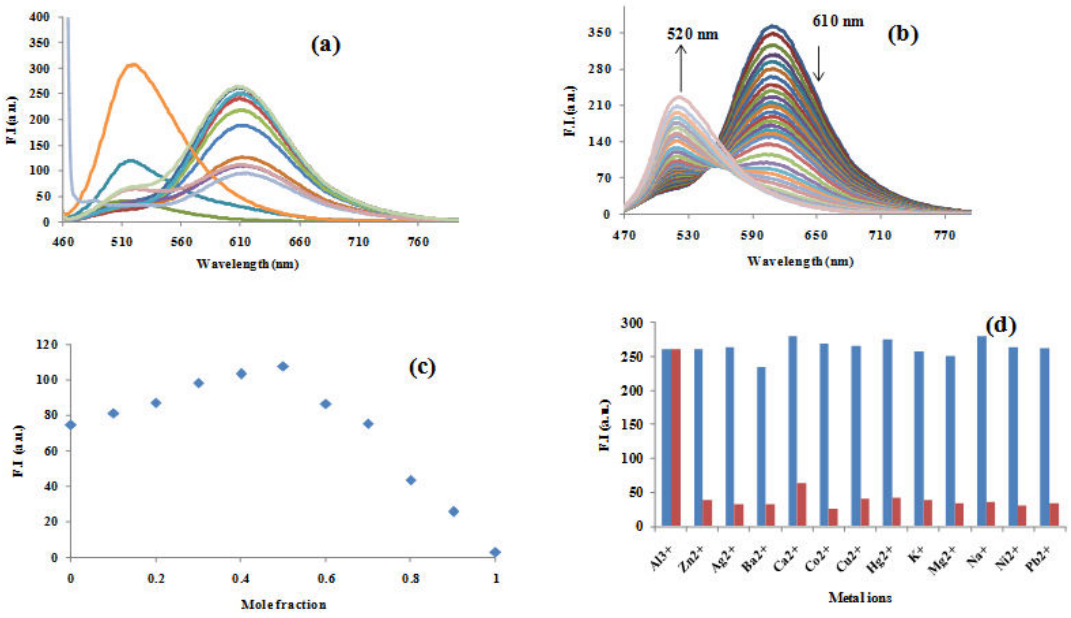

Figure 10: (a) Emission spectra on addition of 50 eq. of different metal ions to probe **7** (20 µM, CH_3CN); (b) Changes in emission spectra on addition of Al^{3+} (1-25 µM) to 20 µM of **7** in CH_3CN; (c) Jobs plot showing 1:1 stoichometric complex of probe **7** with Al^{3+} (20 µM, CH_3CN); (d) Red bars represent selectivity of probe (20 µM) upon addition of different metal ions in CH_3CN and blue bars shows the competitive selectivity of probe in the presence of interfering metal ions.

5.6.2. Photophysical properties towards anions

Upon addition of 50 eq. of tetrabutylammonium salts of various anions viz., F^-, Cl^-, Br^-, I^-, AcO^-, NO_3^-, $H_2PO_4^-$, $HP_2O_7^-$, HSO_4^-, CN^-, SCN^- to probe **7** (20 µM, CH_3CN) in acetonitrile, except F^- ion, no significant change was observed with other ions (Figure 11a). UV-visible spectra of probe **7** showed two absorption bands at 340 nm and 460 nm. On incremental addition of F^- ion (0.5-12.5 µM), the absorption band at 460 nm quenched followed by red shift of band at 395 nm from 340 nm with concomitant appearance of new band at 570 nm (Figure 11b). The interaction of fluoride with probe **7** showed hydrogen bonding interactions followed by deprotonation. The quenching followed by red shift and formation of new band prompted us to determine the F^- ion

ratiometrically. Selectivity of probe **7** as F^- selective chemosensor was confirmed by competitive experiments with 50 eq. of F^- and 50 eq. of other anions. Addition of various competing ions to probe **7** complexed with F^- ion did not affect the absorption spectra. Therefore it can be inferred as F^- selective chemosensor (Figure 11c). The association constant for binding of F^- ion with probe **7** was 1.14×10^3 M^{-1}. The lowest detection limit was 0.5 µM. Visible colour change from orange to purple was observed on addition of 50 eq. F^- ion to 20 µM of **7** (Figure 11d).

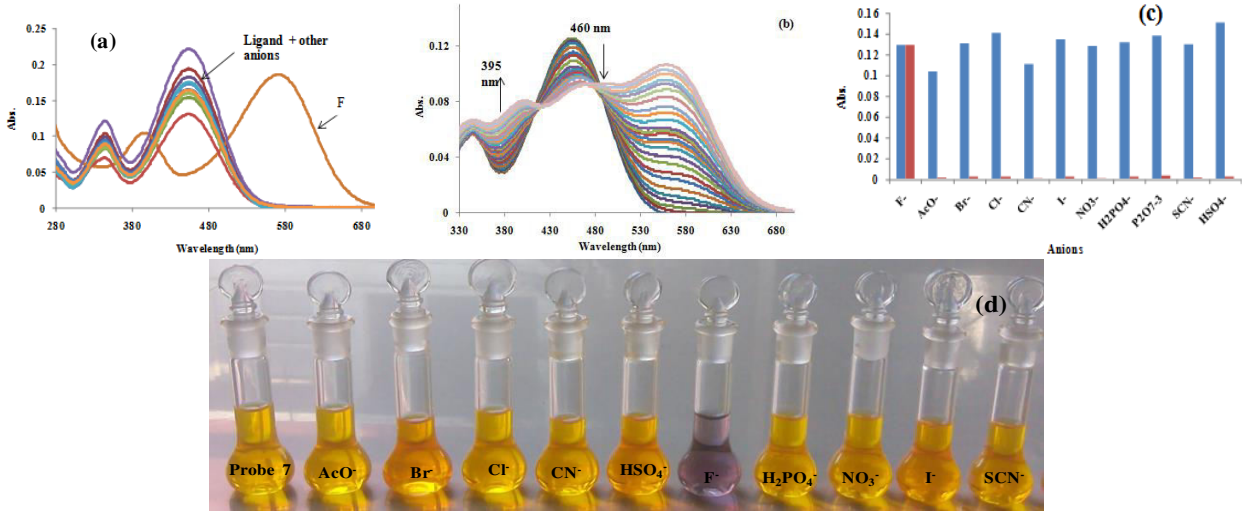

Figure 11: (a) Absorption spectra on addition of 50 eq. of different anions to probe **7** (20 µM, CH_3CN); (b) Changes in absorption spectra on addition of F^- (0.5-12.5 µM) to 20 µM of **7** in CH_3CN; (c) Red bars represent selectivity of probe (20 µM) upon addition of different anions in CH_3CN and blue bars shows the competitive selectivity of probe in the presence of interfering anions; (d) Color changes observed by naked eye on addition of 50 eq. of anions to probe **7** (20 µM).

Further, the effect of various anions on emission spectra of probe **7** was studied. When excited at 450 nm, probe **7** (20 µM, CH_3CN) showed the dual emission bands at 520 nm and 610 nm. Addition of 50 eq. of tetrabutyl ammonium salts of various anions viz., F^-, Cl^-, Br^-, I^-, AcO^-, NO_3^-, $H_2PO_4^-$, $HP_2O_7^-$, HSO_4^-, CN^-, SCN^-, only F- ion showed significant change with probe (Figure 12a). Incremental addition of 1-19 µM of F^- ion to probe **7**, a decrease in emission band at 520 nm and 610 nm was observed (Figure 12b). Ratiometric determination of F^- ion by fluorescence spectroscopy showed the continuous decrease in emission intensity at 610 nm on increasing the equivalents from 1 to 19 µM. The binding constant was found to be 4.4×10^3 M^{-1}. Lowest detection limit was 1 µM.

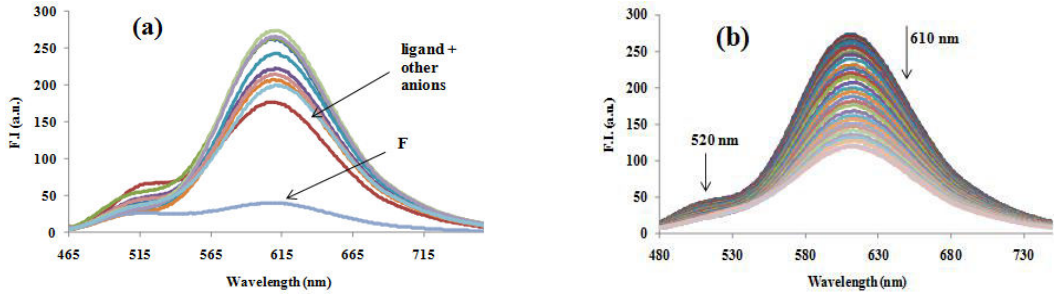

Figure 12: (a) Emission spectra on addition of 50 eq. of different anions to probe **7** (20 µM, CH_3CN); (b) Changes in emission spectra on addition of F^- (1-19 µM) to 20 µM of **7** in CH_3CN

Detailed complexation of probe **7** with Al^{3+} was studied through ^1H NMR titrations on addition of different concentrations of Al^{3+} ions in $CDCl_3$ + CD_3CN. Consecutive additions of Al^{3+} to probe **7** induced significant changes in ^1H NMR spectra. Addition of 0.5 eq. of Al^{3+} ions to probe **7**, resulted in shifting of imine protons at 8.66 ppm of schiff base along with merging with other aromatic protons. Aromatic protons in region 6.16-6.34 ppm showed the downfield shift of 0.08 ppm and the aromatic protons at 7.40 ppm became merged with $CHCl_3$ peak. The major downfield shift was 0.5 ppm of aromatic proton at 7.30 ppm to 7.80 ppm. Further addition of 1.0 and 1.5 eq. of Al^{3+} does not cause an appreciable shift in position of signals suggesting the formation of 1:1 complex between the probe **7** and Al^{3+} (Figure 13a). Interactions between the probe **7** and F^- ion were studied through ^1H NMR titrations. Addition of 0.5 to 1.0 eq. of F^- ion to probe **7** showed broadening of OH peak suggesting the hydrogen bonding interactions. Addition of 1.5 eq. of F^- ion resulted in disappearance of OH signal without any change in aromatic signals. No spectral changes were observed on further increase in concentration (Figure 13b).

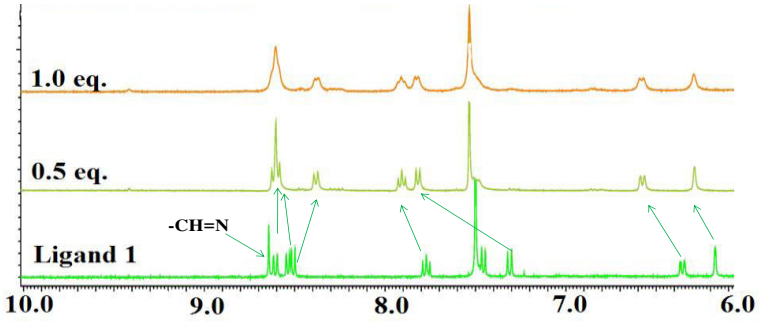

Figure 13a ^1H NMR titration spectra of probe **7** with increasing conc. (0.5-1.0 eq.) of Al^{3+}

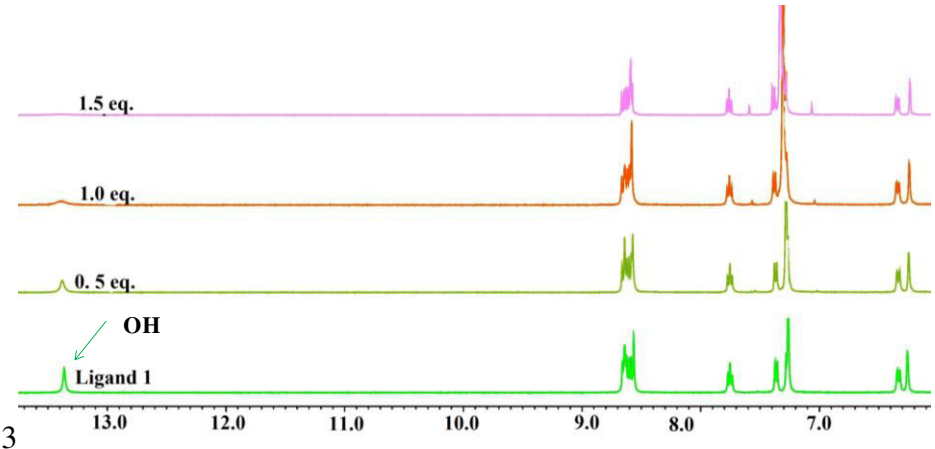

33

Figure 13b ^{1}H NMR titration spectra of probe **7** with increasing conc. (0.5-1.5 eq.) of F^-

5.7. DNA BINDING STUDIES

Interactions of probe **7**.Al^{3+} complex with ct-DNA were determined through UV-visible and fluorescence emission studies. Addition of ct-DNA (10-50 µM) to probe **7**.Al^{3+} complex, showed increase in absorption intensity at 340 nm and 460 nm (Figure 14a). The emission intensity

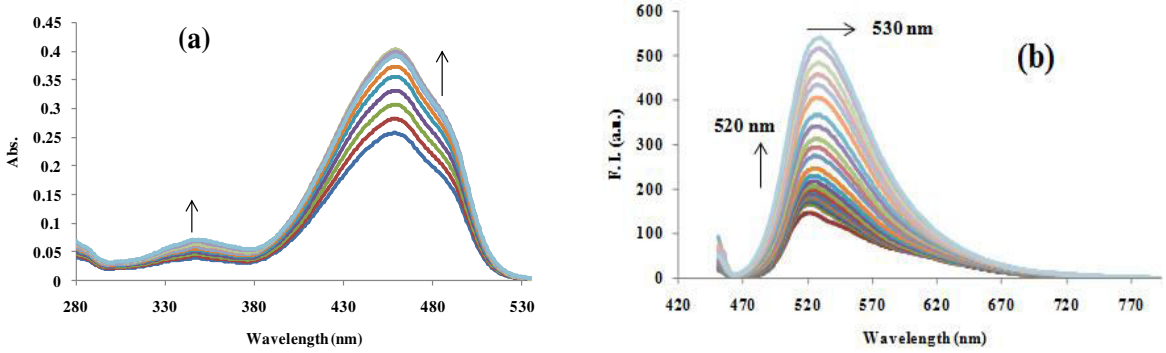

Figure 14: (a) Effect of incremental addition of ct-DNA (10-50 µM) to probe **7.**Al^{3+} complex on absorption spectra; (b) Effect of incremental addition of ct-DNA (4-30 µM) to probe **7.**Al^{3+} complex on emission spectra

increased to a significant extent on addition of 4-30 µM of ct-DNA. Upon incremental addition of 4-30 µM of ct-DNA to **7**.Al^{3+} complex, the emission intensity at 520 nm increases significantly with a red shift to 530 nm (Figure 14b).

Ethidium bromide (EtBr) displacement study

Fluorescence experiments were carried out in order to confirm the reversibility of probe **7**.Al^{3+} complex with DNA. Incremental addition of 50 µM solution of ethidium bromide to probe

7.Al^{3+}.DNA complex, resulted in fluorescence quenching at 520 nm with the simultaneous increase in emission intensity at 615 nm due to formation of EtBr:DNA complex, hence confirming the reversible binding of probe **7.**Al^{3+} complex with DNA (Figure 15a). Competitive binding experiments were carried out to confirm the binding mode of probe **7**.Al^{3+} complex with DNA. To complex containing 10 µM EtBr and 10 µM DNA, addition of 0-20 µM solution of probe **7**.Al^{3+} complex, emission intensity at 615 nm underwent quenching with blue shift to 600 nm and emission enhancement at 520 nm due to displacement of DNA from EtBr complex. Thereby confirming the probe **7**.Al^{3+} complex as a strong DNA intercalator (Figure 15b).

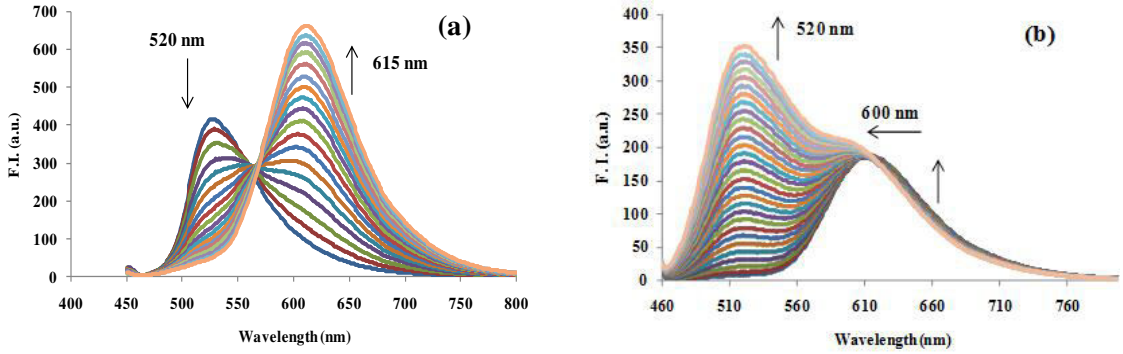

Figure 15: **(a)** Ethidium bromide displacement assay of probe **7**·Al^{3+}·DNA complex; (b) Competitive ethidium bromide displacement assay of probe **7**·Al^{3+}·DNA complex

5.8. CONCLUSION

Napthalimide based schiff base has been synthesized by employing multistep synthesis from commercially available acenaphthene. It has been successfully utilized as a chemosensor for selective detection of Al^{3+} and HSO_4^- ions in polar protic solvent. Owing to the specific reactivity of the Al^{3+}/HSO_4^--catalyzed chemical reaction, probe **6** displayed selectivity response for detection of 0.5 nM to 0.7 µM Al^{3+} ions and 50 nM to 40 µM HSO_4^- ions. Moreover, probe **6** showed the strong DNA intercalation properties through emission enhancement for the probable application as drug candidate.

Similarly, probe **7** has been used as a colorimetric and fluorescent chemosensor capable of sensing the Al^{3+} and F^- ions selectively over other metal ions in acetonitrile. Emission enhancement on addition of DNA to **7**.Al^{3+} complex revealed its strong DNA binding ability. DNA intercalation was also confirmed through ethidium bromide displacement assay.

5.9. Experimental section

Materials and methods

All reagents were purchased from commercial suppliers and used without further purification. TLC analyses were performed on silica gel plates and column chromatography was conducted over silica gel (mesh 60–120). ^{1}H NMR spectra were recorded using JEOL-ECS spectrometers operating at 400 MHz. ^{13}C NMR sepctra were recorded at 100 MHz. All chemical shifts are reported in ppm relative to the TMS as an internal reference. UV-vis studies were carried out on a Shimadzu 2600 machine using slit width of 1.0 nm and matched quartz cells. Fluorescence spectra were determined on a Varian Cary Eclipse fluorescence spectrometer. Stock solution of probes **6** and **7** were prepared at 10^{-3} M in distilled CH_3OH. The resulting solution was shaken well before recording the absorption spectra. All absorption and fluorescence scans were saved as ACS II files and further processed in Excel™ to produce all graphs shown. Solutions of **6** and **7** were typically 20 μM for UV-visible studies.

5.9.1. Synthesis of compound 2

To the mixture of acenaphthene **1** (7.7g, 50mmol) and acetic acid (60 ml), conc. nitric acid (5.5 ml) was added at room temperature. After 4 h, the reaction mixture was poured into ice water. The precipitate was filtered and washed with water. The crude product was recrystallized from acetic acid and then ethanol to afford 1,2-dihydro-5-nitroacenaphthylene **2** in 90% yield.

5.9.2. Synthesis of compound 3

To a stirred solution of sodium dichromate (2.24 g, 7.5 mmol) in acetic acid (5 ml), compound **2** (0.60 g, 3 mmol in 5 ml acetic acid) was added and refluxed for 5 h. The reaction mixture was mixed with cold water (50 ml) at 0 ^{o}C, filtered and washed with water until the filterate became neutral. The residue was dried in vacuo to afford the product 6-nitrobenzo[*de*]isochromene-1,3-dione **3** in 85% yield.

5.9.3. Synthesis of compound 4

To a stirred solution of compound **3** (0.5 gm, 1.77 mmol) in ethanol, allyl amine (0.132 ml, 1.77 mmol) was added and refluxed for 6 h. After completion of the reaction, reaction mixture was quenched with water followed by extraction with chloroform. Chloroform layer was separated

out, dried over anhydrous sodium sulphate and concentrated in vaccum to obtain crude product. The crude product was further purified by silica gel chromatography (60-120 mesh) using hexane: ethyl acetate (9:1) as eluents.

Spectral data of 2-allyl-6-nitro-1*H*-benzo[*de*]isoquinoline-1,3(2*H*)-dione (4): yellow solid

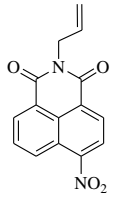

m.p. 146 ^{o}C; yield: 90%; ^{1}H NMR ($CDCl_3$, 400 MHz): δ 4.81 (t, J = 1.40 Hz, 1H, N-CH_2), 4.83 (t, J = 1.38 Hz, 1H, N-CH_2), 5.24-5.27 (dd, ^{2}J = 10.08 Hz, ^{3}J = 1.36 Hz, 1H, allyl-CH_2), 5.33-5.38 (dd, ^{2}J = 16.96 Hz, ^{3}J = 1.38 Hz, 1H, allyl-CH_2), 5.94-6.04 (m, 1H, allyl-CH), 7.98-8.02 (m, 1H, ArH), 8.42 (d, J = 7.80 Hz, 1H, ArH), 8.71 (d, J = 8.24 Hz, 1H, ArH), 8.74-8.76 (dd, ^{2}J = 7.36 Hz, ^{3}J =0.92 Hz, 1H, ArH), 8.84-8.86 (dd, ^{2}J = 8.68 Hz, ^{3}J = 0.92 Hz, 1H, ArH); ^{13}C NMR ($CDCl_3$, 100 MHz): δ 42.6 (N-CH_2), 118.2, 122.7, 123.5, 123.8, 126.6, 128.9, 129.2, 129.8, 129.9, 131.3, 132.4, 149.4, 162.0 (C=O), 162.8 (C=O).

5.9.4. Synthesis of compound 5

To the solution of compound **4** (100 mg, 0.39 mmol) in methanol, 10% Pd/C (5 mg) and hydrazine hydrate were added and stirred at room temperature for 2 h. Reaction mixture was then filtered to remove catalyst followed by washing with methanol. The crude product was then purified by silica gel chromatography in 60-120 mesh silica using hexane : ethyl acetate (7:3) as eluents to get black coloured solid.

Spectral data of 6-amino-2-propyl-1*H*-benzo[*de*]isoquinoline-1,3(2*H*)- dione (5): black

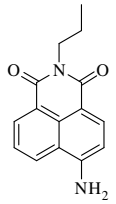

solid; mp: 135 ^{o}C; yield: 78%; ^{1}H NMR (DMSO-d_6, 400 MHz): δ 0.98 (t, J = 7.32 Hz, 3H, CH_3), 1.71 (m, 2H, CH_2), 4.10 (t, J = 7.56 Hz, 2H, N-CH_2), 6.23 (s, 2H, NH_2), 6.87 (d, J = 8.24 Hz, 1H), 7.60 (t, J = 8.02 Hz, 1H), 8.32 (d, J = 8.24 Hz, 1H), 8.40 (d, J = 8.28 Hz, 1H), 8.55 (d, J = 7.32 Hz, 1H); ^{13}C NMR (DMSO-d_6, 100 MHz): δ 10.9 (CH_3), 20.7 (CH_2), 40.7 (N-CH_2), 108.2, 109.0, 114.4, 119.2, 121.8, 123.4, 127.9, 129.33, 130.5, 133.3, 150.9, 163.3 (C=O), 164.0 (C=O); MS (ESI): m/z 255.2 (M^{+}+1).

5.9.5. Synthesis of compound 6

Compound **5** (100 mg, 0.279 mmol) was dissolved in ethanol (10 ml) at room temperature. To this solution, salicylaldehyde (0.072 gm, 0.59 mmol) was added at room temperature and

refluxed for 10 h. After completion of reaction, the bright yellow coloured precipitate was obtained. The solid was filtered and washed with ethanol 2-3 times and then dried under vaccum to get yellow solid product.

Spectral data of (*Z*)-6-(2-hydroxybenzylideneamino)-2-propyl-1*H*-benzo[*de*]isoquinoline-1,3(2*H*)-dione (6): mp: 145 ^{o}C; yield: 90%; ^{1}H NMR ($CDCl_3$, 400 MHz): 1.03 (t, *J* = 7.36 Hz, 3H, CH_3), 1.76-1.82 (m, 2H, CH_2), 4.15-4.19 (m, 2H, N-CH_2), 7.02-7.06 (m, 1H, ArH), 7.13 (d, *J* = 7.80 Hz, 1H, ArH), 7.41 (d, *J* = 7.80 Hz, 1H, ArH), 7.49-7.53 (m, 2H, ArH), 7.78-7.82 (m, 1H, ArH), 8.56-8.59 (dd, ^{2}J = 8.24 Hz, ^{3}J = 0.92 Hz, 1H, ArH), 8.63 (s, 1H, ArH), 8.66-8.68 (dd, ^{2}J = 7.20 Hz, ^{3}J = 1.36 Hz, 1H, ArH), 8.77 (s, 1H, =CH); ^{13}C NMR ($CDCl_3$, 100 MHz): 11.5 (CH_3), 21.4 (CH_2), 41.9 (N-CH_2), 115.3, 117.5, 119.0, 119.7, 120.8, 122.7, 126.4, 127.1, 128.8, 129.7, 131.8, 132.1, 133.1, 134.6, 151.5, 161.3, 163.8, 164.2 (C=O), 165.8 (C=O); MS(ESI): m/z 359.2 (M^{+}+1).

5.9.6. Synthesis of compound 7

Compound **5** (100 mg, 0.279 mmol) was dissolved in ethanol (10 ml) at room temperature. To this solution, 4-diethylaminosalicaldehyde (0.072 gm, 0.37 mmol) was added slowly at room temperature. After refluxing for 7 h, the orange coloured precipitate was obtained. The solid was filtered and washed with ethanol 2-3 times and then dried over vaccum.

Spectral data of (*Z*)-6-(4-(diethylamino)-2-hydroxybenzylideneamino)-2-propyl-1*H*-benzo[*de*]isoquinoline-1,3(2*H*)-dione (7): orange solid; mp: 180 ^{o}C; yield: 95%; ^{1}H NMR ($CDCl_3$, 400 MHz): 1.03 (t, *J* = 7.56 Hz, 3H, propyl CH_3), 1.25 (t, *J* = 7.10 Hz, 6H, CH_3), 1.75-1.81 (m, 2H, propyl CH_2), 3.45 (q, *J* = 7.17 Hz, 4H, CH_2), 4.14-4.18 (m, 2H, NCH_2), 6.25 (d, *J* = 2.28 Hz, 1H, ArH), 6.32-6.34 (dd, ^{2}J = 8.72 Hz, ^{3}J = 2.32 Hz, 1H, ArH), 7.26-7.28 (m, 1H), 7.36 (d, *J* = 8.24 Hz, 1H, ArH), 7.75 (t, *J* = 7.90 Hz, 1H, ArH), 8.57 (s, 1H, = CH), 8.60 (d, *J* = 7.76 Hz, 1H, ArH), 8.63-8.66 (m, 2H), ^{13}C NMR ($CDCl_3$, 100 MHz): 11.54 (Propyl $\underline{CH_3}$), 12.69 (CH_3) 21.42 (propyl $\underline{CH_2}$), 41.88 ($N\underline{CH_2}$), 44.80 (CH_3), 97.43, 104.60, 109.40, 114.50, 119.08, 122.58, 126.56, 126.88, 129.11, 130.17, 131.58, 132.48, 134.74, 152.151, 152.87, 162.89, 164.07 (ArC), 164.14 (C=O), 164.50 (C=O); MS (ESI): m/z 430.2 (M^{+}+1).

5.9.7. UV-vis and fluorescence spectroscopy studies

The absorbance and emission properties of probes **6** and **7** were checked in CH_3OH. The stock solution of probe **6** and **7** were prepared as 10^{-3} M in 25 mL of CH_3OH and then diluted to the desired concentration. Stock solutions of various ions were prepared at the concentration of $\sim 10^{-3}$ M in 25 mL distilled water and then diluted to the desired concentrations. The absorbance and fluorescence spectral data were recorded 10 min after the addition of the ions. For fluorescence measurements, the excitation wavelength was 340 nm (slit width = 10/10 nm) and emission was acquired from 360 nm to 700 nm.

5.9.8. DNA interaction studies

Stock solution of ct-DNA was prepared by dissolving DNA in phosphate buffer (10 mM, pH 7.0). The concentration was estimated from its absorbance intensity at 260 nm with a known molar absorption coefficient value of 6600 $dm^3M^{-1}cm^{-1}$. The purity of DNA was established from ratio of absorbance intensity at 260 nm and at 280 nm. The titration experiments were performed by varying the concentration of Ct-DNA and keeping the compound concentration constant (20 μM). All the UV spectra were recorded after equilibration of solution for 5 min.

REFERENCES

1. S. Demirayak and I. Kayagil, *J. Heterocyclic Chem.*, 2005, **42**, 319.
2. I. Kayagil and S. Demirayak, *Turk. J. Chem.*, 2011, **35**, 13.
3. N. Bouloc, J. M. Large, M. Kosmopoulou, C. Sun, A. Faisal, M. Matteucci, J. Reynisson, N. Brown, B. Atrash, J. Blagg, E. McDonald, S. Linardopoulos, R. Bayliss and V. Bavetsias, *Bioorg. Med. Chem. Lett.,* 2010, **20**, 5988.
4. T. Yu, J. R. Tagat, A. D. Kerekes, R. J. Doll, Y. Zhang, Y. Xiao, S. Esposite, D. B. Belanger, P. J. Curran, A. K. Mandal, M. A. Siddiqui, N.-Y. Shih, A. D. Basso, M. Liu, K. Gray, S. Tevar, J. Jones, S. Lee, L. Liang, S. Ponery, E. B. Smith, A. Hruza, J. Voigt, L. Ramanathan, W. Prosise and M. Hu, *ACS Med. Chem. Lett*., 2010, **1**, 214.
5. M. E. Voss, M. P. Rainka, M. Fleming, L. H. Peterson, D. B. Belanger, M. A. Siddiqui, A. Hruza, J. Voigt, K. Gray and A. D. Basso, *Bioorg. Med. Chem. Lett.,* 2012, **22**, 3544.
6. A. D. Kerekes, S. J. Esposite, R. J. Doll, J. R. Tagat, T. Yu, Y. Xiao, Y. Zhang, D. B. Prelusky, S. Tevar, K. Gray, G. A. Terracina, S. Lee, J. Jones, M. Liu, A. D. Basso and E. B. Smith, *J. Med. Chem*., 2011, **54,** 201.
7. M. P. Dwyer, K. Paruch, C. Alvarez, R. J. Doll, K. Keertikar, J. Duca, T. O. Fischmann, A. Hruza, V. Madison, E. Lees, D. Parry, W. Seghezzi, N. Sgambellone, F. Shanahan, D. Wiswell and T. J. Guzi, *Bioorg. Med. Chem. Lett.,* 2007, **17**, 6216.
8. T. O. Fischmann, A. Hruza, J. S. Duca, L. Ramanathan, T. Mayhood, W. T. Windsor, H. V. Le, T. J. Guzi, M. P. Dwyer, K. Paruch, R. J. Doll, E. Lees, D. Parry, W. Seghezzi and V. Madison, *Biopolymers*, **89**, 372.
9. S. M. Gonzalez, A. I. Hernandez, C. Varela, S. Rodriguez-Aristegui, R. M. Alvarez, A. B. Garcia, M. Lorenzo, V. Rivero, J. Oyarzabal, O, Rabal, J. R. Bischoff, M. Albarran, A. Cebria, P. Alfonso, W. Link, J. Fominaya and J. Pastor, *Bioorg. Med. Chem. Lett.,* 2012, **22,** 1874.
10. H. Zeng, D. B. Belanger, P. J. Curran, G. W. Shipps, H. Miao, J. B. Bracken, M. A. Siddiqui, M. Malkowski and Y. Wang, *Bioorg. Med. Chem. Lett.,* 2011, **21,** 5870.
11. J. G. Kettle, S. Brown, C. Crafter, B. R. Davies, P. Dudley, G. Fairley, P. Faulder, S. Fillery, H. Greenwood, J. Hawkins, M. James, K. Johnson, C. D. Lane, M. Pass, J. H. Pink, H. Plant and S. C. Cosulich, *J. Med. Chem.*, 2012, **55**, 1261.

12. S. A. Mitchell, M. D. Danca, P. A. Blomgren, J. W. Darrow, K. S. Currie, J. E. Kropf, S. H. Lee, S. L. Gallion, J.–M. Xiong, D. A. Pippin, R. W. DeSimone, D. R. Brittelli, D. C. Eustice, A. Bourret, M. Hill-Drzewi, P. M. Maciejewski and L. L. Elkin, *Bioorg. Med. Chem. Lett.*, 2009, **19**, 6991.
13. A. T. Baviskar, C. Madaan, R. Preet, P. Mohapatra, V. Jain, A. Agarwal, S. K. Guchhait, C. N. Kundu, U. C. Banerjee and P. V. Bharatam, *J. Med. Chem.*, 2011, **54**, 5013.
14. T. P. Matthews, T. McHardy, S. Klair, K. Boxall, M. Fisher, M. Cherry, C. E. Allen, G. J. Addison, J. Ellard, G. W. Aherne, I. M. Westwood, R. Van Montfort, M. D. Garrett, J. C. Reader and I. Collins, *Bioorg. Med. Chem. Lett.,* 2010, **20**, 4045.
15. N. S. Reddy, K. Gumireddy, M. R. Mallireddigari, S. C. Cosenza, P. Venkatapuram, S. C. Bell, E. P. Reddy and M. V. R. Reddy, *Bioorg. Med. Chem.*, 2005, **13**, 3141.
16. G. Wells, M. Suggitt, M. Coffils, M. A. H. Baig, P. W. Howard, P. M. Loadman, J. A. Hartley, T. C. Jenkinsd and D. E. Thurstona, *Bioorg. Med. Chem. Lett*., 2008, **18**, 2147.
17. R. M. Mohareb, D. H. Fleita and O. K. Sakka, *Molecules*, 2011, **16**, 16.
18. C. F. Xiao, L. Y. Tao, H. Y. Sun, W. Wei, Y. Chen, L. W. Fu and Y. Zou, *Chin. Chem. Lett*., 2010, **21**, 1295.
19. X. Q. Wu, C. Huang, Y. M. Jia, B. A. Song, J. Li and X. H. Liu, *Eur. J. Med. Chem.*, 2014, **74**, 717.
20. B. B. Friday and A. A. Adjei, *Biochim. Biophys. Acta*, 2005, **1756**, 127.
21. P. Rusconi, E. Caiola and M. Broggini, *Curr. Med. Chem*., 2012, **19**, 1164.
22. J.-F. Cheng, M. Chen, D. Wallace, S. Tith, T. Arrhenius, H. Kashiwagi, Y. Ono, A. Ishikawa, H. Sato, T. Kozono, H. Sato and A. M. Nadzan, *Bioorg. Med. Chem. Lett*., 2004, **14**, 2411.
23. S. Han, V. Zhou, S. Pan, Y. Liu, M. Hornsby, D. McMullan, H. E. Klock, J. Haugen, S. A. Lesley, N. Gray, J. Caldwell and X.-J. Gu, *Bioorg. Med. Chem. Lett*., 2005, **15,** 5467.
24. J. Kazius, R. McGuire and R. Bursi, *J. Med. Chem.*, 2005, **48**, 312.
25. T. Aoki, I. Hyohdoh, N. Furuichi, S. Ozawa, F. Watanabe, M. Matsushita, M. Sakaitani, K. Ori, K. Takanashi, N. Harada, Y. Tomii, M. Tabo, K. Yoshinari,Y. Aoki, N. Shimma and H. Iikura, *Bioorg. Med. Chem. Lett*. 2013, **23**, 6223.
26. M. Basanagouda, V. B. Jambagi, N. N. Barigidad, S. S. Laxmeshwar, V. Devaru and Narayanachar, *Eur. J. Med. Chem.*, 2014, **74**, 225.

27. R. Boutros, C. Dozier and B. Ducommun, *Curr. Opin. Cell Biol*., 2006, **18,** 185.
28. S. W. Ham, H. J. Park and D. H. Lim, *Bioorg. Chem.*, 1997, **25**, 33.
29. E. Bana, E. Sibille, S. Valente, C. Cerella, P. Chaimbault, G. Kirsch, M. Dicato, M. Diederich and D. Bagrel, *Mol. Carcinog*., 2015, **54**, 229.
30. K. B. Puttaraju, K. Shivashankar, C. M. Mahendra, V. P. Rasal, P. N. V. Vivek, K. Rai and M. B. Chanu, *Eur. J. Med. Chem.*, 2013, **69**, 316.
31. S. Harguindey, J. L. Arranz, M. L. Wahl, G. Orive and S. J. Reshkin, *Anticancer Res*., 2009, **29**, 2127.
32. J. Melena, R. Safa, M. Graham, R. J. Casson and N. N. Osborne, *Brain Res*., 2003, **989,** 128.
33. N. Draoui, O. Schicke, A. Fernandes, X. Drozak, F. Nahra, A. Dumont, J. Douxfils, E. Hermans, J. M. Dogne, R. Corbau, A. Marchand, P. Chaltin, P. Sonveaux, O. Feron and O. Riant, *Bioorg. Med. Chem.*, 2013, **21**, 7107.
34. K. M. Amin, A. A. M. Eissa, S. M. Abou-Seri, F. M. Awadallah and G. S. Hassan, *Eur. J. Med. Chem*., 2013, **60**, 187.
35. H. Chen, S. Li, Y. Yao, L. Zhou, J. Zhao, Y. Gu, K. Wang and X. Li, *Bioorg. Med. Chem. Lett*., 2013, **23**, 4785.
36. L. Zhao, Y. Yao, S. Li, M. Lv, H. Chen and X. Li, *Bioorg. Med. Chem. Lett*., 2014, **24**, 900.
37. R. Pingaew, A. Saekee, P. Mandi, C. Nantasenamat, S. Prachayasittikul, S. Ruchirawat and V. Prachayasittikul, *Eur. J. Med. Chem*., 2014, **85**, 65.
38. C. Florean, M. Schnekenburger, C. Grandjenette, M. Dicato and M. Diederich, *Epigenomics*, 2011, **3**, 581.
39. C. Seidel, M. Schnekenburger, C. Zwergel, F. Gaascht, A. Mai, M. Dicato, G. Kirsch, S. Valente and M. Diederich, *Bioorg. Med. Chem. Lett.*, 2014, **24**, 3797.
40. N. E. B. Saidu, S. Valente, E. Bana, G. Kirsch, D. Bagrel and M. Montenarh, *Bioorg. Med. Chem.*, 2012, **20,** 1584.
41. T. D. Penning, G. D. Zhu, V. B. Gandhi, J. Gong, X. Liu, Y. Shi, V. Klinghofer, E. F. Johnson, C. K. Donawho, D. J. Frost, V. B. Diaz, J. J. Bouska, D. J. Osterling, A. M. Olson, K. C. Marsh, Y. Luo and V. L. Giranda, *J. Med. Chem.*, 2009, **52**, 514.
42. H. M. Refaat, *Eur. J. Med. Chem.*, 2010, **45**, 2949.
43. P. Xiang, T. Zhou, L. Wang, C. Y. Sun, J. Hu, Y. L. Zhao and L. Yang, *Molecules*, 2012, **17**, 873.

44. N. R. Gowda, C. V. Kavitha, K. K. Chiruvella, O. Joy, K. S. Rangappa and S. C. Raghavan, *Bioorg. Med. Chem. Lett*., 2009, **19**, 4594.
45. M. A. Omar, Y. M. Shaker, S. A. Galal, M. M. Ali, S. M. Kerwin, J. Li and H. I. El Diwani, *Bioorg. Med. Chem*., 2012, **20**, 6989.
46. T. Liu, C. Sun, X. Xing, L. Jing, R. Tan, Y. Luo and Y. Zhao, *Bioorg. Med. Chem. Lett*., 2012, **22**, 3122.
47. C. Karthikeyan, V. R. Solomon, H. Lee and P. Trivedi, *Arab. J. Chem*., 2013, DOI no: 10.1016/j.arabjc.2013.07.003.
48. Y. K. Yoon, M. A. Ali, A. C. Wei, T. S. Choon, H. Osman, K. Parang and A. N. Shirazi, *Bioorg. Med. Chem*., 2014, **22**, 703.
49. H. B. El-Nassan, *Eur. J. Med. Chem*., 2012, **53**, 22.
50. M. Singh and V. Tandon, *Eur. J. Med. Chem*., 2011, **46**, 659.
51. Q. Zhou and P. Yang, *Inorg. Chim. Acta*, 2006, **359**, 1200.
52. G. Yadav and S. Ganguly, *Eur. J. Med. Chem*., 2015, **97**, 419.
53. F. Gumus and O. Algu,. *J. Inorg. Biochem*., 1997, **68**, 71.
54. F. Gumus, O. Algu, G. Eren, H. Eroglu, N. Diril, S. Gur and A. Ozku, *Eur. J. Med. Chem*., 2003, **38**, 473.
55. F. Gumus, F. Izgu and O. Algu, *FABAD J. Pharm. Sci*., 1996, **21**, 7.
56. F. Gumus, I. Pamuk, T. Ozden, S. Yildis, N. Diril, S. Oksuzoglu, A. Gur, Ozku, *J. Inorg. Biochem*., 2003, **94**, 255.
57. M. Gokce, S. Utku, S. Gur, A. Ozkul and F. Gumus, *Eur. J. Med. Chem*., 2005, **40**, 135.
58. S. A. Galal, K. H. Hegab, A. S. Kassab, M. L. Rodriguez, S. M. Kerwin, A. M. A. El-Khamry and H. I. El Diwani, *Eur. J. Med. Chem*., 2009, **44**, 1500.
59. S. A. Galal, K. H. Hegab, A. M. Hashem, and N. S. Youssef, *Eur. J. Med. Chem*., 2010, **45**, 5685.
60. M. M. Ramla, M. A. Omar, A. M. M. El-Khamry and H. I. El-Diwani, *Bioorg. Med. Chem.*, 2006, **14**, 7324.
61. R. A. Ng, J. Guan, V. C. Alford, J. C. Lanter, G. F. Allan, T. Sbriscia, S. G. Lundeen and Z. Sui, *Bioorg. Med. Chem. Lett.*, 2007, **17**, 955.
62. M. Hranjec, G. Pavlovi, M. Marjanovi, M. Kralj and G. K. Zamola, *Eur. J. Med. Chem*., 2010, **45**, 2405.

63. M. F. Bran˜a, J. M. C. Berlanga and C. M. Roldan, DE patent 2,318,136 (1973), C.A.86; 106,236 (1977).
64. P. A. Panchenko, Y. V. Fedorov, V. P. Perevalov, G. Jonusauskas and O. A. Fedorova, *J. Phys. Chem. A*, 2010, **114**, 4118.
65. R. K. Jackson, Y. Shi, X. Yao and S. C. Burdette, *Dalton Trans*., 2010, **39**, 4155.
66. (a) A. P. de Silva, A. Goligher, H. Q. N. Gunaratne and T. E. Rice, *Arkivoc*, 2003, **8**, 229; (b) A. P. de Silva and T. E. Rice, *Chem. Commun*., 1999, 163.
67. K. D. Krishna, K. S. Ramendra and K. Misre, *Indian J. Chem*., *Sect. B: Org. Chem. Incl. Med. Chem*., 1995, **34**, 876.
68. K. Hanaoka, Y. Muramatsu, Y. Urano, T. Terai and T. Nagano, *Chem. Eur. J.,* 2010, **16**, 568.
69. (a) A. Pardo, J. M. L. Poyato, J. J. Camacho, M. F. Bran˜a and J. M. Castellano, *J. Photochem*., 1986, **36**, 323; (b) A. Pardo, E. Martin, J. M. L. Poyato, J. J. Camacho, M. F. Bran˜a and J. M. Castellano, *J. Photochem. Photobiol., A*, *1987*, **41**, 69.
70. M. F. Bran˜a, J. M. Castellano, C. M. Rolda´n, A. Santos, D. Va´zquez and A. Jime´nez, *Cancer Chemother. Pharmacol*., 1980, **4**, 61.
71. http://www.chemgenex.com; (b) M. F. Bra˜na, A. M. Sanz, J. M. Castellano, C. M. Roldan and C. Roldan, *Eur. J. Med. Chem*., 1981, **16**, 207.
72. B. S. Andersson, M. Beran, M. Bakic, L. E. Silberman, R. A. Newman and L. A. Zwelling, *Cancer Res*., 1987, **47**, 1040; (b) G. H. Su, T. A. Sohn, B. Ryu and S. E. Kern, *Cancer Res*., 2000, **60**, 3137; (c) J. Keen, L. Yan, K. Mack, C. Pettit, D. Smith, D. Sharma and N. Davidson, *Breast Cancer Res. Treat*., 2003, **81**, 177.
73. M. J. Waring, A. Gonzalez, A. Jimenez and D. Vazquez, *Nucleic Acids Res*., 1979, **7**, 217.
74. C. Bailly, M. Bran˜a and M. J. Waring, *Eur. J. Biochem*., 1996, **240**, 195.
75. J. Gallego and B. R. Reid, *Biochemistry*, 1999, **38**, 15104.
76. L. Gonzalez-Bulnes and J. Gallego, *J. Am. Chem. Soc*., 2009, **131**, 7781.
77. (a) R. J. McRipley, P. E. Burns-Horwitz, P. M. Czerniak, R. J. Diamond, M. A. Diamond, J. L. D. Miller, R. J. Page, D. L. Dexter, S.-F. Chen, J.-H. Sun, C. H. Behrens, S. P. Seitz and J. L. Gross, *Cancer Res*., 1994, **54**, 159; (b) M. R. Kirshenbaum, S.-F. Chen, C. H. Behrens, L. M. Papp, M. M. Stafford, J.-H. Sun, D. L. Behrens, J. R. Fredericks, S. T. Polkus, P. Sipple, A. D. Patten, D. Dexter, S. P. Seitz and J. L. Gross, *Cancer Res*., 1994, **54**, 2199; (c)

J. L. Nitiss, J. Zhou, A. Rose, Y. Hsiung, K. C. Gale and N. Osheroff, *Biochemistry*, 1998, **37**, 3078.

78. R. J. Cherney, S. G. Swartz, A. D. Patten, E. Akamike, J.-H. Sun, R. F. Kaltenbach III, S. P. Seitz, C. H. Behrens, Z. Getahun, G. L. Trainor, M. Vavala, M. R. Kirshenbaum, L. M. Papp, M. P. Stafford, P. M. Czerniak, R. J. Diamond, R. J. McRipley, R. J. Page and J. L. Gross, *Bioorg. Med. Chem. Lett*., 1997, **7**, 163.
79. (a) E. B. Veale, D. O. Frimannsson, M. Lawler and T. Gunnlaugsson, *Org. Lett*., 2009, **11**, 4040; (b) E. B. Veale and T. Gunnlaugsson, *J. Org. Chem*., 2010, **75**, 5513.
80. S. Murphy, S. A. Bright, F. E. Poynton, T. McCabe, J. A. Kitchen, E. B. Veale, D. C. Williams and T. Gunnlaugsson. *Org. Biomol. Chem*., 2014, **12**, 6610.
81. K. Suzuki, H. Nagasawa, Y. Uto, Y. Sugimoto, K. Noguchi, M. Wakida, K. Wierzba, T. Terada, T. Asao and Y. Yamada, *Bioorg. Med. Chem*., 2005, **13**, 4014.
82. H. Yin, Y. Xu, X. Qian, Y. Li and J. Liu, *Bioorg. Med. Chem. Lett*., 2007, **17**, 2166.
83. Z. Li, Q. Yang, X. Qian, *Bioorg. Med. Chem. Lett*., 2005, **15**, 1769.
84. A. Wu, Y. Xu and X. Qian, *Bioorg. Med. Chem*., 2009, **17**, 592.
85. (a) A. Padwa and S. K. Bur, *Tetrahedron*, 2007, **63**, 5341; (b) D. M. D'Souza and T. J. J. Muller, *Chem. Soc Rev.*, 2007, **36**, 1095.
86. (a) C. Fu. Gregory, *Acc. Chem. Res.*, 2009, **41**, 1555; (b) A. F. Littke and C. Fu. Gregory, *Angew. Chem. Int. Ed.*, 2002, **41**, 4176.
87. (a) B. B. Toure, B. S. Lane and D. Sames, *Org. Lett.*, 2006, **8**, 1979; (b) J. Koubachi, S. El. Kazzouli, S. Berteina-Raboin, A. Mouaddib and G. Guillaumet, *J. Org. Chem*., 2007, **72**, 7650; (c) J. Koubachi, S. El. Kazzouli, S. Berteina-Raboin, A. Mouaddib and G. Guillaumet, *Synthesis*, 2008, **16**, 2537; (d) R. R. Singhaus, R. C. Bernotas, R. Steffan, E. Matelan, E. Quinet, P. Nambi, I. Feingold, C. Huselton, A. Wilhelmsson, A. Goos-Nilsson and J. Wrobel, *Bioorg. Med. Chem. Lett.*, 2010, **20**, 521; (e) J. Koubachi, S. Berteina-Raboin, A. Mouaddib and G. Guillaumet, *Tetrahedron*, 2010, **66**, 1937; (f) P. V. Kumar, W.-S. Lin, J.-S. Shen, D. Nandi and H. M. Lee, *Organometallics*, 2011, **30**, 5160; (g), H. Cao, H. Zhan, Y. Lin, X. Lin, Z. Du and H. Jiang, *Org. Lett*., 2012, **14**, 1688; (h) H. Y. Fu, L. Chen and H. Doucet, *J. Org. Chem*., 2012, **77**, 4473; (i) K. Pericherla, P. Khedar, B. Khungar and A. Kumar, *Chem. Comm*., 2013, **49**, 2924.
88. (a) W. Li, D. P. Nelson, M. S. Jensen, R. S. Hoerrner, G. J. Javadi, D. Cai and R. D. Larsen,

Org. Lett., 2003, **5**, 4835; (b) M. Parisien, D. Valette and K. Fagnou, *J. Org. Chem*., 2005, **70**, 7578.

89. D. B. Belanger, M. J. Williams, P. J. Curran, A. K. Mandal, Z. Meng, M. P. Rainka, T. Yu, N.-Y. Shih, M. A. Siddiqui, M. Liu, S. Tevar, S. Lee, L. Liang, K. Gray, B. Yaremko, J. Jones, E. B. Smith, D. B. Prelusky and A. D. Basso, *Bioorg. Med. Chem. Lett*., 2010, **20**, 6739.
90. L. C. Meurer, R. L. Tolman, E. W. Chapin, R. Saperstein, P. P. Vicario, M. M. Zrada and M. MacCoss, *J. Med. Chem.,*1992, **35**, 3845.
91. O. Vitse, F. Laurent, T. M. Pocock, V. Benezech, L. Zanik, K. R. F. Elliott, G. Subra, K. Portet, J. Bompart, J.-P. Chapat, R. C. Small, A. Michel and P.-A. Bonnet, *Bioorg. Med. Chem*., 1999, **7**, 1059.
92. P. J. Zimmermann, C. Brehm, W. Buhr, A. M. Palmer, J. Volz and W.-A. Simon, *Bioorg. Med. Chem.,* 2008, **16**, 536.
93. S. Myadaraboina, M. Alla, V. Saddanapu, V. R. Bommena and A. Addlagatta, *Eur. J. Med. Chem.,* 2010, **45***,* 5208.
94. A. Brown, A. Heenderson, C. Lane, M. Lansdell, G. Maw and S. Monaghan, *Bioorg. Med. Chem. Lett.,* 2006, **16**, 4697.
95. V. Gembus, J.-F. Bonfanti, O. Querolle, P. Jubault, V. Levacher and C. Hoarau, *Org. Lett*., 2012, **14**, 6012.
96. S. K. Guchhait, S. Kandekar, M. Kashyap, N. Taxak and P. V. Bharatam, *J. Org. Chem.,* 2012, **77**, 8321.
97. B. Jiang, C.-G. Yang, W.-N. Xiong and J. Wang, *Bioorg. Med. Chem.,* 2001, **9**, 1149.
98. C. Bonini, L. Chiummiento, M. D. Bonis, M. Funicello, P. Lupattelli, G. Suanno, F. Berti and P. Campaner, *Tetrahedron,* 2005, **61**, 6580.
99. X. Lu, B. Wan, S. G. Franzblau and Q. You, *Eur. J. Med. Chem.,* 2011, **46**, 3551.
100. M. Z. Elsabee, E. A. Ali, S. M. Mokhtar and M. Eweis, *React. Funct. Polym.,* 2011, **71**, 1187.
101. W. Brandt, L. Mologni, L. Preu, T. Lemcke, C. Gambacorti-Passerini and C. Kunick, *Eur. J. Med. Chem.,* 2010, **45**, 2919.
102. (a) R. Romagnoli, P. G. Baraldi, M. D. Carrion, C. L. Cara, O. Cruz-Lopez, D. Preti, M. Tolomeo, S. Grimaudo, A. D. Cristina and N. Zonta, *Bioorg. Med. Chem.,* 2008, **16**, 5367;

(b) P. Diana, A. Carbone, P. Barraja, A. Montalbano, A. Martorana, G. Dattolo, O. Gia, L. D. Via and G. Cirrincione, *Bioorg. Med. Chem. Lett.,* 2007, **17**, 2342; (c) M. A. Gouda, M. A. Berghot, E. A. Baz and W. S. Hamama, *Med. Chem. Res.,* 2012, **21**, 1062; (d) C. Medower, L. Wen and W. W. Johnson, *Chem. Res. Toxicol.,* 2008, **21**, 1570; (e) L. Brault, E. Migianu, A. Ne guesque, E. Battaglia, D. Bagrel and G. Kirsch, *Eur. J. Med.Chem.,* 2005, **40**, 757.

103. a) R. B. DeVasher, L. R. Moore and K. H. Shaughnessy, *J. Org. Chem.,* 2004, **69**, 7919; (b) R. B. DeVasher, J. M. Spruell, D. A. Dixon, G. A. Broker, S. T. Griffin, R. D. Rogers and K. H. Shaughnessy, *Organometallics,* 2005, **24**, 962.
104. M. Mondal and U. Bora, *Green Chem.*, 2012, **14**, 1873.
105. Crystallographic data for the structural analysis have been deposited at the Cambridge Crystallographic Data Centre. (E-mail: deposit@ccdc.cam.ac.uk).
106. M. R. Grever, S. A. Sehepartz and B. A. Chabners, *Semin. Oncol.*, 1992, **19**, 622.
107. A. Monks, D. Schudiero, P. Skehan, R. Shoemaker, K. Paull, D.Vistica, C. Hose, J. Langley, P. Cronise, A. Vaigro-Wolff, M. Gray-Goodrich, H. Campbell, J. Mayo and M. Boyd, *J. Natl. Cancer Inst.*, 1991, **83**, 757.
108. M. R. Boyd and K. D. Paull, *Drug Dev. Res.*, 1995, **34**, 91.
109. A. Czarnik, *Acc. Chem. Res.*, 1996, **29**, 112.
110. (a) R. Goel, V. Luxami and K. Paul, *RSC Adv.,* 2014, **4**, 9885; (b) R. Goel, V. Luxami and K. Paul, *Org. Biomol. Chem.*, 2015, **13**, 3525.
111. K. S. Currie, J. E. Kropf, T. Lee, P. Blomgren, J. Xu, Z. Zhao, S. Gallion, J. A. Whitney, D. Maclin, E. B. Lansdon, P. Maciejewski, A. M. Rossi, H. Rong, J. Macaluso, J. Barbosa, J. A. Di Paolo and S. A. Mitchell, *J. Med. Chem.*, 2014, **57**, 3856.
112. Y. Chen, H.-R. Liu, H.-S. Liu, M. Cheng, P. Xia, K. Qian, P.-C. Wu, C.-Y. Lai, Y. Xia, Z.-Yu. Yang, S. L. Morris-Natschke and K.-H. Lee, *Eur. J. Med. Chem.,* 2012, **49**, 74.
113. H. Xue, X. Lu, P. Zheng, L. Liu, C. Han, J. Hu, Z. Liu, T. Ma, Y. Li, L. Wang, Z. Chen and G. Liu, *J. Med. Chem.*, 2010, **53**, 1397.
114. A. Manvar, A. Bavishi, A. Radadiya, J. Patel, V. Vora, N. Dodia, K. Rawal and A. Shah, *Bioorg. Med. Chem. Lett.*, 2011, **21**, 4728.
115. G. R. Madhavan, V. Balraju, B. Mallesham, R. Chakrabarti and V. B. Lohray, *Bioorg. Med. Chem. Lett.*, 2003, **13**, 2547.

116. K. Nepali, S. Sharma, M. Sharma, P. M. S. Bedi and K. L. Dhar, *Eur. J. Med. Chem.,* 2014, **77**, 422.
117. K. Paul, S. Bindal and V. Luxami, *Bioorg. Med. Chem. Lett.,* 2013, **23**, 3667.
118. S. G. Kini, S. Choudhary and M. Mubeen, *J. Comput. Methods Mol. Des*., 2012, **2**, 51.
119. K. V. Sashidhara, A. Kumar, M. Kumar, J. Sarkar and S. Sinha, *Bioorg. Med. Chem. Lett.,* 2010, **20**, 7205.
120. J. Bradac, Z. Furek, D. Janezic, S. Molan, I. Smerkolj, B. Stanovnik, M. Tisler and B. Vercek *J. Org. Chem.,* 1977, **42**, 4197.
121. A. I. Caço, L. C. Tome, R. Dohrn and I. M. Marrucho, *J. Chem. Eng. Data*, 2010, **55**, 3160.
122. Compounds were constructed and docked with builder tool kit of software package ArgusLab 4.0.1 (www.arguslab.com).
123. W.-K. Choi, M. I. El-Gamal, H. S. Choi, D. Baek and C.-H. Oh, *Eur. J. Med. Chem*., 2011, **46,** 5754.
124. (a) N. J. Turro, *Modern Molecular Photochemistry*; University Science Books: Sausalito, 1991; (b) J. Fan, M. Hu, P. Zhan and X. Peng, *Chem. Soc. Rev.,* 2013, **42**, 29.
125. (a) D. L. Dexter, *J. Chem. Phys*., 1953, **21**, 836; (b) Y. Zhao, Y. Zhang, X. Lv, Y. Liu, M. Chen, P. Wang, J. Liu and W. Guo, *J. Mater. Chem*., 2011, **21**, 13168; (c) X. Qu, Q. Liu, X. Ji, H. Chen, Z. Zhou and Z. Shen, *Chem. Commun*., 2012, **48**, 4600; (d) J. Fan, P. Zhan, M. Hu, W. Sun, J. Tang, J. Wang, S. Sun, F. Song, and X. Peng, *Org. Lett.,* 2013, **15**, 492.
126. (a) T. Förster, *Ann. Phys*., 1948, **2**, 55; (b) T. Z. Förster, *Naturforsch*, 1949, **4**, 321; (c) N. Kumar, V. Bhalla and M. Kumar, *Analyst*, 2014, **139**, 543; (d) J. Zhang, R. Wang, Z. Zhu, L. Yi and Z. Xi, *Tetrahedron*, 2015, **71**, 8572; (e) R. Guliyev, A. Coskun and E. U. Akkaya, *J. Am. Chem. Soc*., 2009, **131**, 9007; (f) Z. Kostereli, T. Ozdemir, O. Buyukcakir and E. U. Akkaya, *Org. Lett*., 2012, **14**, 3636; (g) W. G. Skene and S. Dufresne, *Org. Lett*., 2004, **6**, 2949.
127. a) N. Song, M. Ding, Z. Pan, J. Li, L. Zhou, H. Tan and Q. Fu, *Biomacromolecules*, 2013, **14**, 4407; (b) S. Angelos, Y. W. Yang, K. Patel, J. F. Stoddart and J. I. Zink, *Angew. Chem., Int. Ed*., 2008, **47**, 2222.
128. C. W. Tornøe, C. Christensen and M. Meldal, *J. Org. Chem.,* 2002, **67***,* 3057.
129. R. Goel, V. Luxami and K. Paul, *RSC Adv*., 2014, **4**, 9885.
130. H. Yu, Y. Xiao, H. Guo and X. Qian, *Chem. Eur. J.,* 2011, **17**, 3179.

131. T. Nagano, H. Takakusa, K. Kikuchi, Y. Urano, S. Sakamoto and K. Yamaguchi, *J. Am. Chem. Soc*., 2002, **124**, 1653.
132. A. Ojida, Y. Kurishita, T. Kohira and I. Hamachi, *J. Am. Chem. Soc*., 2010, **132**, 13290.
133. F. Sozmen, B. S. Oksal, O. A. Bozdemir, O. Buyukcakir and E. U. Akkaya, *Org. Lett*., 2012, **14**, 5286.
134. Y. Ueno, J. Jose, A. Loudet, C. P´erez-Bol´ıvar, P. Anzenbacher Jr and K. Burgess, *J. Am. Chem. Soc*., 2011, **133**, 51.
135. J. K. Heinonen, in Biological Role of Inorganic Pyrophosphate, Kluwer Academic Publishers, Boston, 2001.
136. J. A. Drewry, S. Fletcher, H. Hassan and P. T. Gunning, *Org. Biomol. Chem*., 2009, **7**, 5074.
137. C. P. Mathews and K. E. van Hold, Biochemistry, The Benjamin/Cummings Publishing Company, Inc., Redwood City, CA, 1990.
138. (a) W. N. Limpcombe and N. Sträter, *Chem. Rev*., 1996, **96**, 2375; (b) P. Nyrén, *Anal. Biochem*., 1987, **167**, 235; (c) T. Tabary and L. Ju*, J. Immunol. Methods*, 1992, **156**, 55.
139. (a) E. J. O'Neil and B. D. Smith, *Coord. Chem. Rev*., 2006, **250**, 3068; (b) R. Marťınez-Ḿanez and F. Sancenon, *Chem. Rev*., 2003, **103**, 4419; (c) P. D. Beer and P. A. Gale, *Angew. Chem., Int. Ed*., 2001, **40**, 486.
140. S. Mizukami, T. Nagano, Y. Urano, A. Odani and K. Kikuchi, *J. Am. Chem. Soc*., 2002, **124**, 3920.
141. (a) C. Park and J.-I. Hong, *Tetrahedron Lett*., 2010, **51**, 1960; (b) X.-h. Huang, Y. Lu, Y.-b. He and Z.-h. Chen, *Eur. J. Org. Chem*., 2010, 1921; (c) J. H. Lee, J. Park, M. S. Lah, J. Chin and J.-I. Hong, *Org. Lett*., 2007, **9**, 3729; (d) H. N. Lee, Z. Xu, S. K. Kim, K. M. K. Swamy, Y. Kim, S.-J. Kim and J. Yoon, *J. Am. Chem. Soc*., 2007, **129**, 3828; (e) H. N. Lee, K. M. K. Swamy, S. K. Kim, J.-Y. Kwon, Y. Kim, S.-J. Kim, Y. J. Yoon and J. Yoon*, Org. Lett*., 2007, **9**, 243; (f) A. Ojida, H. Nonaka, Y. Miyahara, S. Tamaru, K. Sada and I. Hamachi, *Angew. Chem., Int. Ed*., 2006, **45**, 5518.
142. C. M. G. dos Santos and T. Gunnlaugsson, *Dalton Trans*., 2009, 4712.
143. S. Mizukami, T. Nagano, Y. Urano, A. Odani and K. Kikuchi, *J. Am. Chem. Soc*., 2002, **124**, 3920.
144. K. M. K. Swamy, S. K. Kwon, H. N. Lee, S. M. S. Kumar, J. S. Kim and J. Yoon, *Tetrahedron Lett*., 2007, **48**, 8683.

145. (a) S. Watchasit, A. Kaowliew, C. Suksai, T. Tuntulani, W. Ngeontae and C. Pakawatchai, *Tetrahedron Lett*., 2010, **51**, 3398; (b) Z. Guo, W. Zhu and H. Tian, *Macromolecules*, 2010, **43**, 739; (c) M. J. Kim, K. M. K. Swamy, K. M. Lee, A. R. Jagdale, Y. Kim, S.-J. Kim, K. H. Yoo and J. Yoon, *Chem. Commun*., 2009, 7215; (d) S. Y. Kim and J.-I. Hong, *Tetrahedron Lett*., 2009, **50**, 1951; (e) X. Huang, Z. Guo, W. Zhu, Y. Xie and H. Tian, *Chem. Commun*., 2008, 5143; (f) Y. J. Jang, E. J. Jun, Y. J. Lee, Y. S. Kim, J. S. Kim and J. Yoon, *J. Org. Chem*., 2005, **70**, 9603; (g) L. Fabbrizzi, N. Marcotte, F. Stomeo and A. Taglietti, *Angew. Chem., Int. Ed*., 2002, **41**, 3811.

146. N. Shao, J. Jin, G. Wang, Y. Zhang, R. Yang and J. Yuan, *Chem. Commun.,* 2008, 1127.

147. (a) T.-M. Fu, C.-Y. Wu, C.-C. Cheng, C.-R. Yang and Y.-P. Yen, *Sens. Actuators B*, 2010, **146**, 171; (b) Z. Xu, J.-Y. Choi and J. Yoon, *Bull. Korean Chem. Soc*., 2011, **32**, 1371; (c) C. Caltagirone, C. Bazzicalupi, F. Isaia, M. E. Light, V. Lippolis, R. Montis, S. Murgia, M. Olivari and G. Picci, *Org. Biomol. Chem*., 2013, **11**, 2445; (d) P. Sokkalingam, D. S. Kim, H. Hwang, J. L. Sessler and C.-H. Lee, *Chem. Sci*., 2012, **3**, 1819.

148. (a) T. Forster, *Ann. Phys*. 1948, **2**, 55; (b) B. W. vander Meer, G. Coker III and S.-Y. Simon Chen, VCH, Weinheim, Germany, 1994; (c) P. Mahato, S. Saha, E. Suresh, R. DiLiddo, P. P. Parnigotto, M. T. Conconi, M. K. Kesharwani, B. Ganguly and A. Das, *Inorg. Chem*., 2012, **51**, 1769.

149. (a) J. Wu, W. Liu, J. Ge, H. Zhang and P. Wang, *Chem. Soc. Rev*. 2011, **40**, 3483; (b) X. Chen, T. Pradhan, F. Wang, J. S. Kim and J. Yoon, *Chem. Rev*. 2012, **112**, 1910.

150. (a) C. Ma, F. Zeng, L. Huang and S. Wu, *J. Phys. Chem*. B, 2011, **115**, 874; (b) B. R. White, H. M. Liljestrand and J. A. Holcombe, *Analyst*, 2008, **133**, 65; (c) G. Fang, M. Xu, F. Zeng and S. Wu, *Langmuir*, 2010, **26**, 17764.

151. H. Yu, Y. Xiao, H. Guo and X. Qian, *Chem.–Eur. J.,* 2011, **17**, 3179.

152. H. A. Benesi and J. H. Hildebrand, *J. Am. Chem. Soc.* 1949, **71**, 2703.

153. H. Kobayashi and P. L. Choyke, *Acc. Chem. Res*. 2011, **44**, 83.

154. (a) J. Chan, S. C. Dodani and C. J. Chang, *Nat. Chem*. 2012, **4**, 973; (b) E. M. S. Stennett, M. A. Ciuba and M. Levitus, *Chem. Soc. Rev*. 2014, **43**, 1057; (c) J. Wu, B. Kwon, W. Liu, E. V. Anslyn, P. Wang and J. S. Kim *Chem. Rev.* 2015, **115**, 7893; (d) E. M. Nolan and S. J. Lippard *Chem. Rev.*, 2008, **108**, 3443; (e) C. McDonagh, C. S. Burke and B. D. MacCraith *Chem. Rev.*, 2008, **108**, 400; (f) X. Li, X. Gao, W. Shi, and H. Ma, *Chem. Rev.*, 2014, **114**,

590; (g) D. T. Quang and J. S. Kim, *Chem. Rev.*, 2010, **110**, 6280; (h) K. Kaur, R. Saini, A. Kumar, V. Luxami, N. Kaur, P. Singh and S. Kumar, *Coord. Chem. Rev*., 2012, **256**, 1992.

155. Recent examples of the use of 1,8-naphthalimides based probes and sensors in cells: (a) J. Pancholi, D. J. Hodson, K. Jobe, G. A. Rutter, S. M. Goldup and M. Watkinson, *Chem. Sci*., 2014, **5**, 3528; (b) X. Sun, Q. Xu, G. Kim, S. E. Flower, J. P. Lowe, J. Yoon, J. S. Fossey, X. Qian, S. D. Bull and T. D. James, *Chem. Sci*., 2014, **5**, 3368; (c) M. H. Lee, B. Yoon, J. S. Kim and J. L. Sessler, *Chem. Sci*., 2013, **4**, 4121; (d) E. E. Langdon-Jones, N. O. Symonds, S. E. Yates, A. J. Hayes, D. Lloyd, R. Williams, S. J. Coles, P. N. Horton and S. J. A. Pope, *Inorg. Chem*., 2014, **53**, 3788; (e) M. Hee Lee, H. Mi Jeon, J. H. Han, N. Park, C. Kang, J. L. Sessler and J. Seung Kim, *J. Am. Chem. Soc.,* 2014, **136**, 8430; (f) S. U. Hettiarachchi, B. Prasai and R. L. McCarley, *J. Am. Chem. Soc*., 2014, **136**, 7575; (g) X. Wu, X. Sun, Z. Guo, J. Tang, Y. Shen, T. D. James, H. Tian and W. Zhu, *J. Am. Chem. Soc*., 2014, **136**, 3579; (h) L. Zhang, D. Duan, Y. Liu, C. Ge, X. Cui, J. Sun and J. Fang, *J. Am. Chem. Soc*., 2014, **136**, 226.

156. (a) B. M. Aveline, S. Matsugo and R. W. Redmond, *J. Am. Chem. Soc*., 1997, **119**, 11785; (b) Z. Xu, Y. Xiao, X. Qian, J. Cui and D. Cui, *Org. Lett*., 2005, **7**, 889; (c) Z. Zhou, M. Yu, H. Yang, K. Huang, F. Li, T. Yi and C. Huang, *Chem. Commun*., 2008, 3387.

157. (a) H. Cao, T. McGill and M. D. Heagy, *J. Org. Chem.,* 2004, **69**, 2959; (b) D. Esteban-Gómez, L. Fabbrizzi and M. Licchelli, *J. Org. Chem*., 2005, **70**, 5717; (c) D. Srikun, E. W. Miller, D. W. Domaille and C. J. Chang, *J. Am. Chem. Soc*., 2008, **130**, 4596; (d) B. Zhu, X. Zhang, H. Jia, Y. Li, H. Liu and W. Tan, *Org. Biomol. Chem*., 2010, **8**, 1650; (e) R. M. Duke, E. B. Veale, F. M. Pfeffer, P. E. Kruger and T. Gunnlaugsson, *Chem. Soc. Rev*., 2010, **39**, 3936.

158. (a) Z. Li, L. Zhang, L. Wang, Y. Guo, L. Cai, M. Yu and L. Wei, *Chem. Commun*. 2011, **47**, 5798; (b) Y. H. Lau, J. R. Price, M. H. Todd and P. J. Rutledge, *Chem. Eur. J*. 2011, **17**, 2850; (c) Y. Zhao, X. Zhang, Z. Han, L. Qiao, C. Li, L. Jian, G. Shen and R. Yu, *Anal. Chem*. 2009, **81**, 7022; (d) D. W. Domaille, L. Zeng and C. J. Chang, *J. Am. Chem. Soc*. 2010, **132**, 1194. (e) M. Kumar, A. Dhir and V. Bhalla, *Org. Lett*. 2009, **11**, 2567; (f) H. S. Jung, M. Park, D. Y. Han, E. Kim, C. Lee, S. Ham and J. S. Kim, *Org. Lett*. 2009, **11**, 3378. (g) H. J. Kim, J. Hong, A. Hong, S. Ham, J. H. Lee and J. S. Kim, *Org. Lett*. 2008, **10**, 1963; (h) Y. Zhou, F. Wang, Y. Kim, S. Kim and J. Yoon, *Org. Lett*. 2009, **11**, 4442. (i) M. Yu,

M. Shi, Z. Chen, F. Li, X. Li, Y. Gao, J. Xu, H. Yang, Z. Zhou, T. Yi and C. Huang, *Chem. Eur. J*. 2008, **14**, 6892; (j) Q. Zhao, F. Li and C. Huang, *Chem. Soc. Rev.* 2010, **39**, 3007; (k) M. Yu, Z. Li, L. Wei, D. Wei and M. Tang, *Org. Lett*. 2008, **10**, 5115.

159. V. K. Gupta, A. K. Singh and N. Mergu, *Electrochim. Acta*, 2014, **117**, 405.
160. P. D. Darbre, *J. Inorg. Biochem.*, 2005, **99**, 1912.
161. D. P. Perl, D. C. Gajdusek, R. M. Garruto, R. T. Yanagihara and C. J. Gibbs, *Science*, 1982, **217**, 1053.
162. J. Wergedal and D. Baylink, *Science*, 1983, **222**, 330.
163. B. L. Riggs, *Bone and Mineral Research, Annual 2*, Elsevier, Amsterdam, 1984.
164. Y. Zhou, J. F. Zhang and J. Yoon, *Chem. Rev*., 2014, **114**, 5511.
165. S. H. Mashraqui, S. S. Ghorpade, S. Tripathi and S. Britto, *Tetrahedron Lett.*, 2012, **53**, 765.
166. (a) B. C. Zhu, C. C. Gao, Y. Z. Zhao, C. Y. Liu, Y. M. Li, Q. Wei, Z. M. Ma, B. Du and X. L. Zhang, *Chem. Commun*. 2011, **47**, 8656; (b) C. Y. Liu, H. F. Wu, Z. K. Wang, C. X. Shao, B. C. Zhu, and X. L. Zhang, *Chem. Commun*. 2014, **50**, 6013; (c) X. Yan, H. X. Li, W. S. Zheng and X. G. Su, *Anal. Chem*. 2015, **87**, 8904; (d) Y. Teng, X. F. Jia, J. Li and E. K.Wang, *Anal. Chem*. 2015, **87**, 4897; (e) Y. Wen, K. Y. Liu, H. R. Yang, Y. Li, H. C. Lan, Y. Liu, X. Y. Zhang and T. Yi, *Anal. Chem*. 2014, **86**, 9970.
167. (a) Q. Q. Wan, Y. C. Song, Z. Li, X. H. Gao and H. M. Ma, *Chem. Commun*. 2013, **49**, 502; (b) Q. Q. Wan, S. M. Chen, W. Shi, L. H. Li and H. M. Ma, *Angew. Chem., Int. Ed.* 2014, **53**, 10916; (c) L. Yuan, W. Y. Lin, K. B. Zheng and S. S. Zhu, *Acc. Chem. Res*. 2013, **46**, 1462; (d) H. Chen, W. Y. Lin, W. Q. Jiang, B. L. Dong, H. J. Cui and Y. H. Tang, *Chem. Commun*. 2015, **51**, 6968; (e) L. W. He, W. Y. Lin, Q. Y. Xu and H. P. Wei, *Chem. Commun*. 2015, **51**, 1510; (f) Li, L. H.; Li, Z.; W. Shi, X. H. Li and H. M. Ma, *Anal. Chem*. 2014, **86**, 6115.
168. Y. Jia and J. Li, *Chem. Rev.*, 2015, **115**, 1597.
169. G. J. Ryan, S. Quinn and T. Gunnlaugsson, *Inorg. Chem.*, 2008, **47**, 401.
170. (a) E. B. Veale, D. O. Frimannsson, M. Lawler and T. Gunnlaugsson, *Org. Lett*., 2009, **11**, 4040; (b) E. B. Veale and T. Gunnlaugsson, *J. Org. Chem.*, 2010, **75**, 5513; (c) S. Murphy, S. A. Bright, F. E. Poynton, T. McCabe, J. A. Kitchen, E. B. Veale, D. C. Williams and T. Gunnlaugsson, *Org. Biomol. Chem.*, 2014, **12**, 6610.
171. (a) R. B. P. Elmes, M. Erby, S. A. Bright, D. C. Williams and T. Gunnlaugsson, *Chem.*

Commun., 2012, **48**, 2588; (b) A. M. Nonat, S. J. Quinn and T. Gunnlaugsson, *Inorg. Chem.*, 2009, **48**, 4646; (c) S. Banerjee, E. B. Veale, C. M. Phelan, S. A. Murphy, G. M. Tocci, L. J. Gillespie, D. O. Frimannsson, J. M. Kelly and T. Gunnlaugsson, *Chem. Soc. Rev*., 2013, **42**, 1601.

172. (a) S. Banerjee, J. A. Kitchen, T. Gunnlaugsson and J. M. Kelly, *Org. Biomol. Chem*., 2013, **11**, 5642; (b) S. Banerjee, J. A. Kitchen, T. Gunnlaugsson and J. M. Kelly, *Org. Biomol. Chem*., 2012, **10**, 3033; (c) S. Banerjee, S. A. Bright, J. A. Smith, J. Burgeat, M. Martinez-Calvo, D. C. Williams, J. M. Kelly and T. Gunnlaugsson, *J. Org. Chem*., 2014, **79**, 9272.
173. S. Banerjee, J. A. Kitchen, S. A. Bright, J. E. O'Brien, D. C. Williams, J. M. Kelly and T. Gunnlaugsson, *Chem. Commun*., 2013, **49**, 8522.

SUMMARY

Cancer is not a disease but a group of diseases that is characterized by the uncontrolled growth and division of abnormal cells. Uncontrolled division of cells and spread resulted in death. Various factors for induction of cancer are tobacco, unhealthy diet, infectious organisms and internal factors like inherited genetic mutations, hormonal changes and immune conditions. Cancer is a major health problem in developed countries and is the second largest cause of death after heart disease[1] due to ageing and lifestyle. It is predicted that by 2030, cancer can affect 22 million people.[1] Surgical and radiation therapies for treatment of local cancer is not specific due to tumor position in the body and is not completely successful treatment in removing tumors. Chemotherapy is a systemic cancer treatment involving chemotherapeutic drugs that interfere with the cell cycle and division of cells, inducing apoptosis of tumour cell by signaling pathways that improve and eradicate cancer. Various chemotherapeutic drugs that are clinically known are 5-fluorouracil, methotrexate, Doxorubicin, Epirubicin etc. Anticancer agents acted through *in vitro* inhibition of various cancer cell lines viz., breast cancer, ovarian cancer, non small cell lung cancer, melanoma, leukemia at single dose conc. of 10 μM. However, due to the high cancer mortality rate, development of drug resistance and undesirable side effects of previously reported anticancer agents, there is an urgent need to design and synthesise new anti-cancer drugs surpassing the side effects of previous anticancer agents.[2-8] Among fused heterocyclic moieties, imidazo[1,2-*a*]pyrazine, benzimidazole and coumarin moieties have been gaining significant attention in field of organic synthesis and drug discovery.

In present investigation, we have synthesized various imidazo[1,2-*a*]pyrazine derivatives bearing aryl group at different positions and then evaluated them *in vitro* against cancer cell lines. Structure activity relationship predicting the relation of activity with changing substituents. As molecular hybridization is an important technique to combine two active pharmacophores in a single unit. Therefore we have applied this methodology to obtain imidazo[1,2-*a*]pyrazine-coumarin hybrids that have been evaluated against 60 human cancer cell lines along with prediction of SAR. The hybrids have been checked for its cytotoxicity on normal cells. More molecular conjugates/dyads have been synthesized by employing imidazo[1,2-*a*]pyrazine-coumarin linked to triazole and imidazo[1,2-*a*]pyrazine-benzimidaozle linked to triazole via click chemistry and Suzuki-Miyaura coupling reactions. Photophysical properties of all conjugates

have been determined. Naphthalimide derivatives have also been synthesized which have been evaluated for its photophysical sensing towards various anions and metals along with DNA intercalation studies. Characterization of these molecules was done with different spectroscopic techniques such as ^{1}H NMR, ^{13}C NMR and mass spectroscopy.

Results and Discussion

Chapter 2: Covers synthesis, characterization and *in vitro* evaluation of monoarylation, symmetrical/unsymmetrical diarylation of imidazo[1,2-*a*]pyrazines

2.1. Synthesis of 6,8-dibromoimidazo[1,2-*a*]pyrazine

Bromination of 2-aminopyrazine **1** with *N*-bromosuccinamide (NBS) in DMSO and water at room temperature for 6 h gave 2-amino-3,5-dibromopyrazine **2** in 90% yield followed by cyclization with chloroacetaldehyde in the absence of base to obtain 6,8-dibromo-imidazo[1,2-*a*]pyrazine **3** with 80% yield (Scheme 1).

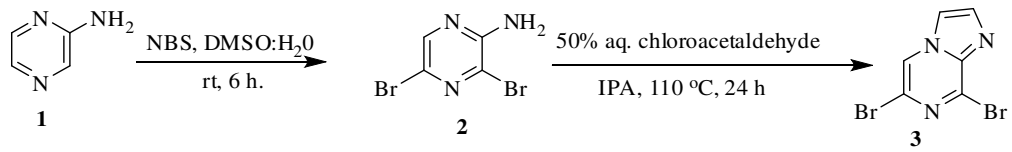

Scheme 1

Palladium catalyzed Suzuki-Miyaura coupling of 6,8-dibromo-imidazo[1,2-*a*]pyrazine **3** with different aryl boronic acids afforded substituted monoarylated and symmetrical diarylated products. During our study of imidazo[1,2-*a*]pyrazine derivatives, thiophen-2-boronic acid served as a model reactant for optimization of the reaction conditions. A survey of different catalysts ($Pd(PPh_3)_4$, $Pd(PPh_3)_2Cl_2$ and $Pd_2(dba)_3$), bases (Cs_2CO_3, Na_2CO_3, K_2CO_3 and DIPEA) and solvents (MeCN:H_2O, Toluene: H_2O, THF, dioxane, DMF, IPA) revealed that $Pd(PPh_3)_4$, Cs_2CO_3 and MeCN:H_2O was found to be the best choice.

With the optimized reaction conditions in hand, we have used 1.0 equivalent of thiophen-2-boronic acid, 5 mol% of $Pd(PPh_3)_4$, Cs_2CO_3 (1 eq.) in MeCN:H_2O (9:1) and evaluated the scope of arylation with variety of aryl boronic acids providing a library of monosubstituted **4a-15a** and disubstituted imidazo[1,2-*a*]pyrazines **4b-15b** (Scheme 2).

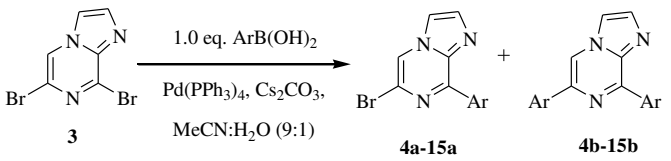

Ar = **4**: 2-thiophene, **5**: 2-furan, **6**: 4-fluorophenyl, **7**: 4-chlorophenyl, **8**: 4-bromophenyl, **9**: 4-methoxyphenyl, **10**: 4-formylphenyl, **11**: 2-hydroxyphenyl, **12**: 1-naphthyl, **13**: phenyl, **14**: 3-methylphenyl, **15**: 4-ethyl phenyl

Scheme 2

We took advantage of the monoarylated products to implement an additional cross-coupling reaction which aimed at providing straightforward access to unsymmetrical imidazo[1,2-*a*]pyrazine. Thus, reactions of of C8 monosubstituted imidazo[1,2-*a*]pyrazines were carried out with 1.0 equivalent of variety of boronic acids in the presence of $Pd(PPh_3)_4$, Cs_2CO_3 in MeCN:H_2O gave unsymmetrical diarylated imidazo[1,2-*a*]pyrazine derivatives (Scheme 3).

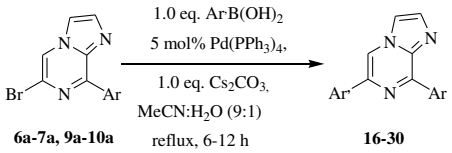

16: Ar = 4-fluorophenyl, Ar' = 4-formylphenyl
17: Ar = 4-fluorophenyl, Ar' = 2-hydroxyphenyl
18: Ar = 4-fluorophenyl, Ar' = 4-chlorophenyl
19: Ar = 4-chlorophenyl, Ar' = 4-2-thiophene
20: Ar = 4-chlorophenyl, Ar' = 4-formylphenyl
21: Ar = 4-chlorophenyl,, Ar' = 2-hydroxphenyl
22: Ar = 4-chlorophenyl, Ar' = 2-furan
23: Ar = 4-chlorophenyl, Ar' = 4-fluorophenyl
24: Ar = 4-chlorophenyl, Ar' = 4-methoxyphenyl
25: Ar = 4-formylphenyl, Ar' = 2-thiophene
26: Ar = 4-methoxyphenyl, Ar' = 4-formylphenyl
27: Ar = 4-methoxyphenyl, Ar' = 2-hydroxyphenyl
28: Ar = 4-methoxyphenyl, Ar' = 4-fluorophenyl
29: Ar = 4-methoxyphenyl, Ar' = 4-chlorophenyl
30: Ar = 4-methoxyphenyl, Ar' = 2-thiophene

Scheme 3

2.2. Characterization

(a) All the synthesized compounds were characterized by ^1H and ^{13}C NMR spectra (JEOL ECS-400 MHz spectrometers) and mass spectra (Waters QTOF Micro).

(b) Single X-ray crystallography of compounds 9b and 20 was grown in ethanol to develop single crystal with Crystalispro diffractometer with graphite monochromated Mo Kα radiation (λ = 0.7107 Å) using SHELX-97, full-matrix least-square refinement method.

2.3. Biological evaluation

Preliminary anticancer activity revealed that monoarylated, symmetrical diarylated compounds **(4a-b, 5a-b, 7a, 8a-b, 9a-b, 11a-b** and **13b)** and unsymmetrical diarylated compounds **(18-19, 21-23, 27-28** and **30)** were selected by National Cancer Institute, Bethesda, Maryland, USA on the basis of structure variation for evaluation of its anticancer activity. The selected compounds were subjected to *in vitro* anticancer assay against tumor cells in a full panel of 60-cell lines at single dose concentration of 10 μM, and the percentages of growth inhibition over sixty tested cancer cell lines were determined.

2.4. Structure activity relationship (SAR studies)

The structure-activity relationship (SAR) emerged from activity results showed that monoaryl

and diaryl imidazo[1,2-*a*]pyrazines were well tolerated for *in vitro* anticancer activities. (i) The monosubstituted and disubstituted imidazo[1,2-*a*]pyrazines with variations of different functional groups on aryl moiety play a key role in varying the efficiency of antitumor activities. (ii) The diaryl imidazo[1,2-*a*]pyrazines positively influence the antitumor effectiveness, inducing good activity than mono aryl imidazo[1-2-*a*]pyrazines against most of the cancer cell lines. (iii) Unsymmetrical diaryl imidazo[1,2-*a*]pyrazine showed broad spectrum antitumor activity than symmetrical diaryl analogue. (iv) Introduction of 2-hydroxy phenyl (**21**), 2-furanyl (**22**) and 4-fluorophenyl (**23**) at C6 position with 4-chlorophenyl at C8 position of imidazo[1,2-*a*]pyrazine led to a broad spectrum antitumor activity. Thus 4-chloro phenyl at C8 position of imidazo[1,2-*a*]pyrazine plays an important role for the activity. (v) Presence of 4-chlorophenyl (**19**) and 4-methoxyphenyl (**30**) at C8 position and 2-thiophene at C6 position of imidazo[1,2-*a*]pyrazine has slightly improved the activity. (vi) Amongst symmetrical diaryl analogues, 4-bromophenyl at C6 and C8 positions of imidazo[1,2-*a*]pyrazine (**8b**) has improved the antitumor activity.

Chapter 3: Covers synthesis, characterization and *in vitro* evaluation of imidazo [1,2-*a*] pyrazine-coumarin hybrids.

3.1. Synthesis of imidazo[1,2-*a*] pyrazine-coumarin hybrids.

2-Aminopyrazine **1** was treated with *N*-bromosuccinimide (NBS) in DMSO and water (9:1) at room temperature for 6 h to give 2-amino-3,5- dibromopyrazine **2** in 90% yield followed by cyclization with 50% aq. chloroacetaldehyde in isopropyl alcohol at 110 ^{o}C for 12 h to obtain 6,8-dibromoimidazo[1,2-*a*]pyrazine **3** in 80% yield. Compound **3** was again brominated with NBS in acetonitrile (ACN) at room temperature for 2 h to afford 3,6,8-tribromoimidazo[1,2-*a*]pyrazine **4** in 90% yield. 3,6,8-Tribromoimidazo[1,2-*a*]pyrazine **4** was then stirred with 7-hydroxy-4-methylcoumarin **5** in the presence of K_2CO_3 and DMF at room temperature for 12 h to afford 7'-(3,6-dibromoimidazo[1,2-*a*]pyrazin-8-yloxy)-4'-methyl-2*H*-chromen-2'-one **6** in 85% yield (Scheme 1).

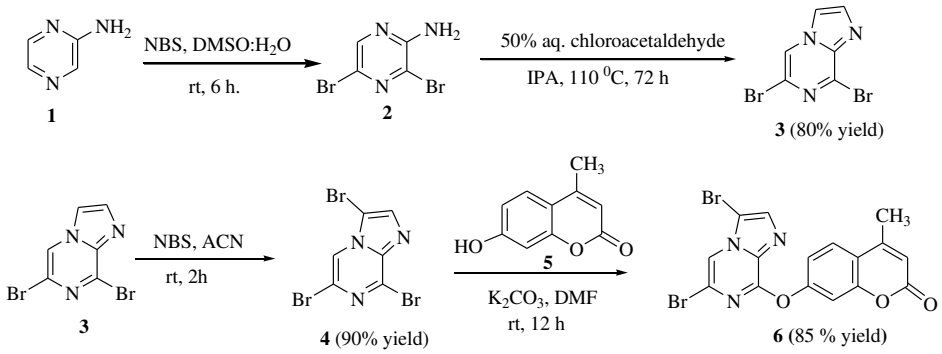

Scheme 1

Palladium catalyzed Suzuki-Miyaura cross coupling of compound **6** with 2-methoxyphenyl boronic acid (1 eq.) in the presence of K_2CO_3 (1 eq.) and 5 mol% of $Pd(PPh_3)_4$ in DME:H_2O (9:1) under inert atmosphere afforded C6-monoarylated **7a** and C3, C6 diarylated **7b** products in 61% and 33% yields respectively. Similarily, compound **6** was also treated with 2-furan boronic acid under same reaction conditions to give compounds **8a** and **8b** in 48% and 25% yields respectively. Reaction of compound **6** with 4-chlorophenyl boronic acid afforded C6 monoarylated product **9a** and C3, C6 diarylated product **9b** in 40% and 42% GCMS yields respectively. These two compounds could not be separated through column chromatography and used as such without purification. However, reactions of **6** with other aryl boronic acids under the same reaction conditions gave only C3, C6 diarylated products **10b-19b** with 54-74% yields. Monoarylated products with these boronic acids could not be separated as these were formed only in traces <5% (determined by GC-MS) (Scheme 2).

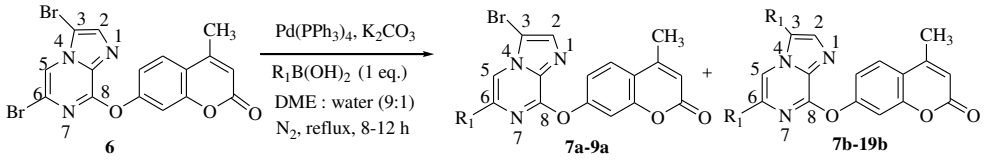

7, R_1 = 2-methoxyphenyl
8, R_1 = 2-furan
9, R_1 = 4-chlorophenyl
10, R_1 = 2-thiophene
11, R_1 = phenyl
12, R_1 = 3-methylphenyl
13, R_1 = 4-ethylphenyl
14, R_1 = 4-fluorophenyl
15, R_1 = 3-t(rifluromethyl)phenyl
16, R_1 = 4-methoxyphenyl
17, R_1 = 4-formylphenyl
18, R_1 = 2-hydroxyphenyl
19, R_1 = 4-acetylphenyl

Scheme 2

Subsequently use of monoarylated product has been implemented for unsymmetrical diarylation via cross coupling reaction at C3 position. C6 Monoarylated imidazo[1,2-*a*]pyrazine-coumarin hybrid **7a** was further refluxed with variety of aryl boronic acids (1.0 eq.) in the presence of 5

mol% of $Pd(PPh_3)_4$, K_2CO_3 (1.1 eq.) in DME:H_2O (9:1) for 6-8 h to give C3, C6 unsymmetrical diarylated imidazo[1,2-*a*]pyrazine-coumarin hybrids **20**-**29** in 52-75% yields. However Suzuki reaction of mixture of monoarylated and symmetrical diarylated compounds (**9a** and **9b)** with 2-thiophene boronic acid under the same reaction conditions and after column chromatography afforded C3, C6 symmetrical and unsymmetrical disubstituted imidazo[1,2-*a*]pyrazine-coumarin hybrids **9b** and **30** in 42% and 61% isolated yields respectively (Scheme 3).

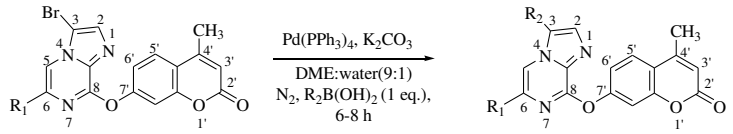

7a, R_1 = 2-methoxy phenyl
9a, R_1 = 4-chloro phenyl

20-30

20, R_1 = 2-methoxyphenyl, R_2 = 2-thiophene
21, R_1 = 2-methoxyphenyl, R_2 = 2-furan
22, R_1 = 2-methoxyphenyl, R_2 = phenyl
23, R_1 = 2-methoxyphenyl, R_2 = 3-methylphenyl
24, R_1 = 2-methoxyphenyl, R_2 = 4-ethylphenyl
25, R_1 = 2-methoxyphenyl, R_2 = 4-fluorophenyl
26, R_1 = 2-methoxyphenyl, R_2 = 4-chlorophenyl
27, R_1 = 2-methoxyphenyl, R_2 = 3-(trifluoromethyl)phenyl
28, R_1 = 2-methoxyphenyl, R_2 = 4-methoxyphenyl
29, R_1 = 2-methoxyphenyl, R_2 = 2-hydroxyphenyl
30, R_1 = 4-chlorophenyl, R_2 = 2-thiophene

Scheme 3

3.2. Characterization

All the synthesized compounds were characterized by ^1H and ^{13}C NMR spectra (JEOL ECS-400 MHz spectrometers) and mass spectra (Waters QTOF Micro).

3.3. Biological evaluation

Compounds **6**, **7a**, **9b**, **10b**, **11b**, **16b**, **28** and **30** were submitted to NCI, USA to test their *in vitro* anticancer activities against a panel of 60 human cancer cell lines at a single dose concentration of 10 μM. Compound **16b** was also evaluated for toxicity to Hek293 (human embryonic kidney) cell lines using the MTT assay. It was observed that compound **16b** showed only 17%, 15%, 9%, 5% and 3% cytotoxicity to Hek293 cells at $10^{-}4$, $10^{-}5$, $10^{-}6$, $10^{-}7$ and $10^{-}8$ M concentrations, respectively. The compound showed only 17% of toxicity to Hek293 cells even at 100 μM concentration. These data indicated that compound **16b** showed potent anticancer activity and low toxicity to normal cells.

3.4. Structure activity raltionship (SAR) studies

Structure–activity correlation, based on the number of cancer cell lines that were inhibited by each compound revealed that the nature of the substituents at the C3- and C6-positions of imidazo[1,2-*a*]pyrazine affected the biological activity. Compounds **10b**, **11b** and **16b** showed comparatively higher activity than **6**, **7a**, **9b**, **28** and **30**, suggesting that there is much difference

in antitumor activity with different substitutions of phenyl rings. The antitumor results indicated that compound **6** with a coumarin moiety at the C8 position and bromo at the C3 and C6 positions displayed only moderate anticancer activity. The anticancer activity has been slightly increased with the substitution of 2-thiophene rings at the C3 and C6 positions, as in the case of compound **10b**. Higher activity has been achieved with substitution of phenyl rings **11b** and 4-methoxyphenyl rings 1**6b** at the C3 and C6 positions. On the other hand, substitution with 4-chlorophenyl at the C6 position and 2-thiophene at the C3 position as in case of compound **30** decreased the activity. It has been revealed that symmetrical diarylated imidazo[1,2-*a*]pyrazine–coumarin hybrids **11b** and **16b** showed higher activity than unsymmetrical diarylated hybrids **28** and **30**. These studies indicated that substitution of the coumarin heterocycle with various phenyl derivatives on imidazo[1,2-*a*]pyrazine gave highly potent anticancer activities towards 60 human cancer cell lines. Overall, **16b** has been found to be the most effective member of this series of compounds and showed a broad spectrum of activity against melanoma cancer cell lines.

3.5. Lipophilicity determination by Shake Flask Method

The partition coefficient of the compounds was also studied in an octanol/water system for the determination of log P values by a shake-flask method[9]. It was observed that compounds **11b** and **16b** showed higher log P values (3.40 and 2.88 respectively), which suggested that the higher antitumour activity of these compounds was related to the lipophilicity. Thus, lipophilicity is a crucial factor for the activity of the synthesized compounds.

3.6. Molecular docking studies

Preliminary anticancer screening showed that compound **16b** has been found to be the most active member of imidazo[1,2-*a*]pyrazine-coumarin hybrids and showed excellent inhibition against melanoma than other cancer cell lines. So in order to observe the molecular interactions of compound in the active site of enzyme for melanoma cancer, docking experiment was performed. Therefore, docking of compound **16b** in the active site of this enzyme indicated the probable mode of action for anticancer activities.

Chapter 4: Covers synthesis and photophysical properties of triazole tethered imidazo[1,2-*a*]pyrazine-coumarin hybrids

4.1.1. Synthesis of triazole tethered imidazo[1,2-*a*]pyrazine-coumarin hybrids

2-bromoethylamine hydrobromide **1** was refluxed with sodium azide in water for 12 h followed

by stirring with sodium hydroxide at room temperature to give 2-azidoethanamine **2**. To obtain the first precursor, we have treated 6,8-dibromoimidazo[1,2-*a*]pyrazine **3** (obtained from bromination of 2-aminopyrazine followed by cyclization with 50% aqueous chloroacetaldehyde) with 2-azidoethanamine **2** in the presence of diisopropylethylamine (DIPEA) in acetonitrile at reflux temperature for 24 h to obtain *N*-(2-azidoethyl)-6-bromoimidazo[1,2-*a*]pyrazin-8-amine **4** in 72% yield (Scheme 1).

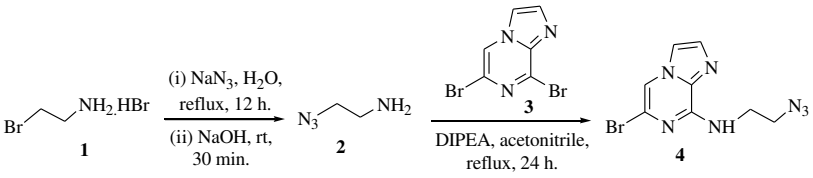

Scheme 1

Second precursor 4-methyl-7-(prop-2-ynyloxy)-2*H*-chromen-2-one **6** was obtained in 81% yield by the reaction of 7-hydroxy-4-methyl-2*H*-chromen-2-one **5** with 2 equivalents of 80% solution of propargyl bromide in the presence of potassium carbonate and acetone at room temperature for 12 h (Scheme 2).

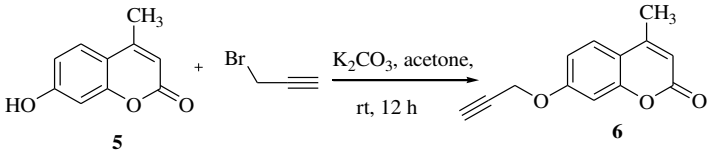

Scheme 2

Compound **4** was treated with 4-methyl-7-(prop-2-ynyloxy)-2*H*-chromen-2-one **6** in the presence of 5 mol% of $CuSO_4.5H_2O$ and 10 mol% of sodium ascorbate in ethanol:water (8:2) at room temperature for 2h to give 1,4-disubstituted triazole **7** in 91% yield. The scope of the reaction was further examined on reaction of compound **7** with various aryl boronic acids to obtain compounds **9**-**24** in 58-92% yields respectively (Scheme 3).

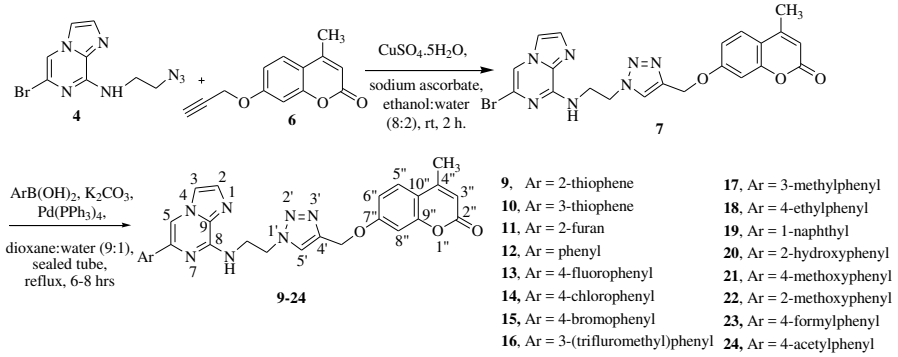

Scheme 3

3-Bromopropylamine hydrobromide **25** was first reacted with sodium azide to give **26** followed by substitution at C-8 position of 6,8-dibromoimidazo[1,2-*a*]pyrazine **3** to give **27** in 65% yield. Compound **27** was then coupled with coumarin **6** via. copper-catalyzed azide-alkyne cycloaddition reaction to give **28** in 82% yield. Compound **28** was further coupled with various aryl boronic acids via Suzuki-Miyaura cross coupling reaction using 5 mol% $[Pd(PPh_3)_4]$, K_2CO_3 and dioxane:water at reflux temperature for 6-8 hrs to obtain compounds **29-38** in 56-90% yields (Scheme 4).

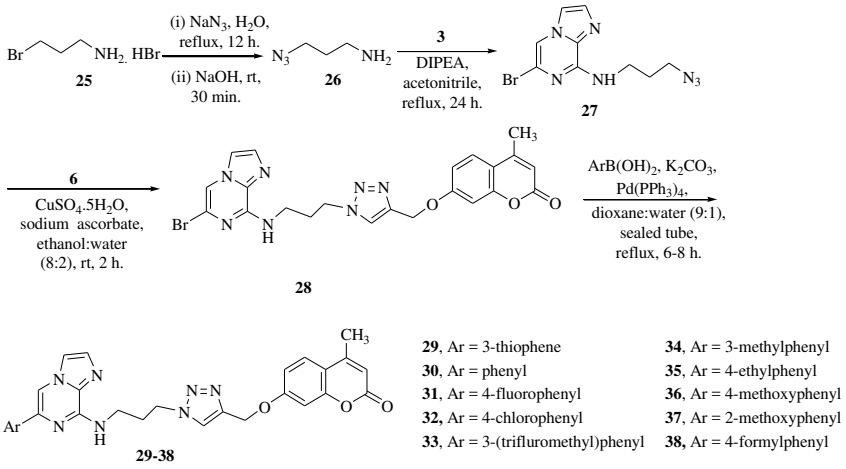

Scheme 4

4.1.2. Characterization

All the synthesized compounds were characterized by ^1H and ^{13}C NMR spectra (JEOL ECS-400 MHz spectrometers) and mass spectra (Waters QTOF Micro).

4.1.3. Photophysical properties

Various spectroscopic measurements (Figure 1,2) were recorded for the molecules to test the cassettes, based on the quantification of their efficiencies. Molar absorptivities (€) and quantum yields (Φ_f) for all 28 compounds were determined in acetonitrile. Overall, it was inferred that compounds with electron donating groups showed lower quantum yields in comparison to compounds with electron withdrawing groups. Increase in linker length also resulted in similar or decrease in quantum yields. Energy transfer efficiencies (ETE) based upon the fluorescence quantum yields have also been determined. Emission spectra of the imidazo[1,2-*a*]pyrazine (donor) and absorption spectra of the coumarin (acceptor) showed significant spectral overlap for the energy transfer.

4.2.1. Synthesis of triazole tethered imidazo[1,2-*a*]pyrazine-benzimidazole hybrids

2-bromoethylamine hydrobromide **1** was refluxed with sodium azide in water for 12 h followed by stirring with sodium hydroxide at room temperature to give 2-azidoethanamine **2**. To obtain the first precursor, we have treated 6,8-dibromoimidazo[1,2-*a*]pyrazine **3** (obtained from bromination of 2-aminopyrazine followed by cyclization with 50% aqueous chloroacetaldehyde) with 2-azidoethanamine **2** in the presence of diisopropylethylamine (DIPEA) in acetonitrile at reflux temperature for 24 h to obtain *N*-(2-azidoethyl)-6-bromoimidazo[1,2-*a*]pyrazin-8-amine **4** in 72% yield (Scheme 1).

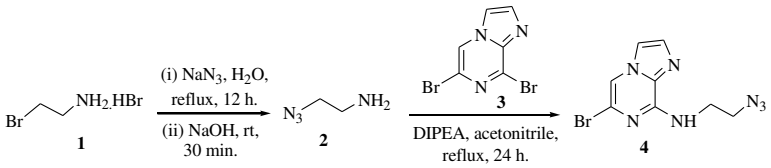

Scheme 1

Reaction of 2-(3-nitrophenyl)-1*H*-benzo[*d*]imidazole **5** with 2 eq. of 80% solution of propargyl bromide, in the presence of potassium carbonate and DMF at room temperature for 12 h to obtain 2-(3-nitrophenyl)-1-(prop-2-ynyl)-1*H*-benzo[*d*]imidazole **6** in 95% yield (Scheme 2).

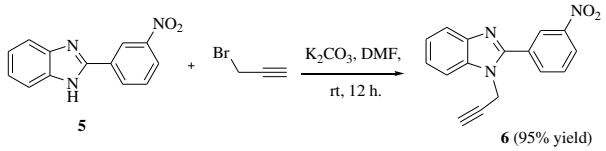

Scheme 2

Keeping both the precursors i.e. azide and alkyne, copper catalyzed azide-alkyne cyloaddition (CuAAC) reaction was performed by reacting azide **4** and alkyne **6** with in the presence of 5 mol% of $CuSO_4.5H_2O$ as catalyst and 10 mol% of sodium ascorbate as reducing agent in ethanol:water (8:2) at room temperature for 2 h to afford triazole linked imidazo[1,2-*a*]pyrazine-benzimidazole conjugate **7** in 81% yield. Conjugate **7** was further reacted with variety of aryl boronic acids through Suzuki-Miyaura cross coupling at C-6 position of imidazo[1,2-*a*]pyrazine using $Pd(PPh_3)_4$ (5 mol%), K_2CO_3 (1 equiv.) in 1,4-dioxane:H_2O (9:1), providing library of arylated compounds **9-24** (Scheme 3).

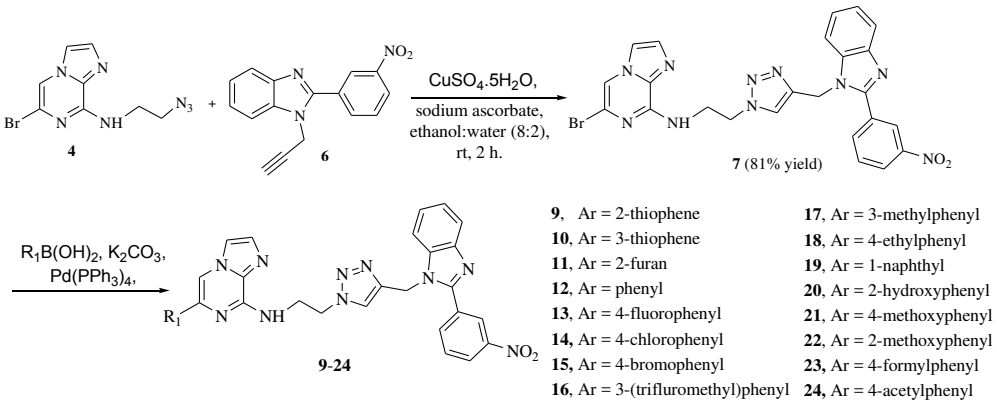

Scheme 3

Reaction of 3-bromopropylamine hydrobromide **25** with sodium azide in water for 12h followed by treatment with NaOH at room temperature to obtain 3-azidopropanamine **26**. Compound **26** was further reacted at C-6 position of 6,8-dibromoimidazo[1,2-*a*]pyrazine **3** to give **27** in 65% yield. Copper catalyzed azide-alkyne cycloaddition of **27** with **6** gave compound **28** in 85% yield. Subsequent reaction of **28** with variety of aryl boronic acids via Suzuki-Miyaura coupling reaction, to obtain compounds **29-38** in 53-83% yields (Scheme 4).

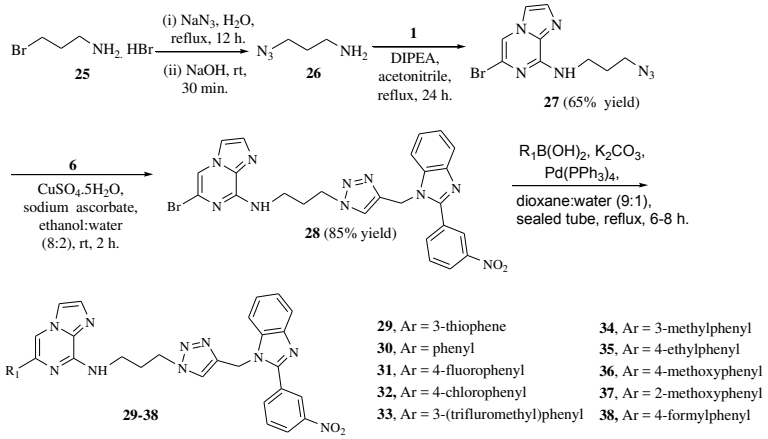

Scheme 4

4.2.2. Characterization

All the synthesized compounds were characterized by ^{1}H and ^{13}C NMR spectra (JEOL ECS-400 MHz spectrometers) and mass spectra (Waters QTOF Micro).

4.2.3 Photophysical properties

Compounds **7-24** and **28-38** were further studied for their photophysical properties. Quantum yields of all compounds were calculated with respect to anthracene in acetonitrile. Further insight and quantitative evaluation of the sensing capability of compounds **7-24** and **28-38** (20 μM,

CH_3CN) with pyrophosphate was obtained from UV-vis and fluorescence experiments. It was surprising that only compound **20** with 2-hydroxylphenyl ring at C6 position of imidazo[1,2-a]pyrazine, showed significant change with pyrophosphate indicating that 2-hydroxyphenyl moiety is responsible for binding with PPi.

Chapter 5: Covers synthesis and photophysical sensing and DNA intercalation studies of naphthalimide derivatives

5.1.1. Synthesis of Naphthalimide based Schiff bases

Schiff bases were synthesized in several steps. Nitration of acenapthene **1** with nitric acid in acetic acid gave **2** followed by oxidation in the presence of sodium dichromate and acetic acid to give **3**. Subsequent reaction with allyl amine in refluxing ethanol gave allylated nitro naphthalimide **4**. Reduction of **4** with palladium carbon in presence of hydrazine hydrate in methanol gave doubly reduced product **5.** Final treatment of intermediate **5** with different aldehydes salicylaldehyde and 4-diethylamino salicaldehyde in ethanol at room temperature for 10-15 h afforded naphthalimide based Schiff bases **6-9** in 85-90% yield (Scheme 1).

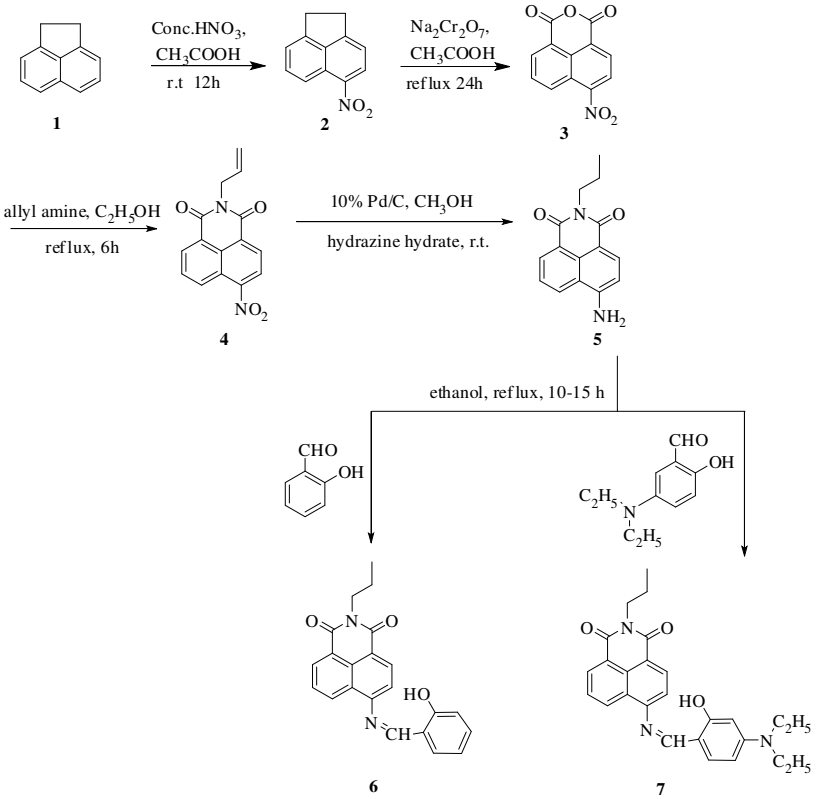

Scheme 1

5.1.2. Characterization

All the synthesized compounds were characterized by ^{1}H and ^{13}C NMR spectra (JEOL ECS-400 MHz spectrometers) and mass spectra (Waters QTOF Micro).

5.1.3.1. Photophysical sensing towards metal ions

Absorption spectra of probe **6** (20 μM, CH_3OH) showed an absorption band centered at 380 nm. On addition of 1000 μM of different metal ions viz., Na^+, K^+, Ca^{2+}, Mg^{2+}, Li^+, Ba^{2+}, Co^{2+}, Ni^{2+}, Zn^{2+}, Hg^{2+}, Ag^+, Pb^{2+} and Al^{3+} as their perchlorate salts, a significant change in UV-visible spectra was observed with Al^{3+} ions, and Hg^{2+} ions showed the sillier results albeit to the lesser extent**.**

Probe **6** (1 μM, CH_3OH, $\Phi = 0.16$) upon excitation at 380 nm showed emission band at 530 nm. After addition of 5.0 equiv of metal ions such as Na^+, K^+, Ca^{2+}, Mg^{2+}, Li^+, Ba^{2+}, Co^{2+}, Ni^{2+}, Zn^{2+}, Hg^{2+}, Ag^+, Pb^{2+} and Al^{3+} under the established conditions, however, discernible changes in both emission color and spectral occurred only in the presence of Al^{3+} ions. Gratifyingly, other metal ions (Hg^{2+}) showed little or no interference.

5.1.3.2. Photophysical sensing towards anions

The sensing behaviour of probe **6** towards anions was determined using tetrabutylammonium salts of various anions viz., F^-, Cl^-, Br^-, I^-, AcO^-, NO_3^-, $H_2PO_4^-$, $HP_2O_7^-$, HSO_4^-, CN^-, SCN^- in CH_3OH. On addition of 50 equiv. of anions to probe **6** (20 μM, CH_3OH), no significant change in absorption spectrum was observed except the HSO_4^-.

In case of addition of various anions to probe **6** (1 μM, CH_3OH), emission changes were observed only in the presence of HSO_4^- ions.

5.1.4. DNA binding studies

Interaction studies of probe **6** with Ct-DNA were performed by spectroscopic means in aqueous phosphate buffer solution at pH 7.0. Thus, the absorption maxima of probe **6**, showed a negligible effect on the change in wavelength position and intensity as Ct-DNA was added gradually. Next, fluorescence titration experiment was carried out. Thus, upon gradual addition of Ct-DNA, the emission intensity (λem = 530 nm) of the probe **6** was found to be significantly enhanced. The association constant of probe **6** with Ct-DNA was also determined by a Benesi-Hildebrand plot. In order to prove the reversibility of probe **6** with DNA, an experiment was performed in the presence of competitive ethidium bromide (standard DNA intercalator).

5.2.1. Photophysical sensing towards metal ions

To examine the binding of sensor **7** with metal ions, the UV-visible and emission studies of sensor **7** towards various metal ions Ag^{2+}, Al^{3+}, Mg^{2+}, Ba^{2+}, Hg^{2+}, Pb^{2+}, Ni^{2+}, Zn^{2+}, Cu^{2+}, Ca^{2+}, Co^{2+}, K^{+} and Na^{+} was carried out in CH_3CN. Binding of **7** with Al^{3+} as its perchlorate salt was examined by UV-visible spectroscopy. UV-visible spectroscopy is complementary part of fluorescence spectroscopy. Therefore to interpret the more precised results, the recognition behaviour of naphthalimide based sensor on various metal ions was investigated by fluorescence studies. Ligand (20 μM) showed dual emission band having weak emission at 520 nm and strong emission at 610 nm when excited at 460 nm. On addition of 50 eq. of different metal ions Ag^{2+}, Mg^{2+}, Ba^{2+}, Hg^{2+}, Pb^{2+}, Ni^{2+}, Zn^{2+}, Cu^{2+}, Ca^{2+}, Co^{2+}, K^{+} and Na^{+} to **7**, no significant change in fluorescence spectrum of different metal ligand complexes was observed. However, a significant change was observed on addition of 50 eq. of Al^{3+} ions.

5.2.2. Photophysical sensing towards anions

Upon addition of 50 eq. of tetrabutylammonium salts of various anions viz., F^-, Cl^-, Br^-, I^-, AcO^-, NO_3^-, $H_2PO_4^-$, $HP_2O_7^-$, HSO_4^-, CN^-, SCN^- to ligand **7** (20 μM, CH_3CN) in acetonitrile, no significant change was observed except F^- ion. A visible colour change from orange to purple was observed on addition of 50 eq. of F^- ion to 20 μM of **7.** UV-visible spectra of ligand showed two absorption bands at 340 nm and 460 nm.

Further the effect of various anions on emission spectra of ligand7 was studied. When excited at 450 nm, ligand **7** (20 μM, CH_3CN) showed the dual emission band at 520 nm and 610 nm. Addition of 50 eq. of tetrabutyl ammonium salts of various anions viz., F^-, Cl^-, Br^-, I^-, AcO^-, NO_3^-, $H_2PO_4^-$, $HP_2O_7^-$, HSO_4^-, CN^-, SCN^- resulted in significant change with only F- ions.

5.2.3 DNA binding studies

Interactions of ligand **7**. Al^{3+} complex with ct-DNA was determined through UV-visible and fluorescence emission studies. Fluorescence experiments (ethidium bromide displacement assay) were carried out in order to confirm the reversibility of ligand **7**.Al^{3+} complex with DNA.

REFERENCES

1. http://www.who.int/mediacentre/factsheets/fs297/en/(accessed 05.01.16).
2. Y. Li, Y. Xu, X. Qian, B. Qu, *Tetrahedron Lett*., 2004, **45**, 1247.
3. Y. Xu, B. Qu, X. Qian, Y. Li, *Bioorg. Med. Chem. Lett*., 2005, **15**, 1139.

4. F. Liu, X. Qian, J. Cui, Y. Xiao, R. Zhanga, G. Lia, *Bioorg. Med. Chem.*, 2006, **14**, 4639.
5. Y. Li, Y. Xu, X. Qian, B. Qu, *Bioorg. Med. Chem. Lett.*, 2003, **13**, 3513.
6. H. B. Mereyala, M. Joe, *Curr. Med. Chem. Anti-Cancer Agents*, 2001, **1**, 293.
7. M. F. Bran˜ a, A. Ramos, *Curr. Med. Chem. Anti-Cancer Agents*, 2001, **1**, 237.
8. X. Qian, Y. Li, Y. Xu, B. Qu, *Bioorg. Med. Chem. Lett.*, 2004, **14**, 2665.
9. A. I. Caço, L. C. Tome, R. Dohrn and I. M. Marrucho, *J. Chem. Eng. Data*, 2010, **55**, 3160.

LIST OF PUBLICATIONS

1. **Richa Goel**, Vijay Luxami and Kamaldeep Paul, "Palladium catalyzed novel monoarylation and symmetrical/unsymmetrical diarylation of imidazo[1,2-*a*]pyrazines and their *in vitro* anticancer activities", *RSC advances*, **2014**, *4,* 9885-9892.
2. **Richa Goel**, Vijay Luxami and Kamaldeep Paul, "Recent advances in development of imidazo[1,2-*a*]pyrazines: synthesis, reactivity and their biological applications", *Organic and Biomolecular Chemistry*, **2015**, *13*, 3525-3555.
3. **Richa Goel**, Vijay Luxami and Kamaldeep Paul, "Synthesis, *in vitro* anticancer activity and SAR studies of arylated imidazo[1,2-*a*]pyrazine-coumarin hybrids", *RSC advances*, **2015**, *5,* 37887-37895.
4. **Richa Goel**, Vijay Luxami and Kamaldeep Paul, "Synthetic approaches and functionalizations of imidazo[1,2-*a*]pyrimidines:an overview of the Decade", *RSC Advances*, **2015**, *5*, 81608.
5. **Richa Goel**, Vijay Luxami and Kamaldeep Paul, "Synthesis of energy transfer cassettes via click and Suzuki Miyaura cross coupling reactions", *RSC Advances*, **2016**, **6**, 37664-37671.
6. **Richa Goel**, Vijay Luxami and Kamaldeep Paul, "Imidazo[1,2-*a*]pyridines: promising drug candidate for antitumor therapy", Current topics in Medicinal Chemistry, **2016** **DOI:** 10.2174/1568026616666160414122644.
7. **Richa Goel**, Vijay Luxami and Kamaldeep Paul, "Synthesis of new triazole based imidazo[1,2-*a*]pyrazine-benzimidazole conjugates: An efficient FRET based ratiometric detection of pyrophosphate, Communicated.
8. **Richa Goel**, Sheryl Sharma, Vijay Luxami and Kamaldeep Paul, "Naphthalimide based chromofluorescent sensor based on Al^{3+}/HSO_4^- triggered cleavage reaction and DNA intercalator, Communicated.
9. **Richa Goel**, Vijay Luxami and Kamaldeep Paul, A 4-imino naphthalimide based selective colorimetric and fluorescent sensor for Al^{3+} and F^- ions, Communicated.

PRESENTATIONS IN CONFERENCES

1 Poster presented at NCIMSF in SCBC, Thapar University, Patiala on 26^{th} -28^{th} Oct 2013.

2 Poster presented at 16^{th} CRSI-NSC in chemistry held at IIT, Bombay on 5^{th}-7^{th} Feb 2014.

3 Poster presented at "Synergistic Aspects of Chemical and Other Sciences-2015 (SACOS-2015)“ held at Punjabi University on 19^{th}-20^{th} Feb 2015, Patiala.

4 Poster presented at 18^{th} CRSI-NSC in chemistry at Punjab University, Chandigarh on 5^{th}-7^{th} Feb 2016.